Cairns, John William (1976) *The strength of lapped joints in reinforced concrete columns.* PhD thesis.

http://theses.gla.ac.uk/1472/

Copyright and moral rights for this thesis are retained by the author

A copy can be downloaded for personal non-commercial research or study, without prior permission or charge

This thesis cannot be reproduced or quoted extensively from without first obtaining permission in writing from the Author

The content must not be changed in any way or sold commercially in any format or medium without the formal permission of the Author

When referring to this work, full bibliographic details including the author, title, awarding institution and date of the thesis must be given

Glasgow Theses Service
http://theses.gla.ac.uk/
theses@gla.ac.uk

THE STRENGTH OF LAPPED JOINTS IN REINFORCED CONCRETE COLUMNS

by

J. Cairns, B.Sc.

A THESIS

PRESENTED FOR THE DEGREE OF DOCTOR OF PHILOSOPHY

of

THE UNIVERSITY OF GLASGOW

by

JOHN CAIRNS, B.Sc.

October, 1976

CONTENTS

CONTENTS contd.

THE STRENGTH OF LAPPED JOINTS IN REINFORCED CONCRETE COLUMNS

by J. Cairns, B.Sc.

SUMMARY

This thesis presents the results of a total of 51 tests on full scale columns in which the main reinforcement was lap jointed. In order to investigate the contribution of the bearing of the ends of the lapped bars to joint strength, several columns were tested with end bearing of bars eliminated, or with bond of bars eliminated within the lap length. Failure of lapped joints was always preceded by extensive splitting of the concrete cover along the line of the lapped bars, and usually took place as the links at the ends of the lap yielded, thus illustrating the bursting nature of the bond action of ribbed reinforcing bars.

At an early stage of the experimental investigation, it was realised that using the results of standard cube tests would not allow the ultimate strength of lapped joints to be calculated with sufficient accuracy. A method was evolved to calculate the stress-strain curve for the concrete in the column, and to extrapolate this relationship to obtain the ultimate strength of the concrete.

The results obtained from the experimental investigation indicate that both the ultimate strength of a short lapped joint confined by links and the net contribution of end bearing to ultimate joint strength vary linearly with concrete compressive strength. Ultimate bond strength was also found to vary linearly with the resistance to splitting of a "push-in" test specimen, and

the quantity and positioning of links is shown to influence ultimate joint strength. Ultimate bond strength was also found to be influenced by the projected rib area/unit length of a bar.

A theoretical analysis of joint strength, based on the Coulomb-Mohr equation of failure, is also presented. The analysis shows that joint strength may be regarded as having two components, one linearly related to the compressive strength of the concrete, the other linearly related to the available resistance to the bursting forces produced by bond and end bearing. Theoretically derived expressions are shown to be in good agreement with experimental results.

The results of the theoretical and experimental investigations are used to formulate design rules for compression lapped joints. A comparison with the requirements of several current codes of practice is made, and it is shown that the requirements of B.S.C.P. 110:1972 may be inadequate in certain cases. It is recommended that increased links be specified at lapped joints.

ACKNOWLEDGEMENTS

The work described was conducted in the Department of Civil Engineering at the University of Glasgow. The author is grateful to Dr. P. D. Arthur, Professor H. B. Sutherland and to the late Professor W. T. Marshall for the facilities, advice and encouragement which they provided, and to the laboratory staff for their interest and assistance. In particular, the help of Messrs. J. Thomson, J. Coleman and A. Galt is gratefully acknowledged.

The author wishes to thank the Associated Portland Cement Co. for the Scholarship which enabled him to undertake the work.

NOTATION

Where applicable, the standard symbols of B.S.C.P.110:1972[9] have been used.

A_r	area of one rib of a ribbed deformed bar projected on a plane perpendicular to the bar axis
A_{sv}	area of one leg of link
c	concrete cover to reinforcement
$E_{c_{500}}$	secant modulus of elasticity of concrete measured at a strain of 500×10^{-6}
F_c	ultimate force available to counteract bursting forces produced by bond or end bearing of reinforcing bar
F_h	bursting force produced in one direction by bond of ribbed deformed bar
F_t	bursting force produced in one direction by end bearing
F_1, F_2	forces exerted on one link by each of a pair of lapped bars
f_c	ultimate compressive strength of concrete in test specimen
f'_c	concrete cylinder compressive strength
f_{c_g}, f_{c_j}	ultimate compressive strength of concrete at height where strains measured, and through lapped joint respectively
f_{c_t}	ultimate tensile strength of concrete
f_{sc_u}, f_{sc_l}	upper and lower limits of ultimate stress developed in compression reinforcement calculated from theoretical analysis
h_r	height of rib above surface of bar core at any point
l_b	length of bar over which bond stresses develop
l_l	lap length

n	no. of turns of wire spiral, or no. of links within lap
s'	clear spacing between pairs of lapped bars
s_t	spacing of ties in computer model
v	velocity of ultrasonic pulse in concrete
v_g, v_j	velocity of ultrasonic pulse at gauge height, and through lapped joint
w	crack width
x	extension
α	inclination of failure wedge and failure cone to bar axis
β	angle of compression cones to bar axis
δ	unit cohesion of concrete
ϵ	strain
ϵ_c	strain in concrete at ultimate compressive stress
ϵ_{ct}	strain in concrete at ultimate tensile stress
θ	angle of internal friction of concrete
λ	ratio of unloaded to loaded area of concrete block
μ	angle
ν	Poisson's ratio
ξ	angle
σ	direct stress
σ_n	normal stress on failure surface below a rib or the end of a bar
σ_q	bearing stress
σ_r	radial stress on bar from failure wedge below rib
σ_t	stress on plane through middle of cone below end of bar

σ_1 , σ_3	major and minor principal stresses
σ_d	standard deviation
τ	shear stress
τ_c	shear strength of concrete
ϕ	diameter of lapped bars
ϕ_c	diameter of wire spiral in push-in tests
γ	ratio = F_1/F_2

Throughout this thesis, all equations are given in S.I. units.

CHAPTER 1

INTRODUCTION

The design of lapped joints between reinforcing bars in compression has received little attention in comparison with the large number of investigations conducted on lapped joints between bars in tension, as it has been assumed that it can be based on the results of tests on tension lapped joints. However, this approach ignores the fact that the bearing of the ends of a reinforcing bar in a compression lapped joint may transfer a substantial proportion of the force in the bar. Compression lapped joints are generally necessary in columns at every floor in a multi-storey structure, and are required to develop the full design strength of the reinforcement, as they cannot be positioned where the stress in the reinforcement is low. Considerable savings might therefore be possible if it could be shown that lap lengths as at present specified by building codes could be reduced with safety.

Research in tension lapped joints has shown the importance of the tensile strength of the concrete forming the cover to the reinforcement in resisting the bursting forces produced by the bond action of ribbed reinforcing bars. The tensile strength of concrete in uniaxial tension is higher than the tensile strength of concrete in biaxial tension-compression, the stress situation which develops round reinforcement in compression lapped joints. This will reduce bond strength in comparison with tension lapped joints.

Only two investigations [1] [2] have been reported in which the contribution of end bearing to the strength of compression lapped joints has been examined. Both investigations were of an exploratory nature, and it was considered that further study of this topic was warranted. The distribution of bond stress within lapped joints was mentioned briefly in both investigations, but no

examination was made of its influence on joint strength. Neither investigation considered the effect of varying the strength of the concrete in the test specimens, and the effect of varying the strength of secondary reinforcement was only considered briefly. It was considered that all the above factors would have a significant influence on the ultimate strength of lapped joints, and should be considered in design. It was also considered advisable to investigate the strength of lapped joints of different lengths in order to formulate design rules, although this variable had been considered in the earlier investigations.

The main section of the experimental programme in the current investigation was conducted on full scale columns. Difficulty was encountered in these tests in evaluating the stress developed in the reinforcement, as using the results of concrete cube compression tests proved to be unsatisfactory. A method was evolved to calculate the stress in the concrete at each load increment from strains measured on the surface of the column, and to extrapolate the stress-strain curve to find the ultimate compressive strength of the concrete. Results calculated by this method compared favourably with the results of a few tests in which strains were measured on the reinforcement. The parameters investigated in the main experimental programme were concrete strength, positioning and strength of links, and the contribution of end bearing. A subsidiary series of 'push-in' tests was also conducted to examine the influence on bond strength of the confining force on a bar, and to compare the bond strength of the two types of ribbed bar used in the main experimental programme.

In previous theoretical investigations of bond strength[3][4][5], it has been assumed that the radial bursting stress produced by the bond action of ribbed reinforcing bars is proportional to the bond

stress around the bar. A theoretical analysis is presented in this thesis, in which it is shown that end bearing strength and bond strength of ribbed bars are made up of two components, one due to the resistance to the bursting forces produced by bond or end bearing, the other related to the compressive strength of the concrete. This theoretical analysis shows good agreement with experimental results.

Expressions derived from the theoretical analysis were used to compare experimental results with the requirements of current codes of practice. This indicated that the provisions of B.S.C.P.110:1972 are inadequate for compression lapped joints, and it is recommended that they be revised to specify that additional confining reinforcement must be provided at the ends of laps in compression lapped joints.

CHAPTER 2

REVIEW OF LITERATURE

2.1. Bond : General

2.1.1. Despite the large amount of research that has been carried out into the bond developed between steel and concrete, few investigators have examined the problem of bond where the reinforcement is in compression. Only two published works, by Pfister and Mattock[1] and by Leonhardt and Teichen[2] deal specifically with the effect of lap length on the strength of lapped joints in reinforced concrete columns. Both Hajnal-Konyi[6] and the 1970 report of the A.C.I. committee on bond[7] mention only research with bars in tension, but an earlier 'State of the Art' report by the same A.C.I.committee[8] did indicate the need for research into compression bond, particularly with large diameter bars.

The scarcity of published work on bond of bars in compression makes it necessary to examine the results of bond tests with bars in tension. However, it has been stated that "a complete bibliography on bond would comprise many hundreds of items,"[6] and the 1970 A.C.I. bond report[7] listed 66 American references. A comprehensive review of all published work on bond is therefore outwith the scope of a thesis of this nature, and so reference will be made only to papers on compression bond and a few major works on tension bond.

2.1.2. B.S.C.P. 110:1972[9] defines two types of bond stress, local bond and anchorage bond. Local, or flexural bond stresses, are caused by a changing force in a continuous bar due to a variation in moment along a member. Anchorage bond stresses develop the force in a bar over the distance between its cut off point, or point of zero stress, and a point at which it is required to carry a certain

load. A lapped joint is a special case of an anchorage, and has been described as "two anchorages back to back" by Roberts and Ho[10].

2.1.3. Roberts[11] has given a good account of the bond action of the three main classes of reinforcing bar available in 1968, plain round bars, square twisted bars, and hot rolled ribbed deformed bars. The main difference between the classes are the amounts of enhancement of bond due to the deformation of the bars, and the various modes of failure. Unless a very large amount of cover or heavy confining reinforcement is provided round a ribbed bar, it will fail by splitting the concrete along the line of the bar. A plain round bar, on the other hand, will pull straight out of the concrete, leaving a smooth hole. The behaviour of a square twisted bar lies somewhere between the other two, with failure often accompanied by an unscrewing of the bar from the concrete.

In America, where only ribbed bars are now used, the A.C.I. committee on bond[8] reporting in 1966, stated that, although bond failure and splitting of the concrete cover are not the same thing, both must be considered together. In the U.K. Hajnal-Konyi[6] has also stressed the importance of the bursting effect where ribbed bars are used. Throughout this review, ribbed bars only are considered, as only they are relevant to the experimental programme reported later in this thesis.

Despite the fact that most of the 'bond' strength of a ribbed bar is due to bearing of the ribs on concrete, the transfer of force between bar and concrete is still referred to as 'bond'. 'Bond stress' is defined as the change in load in a bar divided by the surface area of a plain round bar of equivalent diameter to the deformed bar over which the change in load takes place.

Expressed in mathematical terms,

$$f_{bs} = \frac{\Delta f_{st} \cdot \pi \cdot \phi^2/4}{\Delta l \cdot \pi \cdot \phi} = \frac{\Delta f_{st} \cdot \phi}{4 \cdot \Delta l} \qquad 2.1.$$

where Δf_{st} = change in stress in bar

ϕ = nominal diameter of deformed bar

and Δl = length of bar over which Δf_{st} takes place.

2.2. Anchorage Tests.

2.2.1. In an anchorage test, a reinforcing bar is pulled out of a concrete specimen, load and bar slip usually being recorded. The ultimate bond stress is then obtained from eqtn. 2.1, where Δf_{st} is taken as the maximum stress developed in the bar, and Δl is the length of bar in bond. The simplest form of anchorage test is a straightforward pullout test, as used by Abrams[12] in early studies of bond, in which an axially embedded bar is pulled from a cube or cylinder of concrete. Snowden[13] has examined many variations based on this principle.

In many investigations, heavy binding reinforcement was provided to prevent splitting of the concrete around a bar. Bond stresses of over 20N/mm^2 for a concrete cube strength of 21N/mm^2 were recorded by Snowden[13], while Ferguson[14] reported a bond stress of 2.4N/mm^2 for a similar concrete strength where confining reinforcement was not used. Leonhardt[15] has pointed out that restraint to splitting of pullout specimens may also be provided by the platens of the testing machine. The values of bond stress obtained in tests on specimens with heavy lateral reinforcement provide a measure of the physical properties of a reinforcing bar, but should not be used as the basis of design of structural members, where resistance to splitting will be generally considerably lower.

Results of tests by Mains[16], Bernander[17], and Mathey and

Watstein[18], all showed a similar distribution of bond stress along a bar embedded in a pullout specimen. They found that peak bond stresses occurred initially at the loaded end of a bar, but that the point of maximum bond stress tended to move into the specimen as failure was approached, as indicated in fig. 2.1. Average ultimate bond stress was found to decrease with increasing bond length by all investigators, and Mains concluded that a hook takes only a small proportion of the load on a ribbed bar in a pullout test.

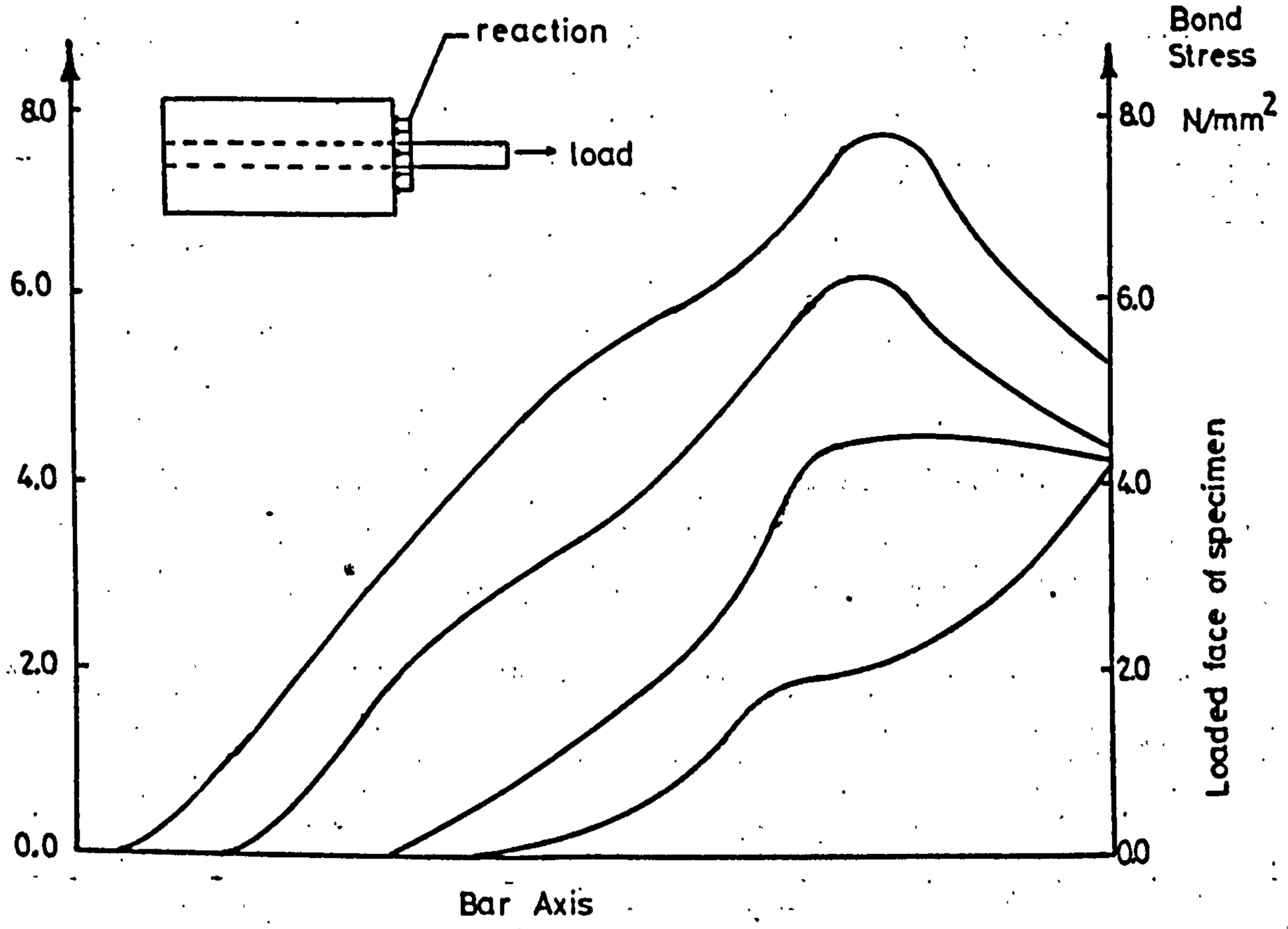

Fig. 2.1 Bond stress distribution in pullout test, from Mains[10].

Ferguson and Thompson, in a series of beam tests[14][19], confirmed that average ultimate bond stress decreases with increasing bond length. A reduction from 5.4 N/mm^2 to 3.5 N/mm^2 was found for an increase in bond length from 16 to 48 bar diameters. In most tests, failure was preceded by splitting of the concrete cover along the reinforcing bar. Additional concrete cover and the

provision of stirrups around a bar were both found to enhance ultimate average bond stress, but bars cast near the top of specimens were found to be weaker. Ferguson and Thompson considered that, for beams without secondary reinforcement, ultimate average bond stress varied with the square root of concrete cylinder compressive strength.

A report of the Dutch organisation for concrete research, the C.U.R.[3], presents the results of 214 tests on eccentric pullout specimens. Sufficient transverse reinforcement to resist the shear on the specimens was provided. The report concluded that the stress developed in a bar varied linearly with the cover ratio c/ϕ, the tensile strength of the concrete as determined by cylinder splitting tests, and, in contrast to the investigations by Ferguson and Thompson, with the bond length of the bar. The results, however, do show a decrease in ultimate average bond strength for longer bond lengths.

Untrauer and Henry[20] investigated the influence of lateral pressure on bond strength, by using a standard pullout test, but with pressure applied to two opposite faces of cubic test specimens. They found that the stress developed by a bar varied with the square root of the lateral pressure, but, as the bars always failed by splitting of the test specimen parallel to the direction of loading, the results were highly dependent on the frictional restraint provided by the steel platens. However, as Hillsdorf, Kupfer and Rusch[21] have shown, the tensile strength of concrete in biaxial tension-compression is lower than the uniaxial tensile strength of concrete, and this must also have affected the resistance to splitting of pullout specimens.

2.2.2. Rehm[22] conducted a study into what he termed "the fundamental law of bond." He used a simple pullout test, with

only a short length of bar, corresponding to rib pitch for deformed bars, allowed in contact with the concrete, the remainder of the bar being debonded. A typical test bar is illustrated in fig.2.2.

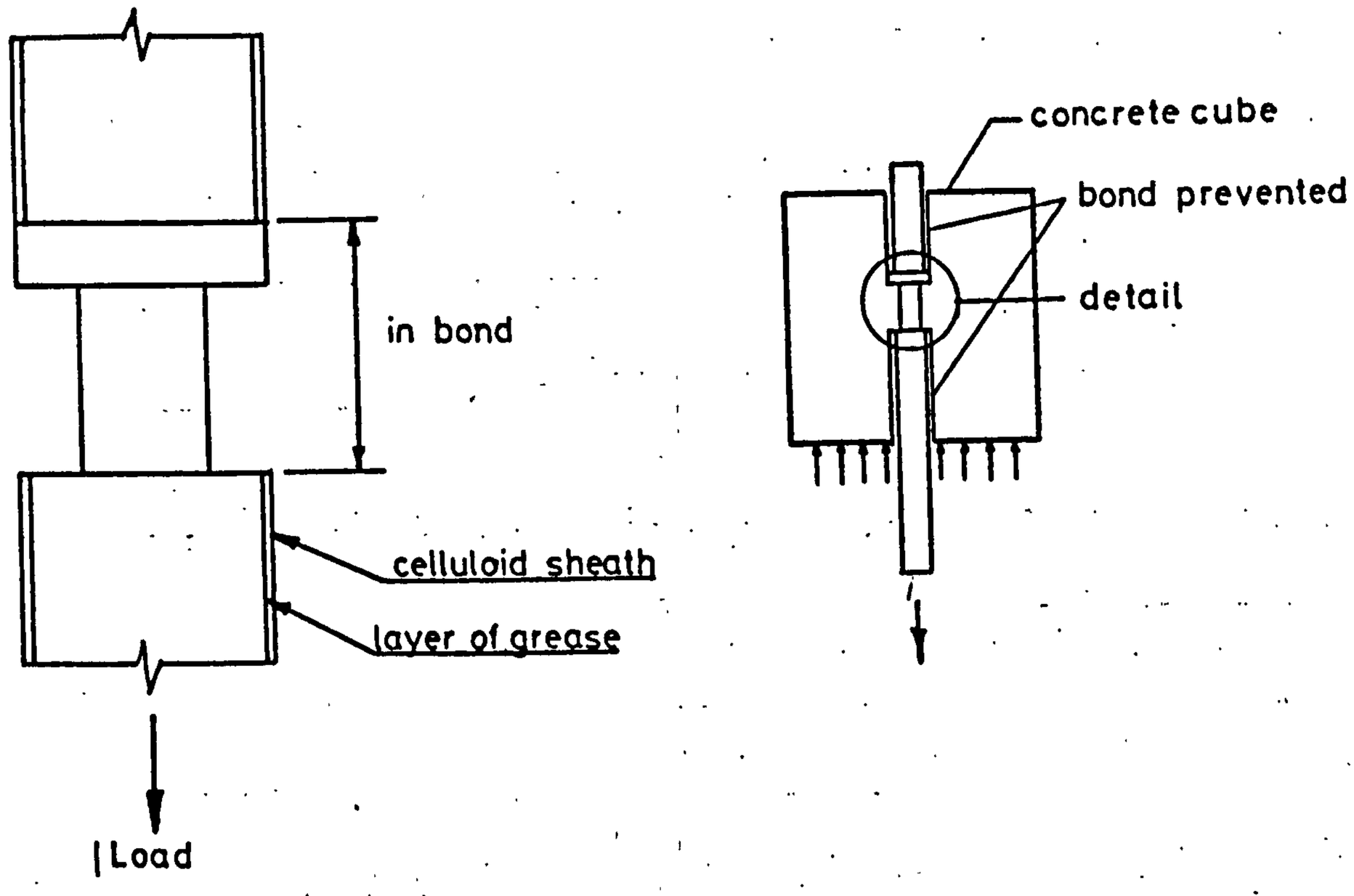

Fig. 2.2. 'Fundamental bond' test specimen.(22)

The low radial stresses set up within the concrete with only one rib acting meant that platen restraint was not significant, but that there was sufficient lateral restraint to prevent the specimen splitting in most cases. Various deformation patterns and rib profiles were investigated, as well as the effect of bar diameter and concrete strength.

Rehm found that the bearing pressure under a rib could be as great as twelve times the cube strength of the concrete, and even higher values were recorded for large values of slip. For the conditions operating in the test, Rehm showed that, if the ratio of the clear distance between ribs to rib height was less than seven,

the bar failed by the concrete shearing across the surface between the tops of the ribs, but that, if the ratio was greater than 10, the concrete first failed below the rib in the direction of the principal shear stress, the subsequent behaviour depending on whether or not the block split. In the first mode, failure started when the value of shear stress over the fracture surface was 0.4 - 0.6 times the cube crushing strength, but the second type of failure started at a lower stress. Rehm states that, in other tests on bars with many ribs, spalling of the concrete revealed wedges of concrete, with a length of 5 - 7 times the rib height, adhering to the ribs.

The cross sectional shape of ribs was found to have little effect on bond-displacement relationships if the angle of the rib face to the bar axis was greater than 45^{o}. At this angle the friction between steel and concrete was sufficient to prevent relative movement, but with lower angle slip could take place on the face of the rib and larger transverse stresses were set up in the concrete. The stress developed by a bar was not found to be affected by the angle between ribs and bar axis, and Rehm concluded that, as long as the projected area of the rib was the same, it was immaterial whether a bar had annular or crescent shaped ribs. In contrast to other investigators, he found that bond strength varied with concrete compressive strength, but it should be borne in mind that these results are based on tests in which failure did not take place by splitting of the test specimen.

Lutz[23] also studied "fundamental" bond, using a different test arrangement from Rehm. He confirmed Rehm's findings with regard to rib face angles, but added that good frictional properties were required to prevent slip between rib face and concrete at all face angles.

Lutz carried out tests on bars with multiple ribs, and found that bars with smaller rib spacings and higher ribs gave better load-displacement relationships, but had only slightly improved *ultimate* bond stresses. His tests showed that lateral reinforcement improved bond strength, the effect increasing with bond length and with bar diameter (cover was not a variable in these tests). Lateral reinforcement was found to have little effect on initial longitudinal crack width and progress, but did appear to inhibit the later stages of cracking, thus increasing bond strength.

2.3. Tension Lapped Joints.

2.3.1. Investigations of many of the factors influencing the strength of tension lapped joints have been made by Ferguson and Breen[24] and by Roberts and Ho[10]. Tepfers[4] has made a particularly comprehensive study of tension lapped joints under static and pulsating loads, and Orangun, Jirsa and Breen[25] have analysed the results of several investigators to produce design rules for tension lapped joints.

2.3.2. The majority of Ferguson and Breen's[24] test specimens did not have confining reinforcement around the lapped joint. However, in those tests where stirrups were provided, an increase in joint strength was obtained, and the failure of the lapped joint was ductile in comparison with the violent failures which took place where stirrups were not used. The authors also noted that stirrups inhibited the formation of diagonal cracks which formed at the end of lapped joints where a bar stopped off near the corner of a beam.

Ferguson and Breen found that no improvement in joint strength was obtained by increasing the length of a lapped joint beyond a certain value. The middle ⅓rd of an 80ϕ lap length apparently played no part in joint strength. It was also observed that,

immediately prior to failure, the splitting cracks that formed longitudinally over lapped bars developed over a smaller proportion of the lap length in the longer lapped joints. The authors concluded that stresses in lapped bars equalized near the ends of long lapped joints, leaving little stress differential, and hence low bond stress, in the middle of the lapped joint.

2.3.3. Roberts and Ho[10] conducted a series of tests on tension lapped joints in which the main variables were lap length, quantity and distribution of links, position of bars as cast, and amount of concrete cover. Only those results applicable to ribbed bars are mentioned here.

Electrical resistance strain gauges were fitted to some bars to examine the variation of steel stress through a lapped joint. The authors found that the distribution of bond stress along a bar was similar for lap lengths of 22ϕ, 33ϕ, and 44ϕ, bond stresses being low in the middle of a lapped joint and high at each end. These findings support the conclusions reached by Ferguson and Breen[24] on bond stress distribution. The results led Roberts and Ho to describe a lapped joint as two anchorages 'back to back' and a comparison of the results of tests on lapped joints with those on pullout specimens showed that a single anchorage could be compared with approximately 40% of the length of a lapped joint.

Electrical resistance strain gauges were also fitted to links in some tests. Roberts and Ho found that, although links contributed little to joint strength until 1.25 times working load, failure was due to yielding of the links at the ends of lapped joints. They also observed that links near the centre of a lapped joint were less highly strained than those near the ends. Heavily ribbed bars were found to produce greater strains in links.

Roberts and Ho found that an increase in concrete cover increased joint strength even where links were present, and recorded an increase in joint strength of 30% for an increase in cover from 1ϕ to 3ϕ. They also found that bars cast near the top of a beam were weaker than those cast near the bottom, due to a combination of settlement of the concrete below the bars whilst still plastic, and a reduction in concrete strength near the top of a beam.

The authors proposed the following expression for the average ultimate bond strength of bottom cast ribbed bars with a cover ratio of unity and a concrete cube strength of $27.5 N/mm^2$.

$$f_{bs} = \left(1.86 + \frac{11.7\phi}{l_l}\right)\left(0.95\ \frac{A_{sv}}{l_l} + 1\right) \qquad 2.2$$

where f_{bs} = average ultimate bond stress.

ϕ = diameter of lapped bars.

l_l = lap length.

and A_{sv} = cross sectional area of one leg of link.

They also recommended that increased links be provided through a lapped joint, and that double links be provided at each end, where bursting forces are greatest.

2.3.4. Tepfers[4] tested over 200 beams with lapped joints under static load, and also conducted a number of tests under fatigue conditions. The tests covered most of the factors which influence the strength of lapped joints.

Tepfers found that the strength of lapped joints without secondary reinforcement increased with the square root of the cube compressive strength of the concrete up to a cube strength of about $40 N/mm^2$, but that at higher concrete strengths the rate of increase was slower, and that at concrete strengths greater than $70 N/mm^2$, joint strength began to decrease with increasing concrete strength. Tepfers considered that the decrease was due to the lower ductility and creep

of high strength concretes, which caused bond stresses to be less uniformly distributed at ultimate load, and hence caused failure at a lower average bond stress.

Tepfers' results showed that increases in concrete cover to the reinforcement produced increases in joint strength similar to those found by Roberts and Ho[10], and that small diameter bars developed higher bond stresses than large diameter for the same cover ratio. Ultimate average bond stress was found to decrease with increasing lap lengths. Although more heavily ribbed bars were found to develop higher bond stresses, the increase in strength was not proportional to the increase in rib area/unit length of bar, and bars with inclined crescent shaped ribs were found to develop the same bond stresses as less heavily ribbed bars with annular ribs.

The influence of secondary reinforcement on joint strength was also investigated. Tepfers found that links improved joint strength, and that the rate of improvement was greater for larger amounts of confining reinforcement, indicating that links tend to take over from concrete in resisting bursting force. However, spirals were found to be more effective than links in confining reinforcing bars, but the presence of spirals did not affect the distribution of bond stress within the lapped joint.

2.3.5. Orangun, Jirsa and Breen[25] compiled the results of several investigations into the strength of lapped joints in tension, and used a non-linear regression analysis to develop an expression for the strength of lapped joints of ribbed deformed bars in tension.

The authors assumed that the component of joint strength due to the presence of secondary reinforcement was additional to the strength of a similar lapped joint without secondary reinforcement. As the ultimate tensile strain of concrete is low, secondary reinforcement

cannot contribute significantly to joint strength until the concrete cover cracks, and the confining force of the concrete itself is lost. However, the B.S.C.P. 110: 1972[9] method for the design of reinforced concrete members in shear is now based on a similar assumption, and there is no reason to believe that the expression derived by Orangun et al is unsuitable.

The expression for the ultimate average bond stress of ribbed deformed reinforcing bars which they derived is as follows:-

$$f_{bs} = \left[0{\cdot}11 + \frac{0{\cdot}28c}{\phi} + \frac{4{\cdot}7\phi}{l_l} + \frac{0{\cdot}027A_{sv}.f_{yv}}{s_v.\phi}\right].\sqrt{f_{cu}} \qquad 2.3.$$

where c = concrete cover to reinforcement

ϕ = diameter of lapped bars

l_l = length of lapped joint

A_{sv} = cross sectional area of stirrups per pair of lapped bars

f_{yv} = yield strength of stirrups

s_v = spacing of stirrups

and f_{cu} = concrete cube strength

2.4. Compression Lapped Joints

2.4.1. A study of column strength, conducted by Richart and Brown[26], provides the earliest record of tests on columns with lapped joints in main reinforcement. Plain untwisted square bars with lap lengths of 20 and 30 bar diameters were used, but the joints were close to the top and bottom of the columns, and well confined by secondary reinforcement. Plowman[27] carried out tests in which plain round mild steel bars were lapped, and found evidence that part of the load in the reinforcement was transmitted by the bearing of the end of the bar on the concrete. Somerville and Taylor[28] examined the effects of joggling bars at a lapped joint, and Pfister and Mattock[1] investigated the effect of lap length and type of confining reinforcement

on joint strength. Leonhardt and Teichen[2] have also conducted tests on columns with lapped joints, to investigate spalling of concrete cover due to end bearing of reinforcement.

2.4.2 Plowman[27] carried out tests on two columns in which plain round bars were lap jointed, with one set of bars joggled. 16mm dia. main bars and 4.7mm dia. links were used. No details of lap length, link spacing or concrete strength are given. Strain readings on the bars within the lap were obtained by welding studs, which projected through the concrete cover, to the bars, and using a 2" Demec demountable mechanical strain gauge to measure strains. A disadvantage of this method is that measurements are taken on one side of a bar only, and so misleading results may be obtained if the load on the bar is not purely axial. However, Plowman's results do indicate a bearing stress of 50 - 100 N/mm^2 on the ends of the joggled bars, with lower stresses recorded at the ends of the other bars. This difference is consistent with Ferguson and Breen's[24] findings that inside bars are better confined than outside bars.

2.4.3 Somerville and Taylor[28] tested 5 columns in which main reinforcement was joggled, 3 columns also having lapped joints. Two lap lengths of 27.5 ϕ and 34.4 ϕ were used, and concrete strength was approximately 60 N/mm^2. In each case the columns were considered to have performed satisfactorily, and the authors concluded that the detailing of secondary reinforcement around joggled bars was not a problem. However, cracking and spalling of the concrete just outwith the lap was noted prior to failure which Somerville and Taylor took to indicate that load was being transferred by the ends of the bars to the concrete. Ferguson and Breen[24], however, also noticed cracking in a similar position in tension splices, where end bearing cannot occur.

Somerville, Morris and Clements[29] in tests on the P. B. column-column joint, where large bars were used, noted that tensile stresses were set up in the concrete, causing spalling and premature failure. They concluded that this was due to the end bearing of the bars.

2.4.4. Pfister and Mattock[1] tested a total of 15 specimens, 7 of which were spirally bound columns of circular cross section, the remainder being tied columns of rectangular cross section. All specimens were 1830mm high, with a maximum slenderness ratio of 7.2. Six 25mm diameter ribbed bars, giving a steel percentage outwith the joint of approximately 4.1%, were used in all columns. Secondary reinforcement was a spiral of 6mm diameter bars at 38mm pitch in the case of circular columns, and ties consisting of 6mm diameter bars at 250mm pitch, which were not positioned relative to the lap, were provided in the rectangular columns. All steel had a yield strength of at least 400N/mm^2, and the average concrete strength was 26N/mm^2. Lap lengths were varied from zero to thirty bar diameters, and one column of each type was tested without joints. The circular columns were cast vertically, and the rectangular columns horizontally.

Electrical resistance strain gauges were used to determine steel strains away from the lap in the rectangular tied columns, but the load carried by the main reinforcement in the circular columns was estimated by comparison with a test in which reinforcement was not jointed. Steel strains had been measured with electrical resistance strain gauges on an unjointed column, and it was assumed that steel strains away from the lap in a column with main reinforcement jointed would be equal to these measured in the unjointed column when both columns were subjected to the same load. This method ignores the effect of a variation in concrete strength, and will overestimate steel stresses once relative movement between steel and concrete

takes place. As a result of this procedure their results may be unreliable in the case of short laps, where slipping was found to start at a lower percentage of ultimate load.

Pfister and Mattock interpreted their results as showing that ultimate joint strength was composed of two parts, a constant average bond stress of 2.55N/mm^2 for both types of column, and an end bearing stress of 130N/mm^2 and 80N/mm^2 for spirally reinforced columns and tied columns respectively. Their findings contradict the results of studies on pullout and tension splice tests, however, where ultimate bond stress has been found to decrease with increasing bond length.

Two tests, in which the main reinforcement was heat treated to produce a steel with a higher limit of proportionality but lower yield strength, gave average bond stresses substantially higher than those achieved with untreated bars for lap lengths of 20 and 30 bar diameters.

Leonhardt and Teichen[2] conducted a series of tests on circular columns reinforced with four pairs of lapped bars. The main reinforcement consisted of 26mm diameter ribbed cold twisted bars confined by 5mm diameter links of plain round bar, at a spacing of 200mm. Lap lengths of 9 ϕ to 37.5 ϕ were investigated, and a concrete cube compression strength of approximately 40N/mm^2 was used throughout the experimental programme, even though columns with lap lengths of 25 ϕ or more developed their full design strength. Strains measured on reinforcing bars indicated that end bearing stresses of up to 120N/mm^2 were achieved, but that end bearing stresses decreased as ultimate load was approached. They concluded that the high end bearing stresses were due to the strains in the lapped bars trying to equalise as close to the ends of the lapped joint as possible, and that this could not be combated by increasing lap lengths. An

increase in concrete cover to the reinforcement was found to produce only a small increase in joint strength, and it was not considered practicable to increase cover beyond the maximum of 39mm investigated. Leonhardt and Teichen therefore concluded that increased links should be provided at both ends of lapped joints, as shown in fig. 2.3. They did find, however, that spalling was less severe in the case of smaller diameter bars, and recommended that extra links need not be provided for bars of 14mm diameter or less.

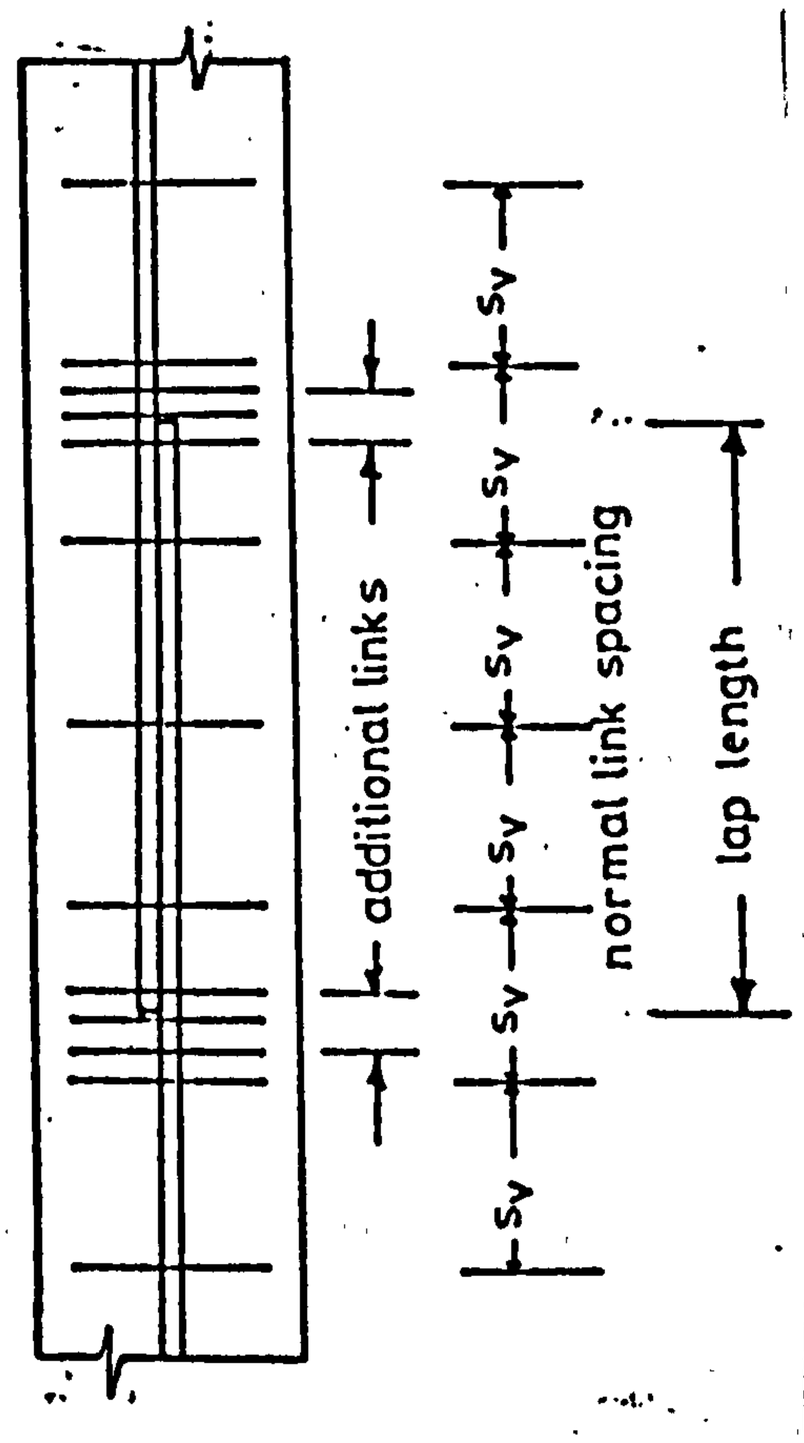

Fig. 2.3 Recommended detailing of secondary reinforcement around compression lapped joints of large diameter reinforcing bars, from Leonhardt and Teichen[2].

In one test, Leonhardt and Teichen eliminated end bearing of the reinforcement, which resulted in a considerable drop in column strength. They found that there was very little increase in joint strength where

the ends of bars were cut square with a saw rather than shear cut, but there did appear to be an improvement in joint strength where lapped joints were staggered longitudinally.

The tensile strength of concrete in biaxial tension-compression may be considerably weaker than the strength of concrete in uniaxial tension.[21] It is therefore considered likely that, as found by Leonhardt and Teichen, the influence of concrete cover on joint strength will be lower in the case of compression lapped joints than in the case of tension lapped joints.

2.5. End Bearing

2.5.1. As has been shown by Leonhardt and Teichen[2], and by Pfister and Mattock[1], the bearing of the end of a reinforcing bar on concrete can transfer a substantial proportion of the total load developed by a bar in a compression lapped joint. Tests on the bearing capacity of concrete, such as those by Hawkins[30] and Hyland and Chen[31], involve a similar stress situation.

2.5.2. Hawkins[30] lists the main conclusions reached in several investigations as follows.

1) failure takes place by the pushing out of a cone of concrete beneath the loaded area.
2) the radial pressures exerted by the cone split the block.
3) the ratio of ultimate bearing strength to concrete compressive strength increases with the ratio, λ , of the loaded to the unloaded area of the block, but the rate of increase is slow for large values of λ .
4) the ratio of ultimate bearing pressure to concrete compressive strength is independent of the depth of the block, provided that the block is deep enough to ensure that the formation of the failure cone is not restricted.

Zielinski and Rowe[32] also produced evidence that embedded and external anchorages in end zones of prestressed concrete members produce similar stress distributions and ultimate loads.

Hawkins also carried out a large number of tests on concentrically and edge loaded concrete blocks, in which the principal variables were concrete strength, ratio of loaded to unloaded area, and size of test specimens. He derived an approximate theoretical analysis, based on a failure criterion suggested by Cowan[33], to estimate the bearing strength of concrete blocks, and obtained the following expression -

$$\frac{\sigma_q}{f_{cu}} = 1 + \frac{K}{\sqrt{f_{cu}}}\left(\sqrt{\lambda} - 1\right) \qquad 2.4$$

where σ_q = ultimate bearing stress

f_{cu} = concrete cube strength

λ = ratio of unloaded area to loaded area

and K = constant depending on the relationship between the tensile and compressive strengths of the concrete, and the angle of internal friction of the concrete, and is usually taken to be 4.1.

Equation 2.4 was found to predict concrete bearing strength satisfactorily for values of λ less than 40.

2.5.3. Hyland and Chen[31] have also investigated the bearing strength of concrete blocks resting on steel or on P.T.F.E. to reduce the effect of platen restraint, or with blocks loaded through punches top and bottom. The punches were 38mm or 51mm in diameter, bearing on cylinders of 152mm diameter, the concrete strength being approximately $40N/mm^2$.

Cones were found to form beneath the punch in all but 51mm high specimens loaded through a 51mm diameter punch, in which cases .

a column of concrete was formed. The authors noted that, although there were differences in strain distribution for the different conditions of test, the ultimate bearing strength of the blocks was not influenced.

Hyland and Chen found that values for the bearing strength of concrete obtained from an expression developed by Chen and Drucker[34] from the theory of perfect plasticity did not show good agreement with their experimental results. Chen and Druckers expression overestimated the effect of specimen height, and Chen and Hyland concluded that complete plasticity could not be considered to develop in specimens where the ratio of punch diameter to specimen height was less than 0.5, or where the ratio of punch diameter to specimen diameter was less than 0.25.

The following points emerge from a review of the above investigations.

1) In a compression lapped joint, transfer of force is achieved by bearing of the ribs of deformed bars and bearing of the end of the bars on the concrete. Both bond and end bearing set up tensile stresses in the concrete cover to the reinforcement, and tend to cause splitting of the cover.

2) Large diameter bars appear to produce the most severe bursting forces.

3) A lap length of 25 ϕ appears to be sufficient to develop the ultimate strength of a deformed bar for a concrete compression strength of 30N/mm^2.

4) No research has been conducted on the influence of concrete strength on the strength of lapped joints in compression.

5) The influence of concrete cover is less significant in compression lapped joints than in tension lapped joints. The influence of secondary reinforcement is therefore likely to be greater.

6) Joggling of lapped bars does not appear to introduce any additional problems.

2.6 Current Codes of Practice

The lap lengths required according to the current British[9], German[35], and American[36], codes of practice and by the Recommendations of the C.E.B.[37], in order to develop the design ultimate stress of compression reinforcement with a characteristic yield strength of 410 N/mm^2 are shown in table 2.1. In addition to these requirements, the British and American codes specify minimum lap lengths of 20ϕ + 150mm and 30ϕ respectively. Although partial safety factors and factors of safety differ in each code, and B.S.C.P.110:1972 assumes a lower ultimate stress for compression reinforcement than the other codes, the design strength of short columns is approximately the same for all codes, and the values presented in table give a true comparison.

All the codes allow a proportional reduction in lap length where less than the design ultimate stress in a bar is required to be developed, subject to a minimum lap length in the range 10ϕ - 12ϕ in all codes except B.S.C.P.110:1972. In B.S.C.P.110 the minimum value of 20ϕ + 150mm still holds.

TABLE 2.1 COMPRESSION LAP LENGTH REQUIREMENTS OF SOME CURRENT CODES OF PRACTICE.

	Lap Length Factor l_l/ϕ Required lap length in terms of diameter of lapped bar.			
Concrete strength N/mm^2	20	30	40	50
Great Britain-B.S.C.P.110:1972[9]	28	22	19	19
U.S.A.- A.C.I. 318-71[36]	26	21	18	16
Germany - D I N 1045:1972[35]	31	25	21	18
C.E.B.Recommendation 1970[37]	39	30	24	21

The design ultimate average bond strength of deformed bars varies approximately with the square root of the concrete strength in all the codes, this having been found to give good agreement with the results of tests where lateral reinforcement was not used. None of the codes allows an increase in bond strength for an increase in concrete cover above the minimum, which is one bar diameter in all cases, except where conditions of exposure demand more. The German code, D I N 1045, and the C.E.B. Recommendations specify that the design ultimate bond stress should be reduced by 50% where reinforcement inclined at less than 45° to the vertical is in the top half of the section as cast, and the American code specifies a 30% reduction where bars are more than 305mm above the bottom of the section.

The C.E.B. Recommendations allow compression bars to be lap jointed at the same position in the length of a member, but the German code specifies that lapped joints must be staggered longitudinally within the member when the percentage of compression reinforcement in the cross section is greater than 3%. The American code allows a maximum of 8% reinforcement at any cross section, while B.S.C.P.110:1972 allows a maximum of 10% at lapped joints.

B.S.C.P.110:1972 is the only code of practice examined which does not recognise the bursting effects of the anchorage of deformed reinforcing bars by specifying additional links, or allowing a reduced lap length for additional links. The German code requires at least 3 transverse bars with a minimum diameter of 0.4 times the main bar diameter to be provided over 0.3 times the lap length at each end of a lapped joint, with a maximum spacing of bars of 4 times the diameter of the main reinforcement, and the C.E.B. Recommendations require transverse reinforcement designed on the lattice analogy to be provided to carry the tangential

forces set up between a pair of lapped bars. The American code allows a reduction of 17% in lap length where links are provided with an effective area of 0.0015 $h.s_v$, where h = overall thickness of member and s_v = spacing of links.

CHAPTER 3

THEORETICAL STUDY OF THE STRENGTH OF LAPPED JOINTS.

3.1. Review of Theoretical Work on Bond Strength

A large number of tests have established that bond failure of lapped joints with ribbed bars takes place by the splitting of the concrete cover along the line of the bars. The bond action of ribbed bars must therefore set up tensile stress in the concrete.

Where force is transferred between bar and concrete, shear stresses parallel to the bar axis will be set up. Compressive and tensile stresses must therefore also be set up. This is shown diagrammatically in fig. 3.1. Since the elastic modulus of concrete is the same in tension and compression, the imaginary 'struts' and 'ties' shown in fig. 3.1 will act at an angle of 45^{o} to the bar axis.

At low bond stress, the forces in struts and ties balance, but as bond stress increases, the deformability of the concrete causes compression struts to be concentrated close to the bearing area of the rib, as shown in fig. 3.2. Elsewhere, a small amount of slip is sufficient to destroy adhesion between bar and concrete, and the tension ties tend to cause separation of the concrete from the bar. The struts, or more correctly, cones of compression, are then balanced by a ring tension in the concrete around the bar, as shown in fig.3.3. A crack forms once the tensile capacity of the weakest part of the concrete ring is exceeded.

Goto[38] has published photographs of cracks formed when a ribbed bar axially embedded in a long concrete cylinder was pulled at both ends. Two different types of cracks were observed, as illustrated in fig. 3.4. The primary cracks, perpendicular to the bar axis and visible externally, are similar to those observed in

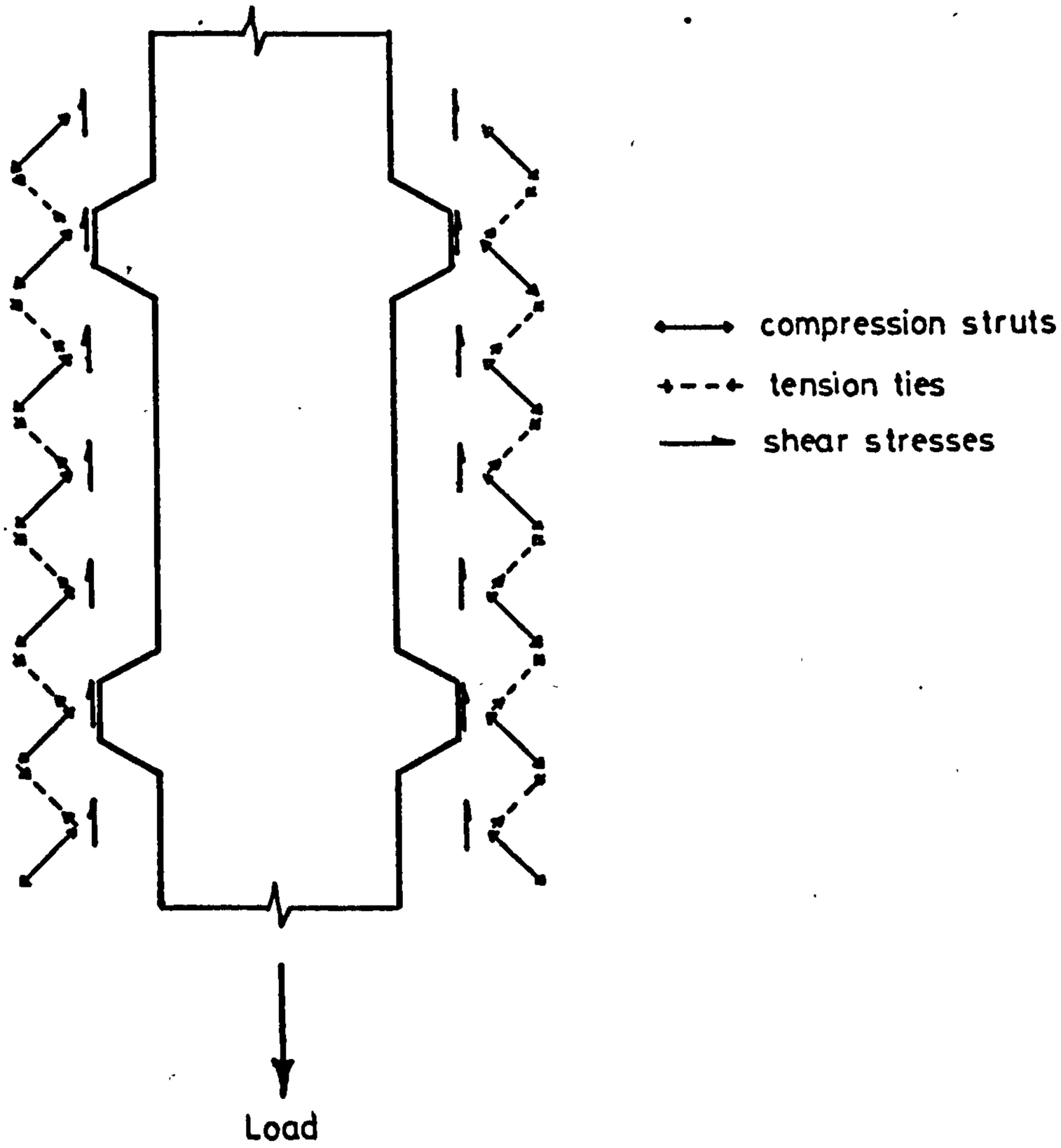

Fig. 3.1 Compression struts and ties around ribbed deformed bar in bond - low bond stress.

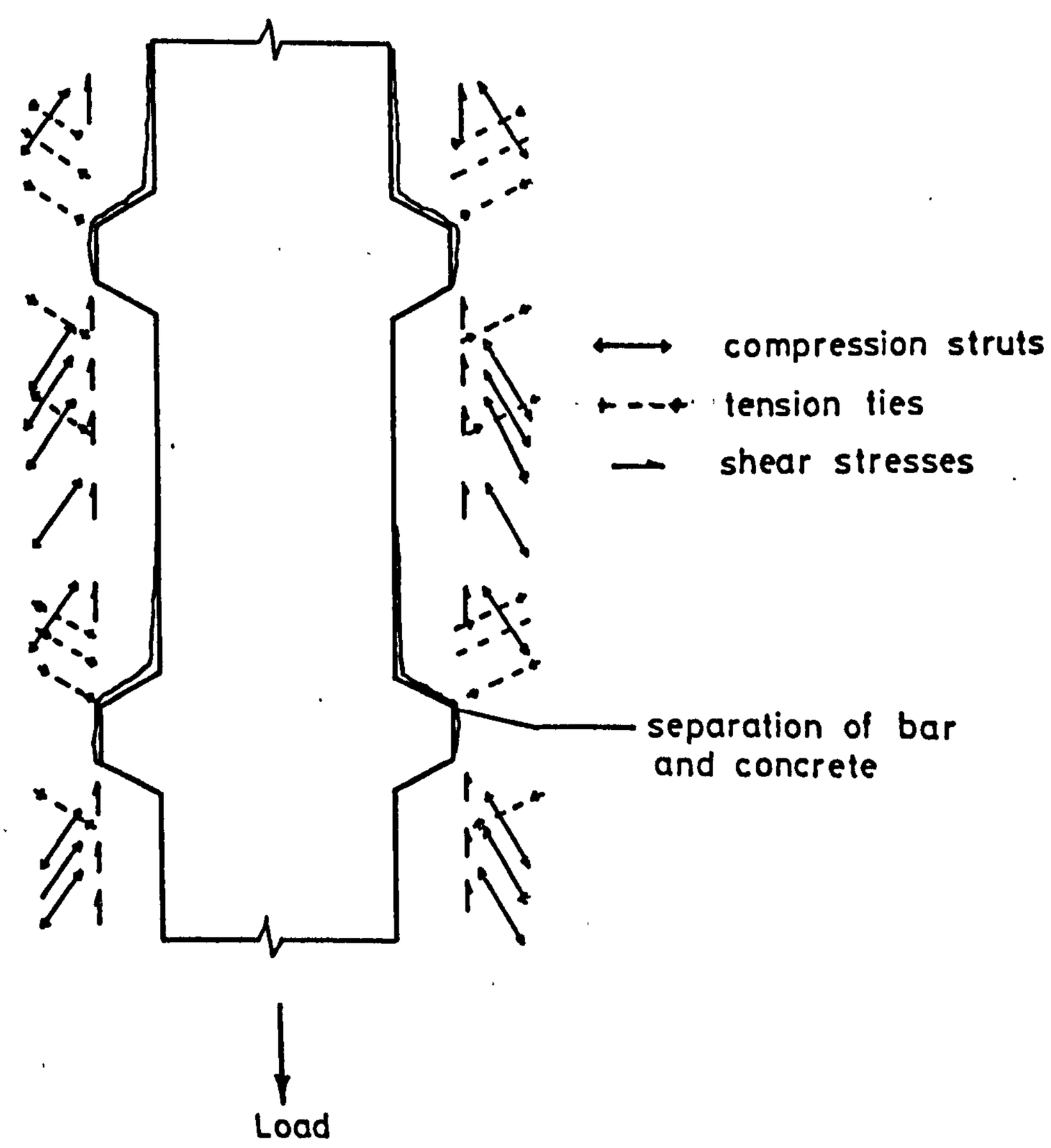

Fig. 3.2 Compression struts and ties around ribbed deformed bar in bond - high bond stress.

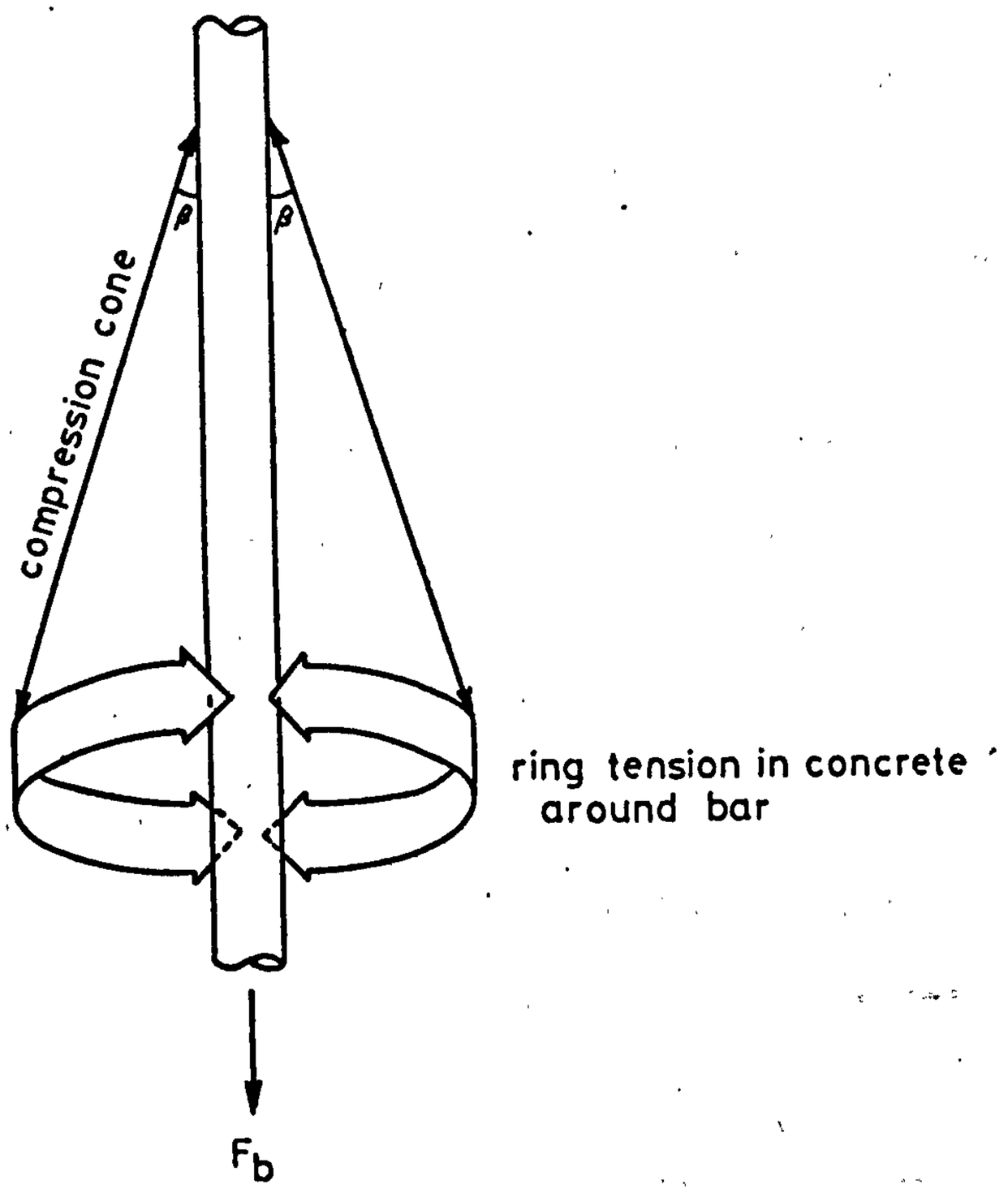

Fig. 3.3 Ring tension around bar to resist radial bursting forces.

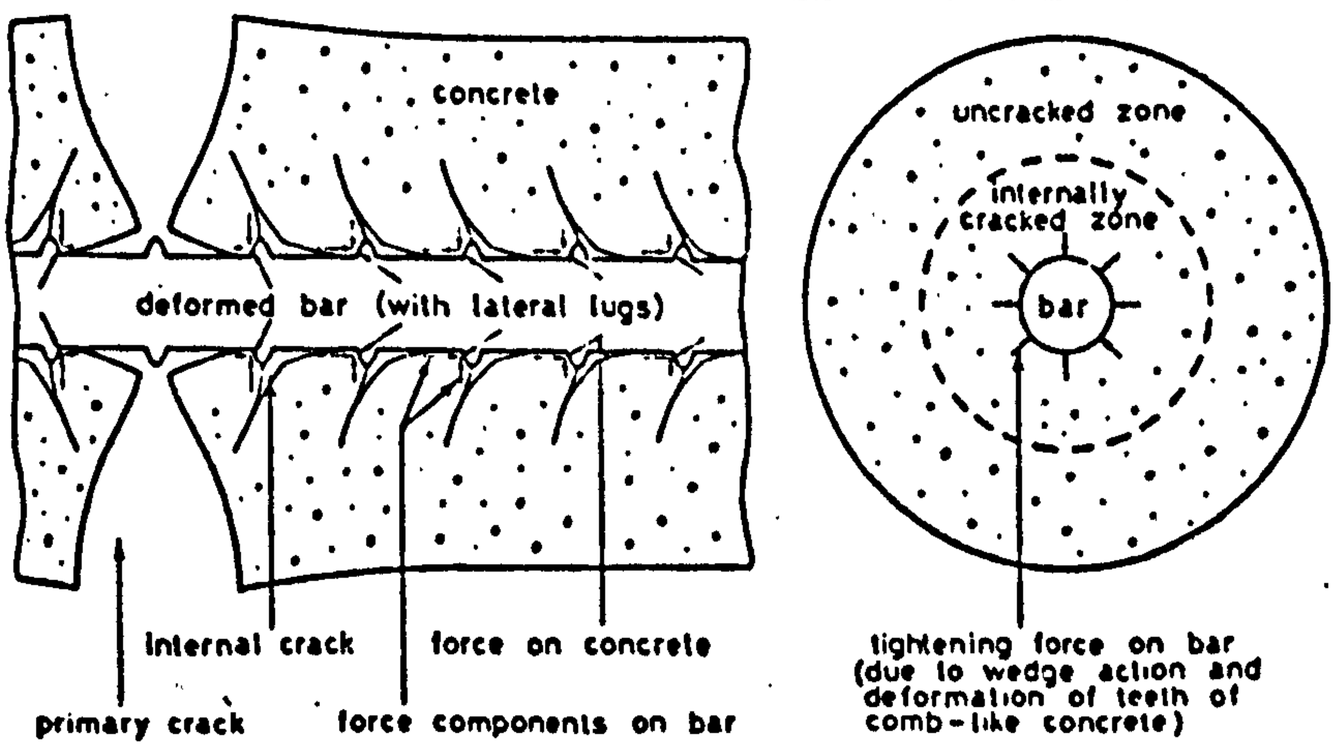

Fig. 3.4 Deformation of concrete around steel reinforcing bar after formation of internal cracks (schematic diagram) by Goto[38]

tests with plain round bars, but the internal cracks, inclined at between 45° and 80° to the bar axis, appear only where ribbed bars are used. The separation of bar and concrete at points distant from the bearing side of the ribs may also be seen in fig. 3.4.

The formation of the internal cracks is due to the principal tensile stress exceeding the tensile strength of the concrete, and so, as major and minor principal stresses are perpendicular to each other, the cracks form parallel to the direction of the principal compressive stress. The angle the compression cones make with the bar axis may therefore be deduced. The steepest internal cracks form midway between primary cracks, as the direction of the principal stresses is influenced by the direct tension carried by the concrete. Near primary cracks, where the direct tension in the concrete is lower, the internal cracks are inclined at approximately 45° to the bar axis. This value indicates that bond stresses produce a radial bursting stress at any point of the same value as the bond stress at that point.

While Goto's results provide confirmation of the concept of compression cones balanced by a ring tension, the inclination of the compression cones deduced from his photographs may not be applicable in other situations, for instance where the concrete around the bars is in compression rather than tension.

3.2. Theoretical studies of the ultimate bond strength of ribbed deformed bars where failure is accompanied by splitting of the concrete cover to the reinforcement have been made by the C.U.R.[3], Ferguson and Krishnaswamy[5], and Tepfers[4], the latter two for the case of lapped joints. Tepfers also considered lapped joints with secondary reinforcement.

3.2.1. The earliest attempt at a theoretical analysis of the factors involved in bond strength was published in a report of

the C.U.R.[3]. An expression was derived by equating the bursting force produced by one rib of a deformed bar to the resistance to splitting of the concrete cover. As indicated in fig. 3.5a the concrete was assumed to behave plastically in tension. Bond strength was calculated by assuming the longitudinal force σ_v , shown in fig. 3.5b, to be proportional to the radial force σ_r , reducing the load carried by each rib to an equivalent bond stress over the bar surface, and adding the effect of the shear stress between the ribs to give the following expression.

$$f_{bs} = \left(A.\, f_{ct} + B\right) + C\,\frac{c}{\phi}\cdot f_{ct} \qquad 3.1$$

where f_{bs} = ultimate bond strength,

A, B and C are experimentally derived constants for each bar.

f_{ct} = ultimate tensile strength of concrete

c = concrete cover

ϕ = diameter of reinforcing bar.

The expression in brackets in equation 3.1 refers to the shear stress between the ribs of a deformed bar, the remainder of the right hand side of the equation being the component of bond strength due to the bearing of the ribs.

Values of the constants A, B and C were determined experimentally for four types of deformed reinforcing bars. However, the results indicated that most of the bond strength of ribbed bars was due to the shear stress between the ribs, and that little load was carried by the ribs. This is unlikely to be correct, as radial cracks formed around the reinforcing bars prior to failure, indicating that there were large tensile strains in the concrete around the bars. There would therefore be little contact between bar and concrete except at the ribs.

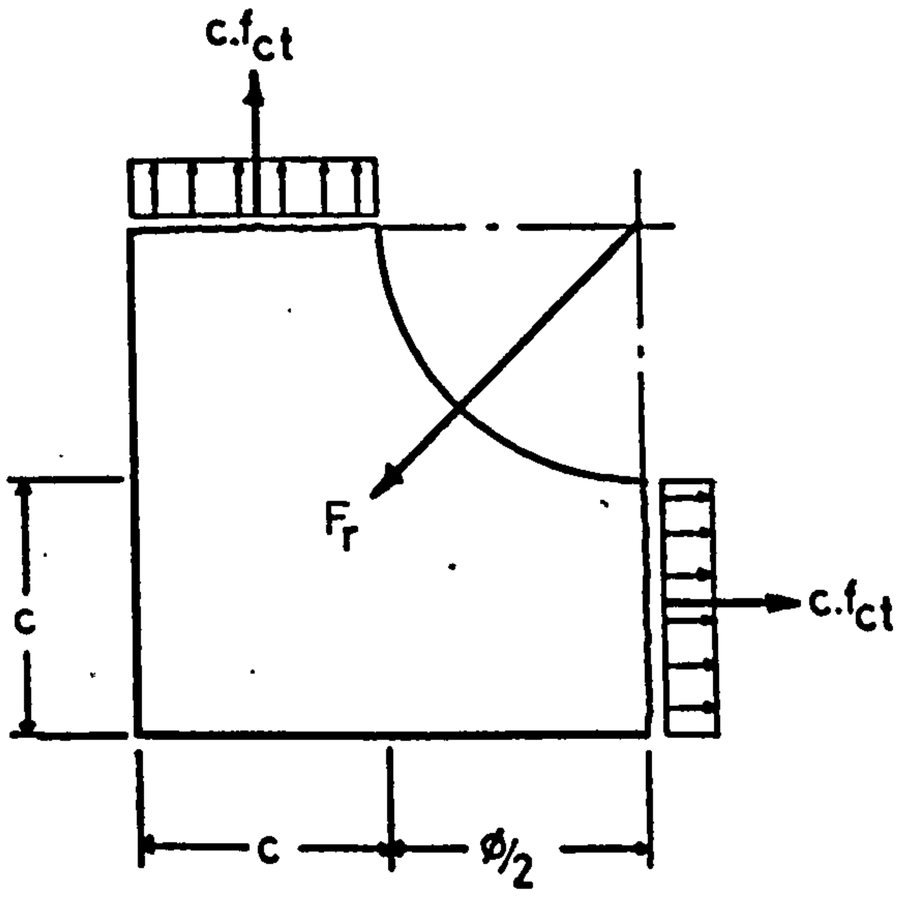

a) corner of pullout specimen

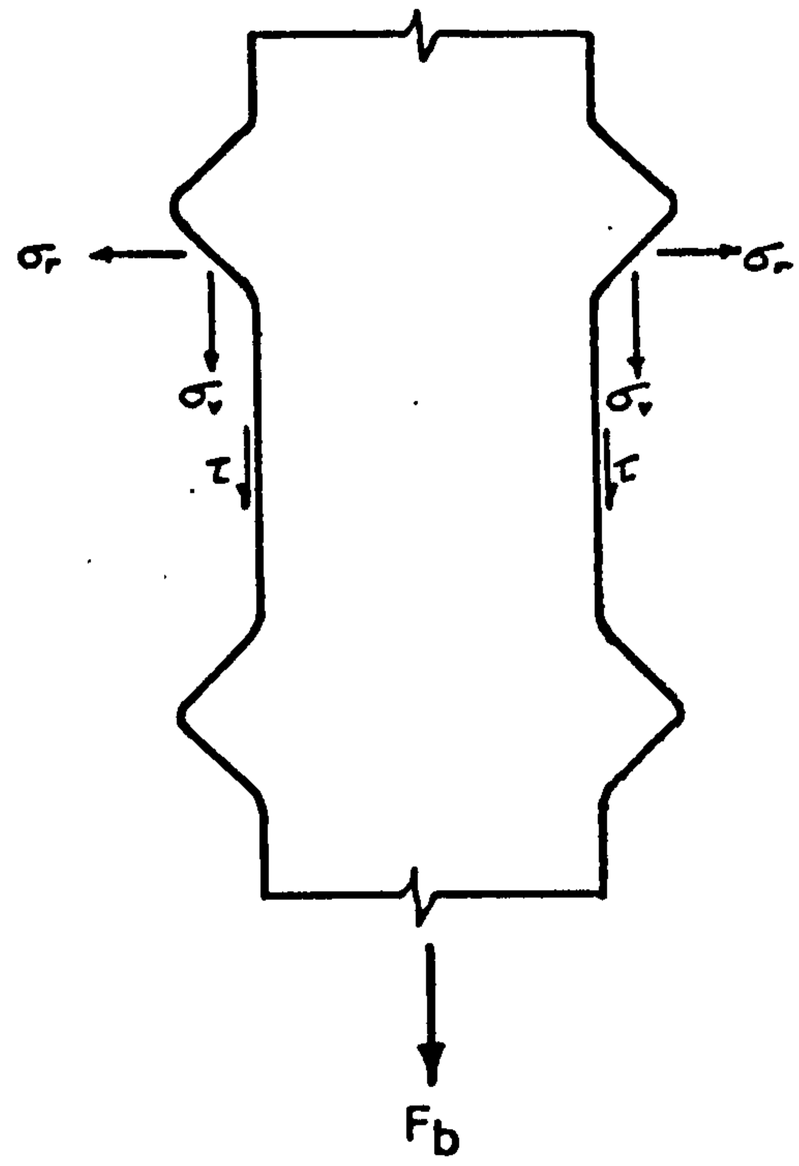

b) Forces exerted by bar

Fig. 3.5 Forces on bar in corner of pullout specimen, from report of C.U.R.[3]

3.2.2 Ferguson and Krishnaswamy[5] identified three patterns of splitting in lapped joints in beams, as shown in fig. 3.6, and used a semi-empirical analysis to relate ultimate average bond strength to cover and spacing of pairs of lapped bars.

Ferguson and Krishnaswamy found that a clear relationship existed between the ratio of clear distance between bars to vertical cover, $s'/_c$, and the failure patterns shown in fig. 3.6, which developed. The 'side split' failure pattern occurred only at ratios lower than1.75, and V type failures were observed only at $s'/_c$ ratios greater than 7.5 No failures were recorded in which only the corner of the beam spalled.

In analysing the load capacity of a lapped joint, Ferguson and Krishnaswamy assumed each bar to have a radial stress component equal in magnitude to the uniform average bond stress along the bar, and equated the bursting force exerted by the bar to the splitting

resistance on a plane through the bar axis, calculated on the assumption that the ultimate tensile strength of the concrete was reached simultaneously at all points on the plane. The ratio of $\frac{\text{resisting force}}{\text{splitting force}}$ was plotted against s'/c and a lower bound obtained. This gave the following expression for the lap length required to develop a stress of 410 N/mm^2 in the reinforcement.

$$l_l = \sqrt{\frac{26{\cdot}5}{f_{cu}}} \cdot 1960\,\phi^2\left(\frac{1}{s'} + \frac{1}{2c}\right) \qquad 3.2$$

where l_l = required lap length

f_{cu} = concrete cube compressive strength

ϕ = diameter of reinforcing bar

s' = clear spacing between bars

and c = vertical concrete cover, as shown in fig. 3.6.

Fig. 3.6 Splitting around splices from Ferguson and Krishnaswamy[5].

3.2.3. Tepfers[4] derived expressions for the bond strength of single bars embedded in cylinders of concrete, and for six failure patterns found in tests on lapped joints in beams. The influence of secondary reinforcement was also considered.

Tepfers analysed the resistance to splitting of thick concrete rings loaded internally by a uniform radial pressure, for the cases of the concrete acting elastically and plastically, and showed that, if the concrete is considered to behave elastically, radial cracks might develop within the concrete ring before its ultimate strength was reached, and it then split completely. However, despite having stated that concrete is unlikely to be sufficiently plastic to allow its ultimate tensile strength to be reached simultaneously everywhere in the ring, Tepfers based his analysis of the strength of lapped joints in beams on that assumption.

In tests on lapped joints confined by secondary reinforcement, it was found that longitudinal cracks appeared over the bars in one face of the beams prior to failure, as shown in fig.3.7. The stress in the reinforcement crossing cracks was determined by taking moments about the point of contact of the two main bars. It was assumed that, where cracks did not appear on the surface of a beam, as in the horizontal beam face in fig. 3.7, the maximum strain in the secondary reinforcement was limited to the ultimate tensile strain of the concrete, taken to be 150×10^{-6}. This last assumption is inconsistent with Tepfers demonstration that cracks can exist in the concrete cover without reaching the surface, and is contradicted by Roberts and Ho's[10] tests, where strains considerably greater than that assumed by Tepfers were recorded on both legs of links prior to ultimate load. The assumption also means that, for lower values of concrete strength and vertical cover c_y, failure was considered to

take place prior to yielding of the secondary reinforcement.

Both Ferguson and Krishnaswamy[5] and Tepfers[4] considered that the bursting forces produced by the bond action of a ribbed bar could be represented by a uniform radial stress equal in magnitude to the bond stress around the surface of an equivalent plain round bar. However Tepfers has shown that, once internal cracks have formed, the magnitude of the radial stress may drop by 30%.

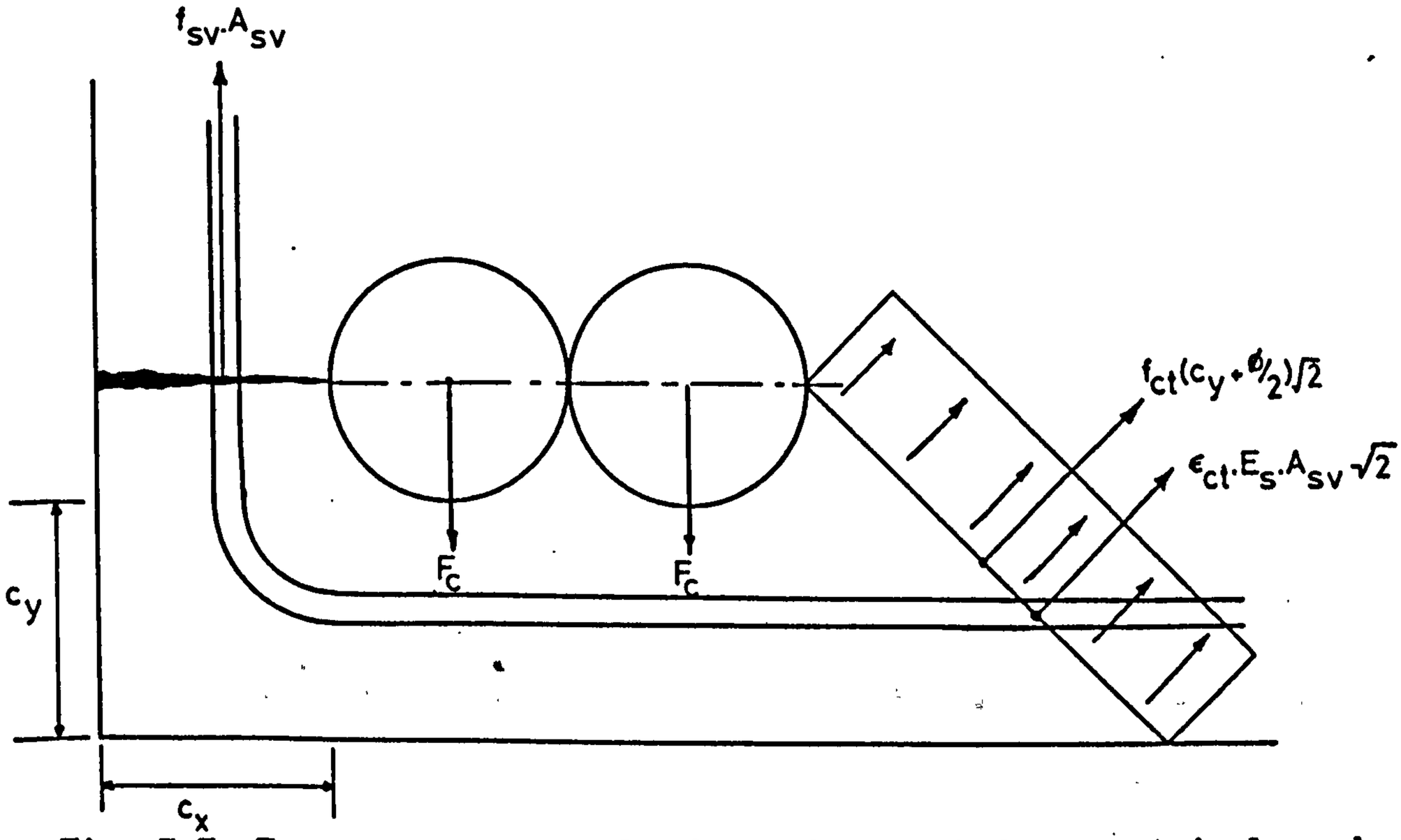

Fig. 3.7 Forces on corner of a beam where reinforcement is lapped after Tepfers[4].

Tepfers made a two dimensional finite element analysis of the interface of a ribbed bar and concrete to investigate the distribution of force from the ribs. He found that, at low bond stresses, where there is still adhesion between bar and concrete at all points on the bar surface, the direction of the maximum shear stress is parallel to the bar axis, and shear stresses are fairly uniform over the rib spacing, as shown in fig. 3.8(a). However, once adhesion is broken, and there is contact only on the bearing surface of the ribs, the direction of the maximum shear stress varies considerably, and the

peak value of shear stress, situated at the bearing surface of the rib, rises to double the average, as shown in fig. 3.8(b).

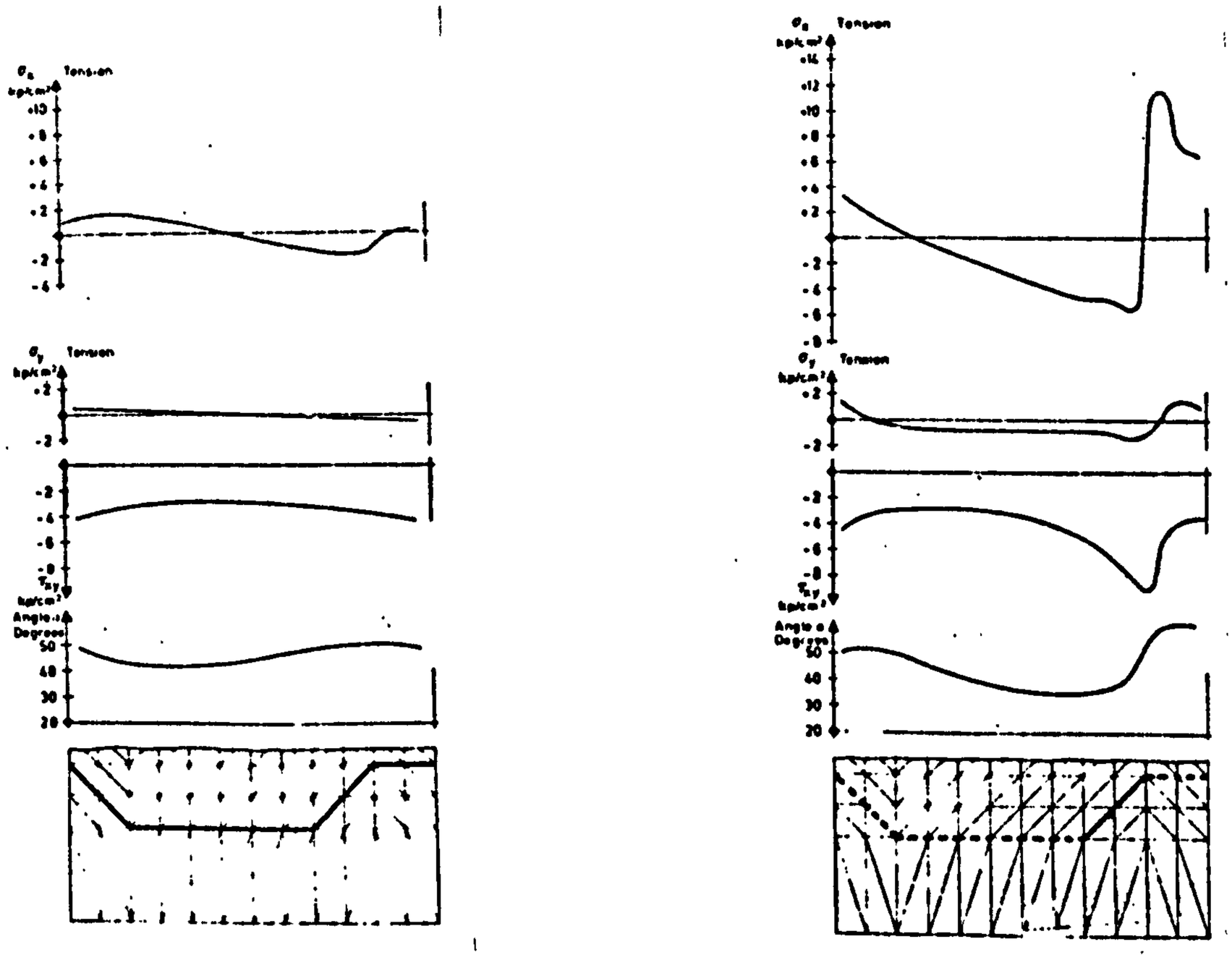

a) Complete bond between steel and concrete.

b) Bond between steel and concrete only on bearing face of ribs.

Fig. 3.8. Tensile and compressive stresses in concrete and direction of principal compressive stress on a plane along the tops of the ribs, from theoretical model used by Tepfers[4].

It may also be seen in fig. 3.8.(b) that the angle between the bar axis and the direction of the principal compressive stress is greatest over the ribs. This is the position at which Goto[38] found internalcracks to form around ribbed deformed bars, and may indicate that the inclination of internal cracks overestimates the average inclination of compression 'cones' to the bar axis, and hence the radial stress produced by the bond action of ribbed deformed bars.

Rehm[22] has suggested that a rib will fracture the concrete on

which it bears in the direction of what is called the 'principal' shear stress. Tepfers[4] analysis shows that a failure surface parallel to the direction of the maximum shear stress and passing through the top of a rib would leave a wedge of concrete against the rib similar to those observed in tests, as shown in fig. 3.9. If adhesion between bar and concrete were not lost, as in the case of strong lateral restraint to splitting, the fracture surface would run across the tops of the ribs.

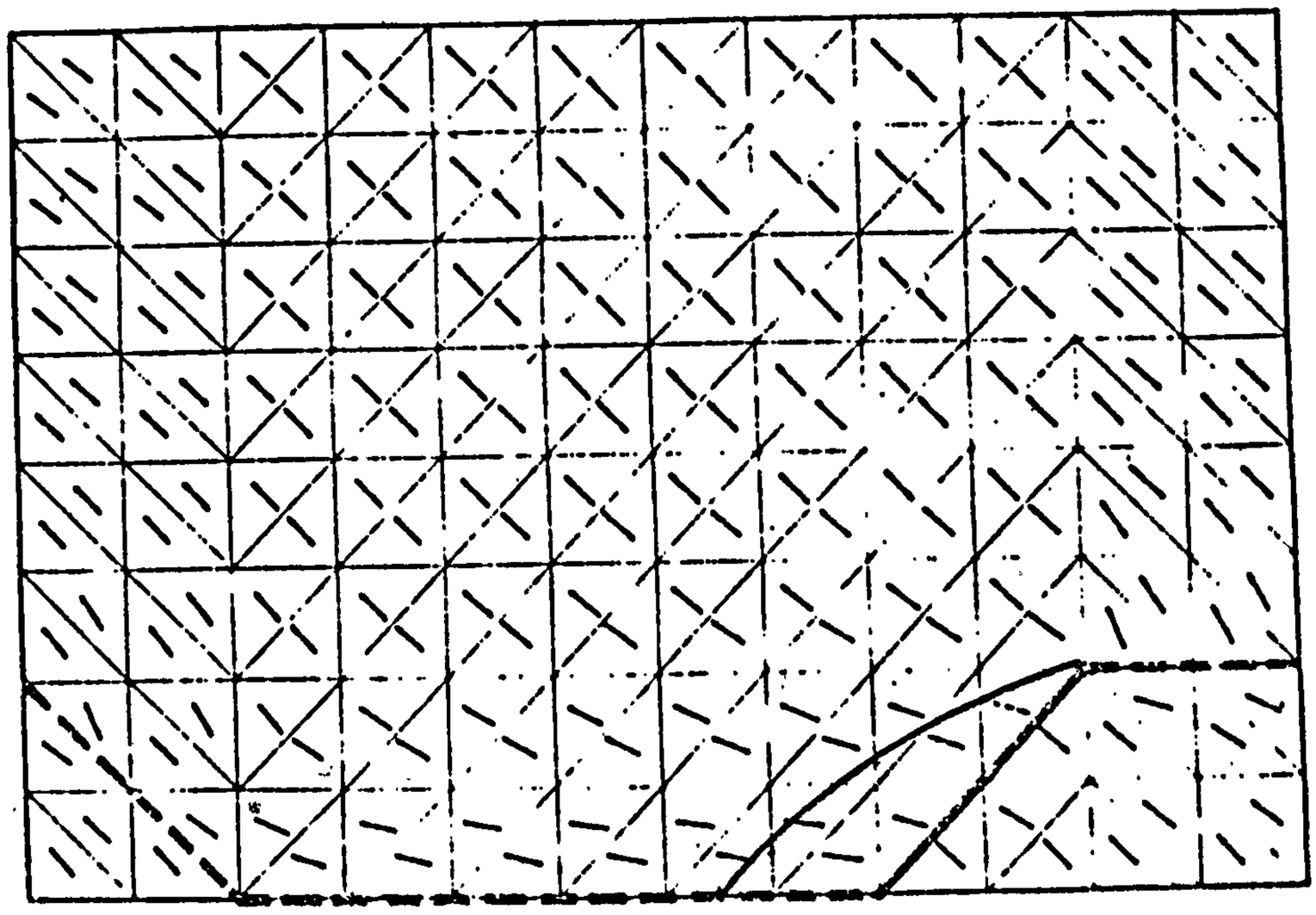

Fig. 3.9 Direction of principal compressive stresses around ribbed deformed bar in bond, from Tepfers[4], and possible failure surface in direction of maximum shear stress. Bond between steel and concrete exists only on the bearing faces of the ribs.

3.2.4 Hawkins[30] has made an approximate theoretical analysis of the failure of a concrete block loaded through a punch, and has obtained good correlation with experimental results.

Failure of a concrete block loaded through a punch is due to the formation of a wedge or cone of material beneath the loaded area, which tends to split the block.

Using the Coulomb-Mohr theory of failure, Hawkins related the bearing stress on the contact area of the punch to the bursting stresses produced in the block by considering the equilibrium of the wedge or cone. He then equated bursting forces to the resistance to bursting of a block, and obtained an expression of the form

$$\sigma_q / f_{cu} = 1 + \frac{K}{\sqrt{f_{cu}}} \left(\sqrt{\lambda} - 1 \right) \qquad 2.4$$

where σ_q = bearing capacity

K = constant - depending on the properties of the concrete

f_{cu} = concrete cube strength

and λ = the ratio of the unloaded to the loaded area of the block.

The Coulomb-Mohr theory is not accepted as a general failure theory for concrete. Goode and Helmy[39] state that it cannot be regarded as such, as the strength of concrete is dependent on the intermediate principal stress, which the Coulomb-Mohr theory assumes to have no effect. Ojha[40] agrees with this, but adds that there is no evidence against it's use in a two dimensional state of stress, and Jensen[41] has shown that the intermediate principal stress is of no significance in a plane stress or plane strain situation, if the intermediate principal stress is perpendicular to that plane.

However, in bearing tests on concrete blocks, intermediate and minor principal stresses will be equal, and therefore the theory may be applied in conjunction with the results of triaxial compression tests.

Although the bearing of the end of a bar in compression bond is obviously a similar problem to that of a punch bearing on a concrete block, it may be less apparent that a ribbed bar fails in bond in a similar manner. In all three situations failure is due to a wedge, or cone, of concrete splitting the surrounding cover.

3.3. Theoretical Approach.

3.3.1. The traditional concept of bond stress, based on the action of plain round bars, is that of a shear stress between bar and concrete. In the case of a ribbed bar, however, the transfer of force close to ultimate strength is due almost entirely to the bearing of the ribs on the concrete. This is illustrated in Goto's[38] photographs, which show the separation of bar and concrete that develops away from the ribs.

The concrete below the ribs is in a state of triaxial compression. The bearing pressure of the rib is the major principal stress, and the restraint from the surrounding concrete determines the minor principal stress. The minor principal stress is the radial component of 'bond stress' of deformed bars.

As stated in section 2.1.3., there are two modes of bond failure of deformed bars. In a type 1 failure, shown in fig.3.10a, the concrete shears on a surface along the tops of the ribs, but this mode of failure only occurs when splitting of the specimen is prevented by strong confining reinforcement. In a type 2 failure, shown in fig. 3.10b, the concrete below the rib fails on an inclined plane, leaving a wedge of concrete adhering to the rib. Movement along the failure plane tends to split the surrounding concrete.

In most practical situations, there will be insufficient confining force to prevent splitting of the test specimen, and type 1 failure will not take place. However, the ultimate bond stress for this mode of failure may be readily determined experimentally if desired.

Type 2 failures occur when the concrete surrounding the bar splits, and any confining reinforcement yields, prior to a type 1 failure. Succeeding sections of this chapter consider only type 2 failures.

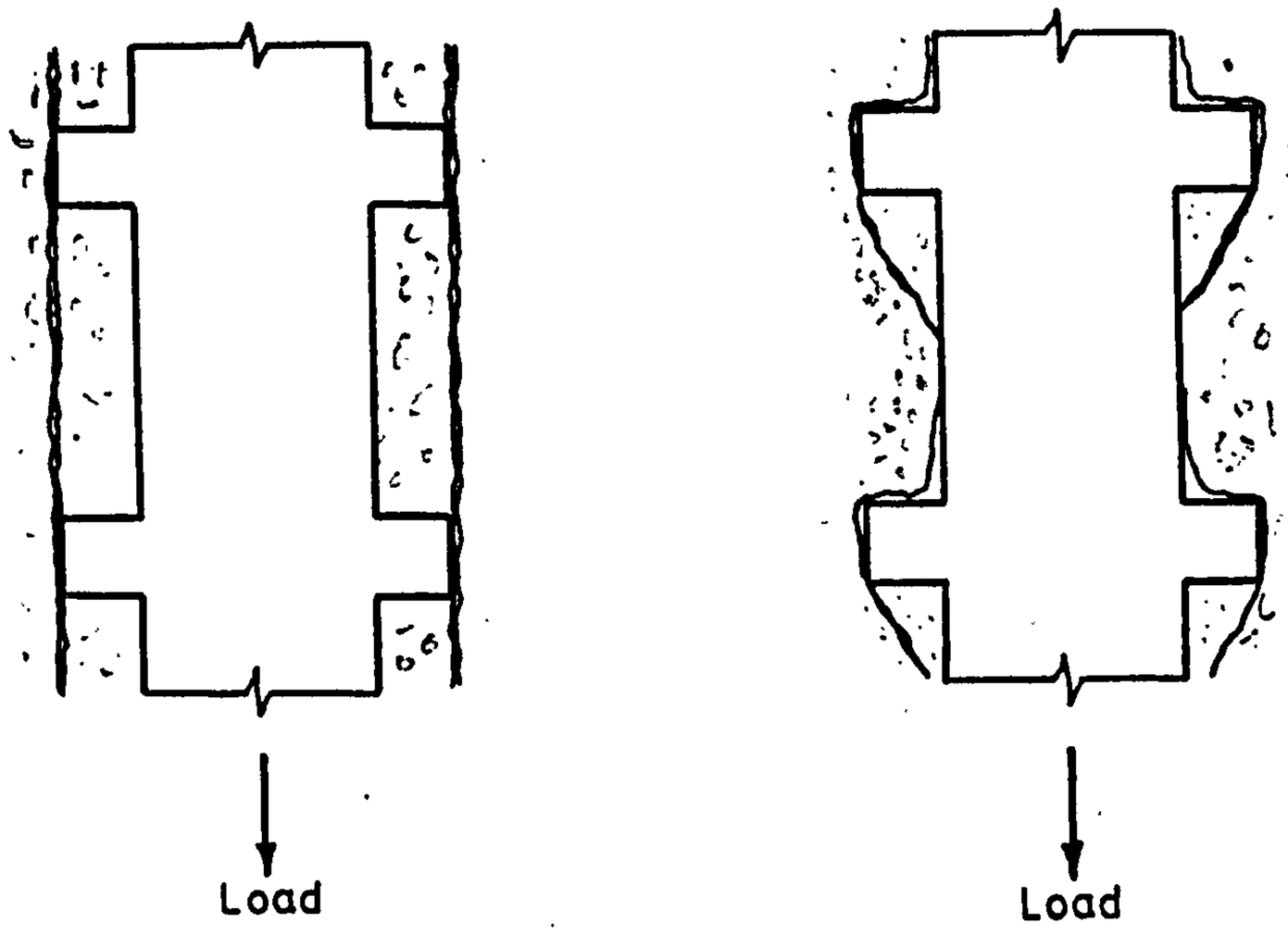

a) Type 1 failure b) Type 2 failure

Fig. 3.10 Modes of failure of ribbed deformed bars in bond.

3.3.2 A short length of an idealised ribbed deformed bar is shown in fig. 3.11. To simplify the analysis a round bar with an annular rib has been chosen. The rib has a face angle of 90^{o}, and the bar surface is assumed to be smooth.

The stresses in the concrete below the rib of a deformed bar are shown in fig. 3.12. If the height of the rib is small in comparison with the radius of the bar, the value of $\sigma_{\theta}.d\mu$ will also be small, and the analysis may be reduced to two dimensions.

According to Ojha[40] and to Jensen[41] the shear strength of concrete in two dimensional problems may be represented by the Coulomb-Mohr equation of failure. The shear strength of concrete below a bar rib is

$$\tau_c = \delta + \sigma_n \tan\theta \qquad 3.3$$

where τ_c = shear strength of concrete

δ = cohesion of concrete

σ_n = normal stress on failure plane

and θ = angle of internal friction of concrete.

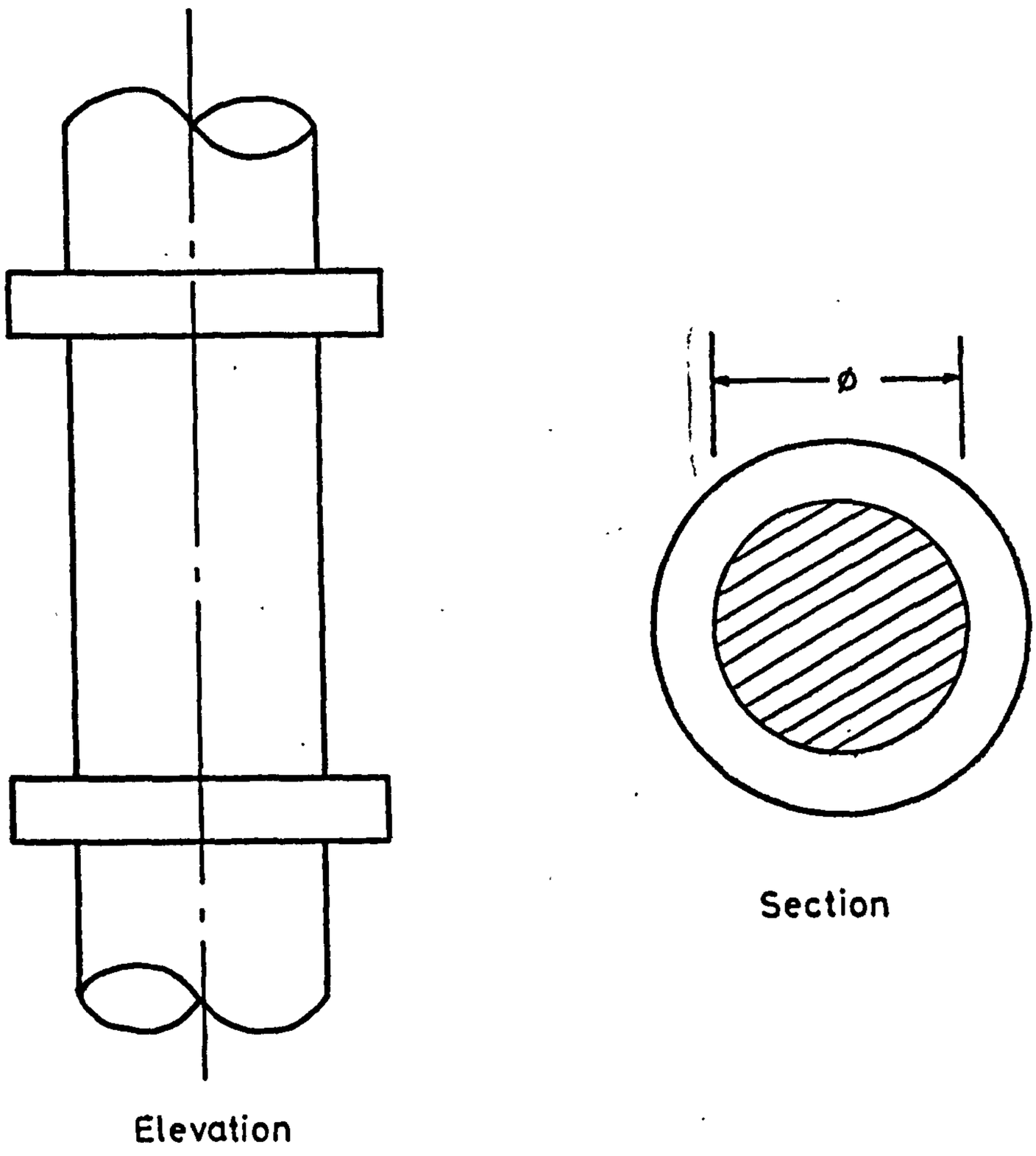

Fig. 3.11 Short length of deformed bar with annular ribs.

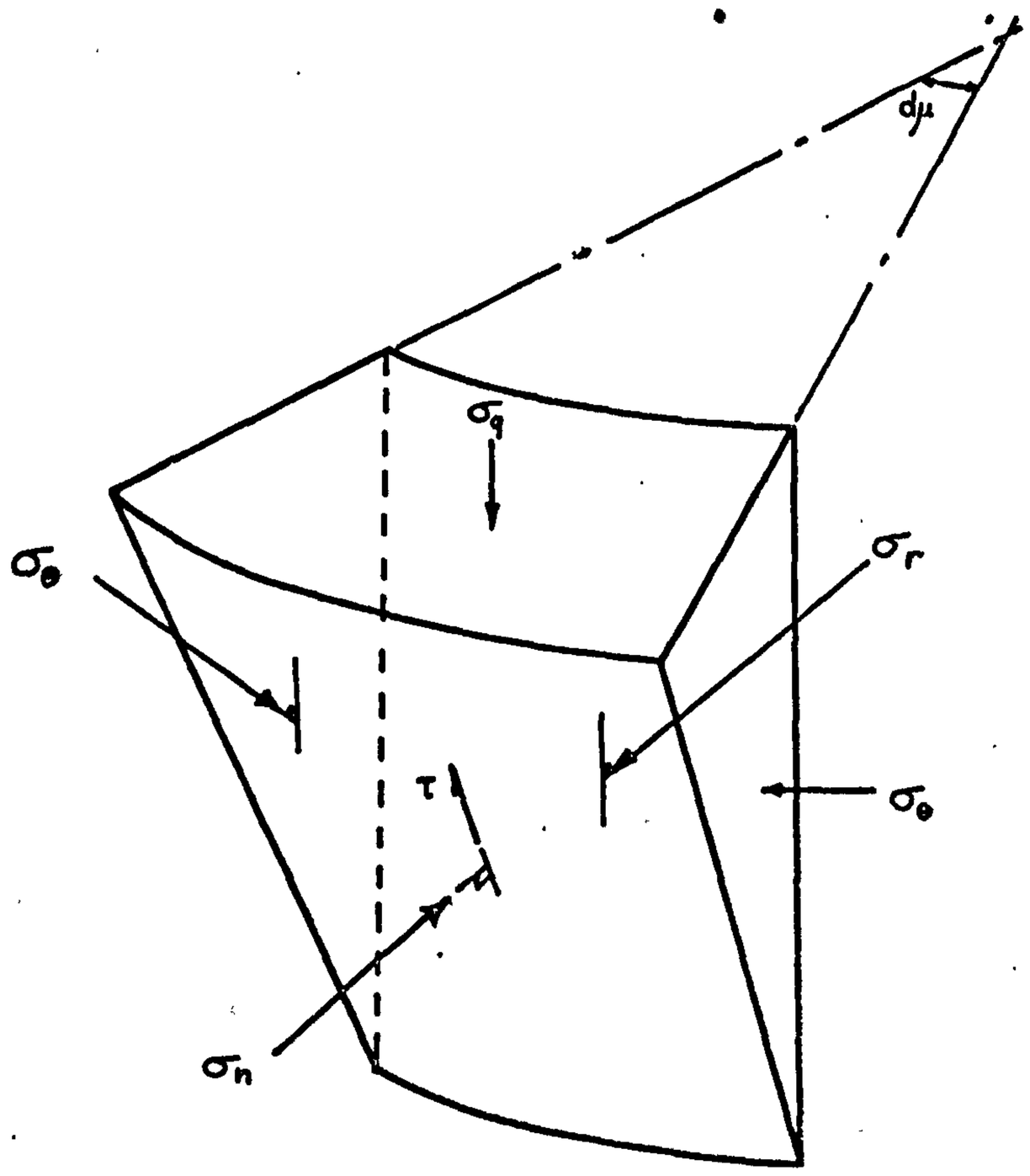

Fig. 3.12 Stresses on concrete wedge below rib.

The shear stress on any plane at an angle α to the direction of the major principal stress is

$$\tau = \tfrac{1}{2}(\sigma_1 - \sigma_3)\sin 2\alpha \qquad 3.4$$

where τ = shear stress

σ_1 = major principal stress

and σ_3 = minor principal stress

The normal stress on the same plane is

$$\sigma = \tfrac{1}{2}(\sigma_1 + \sigma_3) - \tfrac{1}{2}(\sigma_1 - \sigma_3)\cos 2\alpha \qquad 3.5$$

Equations 3.4 and 3.5 may be represented graphically by a method due to Mohr, as indicated in fig. 3.13.

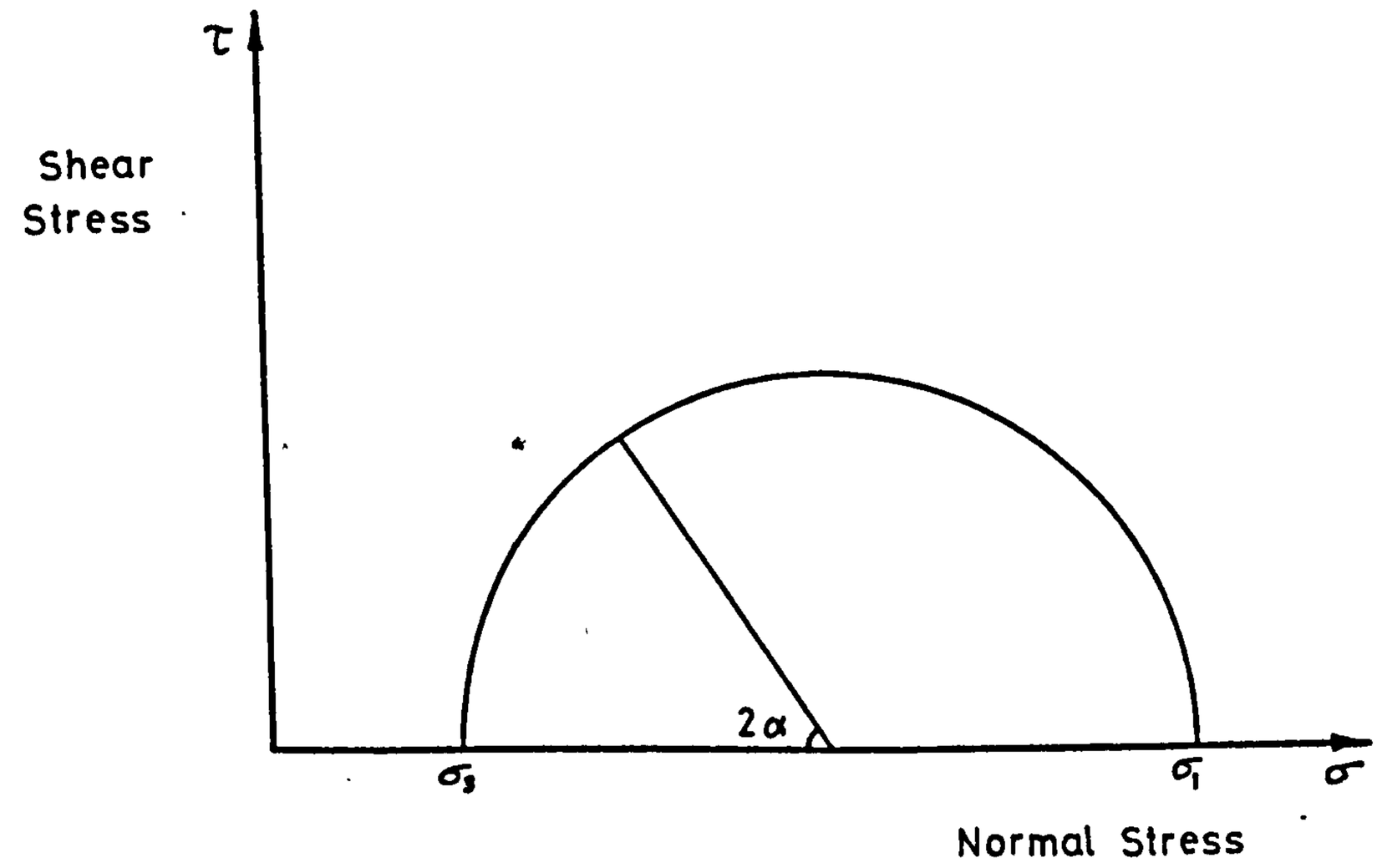

Fig. 3.13 Mohr diagram.

At failure of the concrete below the rib of a deformed bar, the combination of the shear and normal stresses on the failure plane must lie on the Mohr failure envelope, given by equation 3.3, and on a circle to which the line is tangential, as shown in fig. 3.14. The angle between the failure plane and the direction of the major principal stress is, from fig. 3.14.

$$\alpha = 45^\circ - \theta/2 \qquad 3.6$$

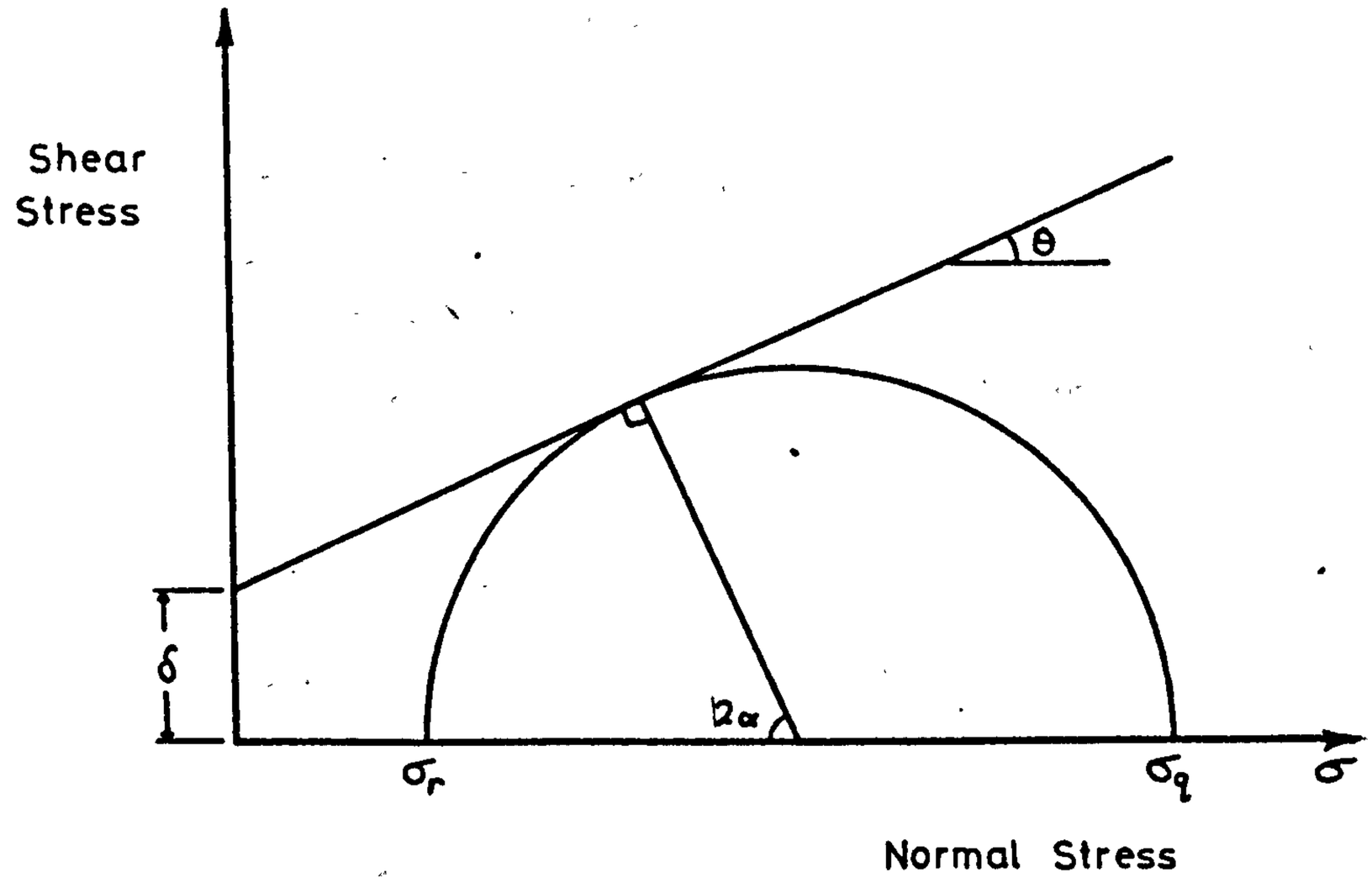

Fig. 3.14 Mohr circle and envelope.

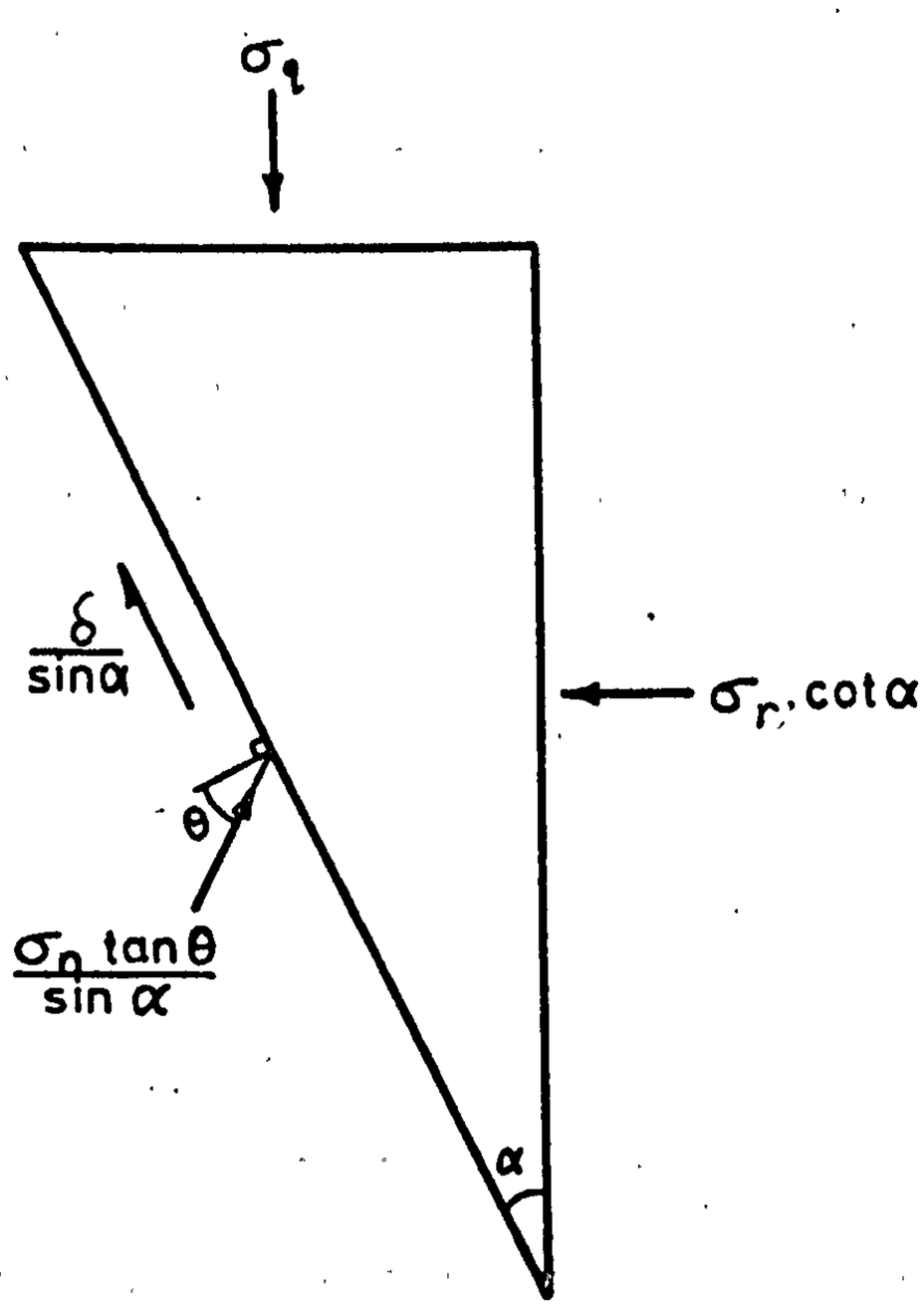

Fig. 3.15 Forces on 2 - D Concrete wedge below rib of deformed bar.

Consideration of the equilibrium of the wedge of concrete below the rib, shown in fig. 3.15, leads to the following expressions.

For $\Sigma V = 0$

$$\sigma_q = \delta \cot\alpha + \sigma_n \tan\theta . \cot\alpha \qquad 3.7$$

For $\Sigma H = 0$

$$\sigma_r \cot\alpha = -\delta + \sigma_n \tan\theta \qquad 3.8$$

where σ_q = bearing pressure of the rib

σ_r = radial stress on the bar

and α = inclination of failure surface to bar axis.

Combining equations 3.7 and 3.8 to eliminate $\sigma_n \tan\theta$ leads to

$$\sigma_q = \sigma_r . \cot^2\alpha + 2\delta \cot\alpha \qquad 3.9$$

and the force developed in a reinforcing bar by bearing of the ribs will be

$$f_{sc} . A_{sc} = \sigma_q . A_r . {}^{l_b}/_{s_r} \qquad 3.10$$

where f_{sc} = stress in bar

A_{sc} = cross sectional area of bar

A_r = bearing area of one rib

l_b = length of bar over which bearing of the ribs takes place

and s_r = spacing of ribs along bar.

The transfer of force by the bearing of the ribs of deformed bars will, from now on, be referred to as 'bond'.

The radial stress σ_r acts over a distance of $h_r . \cot\alpha$ below the rib, and exerts a pressure on the concrete around the bar. The bond strength of a bar therefore depends on the force available to resist the bursting force produced by the bond action of a deformed bar.

Fig. 3.16 shows the forces exerted by the radial stress σ_r on a short length of the bar circumference under one rib. The component of force in the x direction is

$$dF_h = \sigma_r . h_r \cot\alpha . {}^{\phi}/_{2}\, d\mu . \cos\mu . \qquad 3.11$$

The total bursting force produced by the bar is then

$$F_h = \frac{l_b}{S_r} \int_{-\frac{\pi}{2}}^{+\frac{\pi}{2}} \sigma_r \,.\, h_r \,.\, \cot\alpha \,.\, \phi/2 \,.\, \cos\mu \,.\, d\mu \qquad 3.12$$

where F_h = total bursting force produced by the bar.

For a bar with annular ribs, evaluation of the integral leads to the following expression for the total bursting stress produced by the bar.

$$F_h = \frac{l_b}{S_r} \,.\, \phi \,.\, h_r \,.\, \cot\alpha \,.\, \sigma_r \qquad 3.13$$

If the force available to resist bursting forces due to bond is denoted by F_c, then combining equations 3.9, 3.10, 3.11, and simplifying leads to the following expression for the stress developed in a deformed reinforcing bar by bond

$$f_{sc} = \left[\frac{F_c}{\phi \,.\, h_r} + \frac{2\,\delta \,.\, l_b}{S_r}\right] \frac{A_r}{A_{sc}} \,.\, \cot\alpha \leq f_y \qquad 3.14$$

According to equation 3.14, the bond strength of deformed bars is due to two separate factors. One component of bond strength is due to the confining force on the bars from the surrounding concrete, and it is this component which tends to split the concrete cover to the bars. The other component does not cause splitting, and is related to the compressive strength of the concrete.

The values of δ and θ in equation 3.3 may be found from the results of triaxial compression tests on concrete. The results of tests carried out by the author for a concrete with a maximum aggregate size of 2.36mm, presented in Appendix A, showed that the shear strength of concrete under the rib of a deformed bar may be taken to be

$$\tau_c = 0{\cdot}5\, f_c + \sigma_n \tan 32^\circ \qquad 3.15$$

for bars with a rib height of 3mm, and for the range of concrete

strengths and confining pressures considered in this investigation. Substituting in equation 3.14 from 3.15 leads to the following expression for the stress developed by bond of a ribbed deformed bar with annular ribs.

$$f_{sc} = \left[\frac{F_c}{\phi . h_r} + \frac{f_c . l_b}{S_r}\right] A_r . \frac{7.2}{\pi . \phi^2} \qquad 3.16$$

Equation 3.14 does not apply to bars with crescent shaped ribs, for which the integral in equation 3.12 would have to be evaluated separately. For the same rib area, the value of the integral will be greater for a crescent shaped rib with the maximum rib height at $\mu = 0$. A bar with crescent shaped ribs will therefore develop a lower stress than a bar with annular ribs if all other factors are held constant.

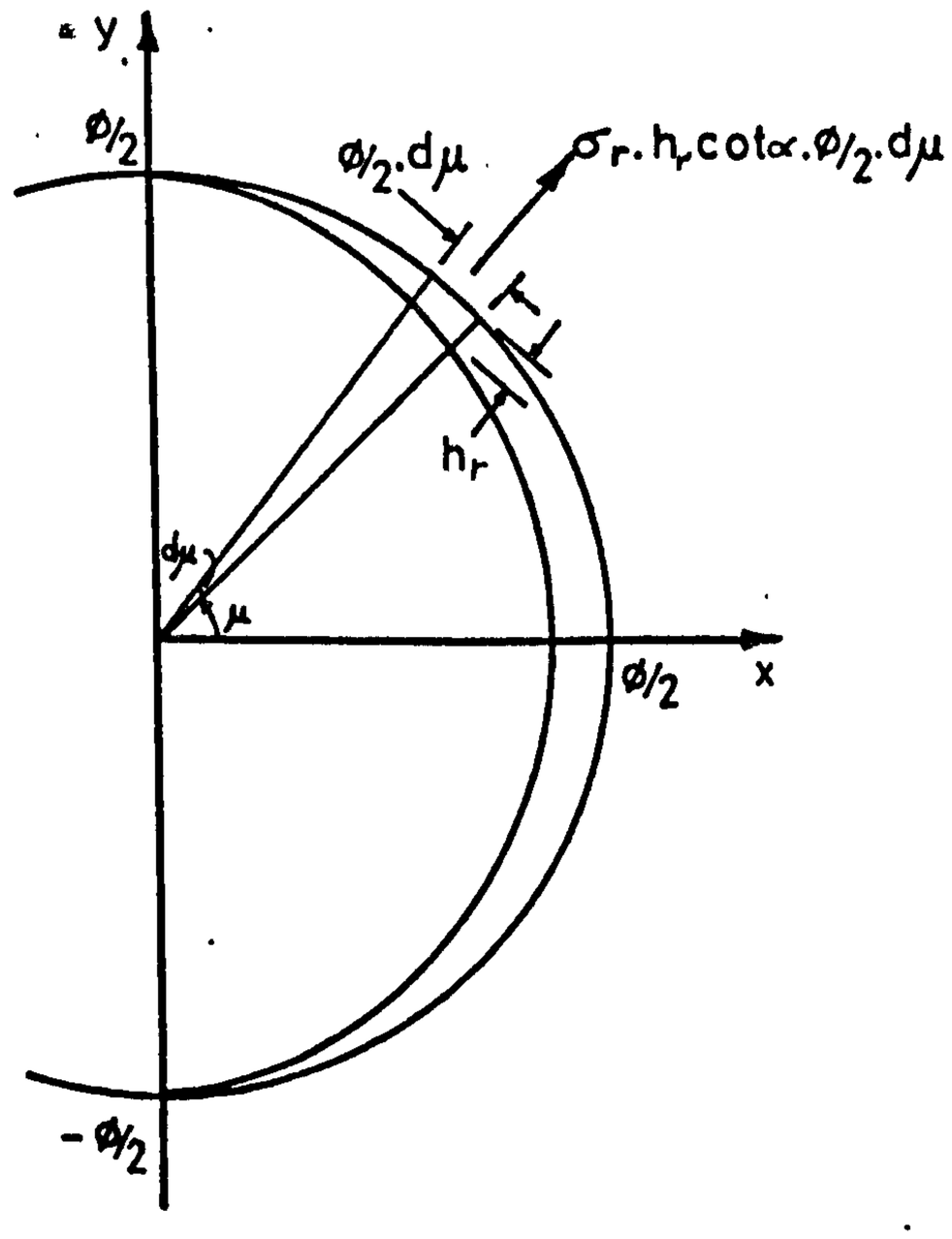

Fig. 3.16 Radial forces set up on bar circumference.

3.3.3. Previous investigators[4][5][25] have considered that the radial stress produced by bond action of ribbed bars may be represented by a uniform radial stress, $f_{bs}.\tan\beta$, acting on the surface of a plain round bar of equivalent diameter to the deformed bar. The angle β may be regarded as the angle the compression 'cones' shown in fig. 3.3. make with the bar axis.

The total confining force on the bar is related to $f_{bs}\tan\beta$ by the following expression

$$F_c = f_{bs}.\tan\beta.\phi.l_b \qquad 3.17$$

f_{bs} is the bond stress on the bar, defined by equation 2.1

Substituting for f_{bs} in equation 3.17 from equations 3.14 and 2.1 leads to

$$\cot\beta = \left[\frac{F_c}{\phi.h_r} + \frac{2\delta l_b}{s_r}\right]\frac{A_r.1{\cdot}8}{\pi.F_c} \qquad 3.18$$

The projected area of an annular rib is

$$A_r = \frac{\pi}{4}\left[(\phi+2h_r)^2 - \phi^2\right] \doteq \pi.\phi.h_r \quad \text{for } h_r \ll \phi \qquad 3.19$$

Equation 3.18 then becomes

$$\cot\beta = 1{\cdot}8\left[1 + \frac{2.\delta.l_b.\phi.h_r}{F_c.s_r}\right] \qquad 3.20$$

The value of the angle β is dependent on many variables, but, as cot cannot be less than 1.8, at its maximum $\beta = 29^\circ$. This value is considerably lower than that obtained by Goto[38], and outwith the range of 37° to 53° suggested by Orangun, Jirsa and Breen[25].

3.4. <u>End Bearing</u>

3.4.1. As mentioned in section 3.2, Hawkins[30] derived an expression, based in part on Coulomb-Mohr failure criteria, for the bearing strength of concrete blocks loaded through steel punches. The analysis equated the forces on a cone of concrete below the punch

to the resistance to splitting of the concrete blocks. An amended form of the analysis is presented here.

Stresses acting on the concrete cone are shown in Fig. 3.17

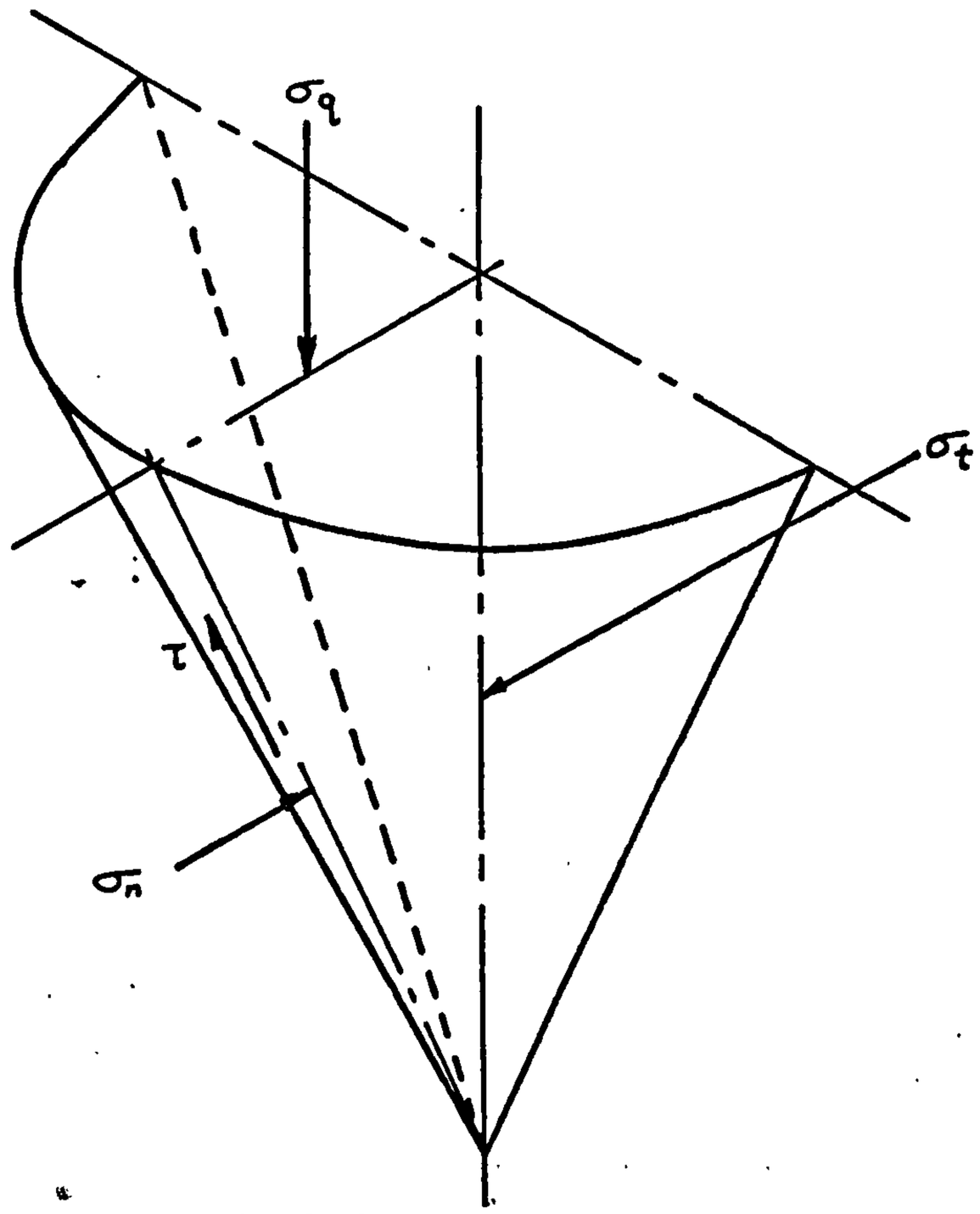

Fig. 3.17 Stresses on concrete below end of bar.

By an analysis similar to that presented in section 3.3.2, it can be shown that the ultimate bearing strength of the end of a bar on concrete is

$$\sigma_q = \sigma_t \cot^2\alpha + 2\delta \cot\alpha$$

where σ_q = bearing stress on concrete 3.21

σ_t = compressive stress on section through middle of cone

δ = cohesion of concrete

and $\alpha = 45° - \frac{\theta}{2}$ where θ is the angle of internal friction of the concrete.

The total force on a section through the middle of the cone will be

$$F_t = \sigma_t \cdot \phi^2/4 \cot\alpha \qquad 3.22$$

If the force available to resist the bursting force produced by the cone is denoted by F_c then combining equations 3.21 and 3.22 leads to the following expression

$$\sigma_q = \left[\frac{4.F_c}{\phi^2} + 2\delta\right]\cot\alpha \leq f_y \qquad 3.23$$

Equation 3.23 shows that, as with bond strength of deformed bars, end bearing strength is due to two factors, the confining force on the cone from the surrounding concrete, and the compressive strength of the concrete.

According to the results of Smee[42] and Richart, Braendtzaeg, and Brown[43], for a concrete with a maximum aggregate size of 20mm, the values of δ and θ to be used in calculation of end bearing strength may be taken to be the same as those used in the calculation of bond strength.

Substituting in equation 3.23 from equation 3.15 leads to the following expression for the ultimate bearing strength below the end of the bar.

$$\sigma_q = 1.8\left[\frac{4.F_c}{\phi^2} + f_c\right] \leq f_y \qquad 3.24$$

3.4.2. It may be seen from equations 3.16 and 3.24 that the steel stress developed by bond of bars and by the bearing of the end of bars depends on the resistance to the bursting forces set up by the transfer of load. The ratio of the force developed in a bar by this confining force to the confining force itself gives an indication of the relative efficiencies of bond and of end bearing in transferring load.

From equation 3.24, setting $\delta = 0$, the force developed in a bar by end bearing due to a confining force F_c is

$$F_b = \frac{\pi\phi^2}{4}\sigma_{qc} = 1.8\pi.F_c \qquad 3.25$$

where F_b = force in bar

and σ_{qc} = bearing pressure due to confining force.

The ratio of bar force to confining force is

$$\frac{F_b}{F_c} = 1.8\pi \qquad 3.26$$

From equation 3.16, putting $\delta = 0$, the force developed by bond of a bar due to a confining force is

$$F_b = \frac{\pi.\phi^2}{4} \cdot f_{sc_c} = \frac{1.8.F_c.A_r}{\phi.h_r} \qquad 3.27$$

where f_{sc_c} = stress developed in bar by confining force.

The ratio of bar force to confining force is

$$\frac{F_b}{F_c} = \frac{1.8.A_r}{\phi.h} \qquad 3.28$$

Substituting for A_r from equation 3.19 leads to

$$\frac{F_b}{F_c} = 1.8\pi \qquad 3.29$$

The efficiency of bond of bars with annular ribs is therefore the same as the efficiency of end bearing. However, if bars with crescent shaped ribs were considered, a lower value of F_b/F_c would be obtained. In this case, the value of $\phi.h_r$ in equation 3.28 is evaluated from the integral in equation 3.12. For the same rib area, a crescent shaped rib produces a greater value of $\phi.h_r$ than an annular rib, and the efficiency of bond is therefore lowered.

3.5 Bond of Single Bars Surrounded by a Spiral

The forces acting on a cylinder of concrete due to the radial component of bond stress of a deformed reinforcing bar are shown in fig. 3.18. It assumed that the concrete cylinder is cracked longitudinally and all the bursting force set up by the reinforcing bar is resisted by a wire spiral around the bar

Equating the total bursting force set up by the bar to the confining force provided by the wire spiral leads to the following expression.

$$F_c = 2.n.\epsilon.E_s..A_{st}. \qquad 3.30$$

where n = no. of turns of spiral around the reinforcing bar

ϵ = strain in wire

E_s = modulus of elasticity of wire

and A_{st} = cross sectional area of wire

If the wire in the spiral yields at the ultimate load developed by the bar, then

$$F_c = 2.n.A_{st}.f_y \qquad 3.31$$

where f_y = yield strength of wire

Substituting for F_c in equation 3.16 leads to the following expression for the ultimate steel stress developed by the reinforcing bar.

$$f_{sc} = \left[\frac{2.n.A_{st}.f_y}{\phi.h} + \frac{f_c.l_b}{S_r}\right] A_r.\ \frac{7.2}{\pi.\phi^2} \qquad 3.32$$

Equation 3.32 holds in cases where the wire spiral yields along the length of the bar at the ultimate load developed by the bar, and the non-splitting component of bond strength, given by the right hand part of the expression in brackets is equation 3.32 is fully mobilised along the bar length.

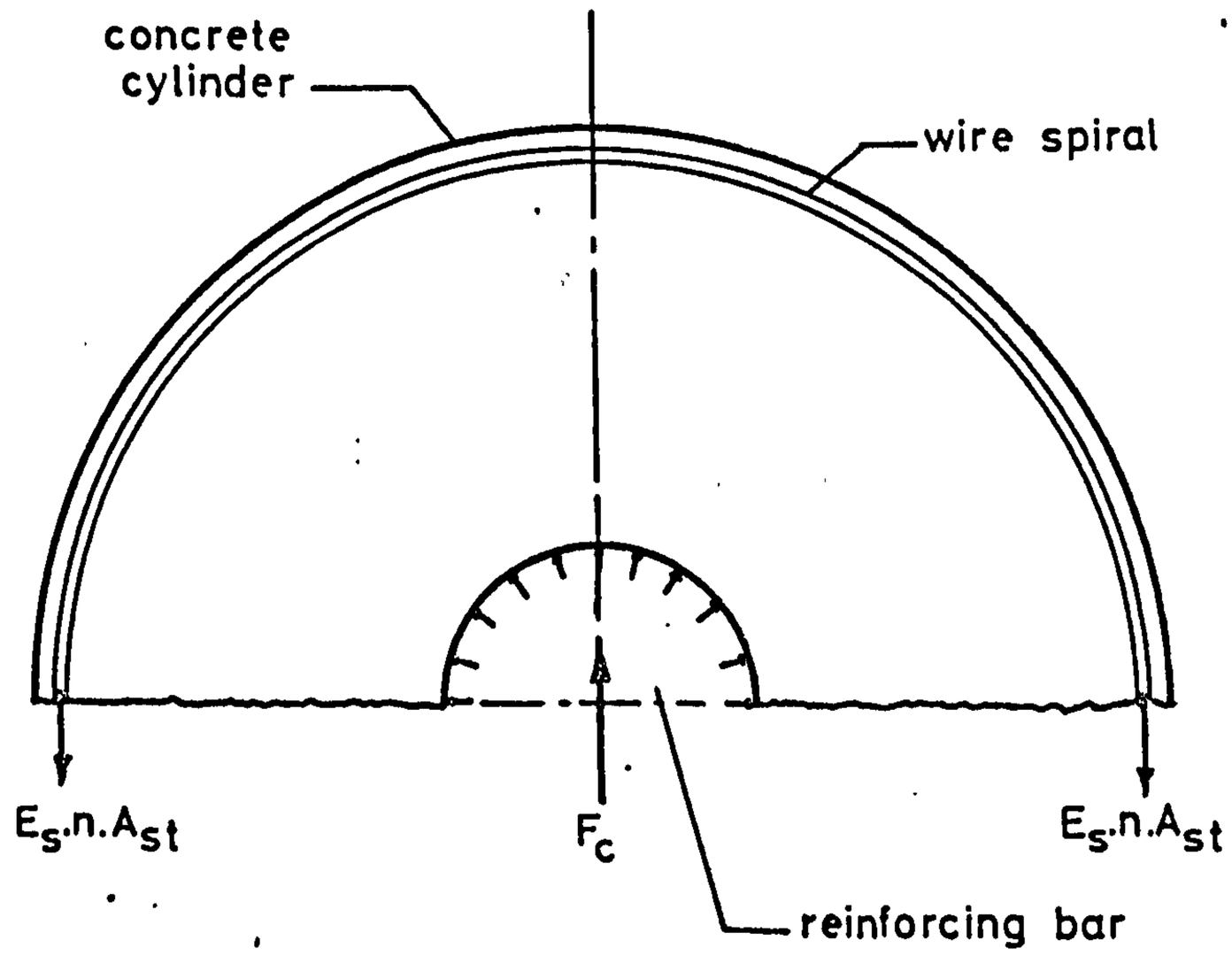

Fig. 3.18 Forces on concrete cylinder.

3.6 Lapped Joints.

3.6.1 From observations of the formation and growth of cracks in test specimens in the current investigation, it can be inferred that failure of compression lapped joints is due to yielding of the links confining the lapped bars. Strains measured on links in a few test specimens support this conclusion.

Previous analysis of the failure of lapped joints have emphasised the importance of the tensile strength of the concrete cover. However, the tensile strength of the concrete cover could have made no contribution to joint strength in the present series of tests, as cracks along the line of the main reinforcement usually extended throughout the length of the lapped joint in all column faces at ultimate load. Large strains, considerably greater than that at which concrete cracks in tension, were measured in both legs of links at the end of lapped joints. In the following analysis, it is assumed that all bursting forces produced by the transfer of load between reinforcement and concrete are carried by tension in the secondary reinforcement confining the bars.

3.6.2 Bars with bond only. A corner of a column is shown in fig. 3.19. As discussed in sections 3.7 and 6.2, bond stresses, and hence bursting forces, are not evenly distributed throughout the lap length, and so different values of bursting forces are assigned to each. Taking moments about point M, on the axis of the link at its point of contact with the main bar, and assuming that the bursting forces produced by the bars act in the directions shown, leads to the expression

$$F_1 \cdot \frac{5\phi}{8\sqrt{2}} + F_2 \cdot \phi \cdot \left(1 + \frac{5}{8\sqrt{2}}\right) = A_{sv} \cdot f_{yv} \cdot \phi \cdot \left(\frac{5}{8} + \frac{1}{\sqrt{2}}\right) \qquad 3.33$$

where F_1 and F_2 are the bursting forces exerted on the link by each bar

and $A_{sv} \cdot f_{yv}$ = ultimate tensile strength of one leg of the link.

Putting

$$F_1 = \psi \ F_2 \qquad 3.34$$

where ψ is a coefficient not greater than unity and not less than zero, leads to the following expression for the restraining force on a bar due to one link.

$$F_2 = \frac{0{\cdot}93 . A_{sv} . f_{yv}}{(1 + 0{\cdot}31 \psi)} \qquad 3.35$$

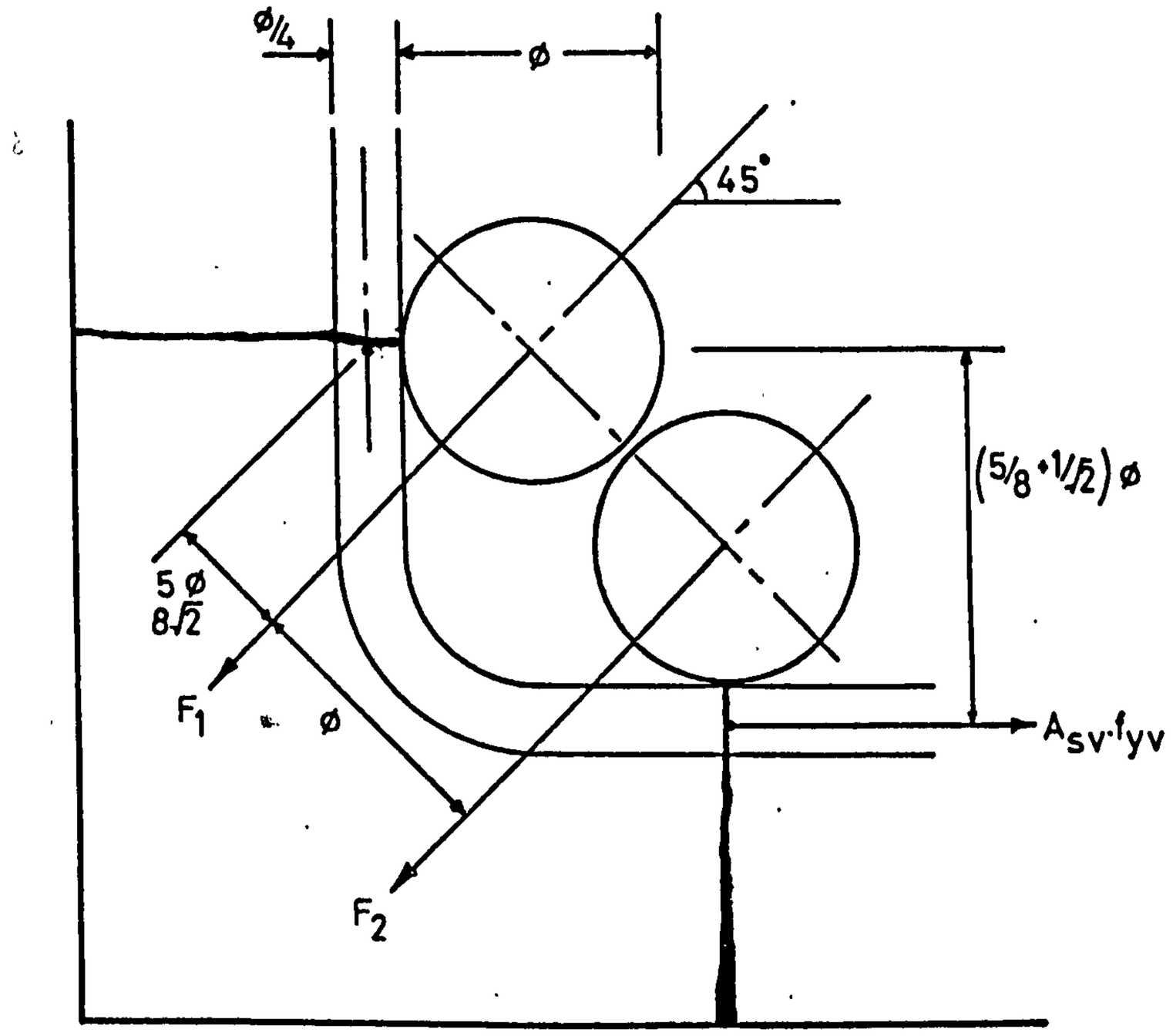

Fig. 3.19 Ultimate splitting pattern around lapped bars and forces on corner of column.

As indicated in fig. 3.20 the distribution of bond stress through a lapped joint may be considered to lie between two extremes. Where bond stresses are uniformly distributed along the bars within the lap length, as shown in fig. 3.20(a), equal bursting forces are set up by both bars, and $F_1 = F_2$, i.e. $\psi = 1$. Where bond stresses are concentrated close to the end of the bars in lapped joint, as shown in fig. 3.20(c), one bar will exert no force on a link at the end of

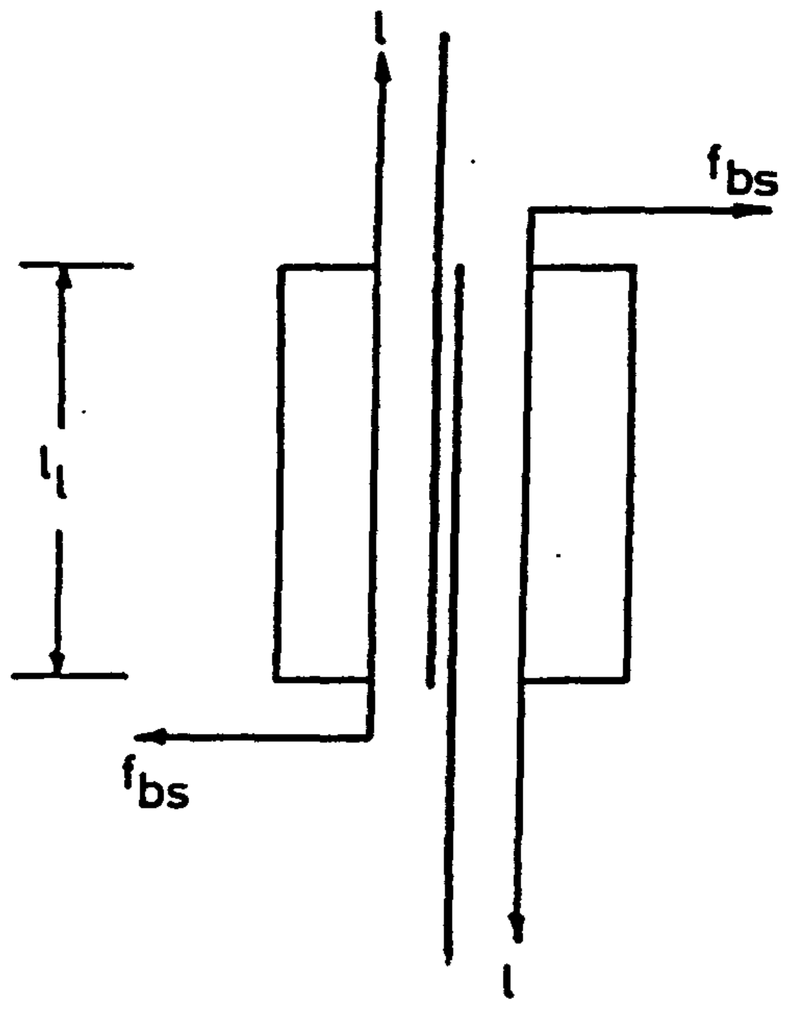

a) Uniform bond stress through lapped joint $\psi = 1$

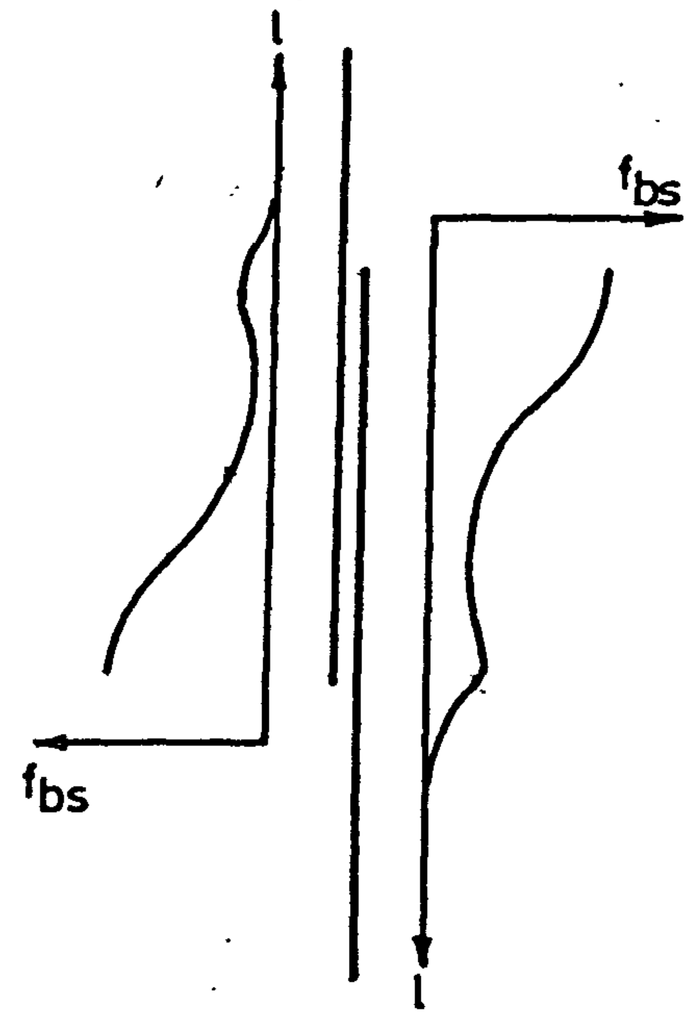

b) Typical bond stress distribution found in tests $0 < \psi < 1$

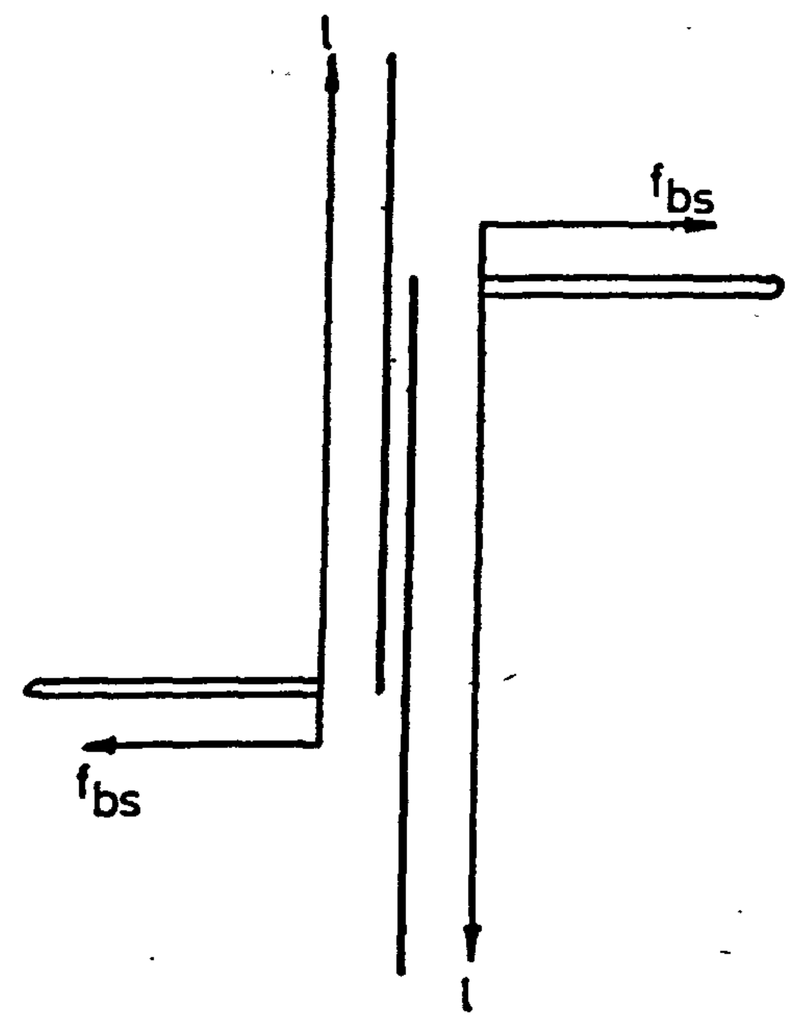

c) All force transferred close to ends of lapped joint $\psi = 0$

Fig. 3.20 Influence of bond stress distribution on value of ψ - bars with end bearing eliminated.

the lapped joint, and $F_1 = 0$, i.e. $\psi = 0$.

The assumption in fig. 3.19 of the directions in which the bursting forces act is only correct when $F_1 = F_2$. As the value of ψ decreases, the direction of F_2 will tend to move closer to the horizontal, as indicated in fig 3.21, and equation 3.35 will underestimate the available resistance to the bursting forces. Fig. 3.21 shows the forces acting on the corner of a column when $F_1 = 0$. Taking moments about point M, on the axis of the link at its point of contact with the main bar, leads to the following expression.

$$F_2 \cdot \phi \left[\left(\frac{5}{8} + \frac{1}{\sqrt{2}}\right)^2 + \frac{1}{2}\right]^{\frac{1}{2}} \cdot \sin 2\xi = \left(\frac{5}{8} + \frac{1}{\sqrt{2}}\right) A_{sv} \cdot f_{yv} \qquad 3.36$$

For horizontal equilibrium

$$F_2 \cdot \cos \xi = A_{sv} \cdot f_{yv}. \qquad 3.37$$

Solving for ξ in equations 3.36 and 3.37 leads to a value of 26.5° for ξ.

Substituting for ξ in equation 3.37 leads to the following expressions for the force exerted on each of the pair of lapped bars by one link when $\psi = 0$.

$$F_2 = 1{\cdot}13\ A_{sv} \cdot f_{yv} \qquad 3.38$$

$$F_1 = 0 \qquad 3.39$$

From equation 3.35, the force exerted on each of the pair of lapped bars by one link when $\psi = 1$ is given by

$$F_1 = F_2 = 0{\cdot}71\ A_{sv} \cdot f_{yv}. \qquad 3.40$$

In the above analysis, the influence of aggregate interlock across the cracks and the dowel action of the links has been neglected, as it is impossible to evaluate their contribution, if any. The presence of either will increase the confining force on the bars.

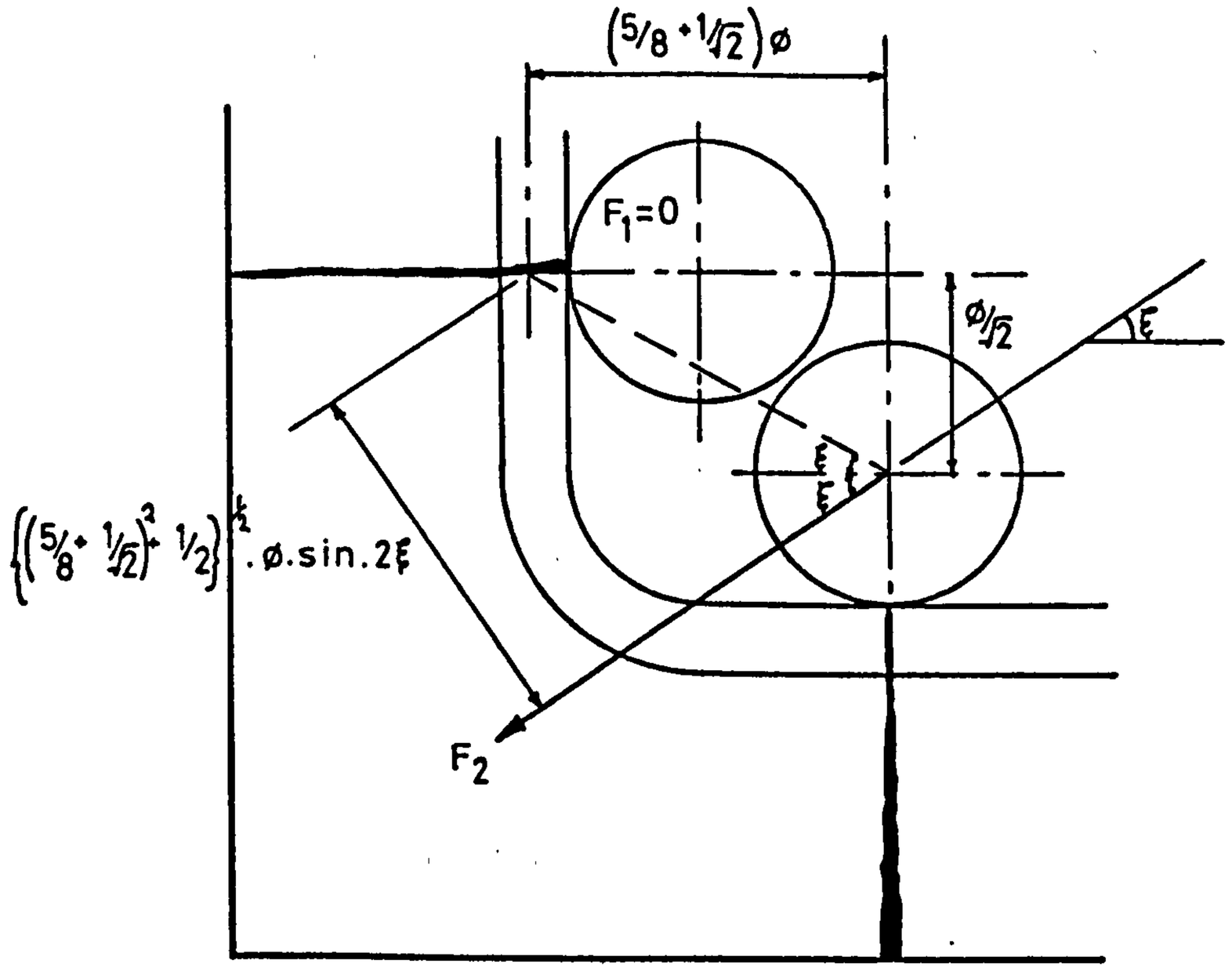

Fig. 3.21 Forces on corner of column. $\psi = 0$

The total confining force on a bar in a lapped joint may also be evaluated for the limits of bond stress distribution illustrated in figs. 3.20(a) and 3.20(c).

Where bond stresses are uniformly distributed throughout the lap length, all the links within the lap length act in resisting the bursting force exerted by the lapped bars. The total confining force on one bar is then

$$F_c = n . F_1 = 0{\cdot}71 . n . A_{sv} . f_{yv} \qquad 3.41$$

where n is the total number of links confining the pair of lapped bars.

Where bond stresses are concentrated close to the end of each of the pair of lapped bars, only the links closest to the ends of the lapped joint will act. The confining force on each bar is then

$$F_c = 1{\cdot}13\, A_{sv} . f_{yv} \qquad 3.42$$

Equation 3.42 holds where there are two or more links in the lap length. If only one link positioned in the middle of the lapped joint is present, the confining force on each bar is given by equation 3.41.

Equations 3.41 and 3.42 may be substituted in equation 3.16 to give upper and lower limits for the stress developed by a lapped bar for the joint detail used in the current investigation.

At the upper limit,

$$f_{sc_u} = \left[\frac{0.71.n.A_{sv}.f_{yv}}{\phi.h_r} + \frac{f_c.l_b}{s_r}\right] A_r.\frac{7.2}{\pi.\phi^2} \leq f_y \qquad 3.43$$

At the lower limit

$$f_{sc_l} = \left[\frac{1.13\ A_{sv}.f_{yv}}{\phi.h_r} + \frac{f_c.l_b}{s_r}\right] A_r.\frac{7.2}{\pi\phi^2} \leq f_{yv} \qquad 3.44$$

When n = 1, equation 3.43 applies at both limits.

3.6.3 Bars with end bearing only. The same joint detail was used in tests on bars with end bearing only as in tests with bond only. Equations 3.38 and 3.40 are therefore still applicable, but the values of ψ and n to be used where bars have end bearing only must be considered separately.

As bursting forces due to end bearing are set up only at the ends of a lapped joint, only the links at the end of the lap can be expected to provide resistance to bursting forces.

Bursting forces additional to those produced by end bearing are set up by the bond stresses that develop outwith the lap length on one bar to transfer force to the end of the other bar, shown in fig. 3.22. The value of this bursting force on the links at the ends of the lap depends on the distribution of bond stresses outwith the lapped joint. If bond stresses are concentrated near the end of the lapped joint, as indicated in fig. 3.22(a), both lapped bars will

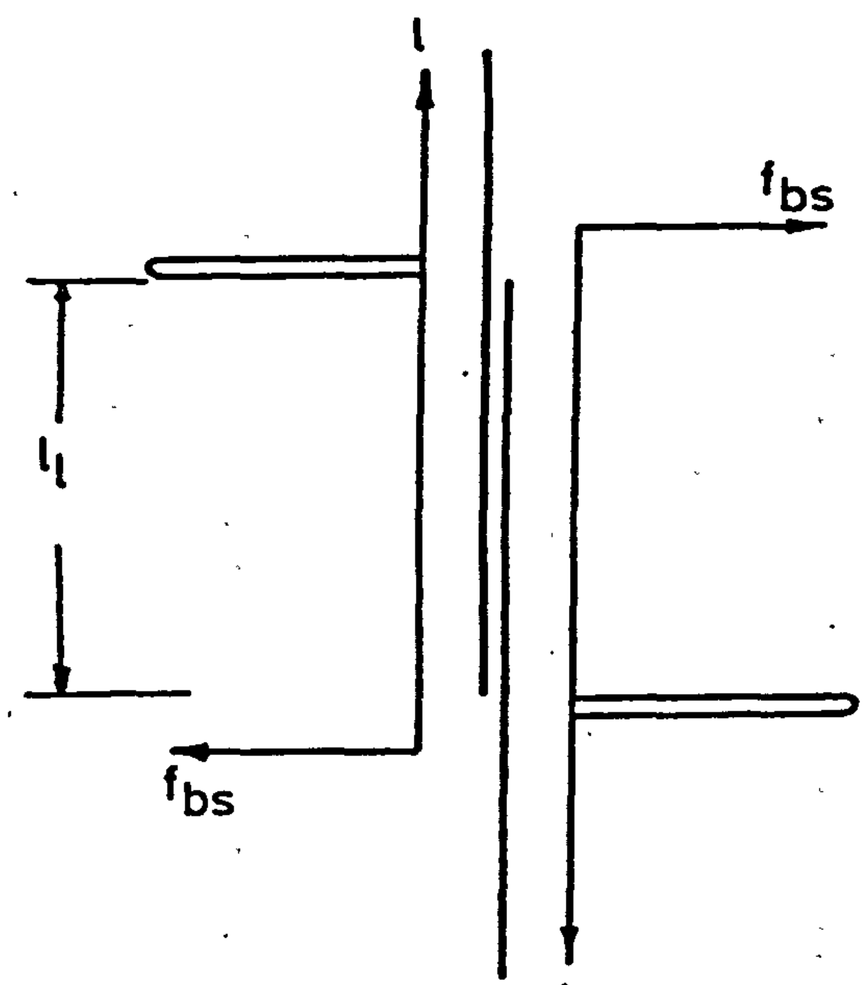

a) High bond stresses close to ends of lapped joint $\psi = 1$

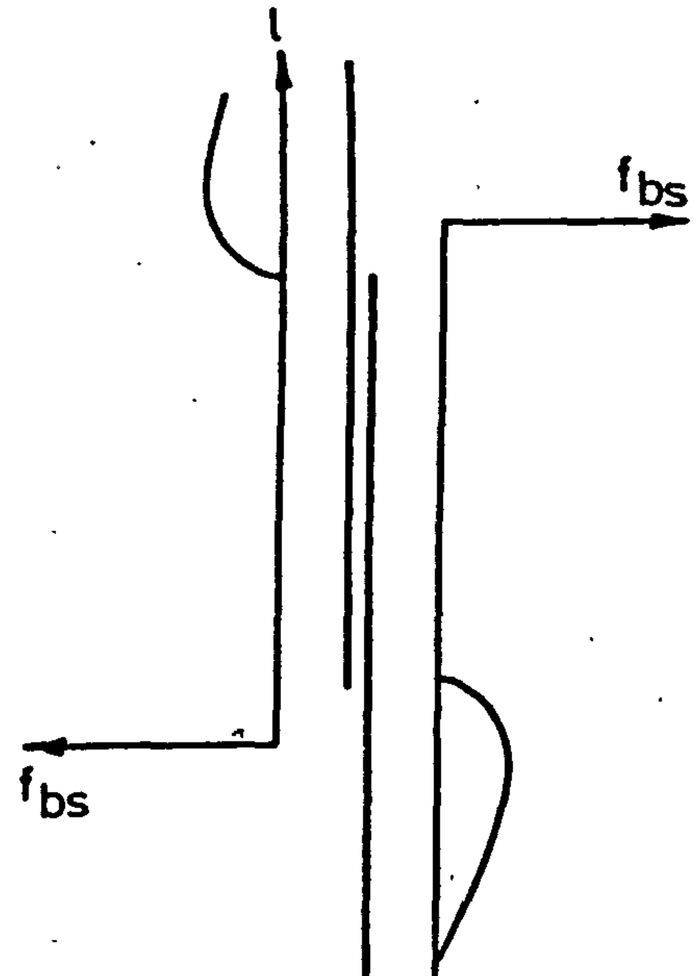

b) Typical bond stress distribution found in tests $0 < \psi < 1$

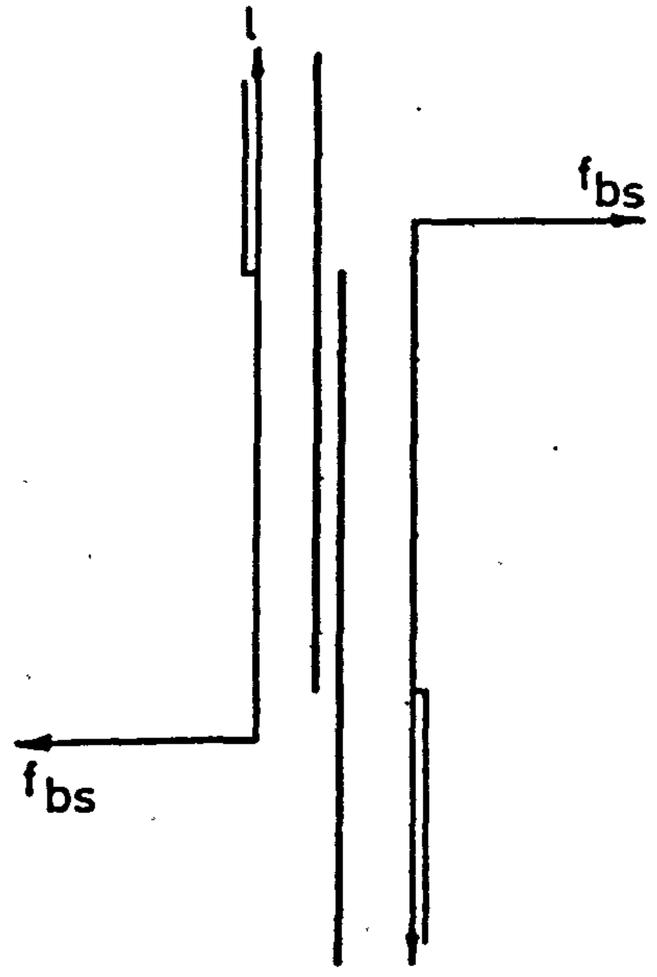

c) Low bond stress over long distance outwith lapped joint $\psi = 0$

Fig. 3.22 Influence of bond stress distribution on value of ψ - bars with bond eliminated over lap length.

exert large bursting forces on the link, and the value of ψ will tend to unity. Where bond stresses are more uniformly distributed over a longer length of bar, as shown in fig. 3.22(c), the non-bursting component of bond stress may carry a higher proportion of the force transferred, and the value of ψ in the links at the ends of the lap will tend to zero.

As in section 3.6.2, upper and lower limits to the transfer of force may be specified. At the upper limit, $\psi = 0$, and the ultimate end bearing strength of a bar is found by combining equations 3.24 and 3.38, which leads to

$$\sigma_q = 1{\cdot}8 \left[\frac{4{\cdot}52\, A_{sv} \cdot f_{yv}}{\phi^2} + f_c \right] \leqslant f_y \qquad 3.45$$

At the lower limit, $\psi = 1$, and the ultimate end bearing strength of a bar is, from equations 3.24 and 3.40.

$$\sigma_q = 1{\cdot}8 \left[\frac{2{\cdot}84\, A_{sv} \cdot f_{yv}}{\phi^2} + f_c \right] \leqslant f_y \qquad 3.46$$

3.6.4. Although only one joint detail was used in the experimental study of joint strength, it is of interest to examine the influence of other joint details on joint strength.

Fig. 3.23 shows one possible detail. The arrangement of bars and links complies with the requirements of B.S.C.P. 110:1972[9]. From the results of tests on tension lapped joints, it is expected that failure would be preceded by cracking of the concrete on the plane through the bar axes, as shown. It is again assumed that failure takes place as the links yield, and that at ultimate load all resistance to bursting is provided by the links. Different values of bursting force are again assigned to each bar of a pair.

Equating the total bursting force produced by the reinforcing bars to the confining force of the secondary reinforcement leads to the following expression

$$3\left(F_1 + F_2\right) = 2\, A_{sv}.\, f_{yv} \qquad 3.47$$

If we again put $F_1 = \psi F_2$, then equation 3.47 becomes

$$F_2 = \frac{0{\cdot}67\, A_{sv}.\, f_{yv}}{(1+\psi)} \qquad 3.48$$

The total confining force on a bar with a uniform distribution of bond stress, i.e. $\psi = 1$, is then

$$F_c = n.F_2 = 0{\cdot}33.n.\, A_{sv}.\, f_{yv} \qquad 3.49$$

where n = No. of links in lapped joint.

This represents a drop of 55% in the confining force on the bar compared with equation 3.41.

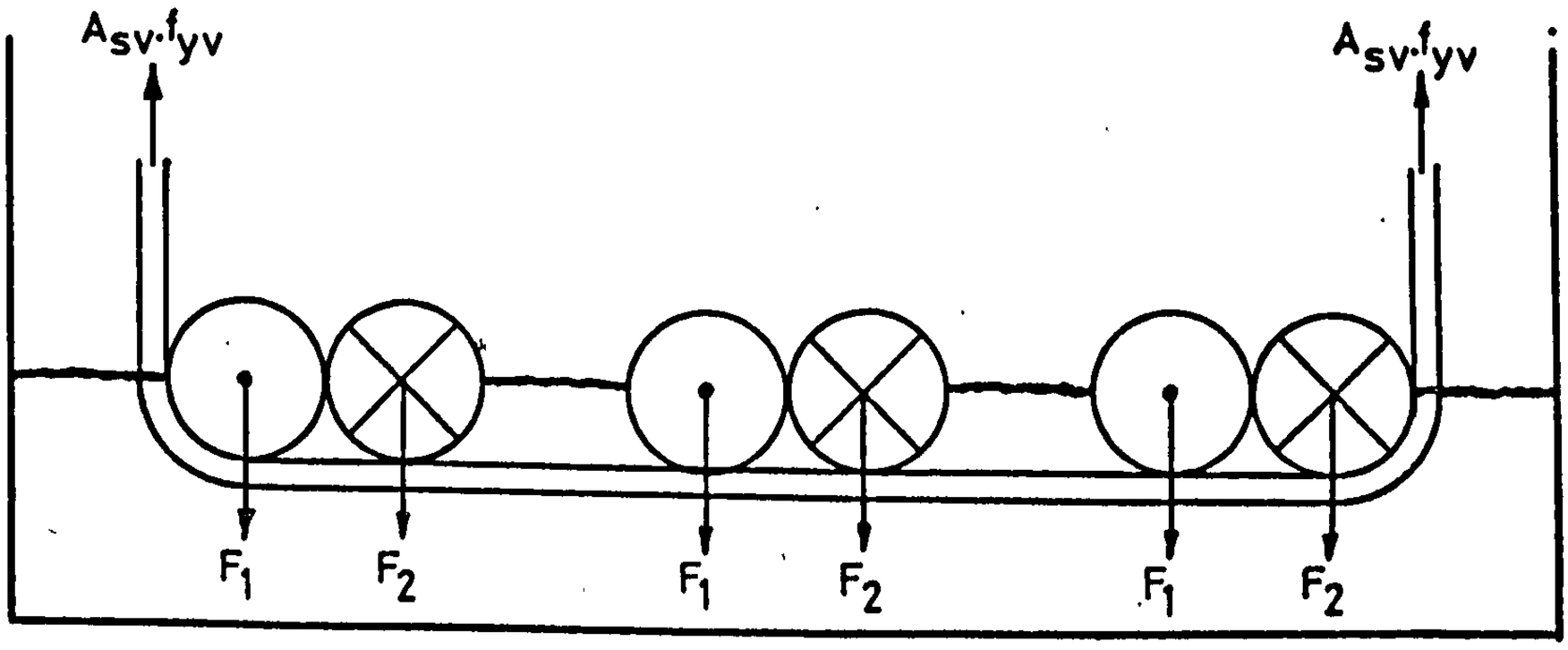

Fig. 3.23 Probable splitting pattern for an alternative joint detail, and forces acting on column face.

3.7 Variation of Steel Stress Through a Lapped Joint

3.7.1 As part of the investigation of the strength of lapped joints, a simple computer model was set up to examine the influence of certain parameters on the variation of stress in a reinforcing bar within a lapped joint.

A plane frame structure, shown in fig. 3.24 was chosen to represent a lapped joint. The middle vertical member represents

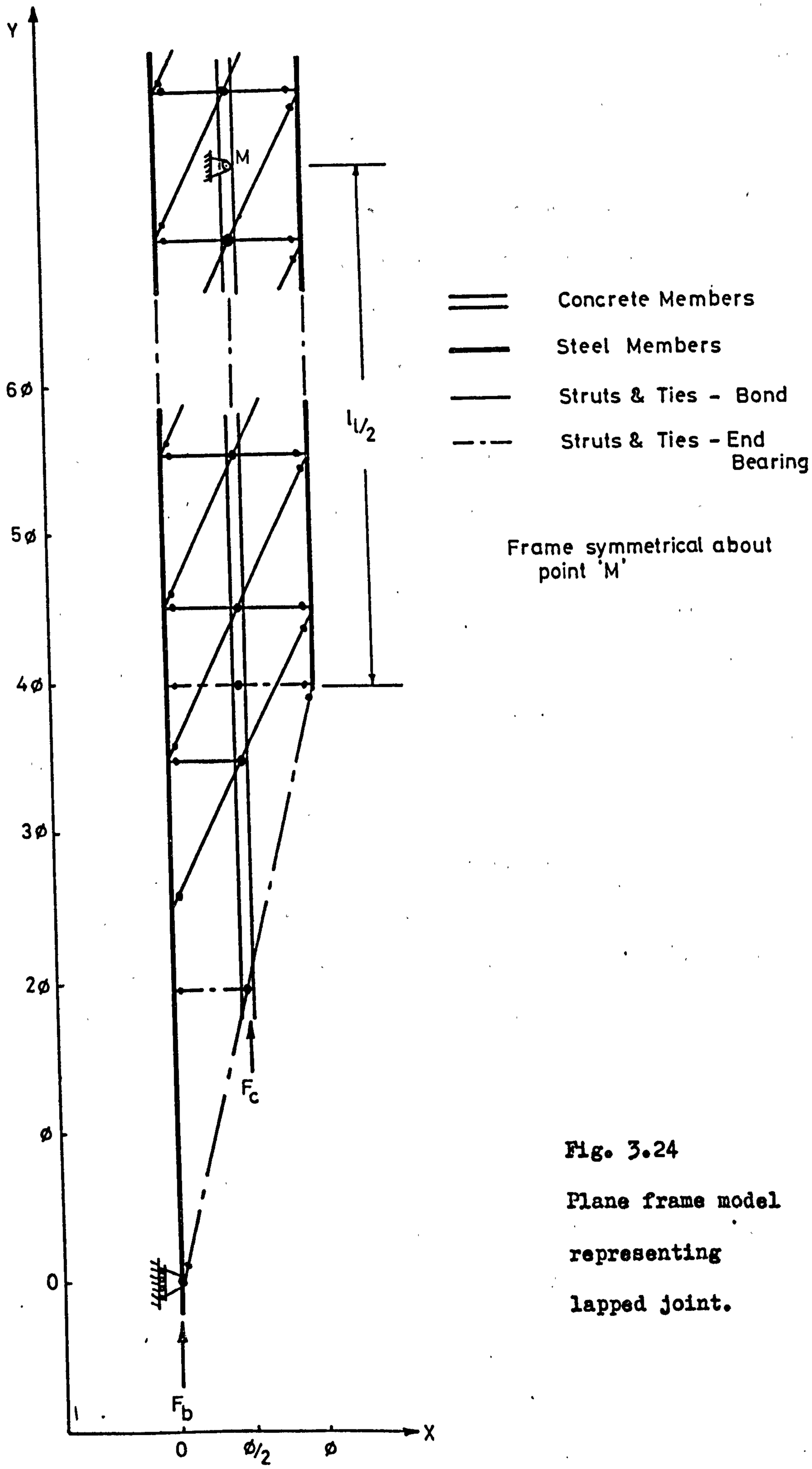

Fig. 3.24

Plane frame model representing lapped joint.

the cross sectional area of concrete in the column, the outside vertical members represent the main reinforcement, and the connecting members carry the transfer of load between reinforcement and concrete. The inclined members may be regarded as the compression 'cones' mentioned in section 3.1, and the horizontal members as the ring tension around the bars. All three bar conditions used in the experimental study were investigated, i.e. bond only, end bearing only, and bond and end bearing combined, the appropriate members being eliminated from the analysis where either bond or end bearing were eliminated.

The elastic moduli of the concrete and the reinforcement were obtained from test results presented in section 5.2.3 and table 4.3. A value of Young's Modulus of 208 kN/mm^2 was used for the reinforcement, and the stress-strain relationship for the concrete was taken to be

$$\sigma = -1.2\sqrt{f_c} \cdot \epsilon^2 + 4.5\sqrt{f_c} \cdot \epsilon \qquad 3.50$$

where σ = stress in N/mm^2

ϵ = strain x 10^3

and f_c = ultimate compressive strength of concrete in the test specimen

The stiffness of tension ties was found to have little influence on the variation of stress in the reinforcement, and a modulus of elasticity of

$$E_c = 4\sqrt{f_c} \times 10^3 \qquad 3.51$$

was used in all cases.

The inclination of the compression struts or 'cones' was derived from equations 3.20 and 3.25. Values of $\tan^{-1}0.5$ and $\tan^{-1}0.25$ were used for bond and end bearing struts respectively.

The cross-sectional area of the vertical members was varied according to the steel percentage considered, and both were considered to be infinitely stiff in bending. The cross-sectional area of the tension ties was calculated by consideration of the area of concrete in tension resisting the bursting forces, as shown in fig. 3.5(a). This was calculated to be

$$A_{ct} = \sqrt{2} \cdot c \cdot s_t \qquad 3.52$$

where A_{ct} = cross-sectional area of tie

c = minimum concrete cover to bar

s_t = spacing of ties in model

The cross-sectional area of the struts was determined from experimental results. Strut areas were chosen to give good agreement between computer model results and strains measured on the main reinforcing bars in actual column test specimens. The cross-sectional area of 'bond' members was constant throughout the lap length, and was the same whether end bearing was present or not, but the cross-sectional area of 'end bearing' members was reduced by 25% where both bond and end bearing were present to conform with experimental results. The area of the bond struts was equal to the area of the reinforcing bar, and the area of the end bearing struts was 4.8 or 3.6 times the area of the reinforcing bar. Both ties and struts were assumed to be pinned at each end. Loads on the vertical members were determined by strain compatibility in the column cross-section outwith the lapped joint.

No allowance was made for the presence of secondary reinforcement, or for slip between concrete and reinforcement. The model therefore represents a lapped joint at a low load, before the concrete cover cracks. At higher loads, the variation of steel stress

through a lapped joint will tend to even out, but the qualitative effect of the parameters investigated in the following sections will be the same as at lower loads. The model is intended to be simple, however, and is adequate for the purpose of showing the influence of the various parameters.

3.7.2 Fig. 3.25 shows the variation of stress in the reinforcement through a lapped joint for each of the three bar conditions investigated, i.e. bond only, end bearing only, and bond and end bearing combined. The analysis is made for a 20ϕ lap length, a concrete strength of 18 N/mm^2, a steel percentage of 3.2%, and for a load of 2000 kN on the column in each case.

It may be seen that, where bond of bars was eliminated within the lapped joint, over 30% of the total stress developed by the bars was developed by bond outwith the lapped joint. This proportion will increase with increasing load on the column. As these bond stresses also cause bursting forces, the value of the coefficient ψ used in equation 3.35 to calculate the ultimate bearing strength of the end of a bar will be greater than zero. Both the other bar conditions develop steel stresses mainly near the end of the bar, indicating a low value of ψ .

As all the parameters considered in the remainder of this section exert a similar influence on the variation of stress along a lapped bar whether bond or end bearing is present or not, results are presented only for bars with bond and end bearing combined.

3.7.3 The variation of steel stress through a 20 bar diameter lapped joint with a compression steel percentage of 3.2% is shown for various concrete strengths in fig. 3.26. The load on each column is that required to develop a steel stress outwith the lap of 115 N/mm^2.

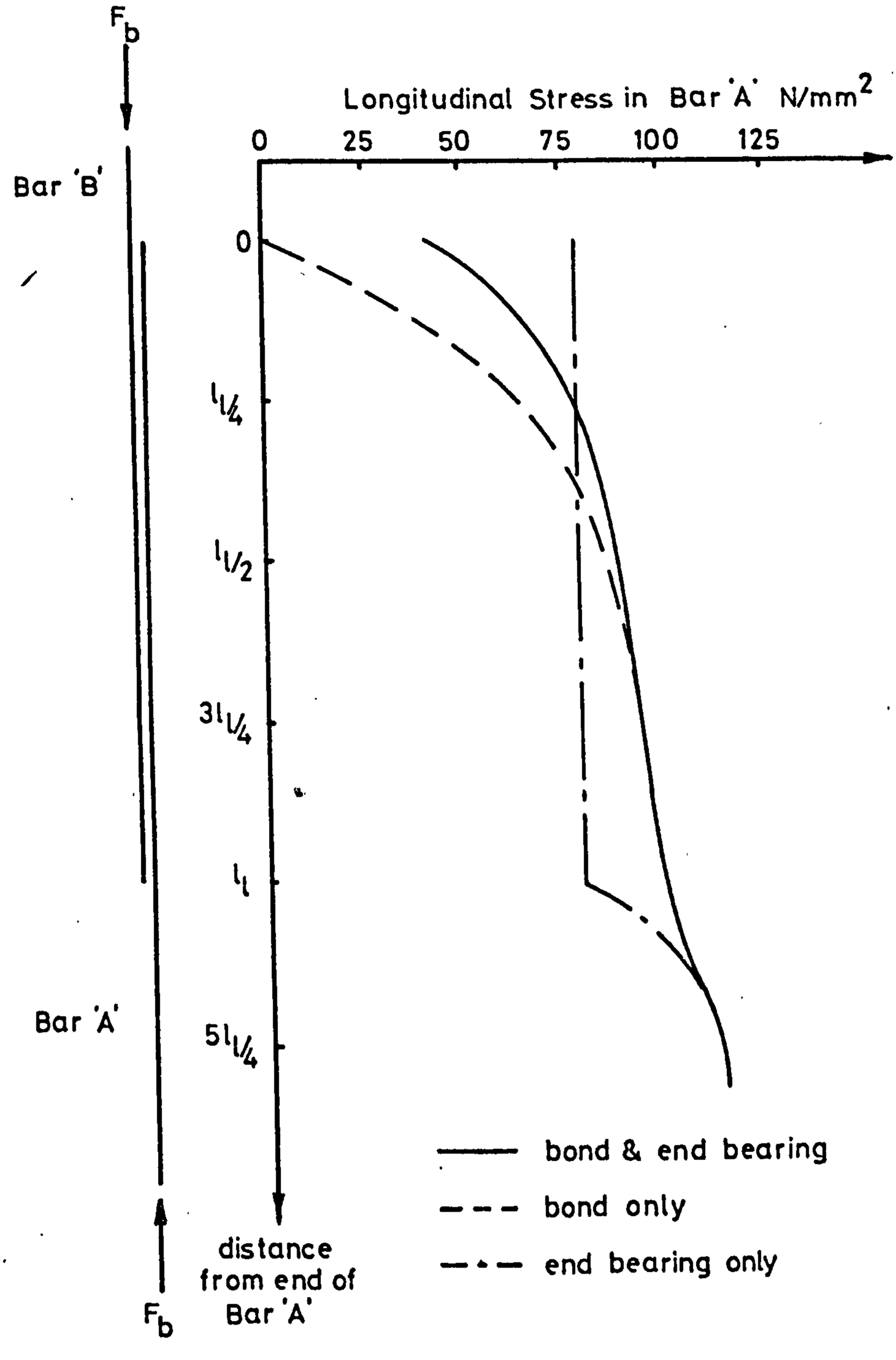

Fig. 3.25 Results of model analysis - variation of longitudinal stress in reinforcement for each bar condition.

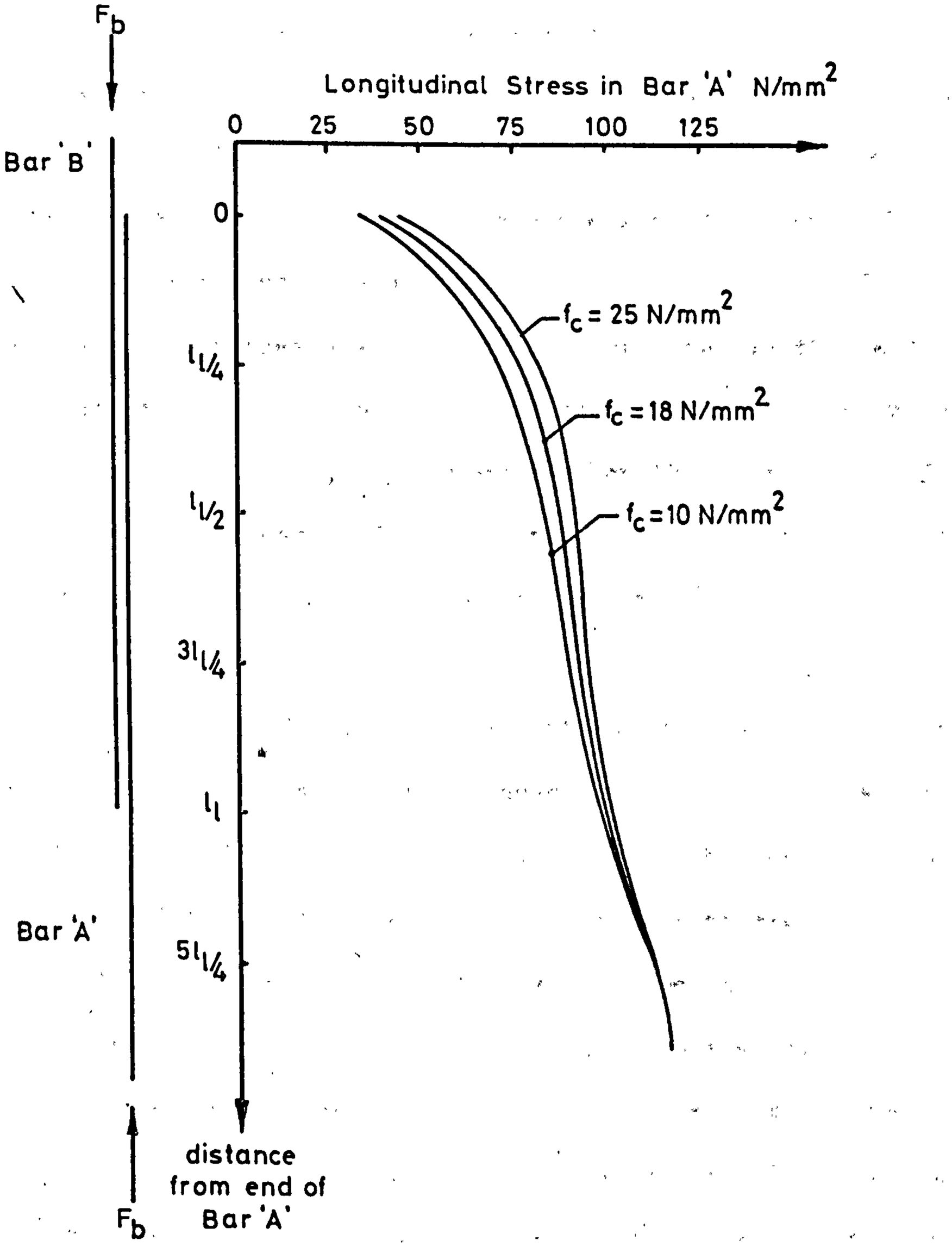

Fig. 3.26 Results of model analysis - variation of longitudinal stress in reinforcement through lapped joint for various concrete strengths - bars with bond and end bearing.

As would be expected, steel stresses vary more evenly with weaker and hence less stiff concrete. However, as the contribution of end bearing is lower, the load transferred by bond will be greater. The value of ψ will be greater for weaker concrete.

3.7.4 The variation of steel stress through lapped joints with lap lengths of 10 and 20 bar diameters is shown in fig. 3.27 for a concrete strength of 18 N/mm^2, a steel percentage of 3.2%, and a load of 2000 kN on the column in each case.

End bearing stresses are the same for both lap lengths, and develop about one third of the stress in the reinforcement outwith the lapped joint. However, the longer lap length has a less uniform variation of steel stress, and hence a more uneven distribution of bond stress and a lower value of the coefficient ψ defined in section 3.6.

3.7.5 The influence of the percentage of compression reinforcement in the cross section of a column is shown in fig. 3.28, for a concrete strength of 18 N/mm^2 and a 20 bar diameter lap length. The load on each column is that required to develop a stress of 115 N/mm^2 in the reinforcement outwith the lap. A steel percentage of 1% is the minimum allowed by B.S.C.P. 110:1972 in columns where other than nominal reinforcement is provided, and 5% is the maximum allowed when all reinforcement is lap jointed at the same height. 3.2% was the value most commonly used in specimens in the experimental part of the investigation.

For comparison, the variation of the stress in the reinforcement through a lapped joint is also shown for a steel percentage of infinity, i.e. no interaction between steel and concrete. This is an approximation to the situation in tension lapped joints, where tensile strength of the concrete contributes little to member

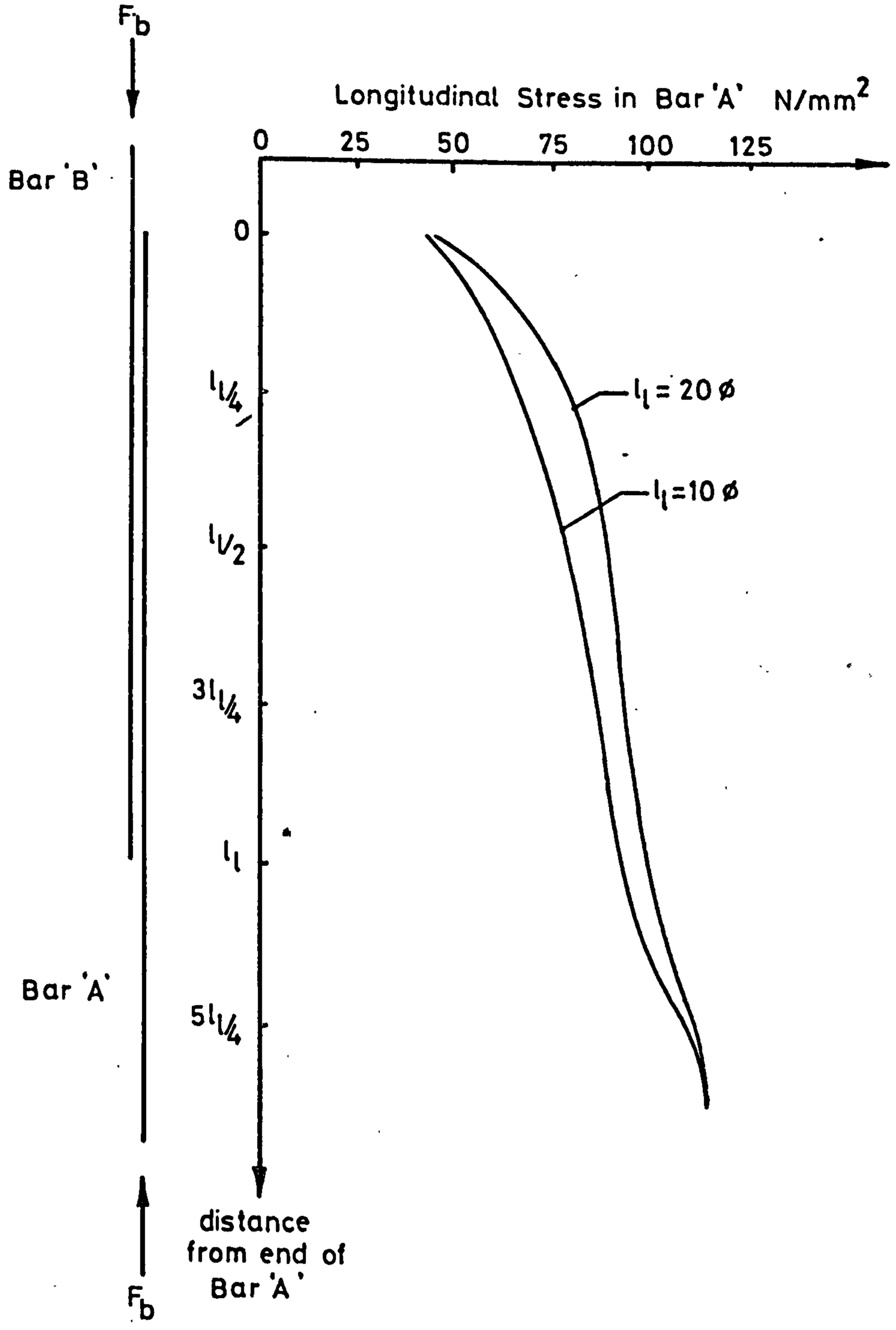

Fig. 3.27 Results of model analysis - variation of longitudinal stress in reinforcement for different lap lengths - bars with bond and end bearing.

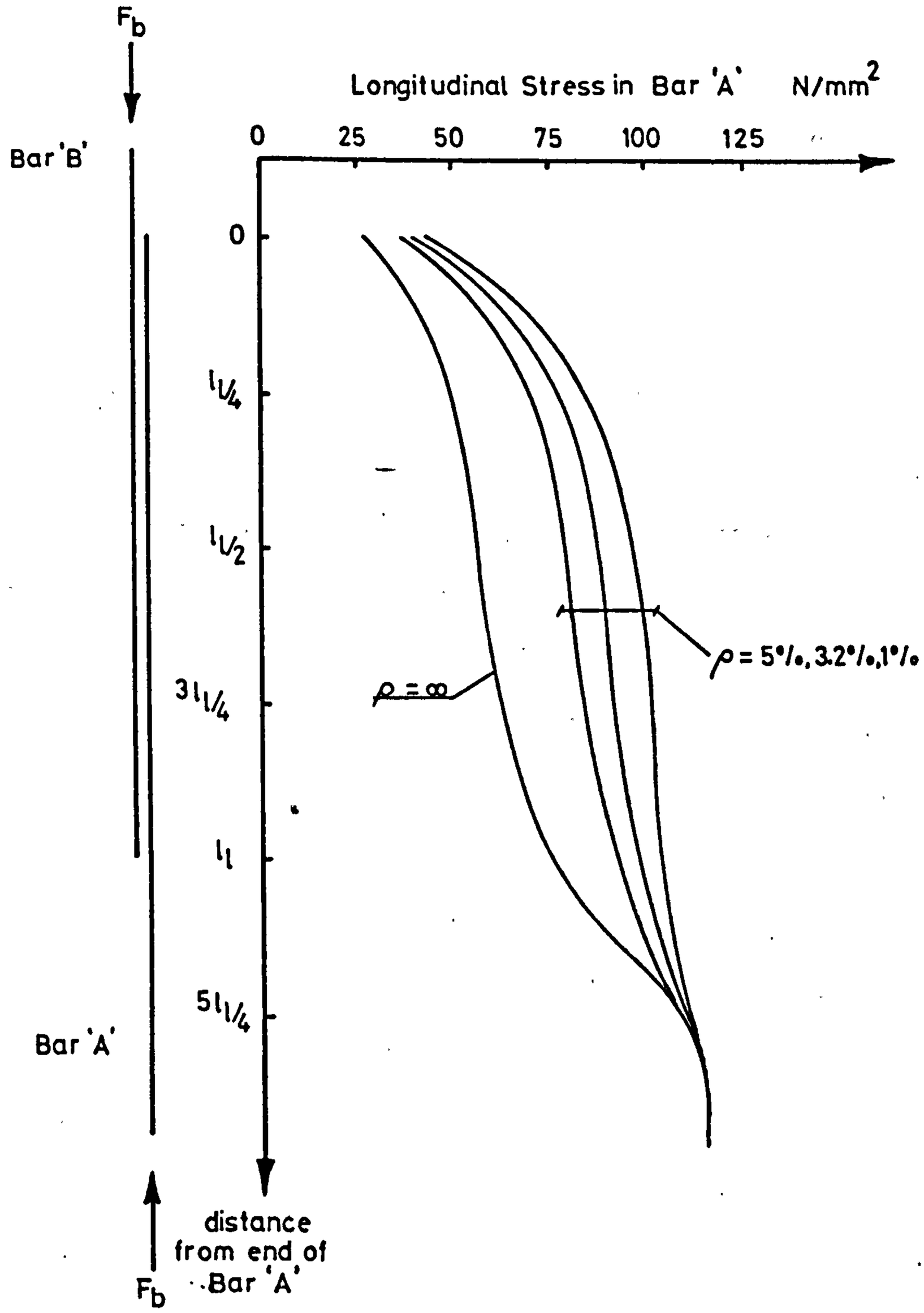

Fig. 3.28 Results of model analysis - variation of longitudinal stress in reinforcement through lapped joint for various steel/concrete ratios - bars with bond and end bearing.

strength. The line may be considered to represent a tension lapped joint with a tensile 'bearing stress' on the end of the bar.

Fig. 3.28 shows that higher steel percentages produce a more even build-up of steel stress in the main columns bars. A steel percentage of infinity produces a steel stress variation with the value of steel stress in the middle of the lapped joint 50% of the value outside. The transfer of force in each half is even, and so $\psi = 1$. In comparison, the ratio of steel stresses in the middle of a lapped joint to the steel stress outside are 0.7, 0.77 and 0.84 for steel percentage of 5%, 3.2% and 1% respectively, indicating successively lower values of ψ . However, even if $\psi = 1$, the total confining force on a bar will be overestimated by equation 3.41 unless the bursting forces produced by the bar are uniformly distributed, and all the confining reinforcement yields simultaneously.

Roberts and Ho[10] have suggested that a tension lapped joint may be regarded as two anchorages "back to back", as shown in fig.3.29, with each anchorage being half the length of the lapped joint and developing approximately half the total stress developed by the lapped joint.

The model analysis showed that the slope of variation of steel stress along a lapped bar was always a minimum in the middle of the lap. If Roberts and Ho's[10] concept is applied to compression lapped joints, the two "back to back" anchorages must therefore be of the same length, but the relative proportions of the stress developed by each anchorage will depend on many factors, such as the concrete strength, lap length, and the percentage of reinforcement in the cross section. For a 20 ϕ lap length, 1% compression reinforcement in the cross section and a concrete strength of 18 N/mm^2, one anchorage would be required to develop 84% of the total stress

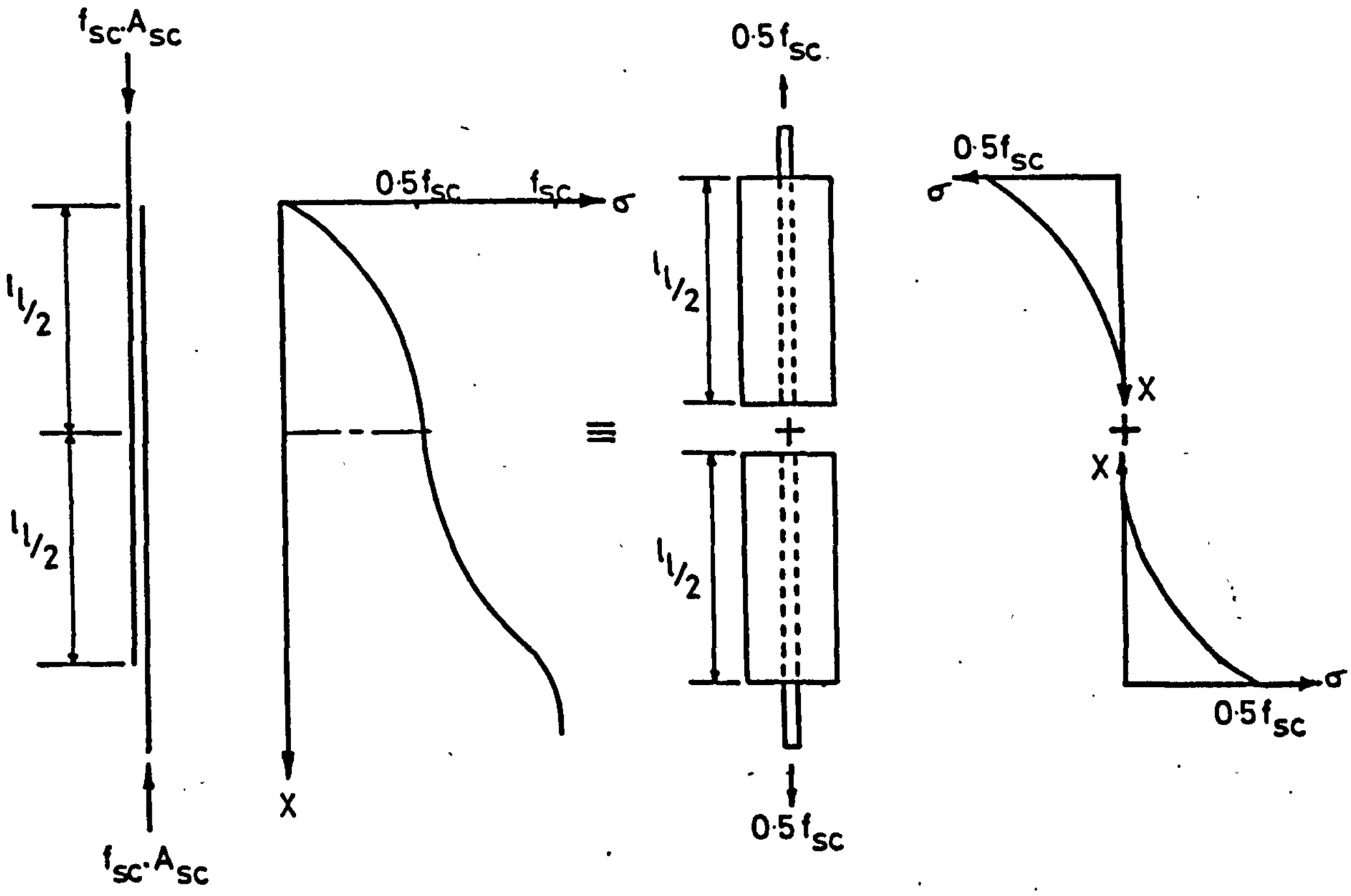

σ - stress in bar
X - distance along bar

Fig. 3.29 Tension lapped joint and equivalent anchorage, after Roberts and Ho[10].

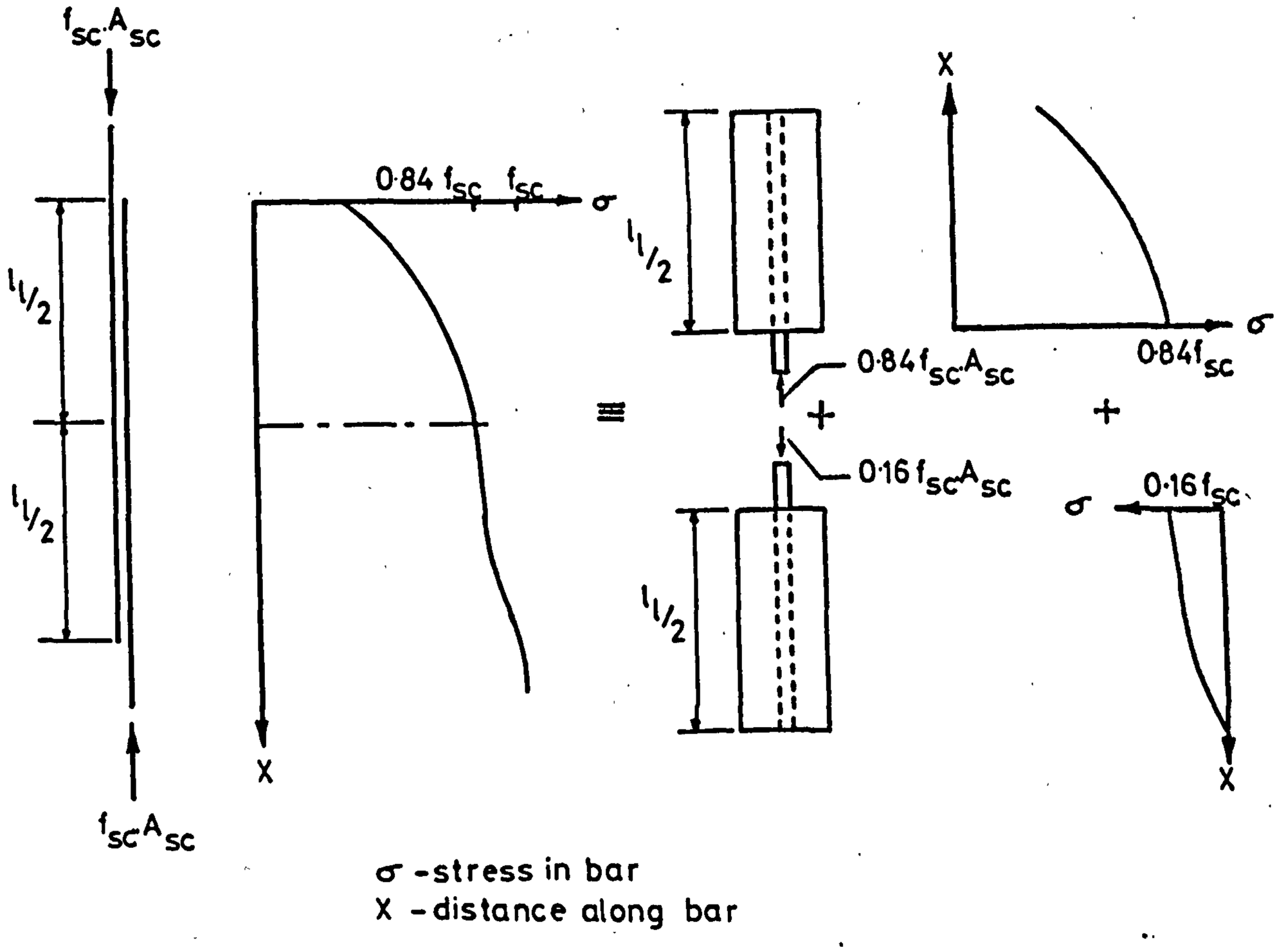

σ - stress in bar
X - distance along bar

Fig. 3.30 Compression lapped joints and equivalent anchorages.

developed by the lapped joint, while the other would only be required to develop 16%, as shown in fig. 3.30. It is concluded that, although Roberts and Ho's concept might be usefully applied to the design of tension lapped joints, it is unsuitable for use with compression lapped joints.

3.8 Design of Experiments

The main experimental study was conducted on full scale columns with lapped joints. The primary aim of the initial test series was to investigate the contribution of the bearing of the ends of the reinforcing bars on the concrete to joint strength. In order to examine the strength of end bearing both by itself and in combination with bond, some specimens were constructed with the bearing of the ends of the bars eliminated, and others with bond eliminated within the lap length. These tests were carried out on specimens with lap lengths of 10, 15 and 20 bar diameters, to see if the contribution of end bearing was affected by lap length. It had originally been intended to investigate longer lap lengths, but as a lap length of 20ϕ was found to develop a stress close to the yield strength of the reinforcement, it was decided that tests with longer lap lengths would yield little additional information. The small range of lap lengths was instead investigated for a range of other parameters.

It was decided to investigate columns with large diameter reinforcing bars, as this was considered to be closest to present construction practices. In addition, Leonhardt and Teichen[2], and Sommerville, Morris and Clements[29] had found that large diameter bars produced the most severe splitting of the concrete where a bar was stopped-off, and, as reported by Tepfers[4] and others, larger bars have been found to give lower values of bond strength. Columns were generally of 400mm.sq. cross section, and were reinforced with

four pairs of lapped bars of 25mm, 32mm and 40mm disc, which corresponds to compression steel percentages of 1.2%, 2.0% and 3.2%. However, it was soon realised that, for the reasons outlined in section 5.2, it was impossible to determine the steel stress developed by a lapped joint with sufficient accuracy for the lower steel percentage. The highest steel percentage used in the initial test series was therefore used in the remaining test series.

The concrete cube strength, initially intended to be constant at 35 N/mm^2 ranged from 29.7 N/mm^2 to 41.8 N/mm^2 at time of test in the first test series, and so a second test series was set up, in which the concrete strength of the specimens was deliberately varied, and all other variables were held constant. In this series the strength of lapped joints both with and without end bearing was investigated. A lap length of 10 bar diameters was used for all but one of the specimens in this series.

A third series examined the influence of secondary reinforcement on joint strength. In the two previous series, links were provided in what was felt to be the optimum arrangement, and in the third test series, the effect of stronger links, weaker links and badly positioned links was investigated.

A cover/bar diameter ratio of 1.25 was used throughout the investigation, as it was felt that it was impracticable to increase the parameter.

In addition to the tests on columns with lapped joints, two columns were tested with continuous reinforcement, to check the accuracy of the method of calculating ultimate bar stress described in section 5.2.

In all the test series, it was considered best to investigate

the many variables briefly, and attempt correlation with the proposed theory, rather than to make large numbers of tests on a few variables, with the aim of a statistical analysis.

A short series of push-in tests was also conducted, to compare the bond strength of the two types of reinforcing bar used in the main series.

CHAPTER 4

DESCRIPTION OF EXPERIMENTAL WORK.

4.1 General Description of Test Specimens.

Details of the test specimens used in the main experimental programme are presented in table 4.1 and in fig. 4.1.

The joint detail chosen for the lapped joint was unusual, but was designed to give a similar column cross-section above and below the lapped joint. This gave the same concrete cover and the same confinement by secondary reinforcement to each bar. Excluding the influence of any variation in concrete strength throughout the height of a column, the strength of specimens was therefore the same above and below the lapped joint. However, the joint detail was not one that could be used in practice, as it would be difficult to position the reinforcement accurately. The centre of the lap was usually at the mid-height of a column, but, where longer laps were used, the position of the lap was raised to permit measurement of strains outwith the lap.

In some tests, it was decided to eliminate the bearing of the ends of the reinforcing bars on the concrete. This was achieved by gluing cylinders of expanded polystyrene, about 25mm thick and of slightly larger diameter than the bar, to the square cut ends of the bars before the concrete was cast.

In other tests, bond between the bars and the concrete was eliminated throughout the length of the lap by wrapping each bar with a 5mm thick layer of expanded polystyrene to prevent bearing by the bar deformations, and a covering of P.V.C. tape, to provide a seal and to protect the polystyrene. At the points where links were provided, the bars were not wrapped, but a deformation was ground off and the bar surface polished, to minimize bond stresses

TABLE 4.1 DETAILS OF REINFORCEMENT

Column	Main Reinforcement		Secondary Reinforcement		Lap Length	No. of Links in Lap	Notes
	Dia (mm)	Yield Strength (N/mm^2)	Dia (mm)	Yield Strength (N/mm^2)	(mm)		
A 101	25	410*	6	310°	250	2	
102	"	410*	"	310°	500	3	
103	"	410*	"	310°	625	4	
104	"	410*	"	310°	500	3	Bond
105	"	410*	"	310°	500	3	E.B.
111	"	472	"	385	250	2	2
113	"	"	"	"	500	3	2
114	"	"	"	"	250	2	Bond. 2
116	"	"	"	"	500	3	Bond. 2
201	32	435	8	310°	640	3	
201B	"	442	"	390	"	3	
202	"	435	"	310°	"	3	Bond
202B	"	442	"	390	"	3	Bond
203	"	435	"	310°	"	3	E.B.
300	40	445	10	310	-	-	C
301	"	"	"	"	400	2	
302	"	"	"	"	600	3	
302B	"	"	"	"	"	3	
302C	"	415	"	390	"	3	
303	"	445	"	310	800	3	
303B	"	"	"	"	"	3	
304	"	"	"	"	400	2	Bond
304B	"	"	"	"	"	2	Bond
305	"	"	"	"	600	3	Bond

TABLE 4.1 Contd.

Column	Main Reinforcement		Secondary Reinforcement		Lap Length	No. of Links in Lap	Notes
	Dia (mm)	Yield Strength (N/mm^2)	Dia (mm)	Yield Strength (N/mm^2)	(mm)		
306	40	445	10	310	800	3	Bond
306B	"	415	"	390	"	3	Bond
307	"	445	"	310	400	2	E.B.
308	"	"	"	"	600	3	E.B.
308B	"	"	"	"	"	3	E.B.
308C	"	415	"	390	"	3	E.B.
308D	"	"	"	"	"	3	E.B.
309	"	445	"	310	800	3	E.B.
B 300	"	415	"	390	-	-	C
301	"	"	"	"	400	2	
301B	"	"	"	"	"	2	
311	"	"	"	"	"	2	
321	"	"	"	"	"	2	
331	"	"	"	"	"	2	
304	"	"	"	"	"	2	Bond
304B	"	"	"	"	"	2	Bond
314	"	"	"	"	"	2	Bond
334	"	"	"	"	"	2	Bond
334B	"	"	"	"	"	2	Bond
313	"	"	"	"	800	3	
C 301	"	"	8	240	400	2	
303	"	"	"	"	800	3	
311	"	"	10	390	400	1	
311B	"	"	"	"	"	1	

TABLE 4.1 Contd.

Column	Main Reinforcement		Secondary Reinforcement		Lap Length (mm)	No. of Links in Lap	Notes
	Dia (mm)	Yield Strength (N/mm^2)	Dia (mm)	Yield Strength (N/mm^2)			
313	40	415	10	390	800	2	
321	"	"	"	"	400	2	
324	"	"	"	"	"	2	
324B	"	"	"	"	"	2	
326	"	"	"	"	800	3	

Notes

Bond - End bearing of the reinforcement eliminated - see section 4.

E.B. - Bond eliminated throughout lap length - see section 4.

C - Column without lap joint.

2 - Type 2 column.

* - Nominal strength.

o - Strength of 10mm diameter secondary reinforcement from same source.

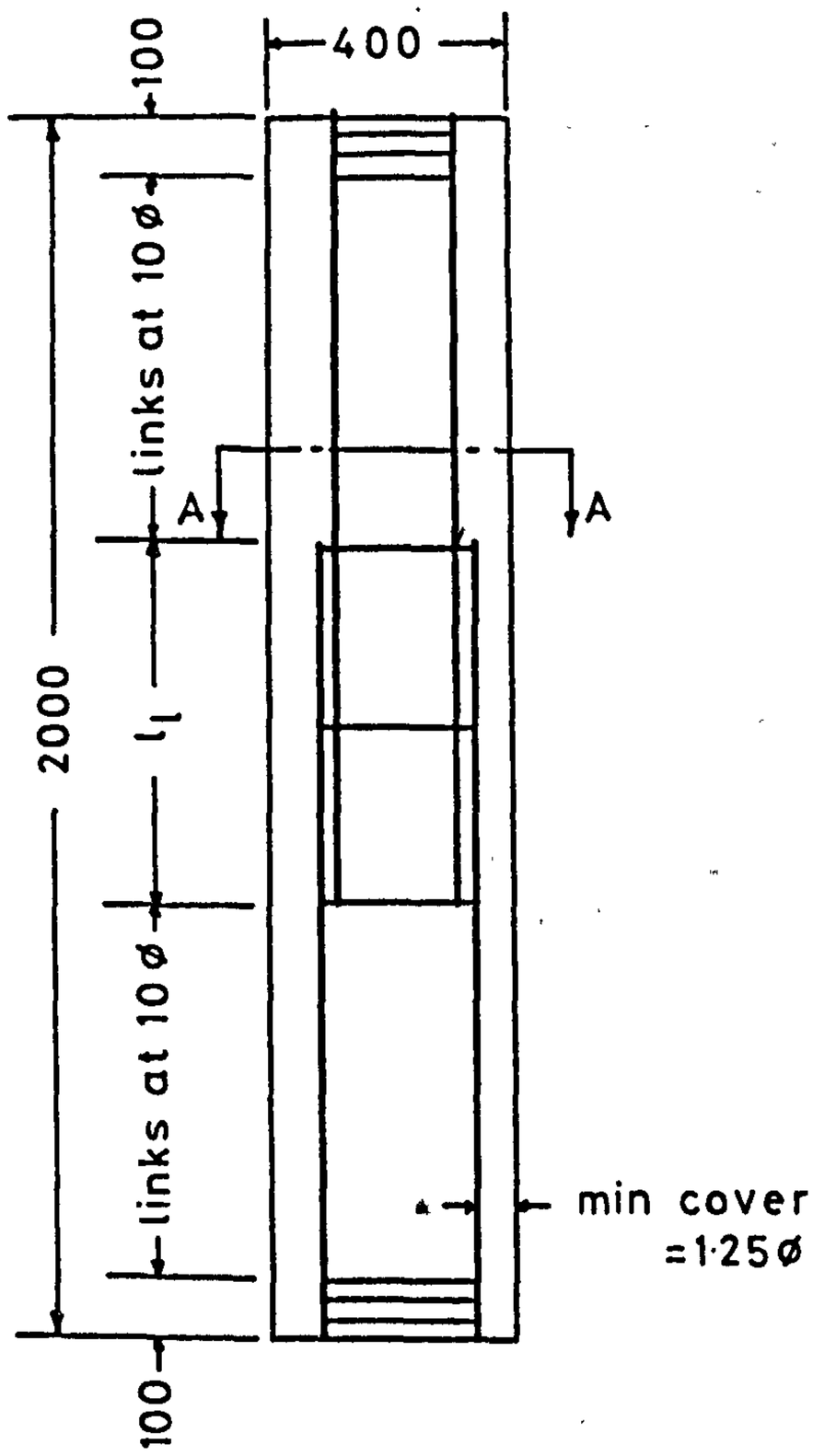

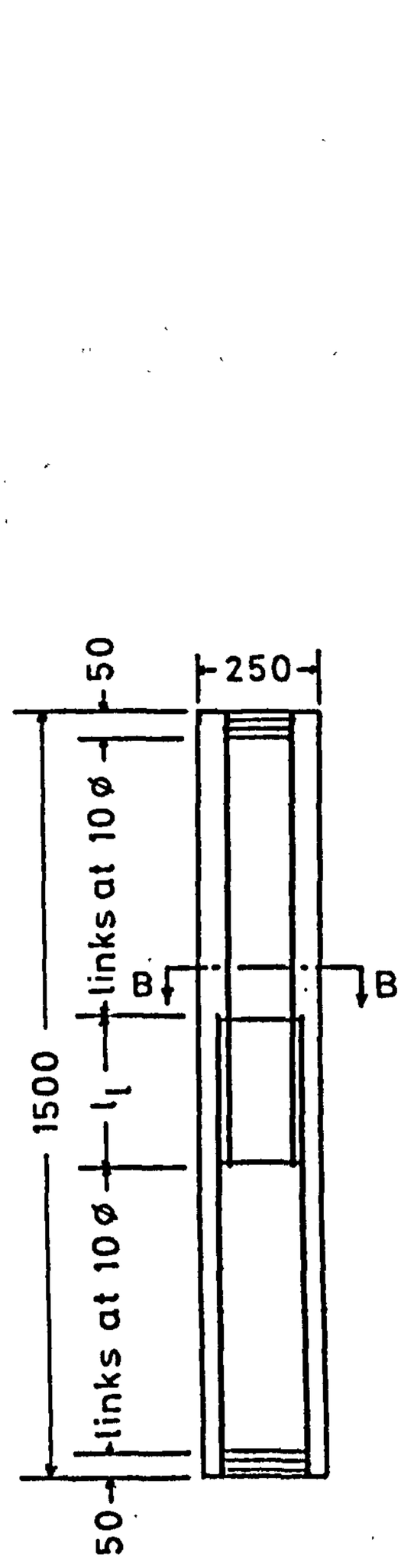

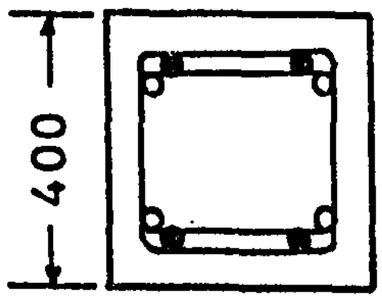

Section A-A

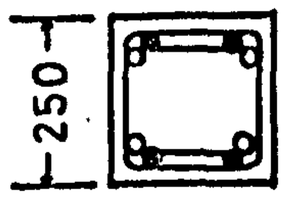

Section B-B

dimensions in mm.

Type 1 Type 2

Fig. 4.1(a) Typical column details.

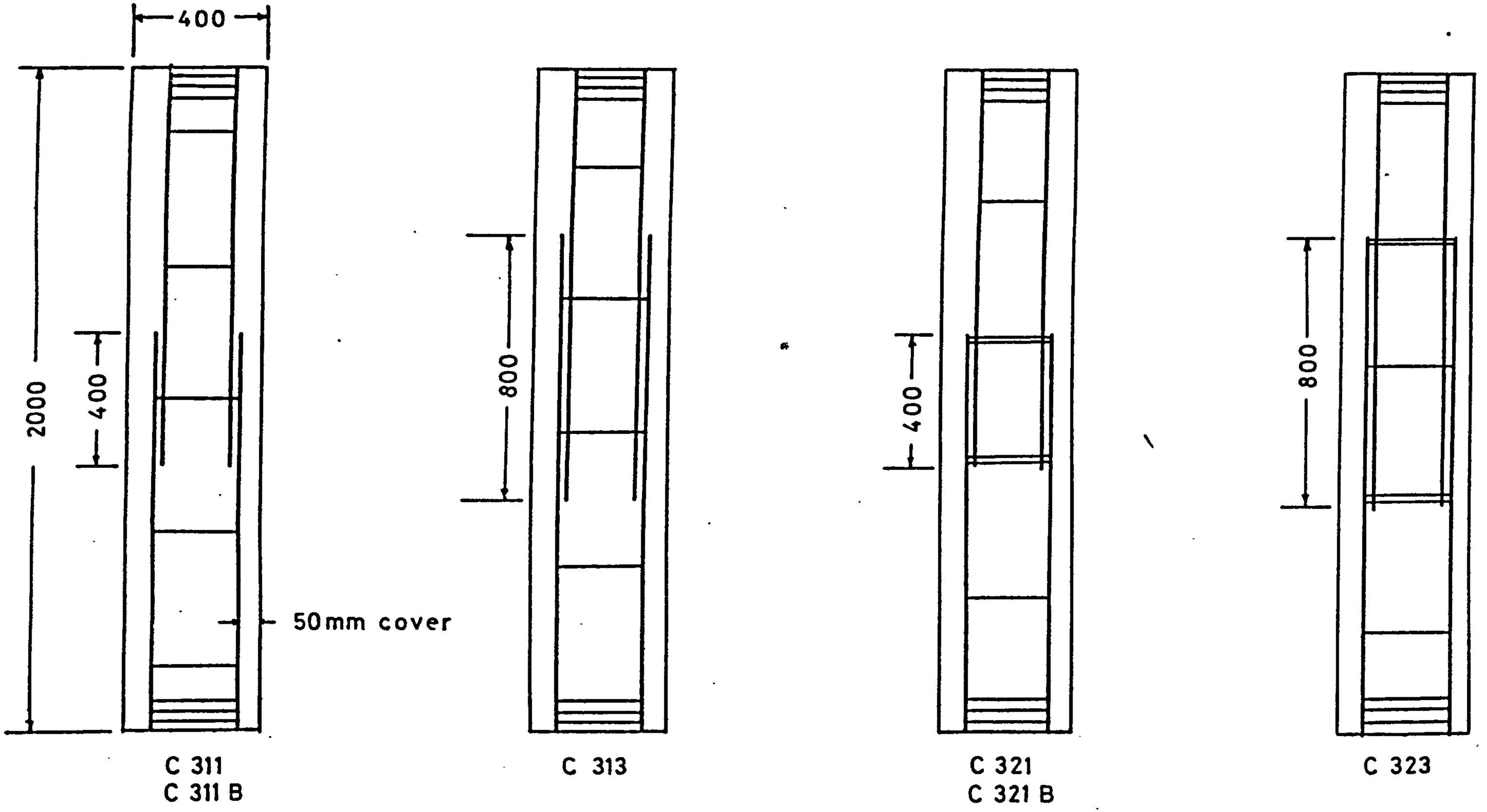

C 311
C 311 B

C 313

C 321
C 321 B

C 323

dimensions in mm.
Column sections as in Fig 4.1a
Spacing of links = 400 mm

Fig. 4.1(b) Special column details.

and to allow the links to act in restraining the main reinforcement.

4.2 Materials

4.2.1 The concrete was manufactured from ordinary Portland cement, 20mm maximum size washed irregular gravel, and washed concreting sand. Variations in grading of aggregates caused slight variations in mix proportions throughout the tests. Three different mixes were used, the weakest having medium workability, and the other two low workability. Full details of mix proportions and the results of tests on standard test specimens are given in Table 4.2.

4.2.2 Two makes of reinforcing bar, shown in fig. 4.2, were used for the main reinforcement.. Earlier specimens were manufactured with 'Unisteel 410' reinforcement, but manufacture of this type of bar ceased 12 months after the start of the experimental investigation. It was decided to continue to use hot rolled ribbed deformed bars rather than to change to hot rolled cold twisted bars, and 'Hybar' reinforcement was chosen as it had a rib pattern similar to that of 'Unisteel 410'. Both reinforcing bars fulfilled the conditions of B.S.C.P. 110; 1972 for type 2 deformed bars. Typical stress-strain curves for each, determined from compression tests, are presented in fig. 4.3. In those tests where the ends of bars bore on the concrete, the 'Unisteel 410' bars had shear cut ends. However, as 'Hybar' reinforcement was obtainable only in 12 m.lengths, bars had to be cut to length by saw in the laboratory, and the ends were therefore square. Plain round mild steel bars were used for secondary reinforcement, with yield strengths ranging from 240 N/mm^2 to 390 N/mm^2. A typical stress-strain curve, determined from a tension test, is shown in fig. 4.4. All bars were used 'as delivered', their condition varying from clean to moderately rusted. Details of reinforcement used are given in tables 4.1 and 4.3.

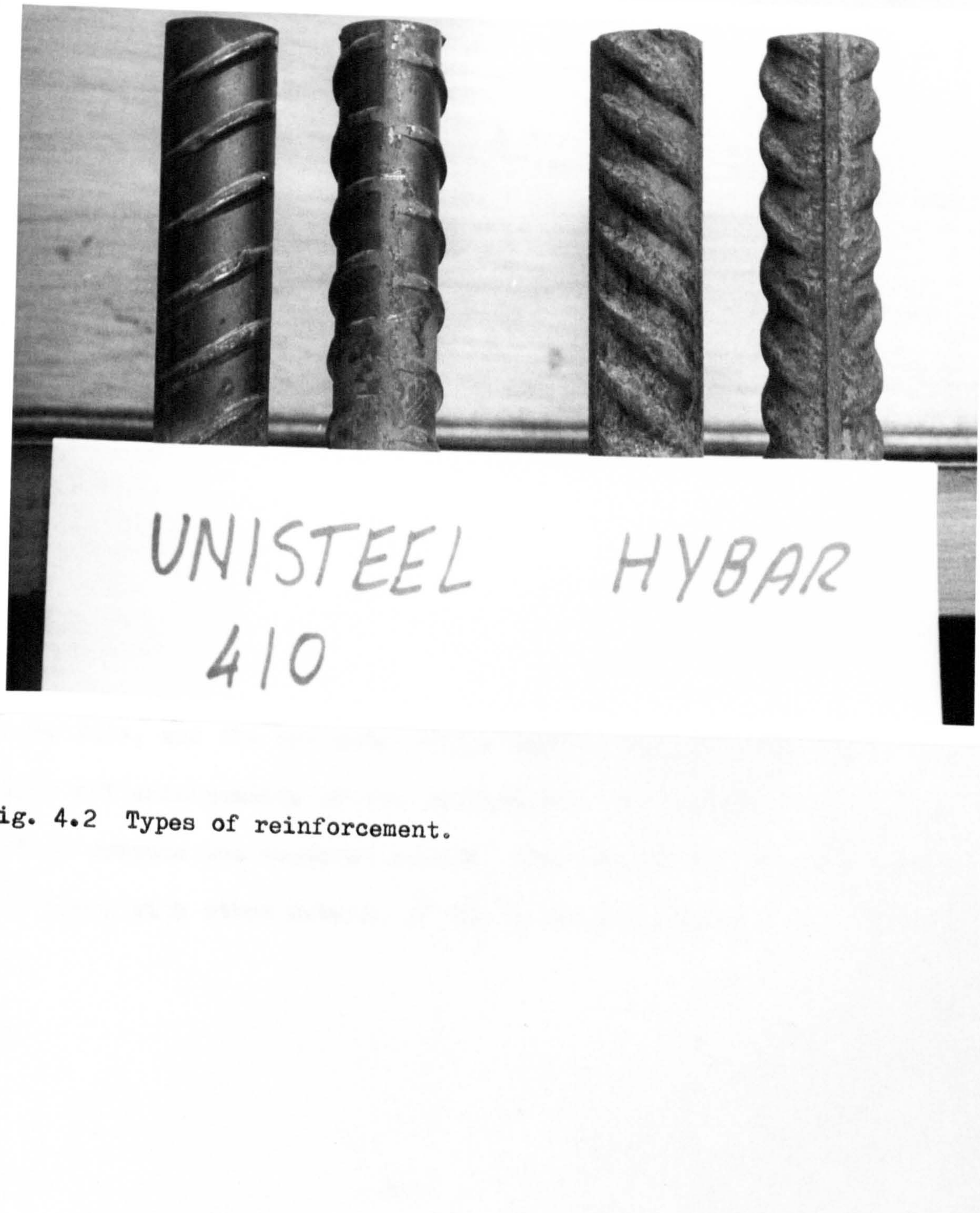

Fig. 4.2 Types of reinforcement.

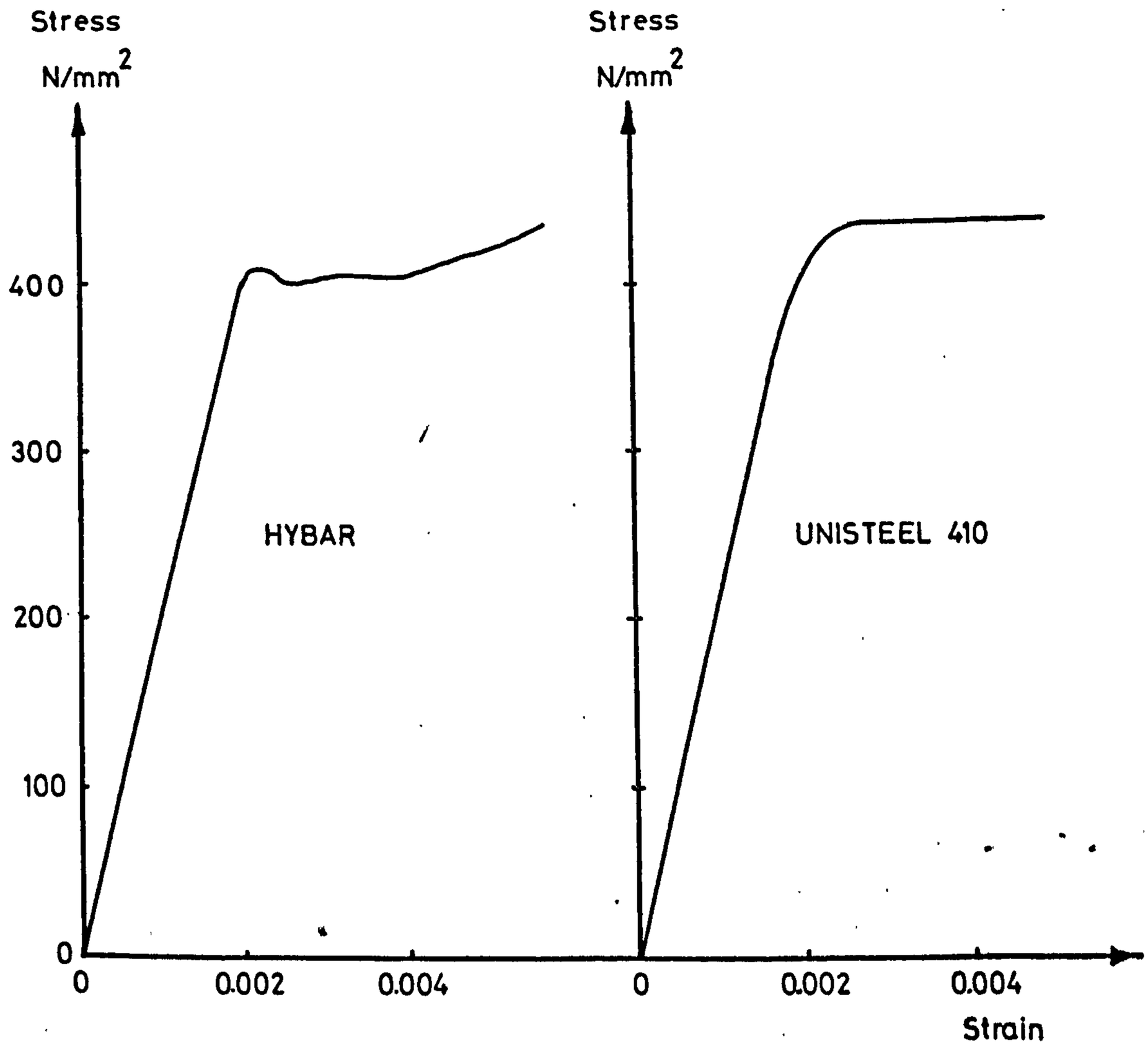

Fig. 4.3 Typical stress-strain relationships for compression reinforcement.

To calculate the area of a rib above the bar surface, and the value of $\int_{-\frac{\pi}{2}}^{\frac{\pi}{2}} \phi_{/2} h_r . \cos\mu . d\mu$ (equation 3.12), bars were saw-cut parallel to the ribs, and the cut ends photographed. Measurements were then scaled off enlargements of the photographs, and numerical integration used to compute the required values. The results are given in table 4.3, along with other details of the reinforcing bars.

TABLE 4.2 CONCRETE MIX PROPORTIONS AND STRENGTHS.

Column	Mix Proportions (By Weight)				Age at Test	Concrete Cube Strengths (cured wet)	Cylinder Splitting Strengths (cured dry)
	Water	Cement	Sand	Aggregate	(days)	N/mm^2	N/mm^2
A 101	0.56	1.0	1.8	3.6	17	31.5	2.5
102	"	"	"	"	16	29.7	2.3
103	"	"	"	"	21	34.0	2.3
104	"	"	"	"	20	32.8	2.9
105	"	"	2.2	"	22	32.2	2.2
111	"	"	"	"	21	39.5	2.7
113	"	"	"	"	21	38.0	2.5
114	"	"	"	"	21	36.0	2.3
116	"	"	"	"	20	40.2	2.3
201	"	"	1.8	"	17	30.2	2.4
201B	"	"	2.2	"	20	41.8	2.6
202	"	"	"	"	22	34.8	2.4
202B	"	"	"	"	22	37.7	2.5
203	"	"	"	"	25	38.0	3.2
300	"	"	"	"	26	41.2	2.2
301	"	"	"	"	21	32.6	2.5
302	"	"	1.8	"	24	32.4	2.4
302B	"	"	2.2	"	21	33.8	2.5
302C	"	"	2.8	3.1	22	41.0	2.8
303	"	"	2.2	3.6	21	31.0	2.6
303B	"	"	"	"	20	37.4	2.3
304	"	"	"	"	22	33.4	2.7
304B	"	"	"	"	22	37.1	2.4
305	"	"	"	"	23	39.8	2.8
306	"	"	"	"	23	37.9	2.3

TABLE 4.2 contd.

Column	Mix Proportions (By Weight)				Age at Test (days)	Concrete Cube Strengths (cured wet) N/mm^2	Cylinder Splitting Strengths (cured dry) N/mm^2
	Water	Cement	Sand	Aggregate			
306B	0.56	1.0	2.7*	3.1	22	35.1	2.3
307	"	"	2.2	3.6	22	35.1	2.5
308	"	"	2.2	3.6	21	36.9	2.6
308B	"	"	2.2	3.6	22	34.6	2.2
308C	"	"	2.6*	3.3*	20	41.0	2.6
308D	"	"	2.6*	3.3*	17	38.2	2.4
309	"	"	2.2	3.6	21	31.9	2.3
B 300	0.80	"	4.0*	4.8*	11	19.1	1.4
301	"	"	3.2	4.8	7	14.2	1.3
301B	"	"	3.6	3.9	6	13.6	1.1
311	0.62	"	2.4	4.5	6	26.5	2.4
321	0.56	"	2.2	3.6	5	29.4	2.5
331	0.56	"	2.2	3.6	19	37.7	-
304	0.80	"	3.8*	4.5*	9	13.9	1.1
304B	0.80	"	4.0*	4.8*	8	14.7	1.6
314	0.62	"	3.0*	3.9*	7	15.7	1.4
334	0.56	"	2.6*	3.3*	20	49.3	-
334B	0.56	"	2.6*	3.3*	18	32.6	2.1
313	0.62	"	3.1	3.4	6	25.2	2.2
C 301	0.56	"	2.6*	3.3*	22	37.7	2.3
303	0.56	"	2.6*	3.3*	20	32.4	2.4
311	0.56	"	2.2	3.6	23	33.4	2.5
311B	0.56	"	2.2	3.6	21	34.1	2.4

TABLE 4.2 Contd.

Column	Mix Proportions (By Weight)				Age at Test (days)	Concrete Cube Strengths (cured wet) N/mm^2	Cylinder Splitting Strengths (cured dry) N/mm^2
	Water	Cement	Sand	Aggregate			
313	0.56	1.0	2.7*	3.1*	21	37.0	2.3
321	0.56	"	2.6*	3.3*	19	31.8	2.2
324	0.80	"	3.2	4.8	6	14.7	1.3
324B	0.80	"	3.5*	4.5*	7	12.2	1.4
326	0.62	"	3.1	3.4	6	21.2	2.0

Sand and aggregate source Mid Ross quarry, except where marked * when Hyndford quarry.

TABLE 4.3 DETAILS OF COMPRESSION REINFORCEMENT

BAR TYPE	UNISTEEL 410			HYBAR		
Diameter mm	25	32	40	25	32	40
X-Sect. Area mm^2	491	804	1220	491	807	1255
Yield Strength N/mm^2	410*	435	445	472	442	415
Young's Modulus kN/mm^2	-	-	209	-	-	207
Rib Area (mm^2)	-	-	185	-	-	220
Rib Spacing (mm)	16+	21+	26	15+	19+	24
$\int_{-\frac{\pi}{2}}^{\frac{\pi}{2}} \frac{\phi}{2} h_r \cos\mu . d\mu .$ (mm^2)	32+	52+	81	38+	62+	96.4
Inclination of Ribs to Bar Axis	45°	45°	45°	45°	45°	45°

* Nominal value

\+ Found by proportion from result for 40mm Diameter Bars.

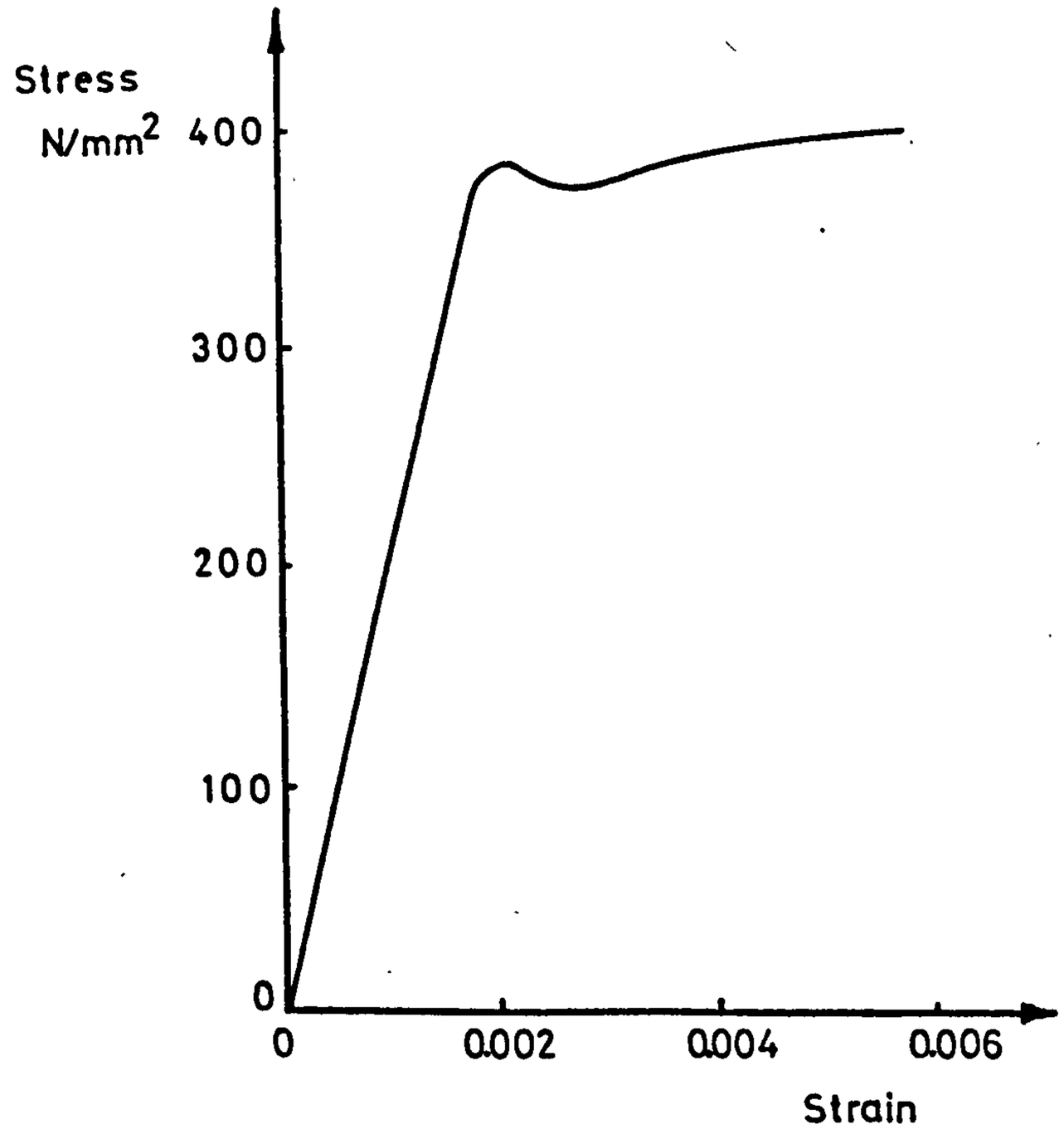

Fig. 4.4 Typical stress-strain relationship for secondary reinforcement.

4.3 Fabrication of Test Specimens

All columns were cast vertically in the laboratory. The aggregates used were surface dry, and the concrete was mixed in a pan mixer. Eight batches were required for a 400mm sq. x 2000mm high column, and two batches for a 250mm sq. x 1500mm high column. Proprietary spacers were used to maintain correct cover during concreting, and the concrete was compacted by internal vibration.

Formwork, of film faced plywood, was stripped approximately 24 hours after casting, and the specimen covered with moist hessian for at least another 24 hours. Specimens were then stored in the laboratory until tested.

Standard 150mm cubes and cylinders were also cast at the same time as the columns. The cubes were cured in water at a temperature

of 20°C. and the cylinders were cured alongside the columns in the laboratory, until required for testing. Cubes and cylinders were tested at the same age as the columns.

4.4 Test Procedure.

A few days before testing, columns were given a coat of thin white emulsion paint, so that cracks could be observed more easily as the test proceeded. Bold red lines were also painted on all column faces to indicate the position of reinforcement within the specimen.

The columns were loaded in a 1,000 tonne capacity Losenhausen testing machine, which was equipped with a servo-valve controlled by feedback from a linear variable displacement transformer, enabling column shortening to be used to control loading. The test set-up is shown in fig. 4.5.

A thin layer of plaster was used to bed the column, and set it vertical. A theodolite was used to check that the specimen was plumb. The top of the column was also bedded in with a thin layer of plaster, and lengths of 25mm sq. hollow steel section were bolted across the column in both directions, top and bottom, to resist premature failure away from the lap.

Just before the start of a test, the transmission time of an ultrasonic pulse between two opposite faces of a column was measured at 100mm vertical intervals throughout the column height, using a 'PUNDIT' digital display tester. This, it was hoped, would give a measure of the variation of concrete strength throughout the column height, and also provide as estimate of concrete strength. The path length of the pulse was measured using calipers, and testing was conducted in accordance with B.S. 4408 part 5[44].

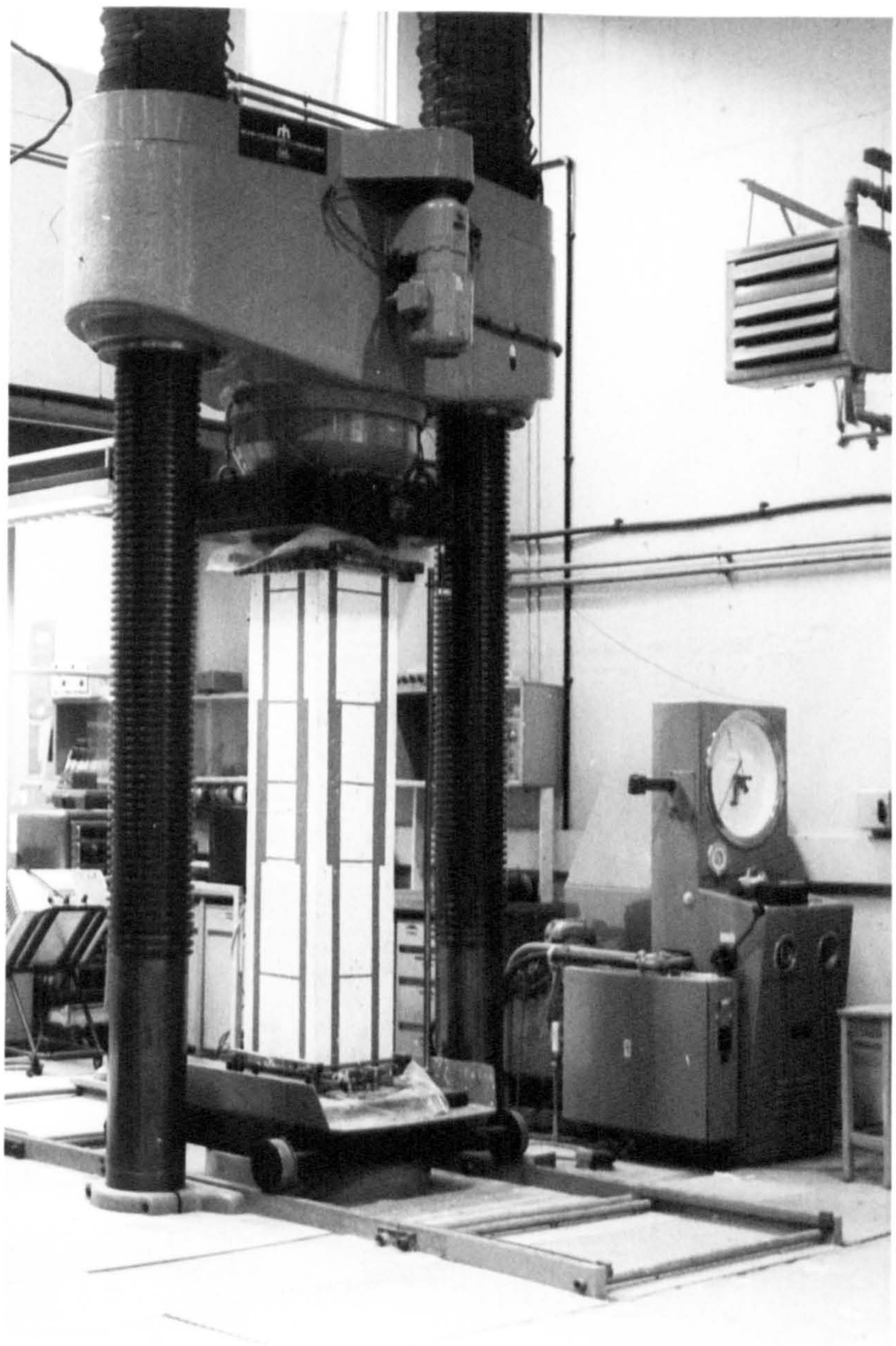

Fig. 4.5 General view of test set-up.

In order to prevent sudden, explosive failures, columns were loaded at a constant rate of deflection, corresponding to an average rate of strain over the column height of approximately 1500 x 10^{-6}/hour. This method of loading also allowed the falling branch of the load-deflection curve to be followed, and permitted study of the ductility of the column. The load on the column was first cycled a few times, between zero and 10% of the predicted ultimate load of the column, before zero readings were taken, to try to eliminate the small concave-up section often found at the start of the load-deflection curve for concrete. Whilst still rising, loading was halted at 200 kN or 250 kN intervals to allow strain readings to be taken, and to record crack development. During tests, the bottom platen of the testing machine was fixed, but the top platen was free to rotate on a spherical seating.

Loading was stopped once the concrete had cracked sufficiently to allow exposure and examination of the bars within the lap. The cones of concrete pushed out by the bearing of the end of the bars were recovered where possible, and the angle of the apex of the cone measured to obtain an estimate of the angle of internal friction of the concrete.

4.5 Instrumentation

The overall shortening of the columns was measured by a linear variable displacement transformer (L.V.D.T.), and the output monitored continuously on a chart recorder in most tests. The tilting of the top platen which occured in some tests will, however, have affected the results, as indicated in fig. 4.6.

Demountable mechanical strain gauges, usually of 50.8mm gauge length, were used to measure concrete surface strains. Generally about 12 gauge points per column were used, but in those tests in

which electrical resistance strain gauges were fitted to the reinforcement, there were up to 30 gauge points. In all but one test, the strains in each face were measured at gauge points out-with the lap, to check that the load was being applied axially. In most tests, strains within the lap were measured in one face only.

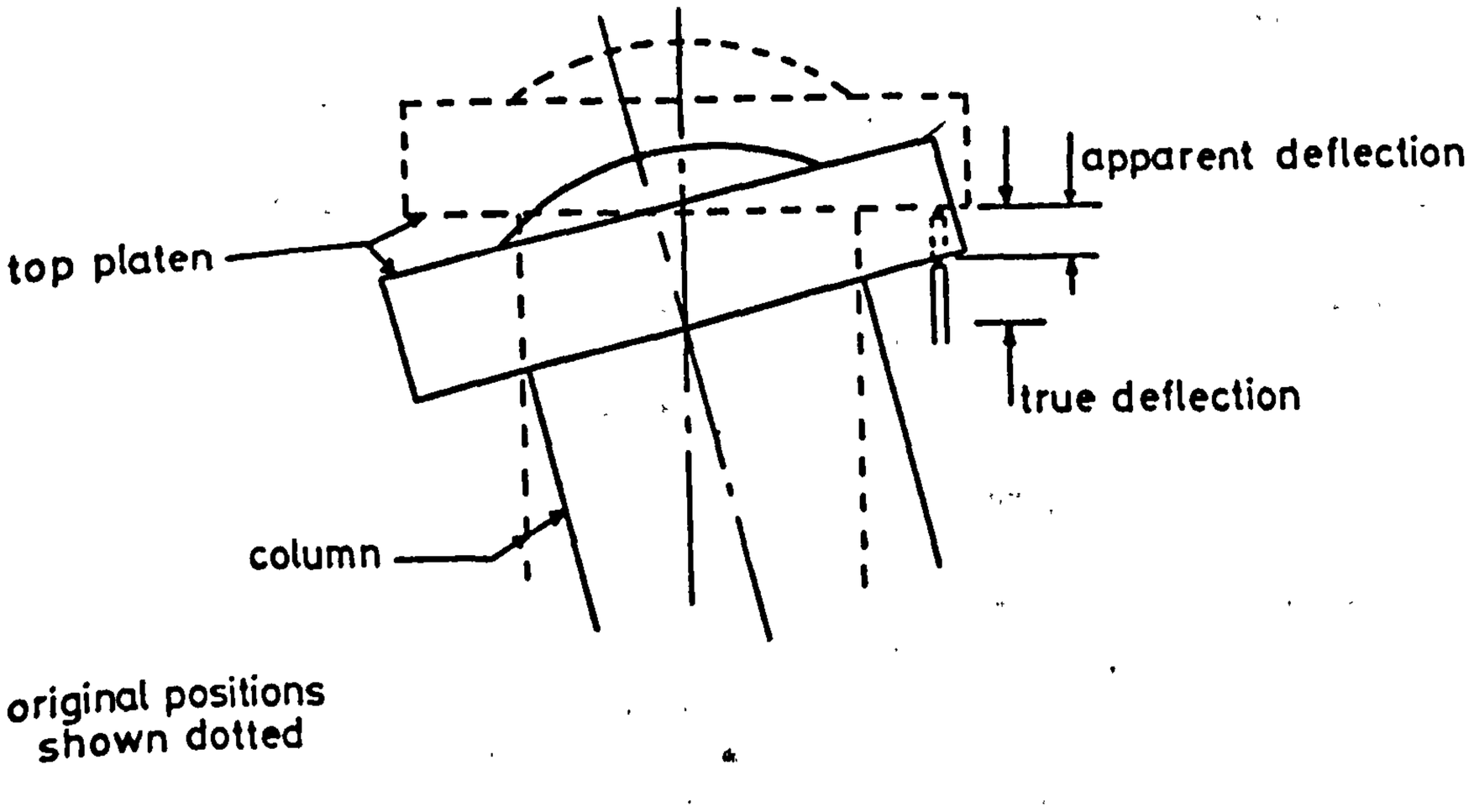

Fig. 4.6 Effect of tilting of top platen.

Metal foil electrical resistance strain gauges were fitted on the surface of the main reinforcing bars and links in four columns. The areas where the gauges were to be fitted were first filed smooth and cleaned, and the gauges were glued to the bars according to manufacturer's instructions. The gauges and connections were later waterproofed and sealed with 'Araldite'. All gauges were of 6mm gauge length, and were mounted in pairs on opposite sides of the bar. 'Unisteel 410' reinforcement was used in the tests, and so the gauges could be fitted with minimal reduction in bar cross section, and without interference to the bearing of bar deformations. The material with which the gauges were waterproofed had a low modulus

of elasticity, and so it was felt that the fitting of gauges would have little effect on bond stress.

During a test, the output from the electrical resistance strain gauges was collected by a multi-channel data-logger, attached to a small computer. A direct read-out of strains was therefore readily available as the test proceeded.

4.6 Push-in Test Specimens

In addition to the main test series described in sections 4.1 to 4.5, a small number of tests were conducted on push-in specimens. In these tests, reinforcing bars embedded in concrete cylinders and surrounded by a wire spiral were loaded in compression, and 'pushed into' the concrete cylinders. Details of the test specimens and the method of loading are shown in table 4.4 and fig. 4.7.

Both makes of reinforcing bar used in the main test series were used in push-in tests. Details of each type are given in table 4.4. Only 40mm diameter bars were used, to ensure that the radial forces set up by the bond action would be adequate to split the concrete cylinder. Bearing of the ends of the bars was prevented by gluing a piece of expanded polystyrene to the ends. The wire used for the confining spiral was of 3mm diameter, and had a yield strength of 450 N/mm^2. It was clean and free of rust. The wire was formed into a 150mm diameter spiral which fitted neatly into the cylinder mould, leaving virtually no concrete cover to the wire.

The concrete was manufactured with water, cement, sand and irregular gravel aggregate in the proportions 0.56 : 1.0 : 2.2 : 3.6 respectively. The specimens were cured in air in the laboratory. Standard test specimens were cast at the same time as the push-in specimens, and cured under water until required for testing.

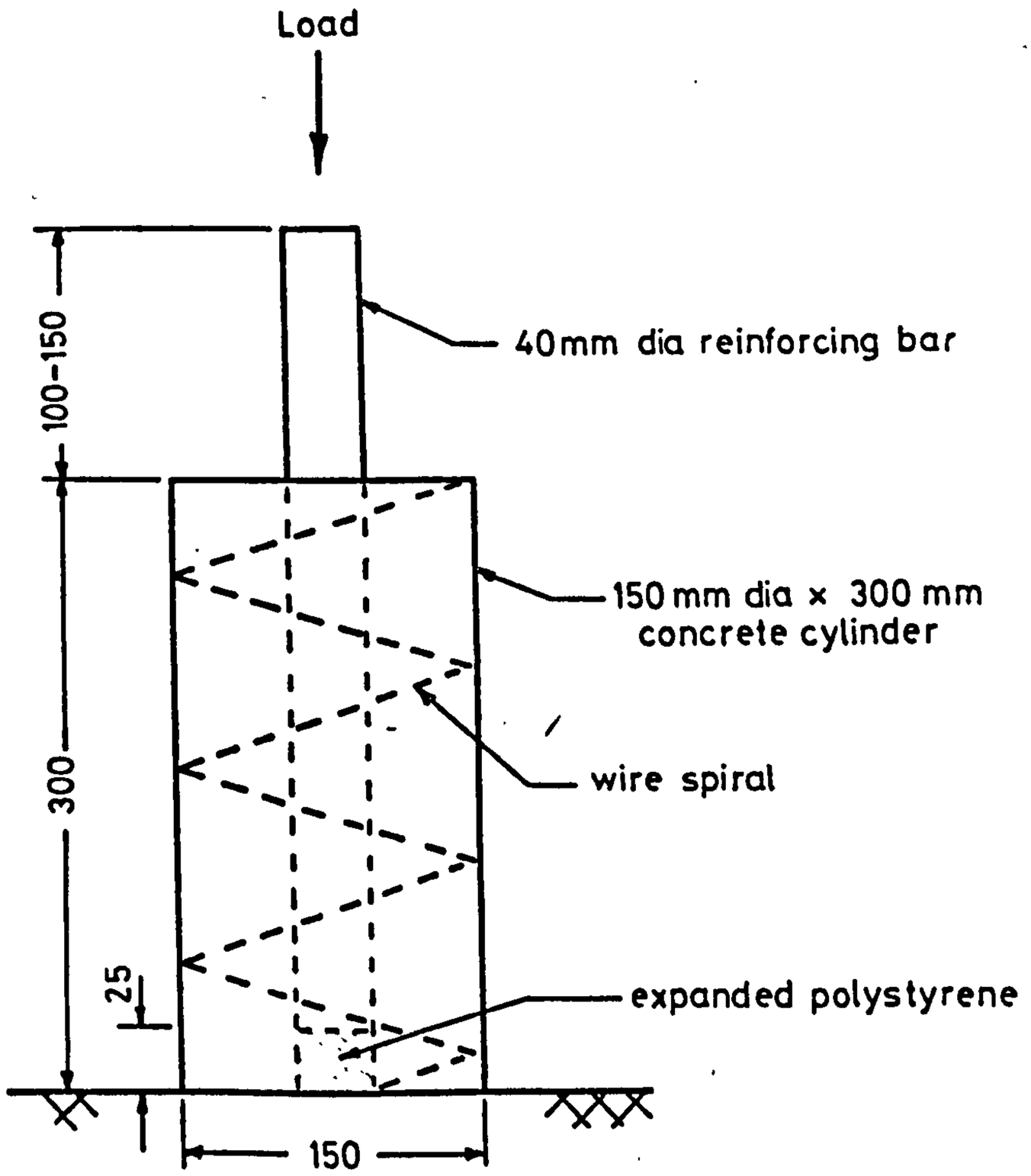

Fig. 4.7 Push-in specimen.

The push-in specimens were tested in a 900 kN Olsen screw type testing machine, and were loaded to failure in approximately five minutes. A typical load-deflection curve is shown in fig. 4.8. Under test, the load on push-in specimens rose steeply to a first peak, then dropped sharply, as longitudinal cracks formed in the cylinder. With further bar movement, the load rose to a second maximum, then dropped slowly, as crack widths and bar slips increased rapidly. In only a few tests did the wire spiral break, although bar-concrete slips of 15mm were usually reached.

The results of these tests are presented in table 4.4.

TABLE 4.4 RESULTS OF PUSH-IN TESTS ON 40mm DIAMETER BARS.

Test No.	Concrete Cube Strength N/mm^2	No. of Turns in Spiral	Steel Stress N/mm^2		Bar Type
			1st Peak	2nd Peak	
U1	42.7	5	165	137	Unisteel 410
		3	146	104	"
U2	35.1	4	159	126	"
		4	116	121	"
U3	35.5	9	110	162	"
		6	?	137	"
		5	107	124	"
		4	113	118	"
H1	36.7	7	143	157	Hybar
		7	146	168	"
		4	143	157	"
		4	147	137	"

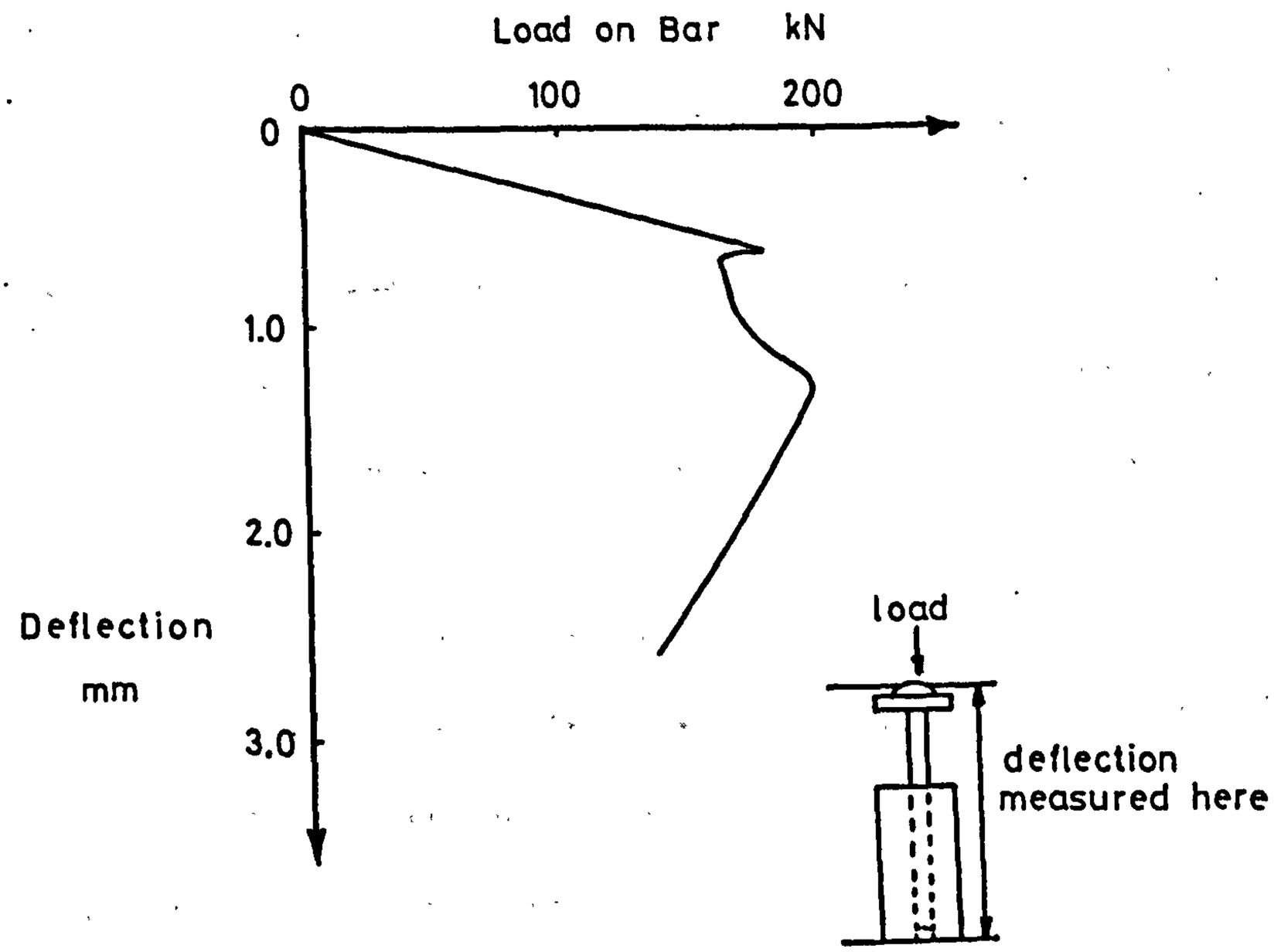

Fig. 4.8 Typical load-deflection curve for push-in test.

CHAPTER 5

PRESENTATION OF TEST RESULTS

5.1 Joint Behaviour

As was expected from observations of the failure of tension lapped joints, failure of compression lapped joints was preceded by extensive splitting of the concrete cover along the line of the reinforcement. Column behaviour beyond ultimate load was not ductile, but complete failure was always preceded by extensive cracking.

Typical load-deflection curves for reinforced concrete columns with and without lapped joints are shown in fig. 5.1. The relative values of deflections are not significant, as tilting of the top platen during tests may have affected deflection measurements. Of the two columns with higher strength concretes, failure was more sudden in the case of the column with a 10ϕ lapped joint than in the case of the column with continuous reinforcement. The much more rapid drop in load capacity in the cases of the columns with lapped joints was due to the reduction in steel stress after failure of the lapped joint, and subsequent spalling of the corners of the column. However, the column with weaker concrete produced by far the most ductile failure, despite presence of the lapped joint.

Cracking developed slightly differently with each of the three bar conditions used in test specimens, i.e. bond and end bearing combined, bond eliminated and end bearing eliminated. First cracks always developed at the ends of a lap, cracks forming where there was least cover to the discontinued bar. However, in the case of bars with end bearing eliminated, cracks then developed mainly within the lap, whereas cracks started to extend in both directions with the other two conditions, but only in the case of bars with bond eliminated

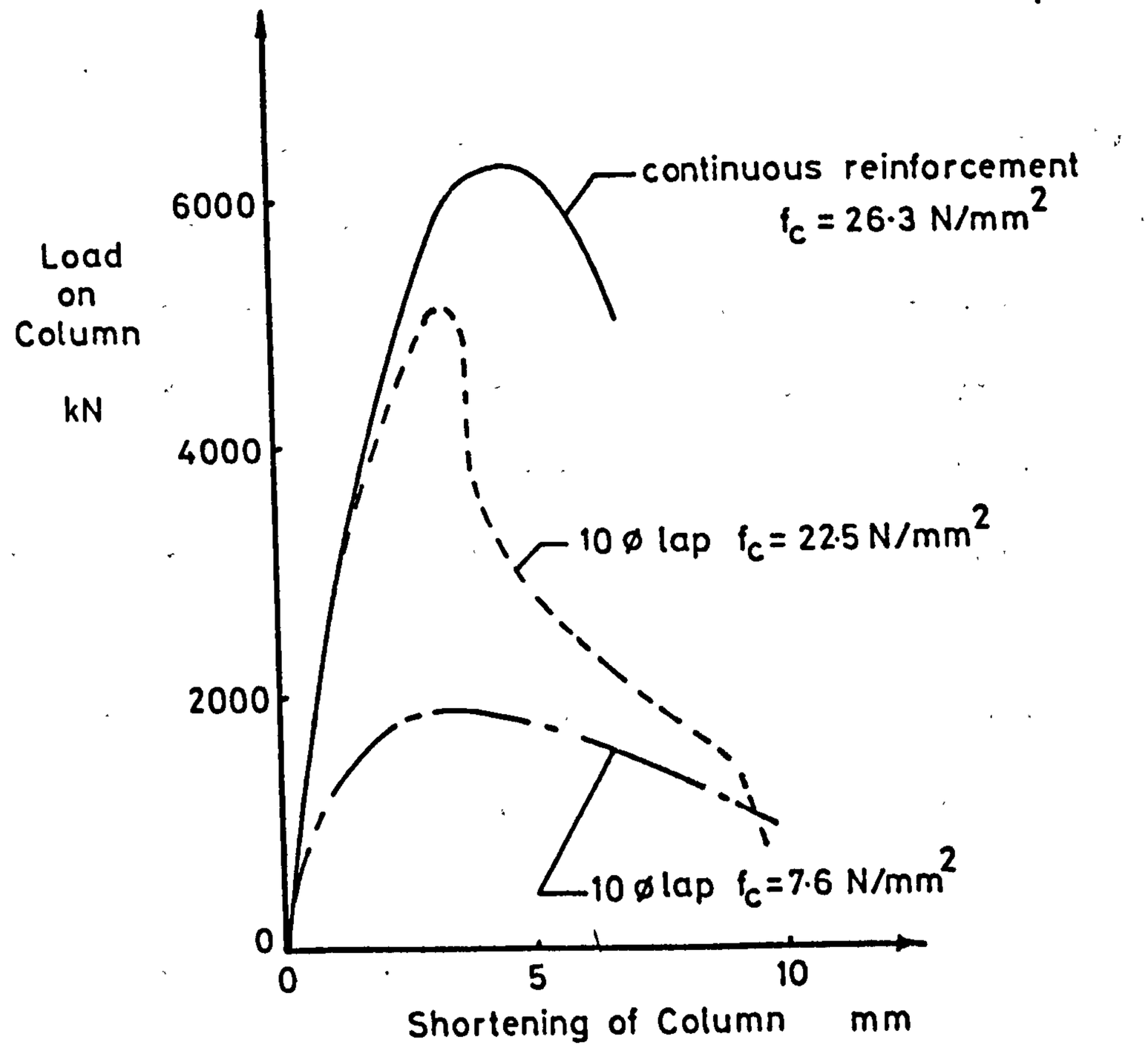

Fig 5.1 Typical load deflection curves for columns with continuous reinforcement and lapped joints.

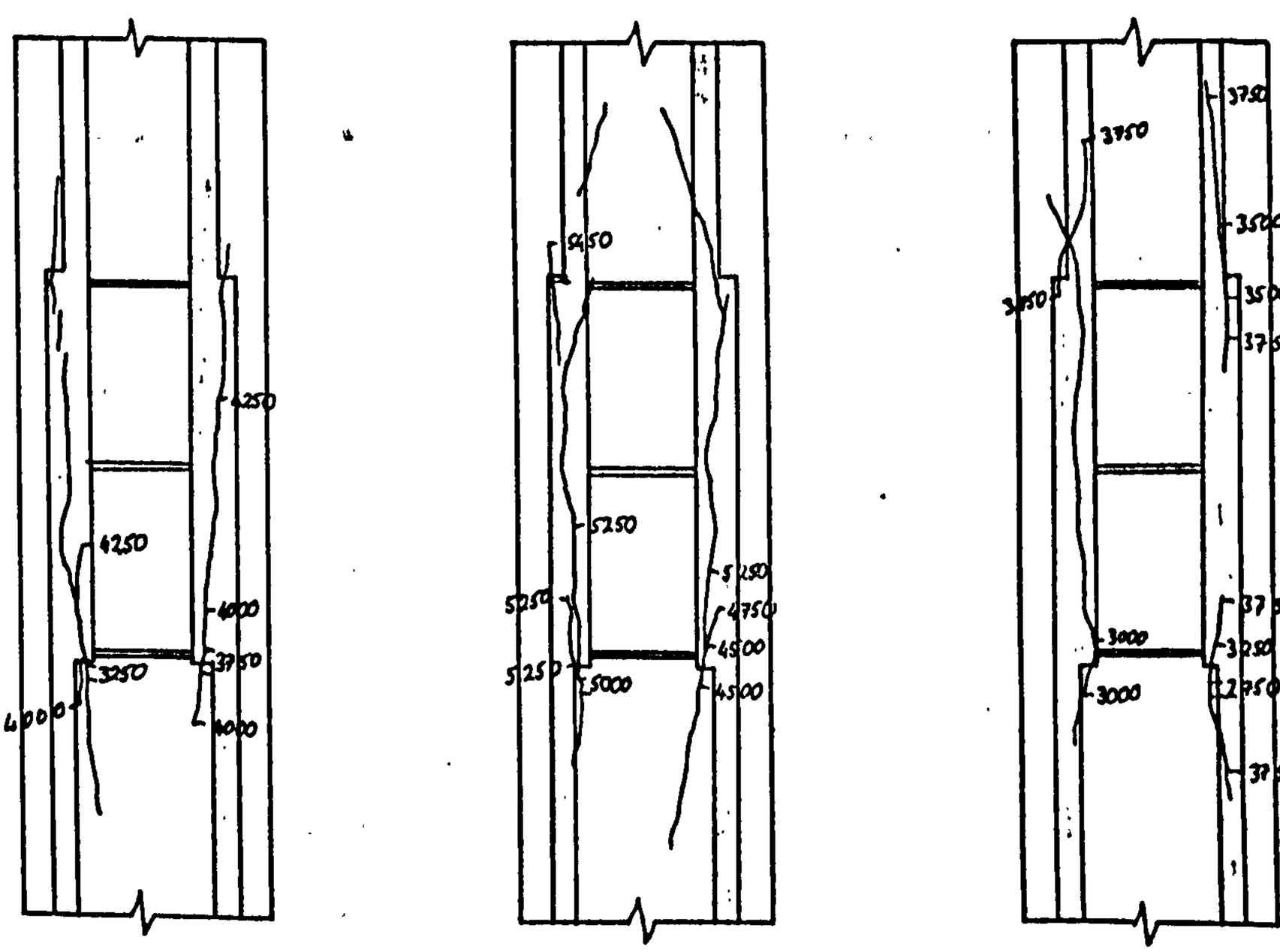

A 302 B
N = 4310 kN
Bond and End Bearing

A 306
N = 5460 kN
Bond only

A 308 B
N = 3920 kN
End Bearing only

Fig 5.2 Typical crack patterns at ultimate load – the numbers on the drawings indicate the load in kN at which the cracks reached these points.

did cracks regularly appear in both column faces adjacent to a bar cutoff before cracks extended throughout the lap. Cracks frequently extended throughout the lap length at ultimate load, particularly with shorter lapped joints. In some tests, horizontal cracks were observed at corners of a column near the ends of a lap close to ultimate load. Typical crack formations for each bar condition are shown in fig. 5.2.

First cracks were observed by the unassisted eye at between 47% and 87% of the ultimate load of a column. However, despite this wide range and the differences in crack development with different bar conditions, subsequent widening of cracks was similar in all tests. When first observed, cracks were about 0.02mm wide, and, with continued loading, increased slowly to around 0.05mm. Close to ultimate load, the rate of increase was much faster, and cracks up to 0.5mm wide were found at ultimate load. Cracks did not narrow appreciably on deloading immediately after ultimate load, and if loading was continued beyond the ultimate load of the column, crack width continued to increase rapidly until the corner of the column spalled. The pattern of crack behaviour and the size of cracks observed indicated that the secondary reinforcement around the lap joint yielded as the joint failed.

Surface strains perpendicular to the bar axis were measured over a discontinued bar at the end of the lap in most tests, and the measurements were plotted against column load. Plots generally showed a sudden change of slope at strains of 50×10^{-6} to 200×10^{-6}, the range of strain in which concrete could be expected to crack.[21] The change of slope, which always occurred at a lower load than the first visually observed crack, is considered to represent the formation of the first splitting crack. Fig. 5.3 shows a typical load-lateral strain curve for a gauge location over the end of a bar,

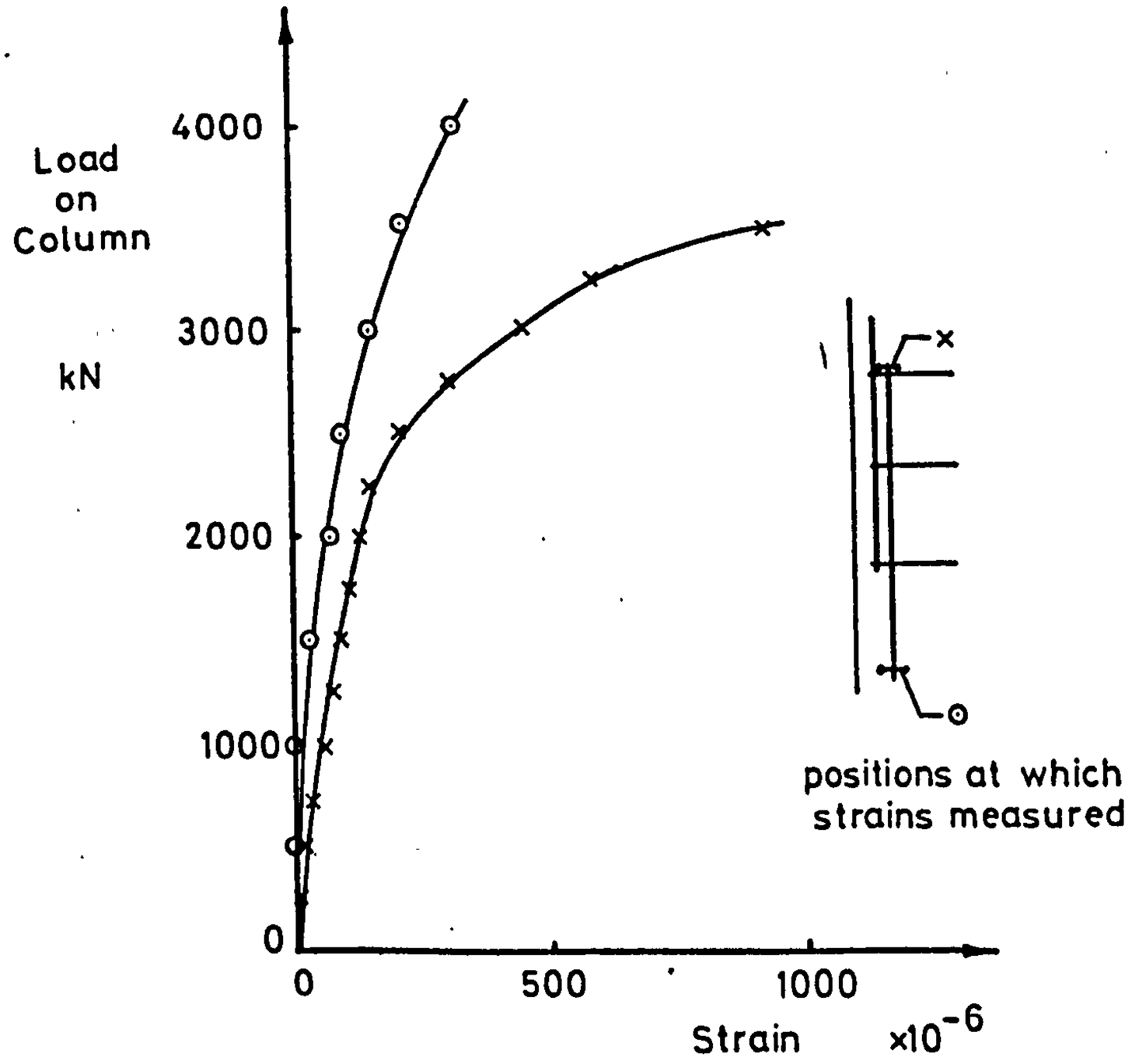

Fig. 5.3 Transverse tensile strains on column face.

and for one outwith the lapped joint. The results of column cracking loads determined from concrete strains are presented in table 5.2.

On exposure of the reinforcing bars after a test, wedges of concrete were found adhering to the bearing surface of the ribs as shown in fig. 5.4. These wedges did not form on ribs at a distance of more than 150mm from the end of a lapped joint. The wedges were more noticeable on 'Unisteel 410' reinforcement, probably due to its steeper rib face angle. Apart from the tests in which bond between reinforcement and concrete was eliminated, the only tests in which these wedges were not found on both sides of the bars were the tests in series 'C' in which double stirrups were used. In these tests, the concrete was sheared on a surface along the tops of the ribs on the side of the bar facing the centre of the column, producing the type 1 failure described in section 3.3.

Figure 5.4 also shows concrete confined under the corners of the links within the lap length. The reinforcement detail used allowed the links to serve in restraining the corner of the column from spalling in addition to restraining the main reinforcement.

Cones of concrete were punched out in the columns by the bearing of the ends of reinforcing bars on the concrete. It was usually possible to recover about four cones intact from each column, and to measure their dimensions.

The cones were usually slightly skewed, with the steeper slope facing the centre of the column. The inclination of the shallower slope was calculated, from which the angle of internal friction of the concrete could be derived by equation 3.6. The results are presented in table 5.2. Up to 10mm relative displacement between bars developed by completion of a test, and there was usually a gap of 1 - 2mm between the end of a bar and the concrete cone when all load was removed from the column.

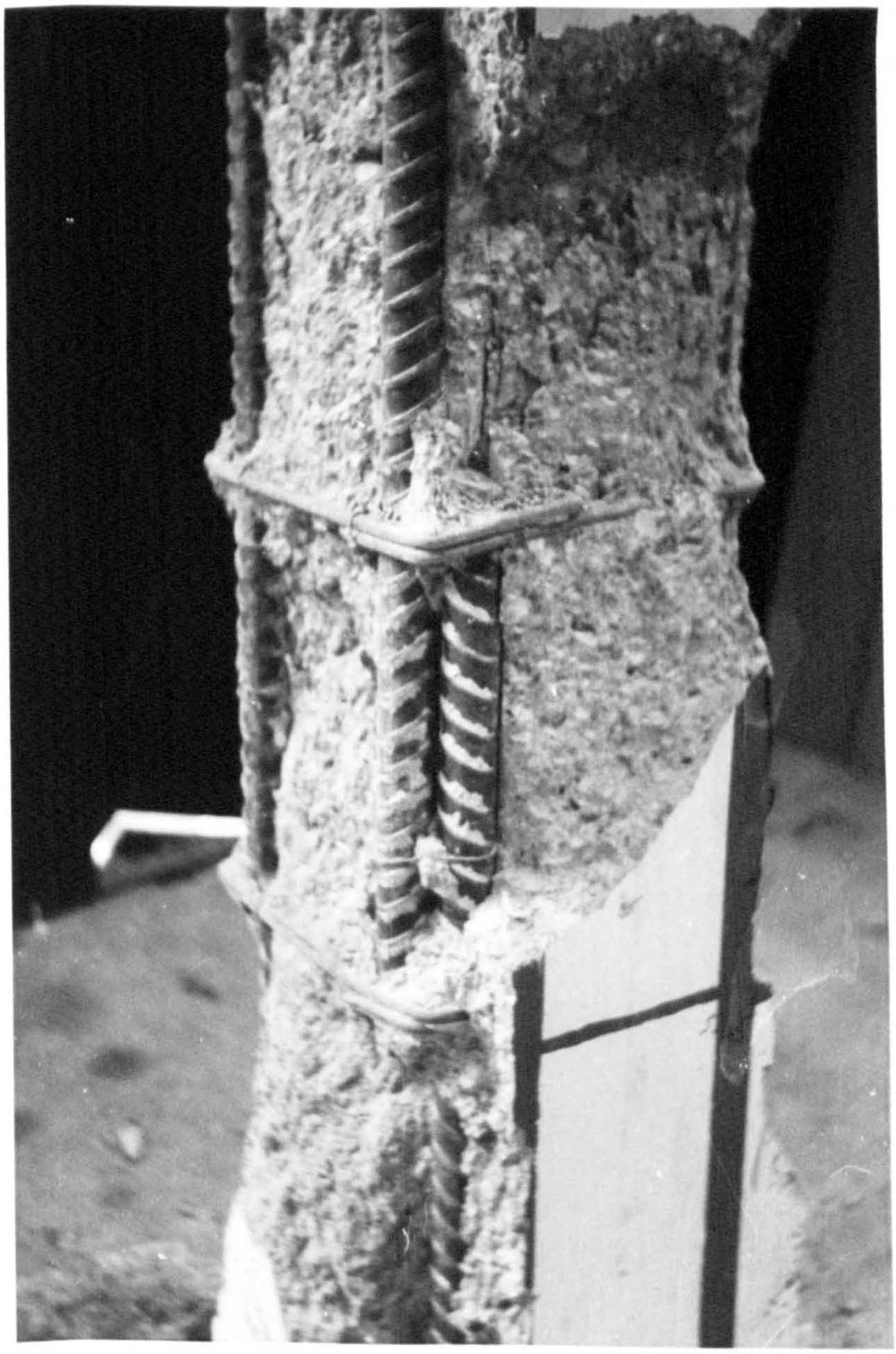

Fig. 5.4 Typical failure of lapped joint, showing wedges of concrete adhering to ribs.

TABLE 5.1 RESULTS OF TESTS ON COLUMNS IN SERIES 'A'.

Column No.	Strength of Concrete in Specimen N/mm^2	Cracking Load kN	Concrete Load at Ultimate kN	Ultimate Load of Column kN	Steel Stress at Ultimate Load N/mm^2	Notes
A101	14.1	-	2260	2960	359	
102	16.7	-	2670	3180	259	
103	20.0	-	3200	3900	359	
104	17.6	-	2820	3420	307	
105	18.8	-	3010	3460	230	
111	20.2	-	1270	2000	371	
113	20.3	-	1280	1990	362	
114	13.8	-	870	1260	199	
116	21.8	-	1370	1880	260	
201	15.3	1750	2430	3860	443	
201B	21.0	1600	3340	4800	454	
202	17.2	1600	2720	4160	448	2
202B	20.9	1700	3320	4250	288	
203	23.7	2000	3770	4350	181	
300	26.3	-	4130	6310	447	
301	22.5	2250	3530	5160	332	
302	16.9	2300	2650	>4190	>315	
302B	17.0	2300	2670	4310	336	
302C	21.6	2600	3390	5400	400	
303	21.2	2200	3330	4750	291	3
303B	22.0	2800	3450	5460	412	4
304	18.2	-	2860	4290	294	
304B	18.5	1800	2900	4120	249	2
305	26.0	3000	4080	5500	291	
306	21.2	2500	3330	5460	435	1, 2
306B	17.9	2150	2810	4510	348	

TABLE 5.1 contd.

Column No.	Strength of Concrete in Specimen N/mm^2	Cracking Load kN	Concrete Load at Ultimate kN	Ultimate Load of Column kN	Steel Stress at Ultimate Load N/mm^2	Notes
307	21.3	1400	3350	4440	223	
308	20.9	1200	3280	4260	201	
308B	18.1	-	2840	3920	221	
308C	23.0	1600	3600	4400	159	1
308D	21.4	1250	3360	4720	271	
309	15.7	900	2460	3350	181	
RESULTS OF TESTS ON COLUMNS IN SERIES 'B' AND 'C'.						
B300	14.6	-	2290	4350	410	
301	6.8	1050	1060	1900	167	
301B	7.6	1070	1190	2190	198	
311	16.2	2050	2540	3830	256	
321	17.5	2600	2750	4390	311	
331	22.9	3000	3600	5500	378	
304	4.8	850	750	1740	196	2
304B	7.0	800	1100	1980	175	
314	10.8	1500	1700	2720	204	
334	25.8	2100	4050	5550	299	
334B	18.3	1500	2870	4080	240	
313	13.6	2300	2140	4390	449	
C301	17.7	2150	2780	4160	275	
303	20.1	2350	3160	5100	387	
311	18.7	2020	2940	3990	210	1
311B	23.7	2050	3720	4600	175	
313	22.2	1650	3490	5310	363	
321	19.1	2500	3000	4710	341	

TABLE 5.1 Contd.

Column No.	Strength of Concrete in Specimen N/mm^2	Cracking Load kN	Concrete Load at Ultimate kN	Ultimate Load of Column kN	Steel Stress at Ultimate Load N/mm^2	Notes
324	6.7	1080	1050	1920	173	
324B	7.6	1090	1190	2150	191	
326	11.6	2100	1820	3980	430	

NOTES

1 Concrete cube strength used to compute results.

2 Some polystyrenes came loose from ends of bars during casting. End bearing was therefore present.

3 Column failed at top, not within lapped joint

4 From measured strains on reinforcement.

TABLE 5.2. DETAILS OF CONES PUNCHED OUT BY END BEARING OF BARS.

Column	Slope of Cone α	Angle of Internal Friction θ
B301	32°	26°
B301B	32°	26°
C324	28°	34°
C324B	28°	34°
B311	20°	50°
B321	25°	40°
B331	24°	42°
A301	21°	48°
A111	24°	42°
C311	20°	50°
C301	24°	42°
A302	25°	40°
B313	27°	36°
C326	24°	42°
C303	25°	40°

(a) Columns with bond and end bearing.

Column	Slope of Cone α	Angle of Internal Friction θ
A307	19°	53°
A308	23°	44°
A203	21°	48°

(b) Columns with end bearing only.

5.2 Analysis of Test Results.

5.2.1 The design of axially loaded short columns is generally based on the formula

$$N = f_c A_c + f_{sc} . A_{sc} \qquad 5.1$$

where N = ultimate load capacity of the column

f_c = compressive strength of concrete in the column usually taken to be 0.67 times the cube compressive strength or 0.85 times the cylinder compressive strength.

A_c = net cross sectional area of concrete

f_{sc} = ultimate steel stress in compression

and A_{sc} = area of main reinforcement.

It is therefore logical to determine the steel stress in a short column in which the main reinforcement is jointed by commuting equation 5.1 to give

$$f_{sc} = \frac{N - f_c . A_c}{A_{sc}} \qquad 5.2$$

However, the earliest test results, when analysed on the conventional assumption that

$$f_c = 0.67 f_{cu} \qquad 5.3$$

produced some negative values for f_{sc}, indicating that equation 5.3 overestimated the strength of the concrete in the test specimens.

Differences in manner and rate of loading are known to affect the ultimate strength of concrete. According to McHenry and Shideler's results[45], loading concrete compression specimens over periods of from 30 to 240 minutes causes failure to take place at about 86% of the ultimate strength of specimens loaded at the more usual rate of 12 $N/mm^2/min$. This value was confirmed by a small number of tests by the author, details of which are presented in table 5.3. It therefore appears that the factor associated with concrete cube strength in these tests should be closer to 0.86 x 0.67=0.58

TABLE 5.3 STRENGTH OF CONCRETE CUBES LOADED AT DIFFERENT RATES

	1 Strength of Cubes Loaded at Standard Rate of 15 $N/mm^2/min$ N/mm^2	2 Strength of Cubes Loaded over Period of 90 - 110 mins. N/mm^2	$^2/_1$
	41.4	35.6	
	40.3	35.1	
	41.4	35.2	
	40.0	36.0	
Average of Four Results	40.8	35.5	0.87

As the cross sectional area of steel compared with concrete is small in a reinforced concrete column, equation 5.2 is very sensitive to a change in the value of f_c. This creates problems as outlined above, and also with regard to the scatter of concrete cube results. It was felt that the results of concrete cube tests could not be considered to give results better than $\pm$ 15%, i.e. within $\pm$ 3N/mm^2 for a 20N/mm^2 concrete. An error of this magnitude in concrete strength would produce an error of $\pm$ 93.6N/mm^2 in steel stress with a steel percentage of 3.2%, the highest and most commonly used value in this investigation. Unless a huge number of tests were to be made, a more accurate method of determining steel stresses was required.

Fitting electrical resistance strain gauges to each reinforcing bar was considered, but rejected on the grounds of inconvenience, delay and expense. Instead, they were used in only four tests, and these results, as well as the results of tests on columns with continuous reinforcement, were used to develop a method for determining the strength of the concrete in the specimens.

5.2.2. As mentioned in section 4.5, strains were measured outwith the lapped joint on each column face, to check that load was being applied axially. In most tests, the gauge points were a sufficient distance from the end of the lap for there to be little slip between bar and concrete at that point, except close to ultimate load. The average surface strain on the column faces and the average of the strains on the four reinforcing bars should therefore be equal, until the column is close to its ultimate load.

To check the validity of this assumption, a comparison was made between surface strains and strains measured with electrical resistance gauges on the reinforcement. Columns A301 and A304B each had one reinforcing bar fitted with electrical resistance strain gauges, and

measured strains were in complete agreement up to loads of 4,000kN and 3,250kN respectively, or about 80% of ultimate load in each case. Results from column A308B, which had four bars gauged, did not show such good agreement, but surface strains measured on one face were almost 50% greater than the average of the other three faces. If the measurements on this face are discounted as being unrepresentative, then steel strains agree well with the measurements on the remaining three faces up to a load of 3,250kN , or 80% of ultimate load. With column A303B, agreement between surface strains and reinforcement strains was poor. It is believed that this is attributable to the proximity of the gauge points to the end of the lap, as the distance of 200mm, half the overall width of the column, may not have been sufficient to allow stresses to "even out". In later tests with 20ϕ lap lengths, the position of the lapped joint within the column was raised to allow room for strains to be measured beneath the lapped joint.

From the above, it was concluded that the assumption of equal average surface strains and average reinforcement strains was justified. The proportion of column load carried by the reinforcing bars could therefore be deduced from measured surface strains and the stress-strain relationship of the reinforcement, and the stress in the concrete at the gauge height could then be found at any load lower than 80% of ultimate load by taking the difference between the total load carried by the column and the proportion taken by the reinforcement, and dividing by the net cross sectional area of concrete.

Fig. 5.5 shows points calculated in this way for column A300, a column with continuous reinforcement. Using the method of least squares, it was found that a parabola provided an excellent fit to the experimental results. If it is assumed that the stress-strain

curve for concrete is parabolic, it may be generally represented by the following expression

$$\sigma = A\epsilon^2 + B\epsilon + C \qquad 5.4$$

where σ = concrete stress

ϵ = concrete strain

and A, B and C are constants depending on the strength of the concrete.

The experimental curve will pass close to the origin and so C will be negligible. Equation 5.4 may therefore be rewritten

$$\sigma = A\epsilon^2 + B\epsilon \qquad 5.5$$

The secant modulus of elasticity of the concrete may be calculated from the experimental results by the following expression

$$E_c = \frac{\sigma}{\epsilon} \qquad 5.6$$

Substituting for σ from equation 5.5 in equation 5.6 leads to

$$E_c = A\epsilon + B \qquad 5.7$$

which is the equation of a straight line. The constants A and B may be evaluated by calculating E_c at various strains from experimental results, and fitting a straight line to these points.

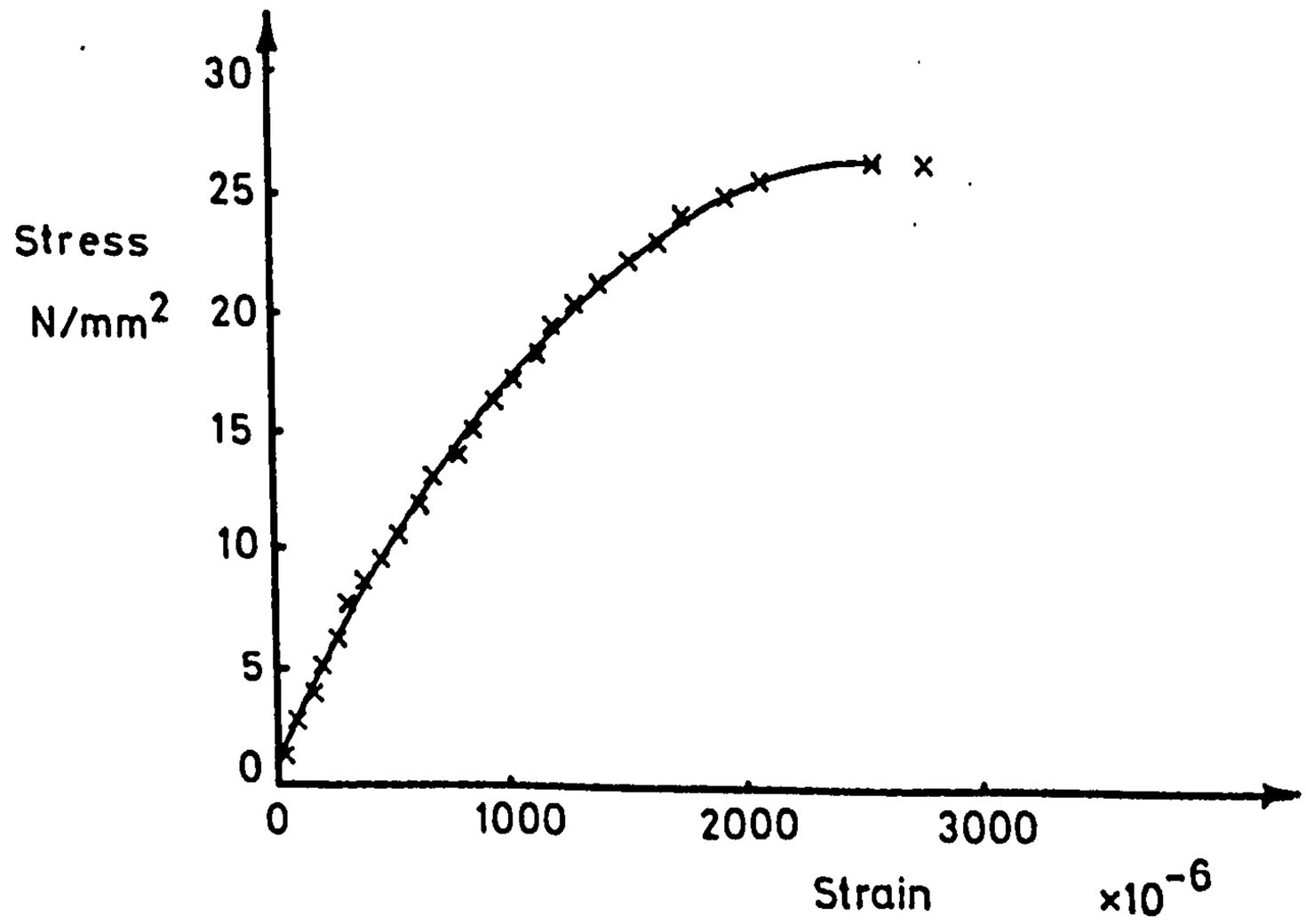

Fig. 5.5 Stress-strain relationship. Col. A 300.

A typical E_c vs. ϵ plot, for column B 321, is shown in fig. 5.6. Although points do not fit well at lower strains, there is good fit to a straight line at strains greater than 250×10^{-6}.

To find the ultimate strength of the concrete, equation 5.5 is differentiated to give

$$\frac{d\sigma}{d\epsilon} = 2A\epsilon + B \qquad 5.8$$

When σ is a maximum, $\frac{d\sigma}{d\epsilon} = 0$, and so the strain at which maximum stress occurs, ϵ max, is given by

$$\epsilon_{max} = -B/2A \qquad 5.9$$

The ultimate strength of the concrete is obtained by substituting ϵ max for ϵ in equation 5.5, which leads to

$$f_c = -B^2/4A \qquad 5.10$$

where f_c = the strength of the concrete in the specimen.

The steel stress developed by a lapped joint may then be calculated by inserting the value of f_c found in this way in equation 5.2.

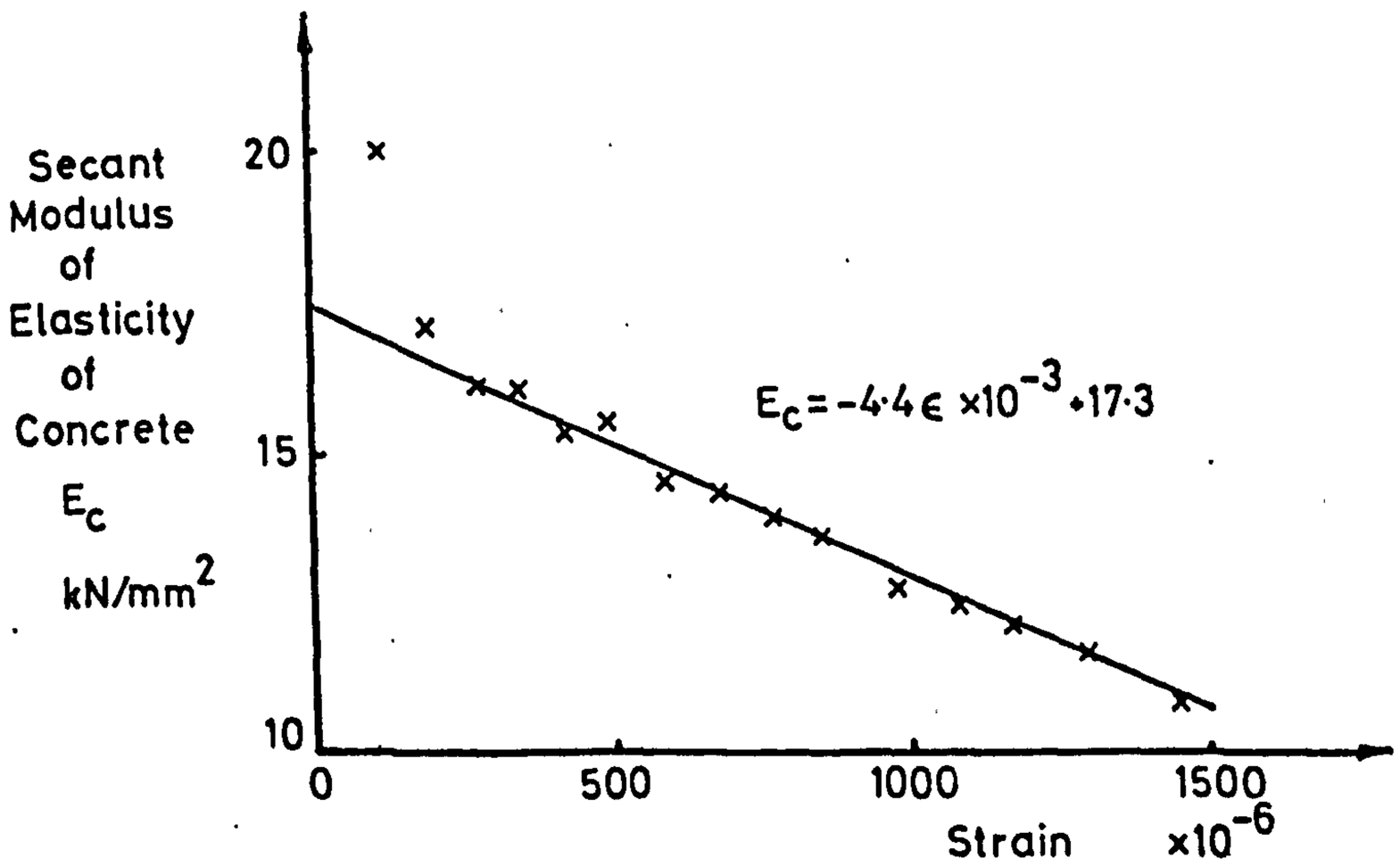

Fig. 5.6 Relationship between secant modulus of elasticity and strain,

5.2.3. As eight batches of concrete were required for each 400mm square x 2000mm column, it was inevitable that there would be some variation of concrete strength throughout the height of columns. Ultrasonic pulse velocity measurements were taken to measure variations, and to attempt to correct the value of f_c found at the gauging height for any difference in concrete strength between the joint region and the height at which strain measurements were taken.

The velocity of an ultrasonic pulse in concrete is directly related to the dynamic modulus of elasticity of concrete, rather than to its strength. The relationship is given by the expression

$$E_{cq} = 1{,}000\,\gamma . V^2 \frac{(1+\nu)(1-2\nu)}{(1-\nu)} \qquad 5.11$$

where E_{cq} = dynamic modulus of elasticity

γ = specific gravity of concrete

V = ultrasonic pulse velocity

and ν = Poisson's ratio for concrete found to be approximately 0.24 in dynamic tests.[46]

According to Takabayashi's results [47], the ratio of dynamic modulus of elasticity to static modulus of elasticity measured as the secant modulus at 15% of ultimate compressive stress is almost constant for concrete strengths greater than 15 N/mm^2, at about 1.30.

Using the results obtained from the U.P.V. and the modulus tests on columns, static modulus of elasticity was plotted against ultrasonic pulse velocity, fig. 5.7. The static modulus of elasticity is the secant modulus measured at a strain of 500 x 10^{-6}, a value chosen as being sufficiently far from zero strain for any inaccuracies in initial strain readings to have little effect, but low enough for there to be negligible slip between reinforcement and concrete.

Unfortunately the wide scatter of U.P.V. results makes the method unsuitable for accurate determination of modulus of elasticity, but many of the factors which caused the scatter, such as type of aggregate, curing methods and age at testing, were identical in each individual column. It is therefore considered that a variation in ultrasonic pulse velocity in a column will represent a variation in the modulus of elasticity of the concrete.

The "best fit" line in fig. 5.7 is

$$E_{c_{500}} = 0{\cdot}73\ V^{2{\cdot}3} \qquad 5.12$$

where $E_{c_{500}}$ = static modulus of elasticity, measured at a strain of 500×10^{-6}.

The results shown in fig. 5.7 are approximately 30% lower than would be expected from equation 5.11 and Takabayashi's[47] results, but in both equation 5.11 and 5.12 the modulus of elasticity of concrete varies with approximately the square of ultrasonic pulse velocity. As Scottish aggregates tend to have low elastic moduli, and, according to Philleo[48], the modulus of elasticity of concrete determined from pulse velocity methods is more strongly influenced than the static modulus by the modulus of elasticity of the aggregate, the relationship suggested by Takabayashi may be low in the present case.

Values of $E_{c_{500}}$ were also plotted against concrete strength, fig. 5.8. Only a limited number of results, in which the same aggregate and mix proportions were used, have been shown. The results show that modulus of elasticity varies with the square root of concrete strength. From equation 5.7, $E_c = B$ when $\epsilon = 0$, and so B is the initial tangent modulus, which varies with the square root of f_c, equation 5.10. As ϵ max is approximately constant for all

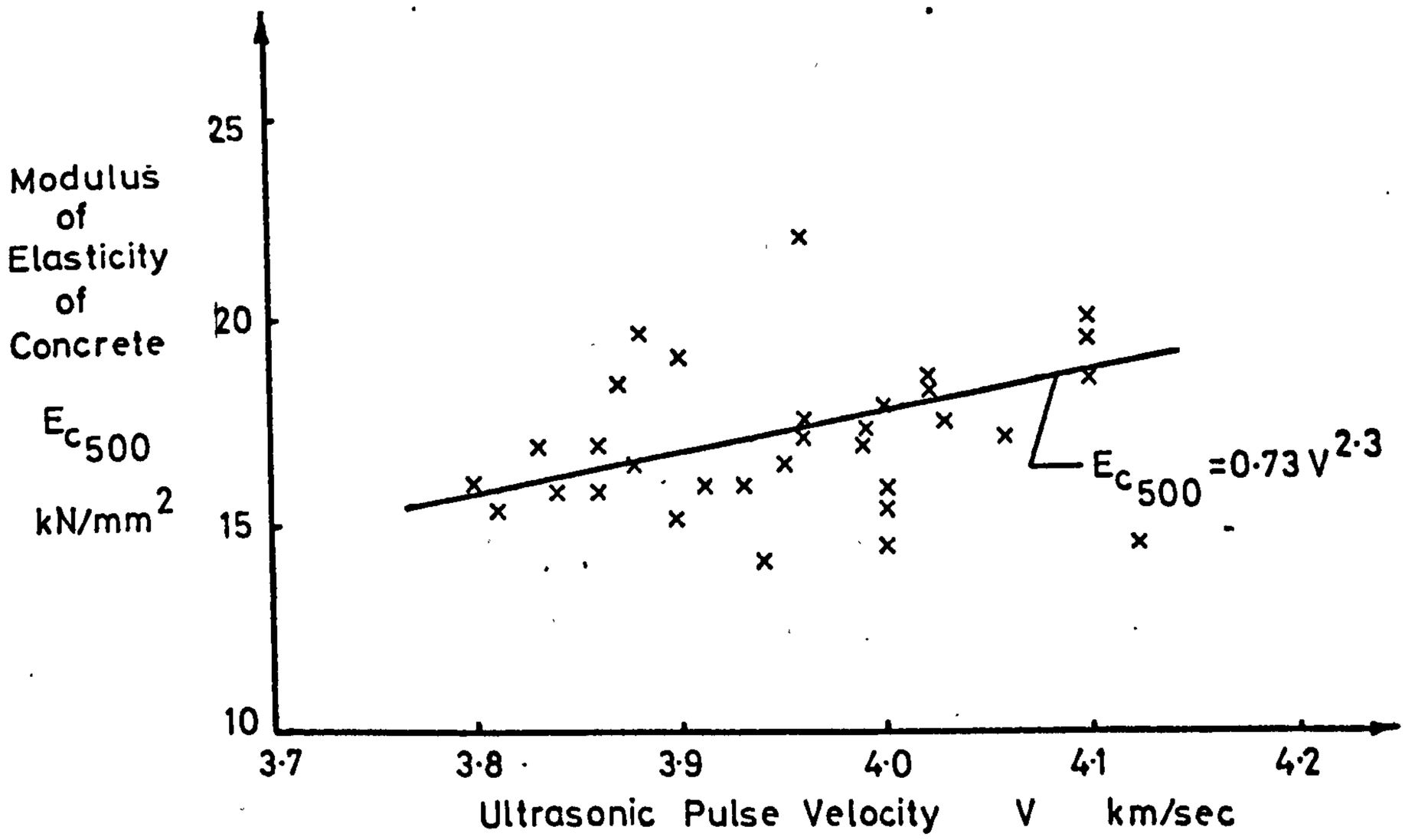

Fig. 5.7 Relationship between secant modulus of elasticity of concrete at a strain of 500 x 10^{-6} and ultrasonic pulse velocity.

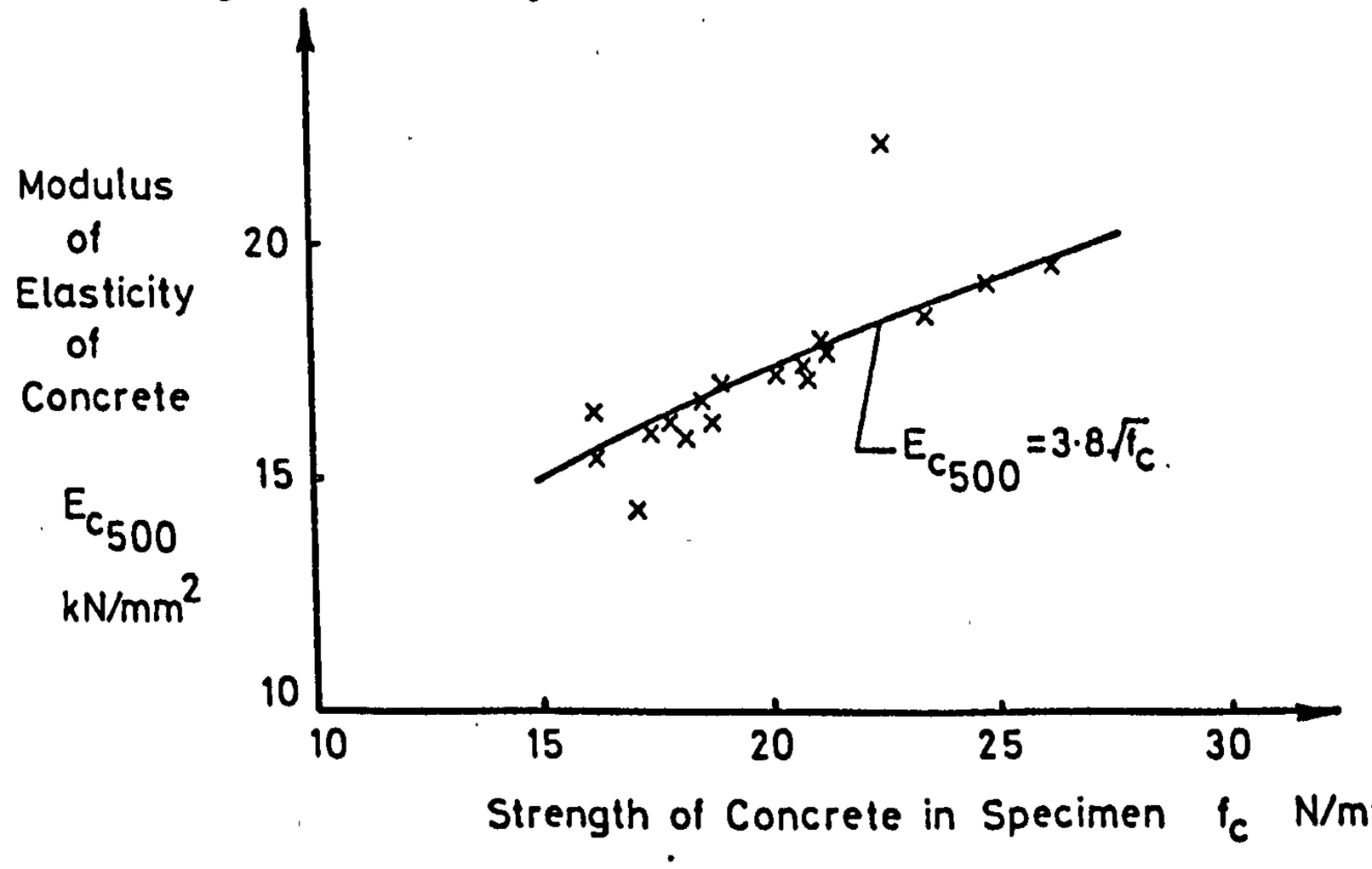

Fig. 5.8 Relationship between secant modulus of elasticity of concrete at a strain of 500 x 10^{-6} and concrete strength.

concrete strengths, it then follows from equation 5.9 that A is proportional to B for all concrete strengths, and so the general form of the relationship between E_c and f_c still hold when E_c is measured at a non-zero strain.

Combining the results of fig. 5.7 and fig. 5.8 gives

$$f_c = 2{\cdot}8 \cdot V^{4{\cdot}6} \qquad 5.13$$

The equipment used to measure the transit time of ultrasonic pulses was guaranteed accurate to within $\pm$ 1%, and the path length was measured accurately. On those columns where there was a difference of more than 1% of ultrasonic pulse velocity between pulse velocities measured at the gauge height and throughout the lap joint, the strength of the concrete at the gauge height, calculated from equation 5.10, was adjusted by equation 5.14

$$f_{cj} = f_{cg} \cdot \left(\frac{V_j}{V_g}\right)^4 \qquad 5.14$$

where f_{cj} = concrete strength throughout lap joint

f_{cg} = concrete strength at gauge height

V_j = average pulse velocity throughout lap joint

V_g = average pulse velocity at gauge height

The value of f_{cj} was then used in equation 5.2 to calculate the steel stress developed by the lap joint.

The value of the index in equation 5.14 was changed from that in equation 5.13 for ease in use, as the change does not greatly influence results.

The value of the index used in equation 5.14 is the same as would be obtained if the results of equation 5.11 and fig. 5.8 were combined.

Sample calculations of the strength of a lapped joint using the method described above are presented in Appendix C.

5.2.4 A comparison of results calculated from equation 5.2 using concrete cube strengths with a factor of 0.56, and using the value of "insitu" strength calculated from equations 5.10 and 5.14 is given in table 5.4 for columns where electrical resistance strain gauges were fitted to the bars, or where the reinforcement was not lap jointed. The average of all four surface strain readings was used in each case to calculate the constants A and B. Also shown in table 5.4 are the steel stresses at ultimate load derived from measured strains on bars, or the yield strength of the reinforcement where bars were continuous. It may be seen that the proposed method compares favourably with the results from measured steel strains except in the case of column A 303B, but that results obtained from concrete cube strength were up to 100 N/mm^2 out.

It was concluded that, in most cases, the proposed method offered the best means available of calculating the steel stress developed by a lap joint.

With a few tests, however, results calculated by the proposed method were obviously in error. In some cases, such as column A 303B, results were above the yield strength of the steel, or indicated higher steel strains at ultimate load than were measured on the column face, while in others it was impossible to fit a reliable straight line to the graph of E_c v. ϵ.

Under these circumstances, concrete cube strengths were used to determine steel stresses at ultimate load, but such tests were usually replicated, to remove any possibility of doubt.

As stated in section 5.2, there was doubt as to what factor should be applied to concrete cube strengths in equation 5.2. To investigate this, the values of concrete strength derived from

equation 5.10 which were considered to be satisfactory were plotted against concrete cube strength for each column, fig. 5.9. This shows that over 90% of the points lie within 16% of the line

$$f_c = 0{\cdot}56\ f_{cu} \qquad 5.15$$

which agrees well with the relationship predicted from McHenry and Shideler's[45] results.

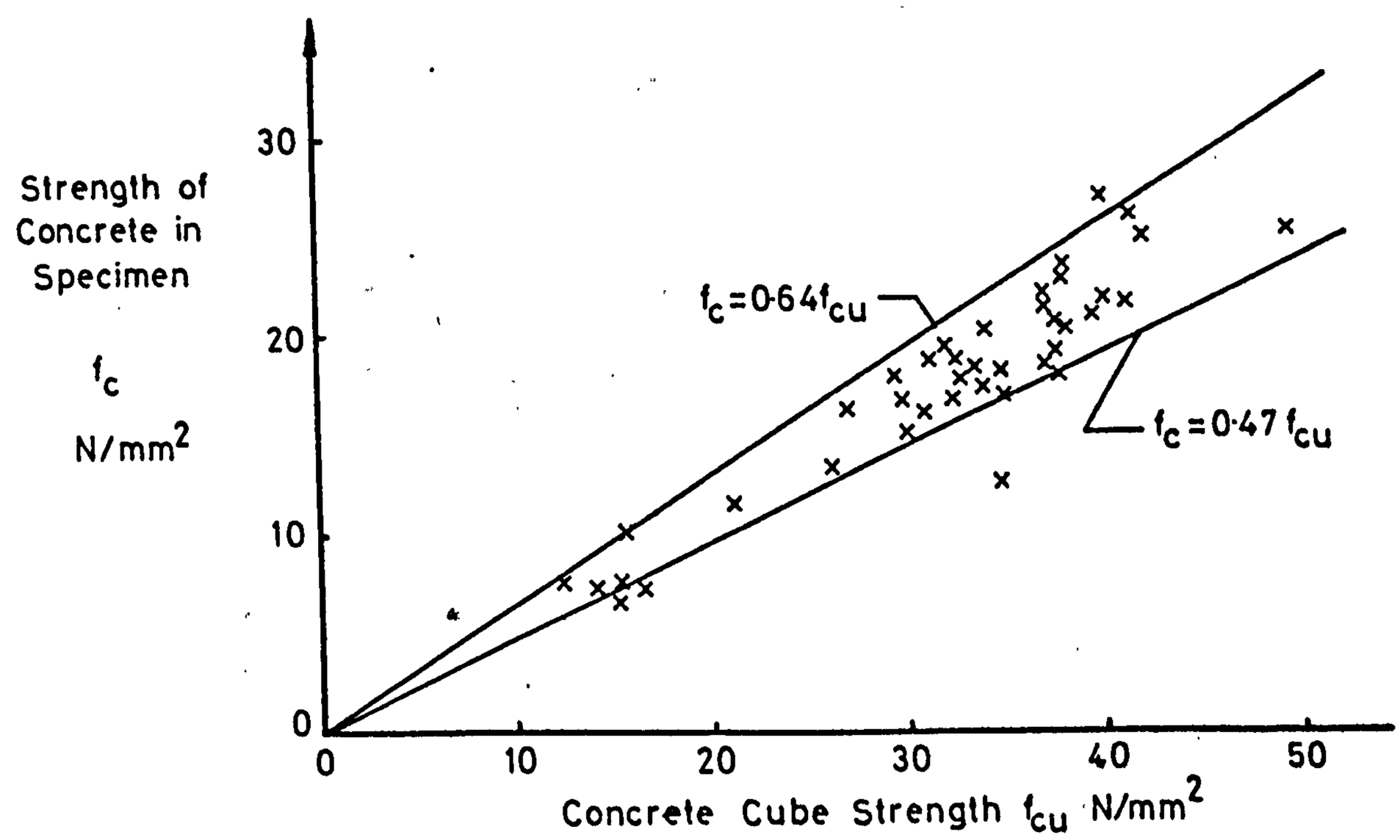

Fig. 5.9 Relationship between strength of concrete in specimen and concrete cube strength.

TABLE 5.4 COMPARISON OF STEEL STRESS AT ULTIMATE LOAD DERIVED BY VARIOUS METHODS.

Column No.	Steel Stress at Ultimate Load (N/mm^2)			Comments
	Method Using Strains on Column Faces and U.P.V.	Method Using 0.56 f_{cu}	Measured Strains or Yield Stress	
A 300	447	551	445	No lapped joint
B 300	410	532	415	No lapped joint
A 301	332	470	316	
A 303B	582	445	412	Gauges close to end of lap
A 304B	249	176	245	
A 308B	221	180	207	

CHAPTER 6

DISCUSSION OF TEST RESULTS

6.1 Introduction

In this discussion, the ultimate strength of a lapped joint is presented in terms of the steel stress developed by a joint, rather than as a uniform average bond stress over the surface of the bar within the lapped joint. Load transmitted by bearing of the end of a bar would give an inflated value of 'bond' stress, and the contribution of end bearing would appear different in lapped joints of different lengths, even if its value were the same. The term 'bond' refers only to the transfer of force by bearing of the ribs of deformed bars, and 'bond stress' is defined by equation 2.1.

The influence of the steel percentage in a column cross section on the accuracy of the calculation of ultimate joint strength has been discussed in section 5.2. Columns A 101 to A 105 had a steel percentage of only 1.23%, and it is considered that the accuracy of these results is low. They are therefore omitted in this discussion of test results.

Unfortunately, it was not possible to obtain the same type of reinforcement throughout the duration of the experimental programme. Differences in bar deformations and the strength of secondary reinforcement meant that results of tests in series 'A' were not always directly comparable with each other and accounts for the replication of certain tests. In analysing the ultimate strength of lapped joints, each type of reinforcement is considered separately.

The effect of certain other differences between the two types of main reinforcement used in test specimens should be small, however. Leonhardt and Teichen[2] state that there is little difference in joint strength between bars with ends shear cut and ends cut square

with a saw, and although the stress-strain curve of reinforcement has been found to influence joint strength[1], the difference between the two types of bars used in this investigation was small.

6.2 General Behaviour of Lapped Joints

In all the tests on columns with lapped joints, extensive longitudinal cracking developed over the lapped bars prior to the column reaching its ultimate load. This type of cracking was not observed in tests on specimens where there were no lapped joints in the reinforcement. Cracking developed with all three bar conditions used, viz. bond and end bearing, bond alone, and end bearing alone although there were differences in crack formation and development with each condition, as described in section 5.1. Both bond and end bearing therefore produce bursting forces which tend to crack the concrete cover to the reinforcement.

The mode of failure of lapped joints in this investigation was similar to the 'face and side split' failure described by Ferguson and Krishnaswamy[5], Figs. 3.6 and 6.1. Cracks first appeared on the column face at point 'C' in fig. 6.1, where large tensile strains were recorded. At point 'E' tensile strains rose slowly at first with increasing column load, but then dropped back, even becoming compressive in some cases, before rising rapidly as cracks developed. Large strains were measured on both legs of links, with slightly higher strains recorded at point 'D' than at point 'E'. The decrease in tensile strains on the surface of a column at point 'E' must therefore have been due to rotation of the corner of the column as a crack developed outwards from the reinforcement at point 'F' towards point 'E'.

Complete failure of lapped joints was accompanied by spalling of the concrete cover to the reinforcement, first at the corners of the column and later across the face. Concrete generally spalled

over a distance of between 6 and 10 times the main bar diameter above and below the lapped joints. However, there was no evidence that cracks extended between pairs of lapped bars at ultimate load, as in fig. 3.6, and it is felt that the spalling of the column faces was due to the outwards movement of the reinforcing bars after ultimate load was reached, thus causing the yielded links to pull the face of the column away from the core, as shown in fig. 6.2.

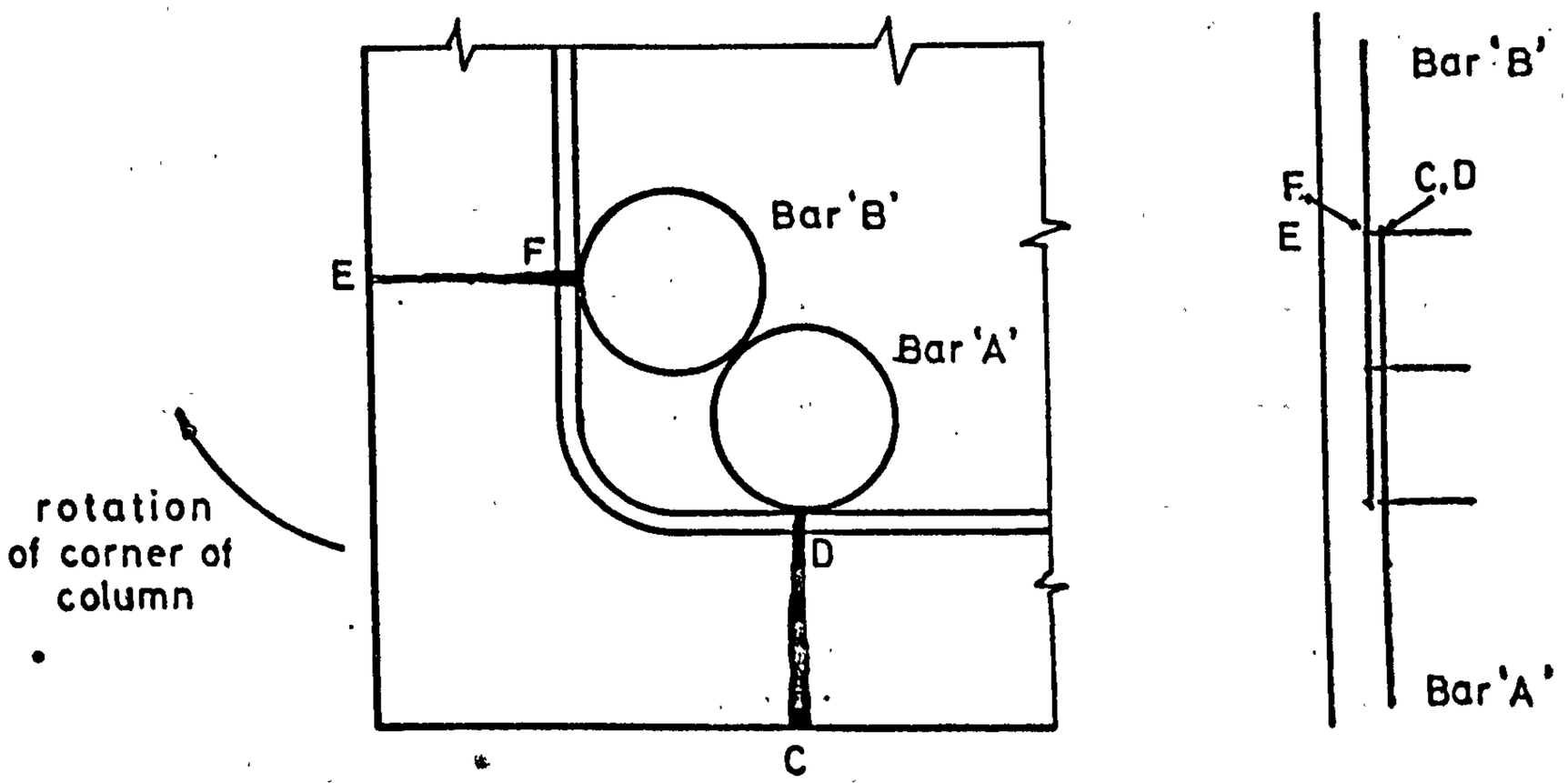

Fig. 6.1 Development of longitudinal cracks around reinforcement.

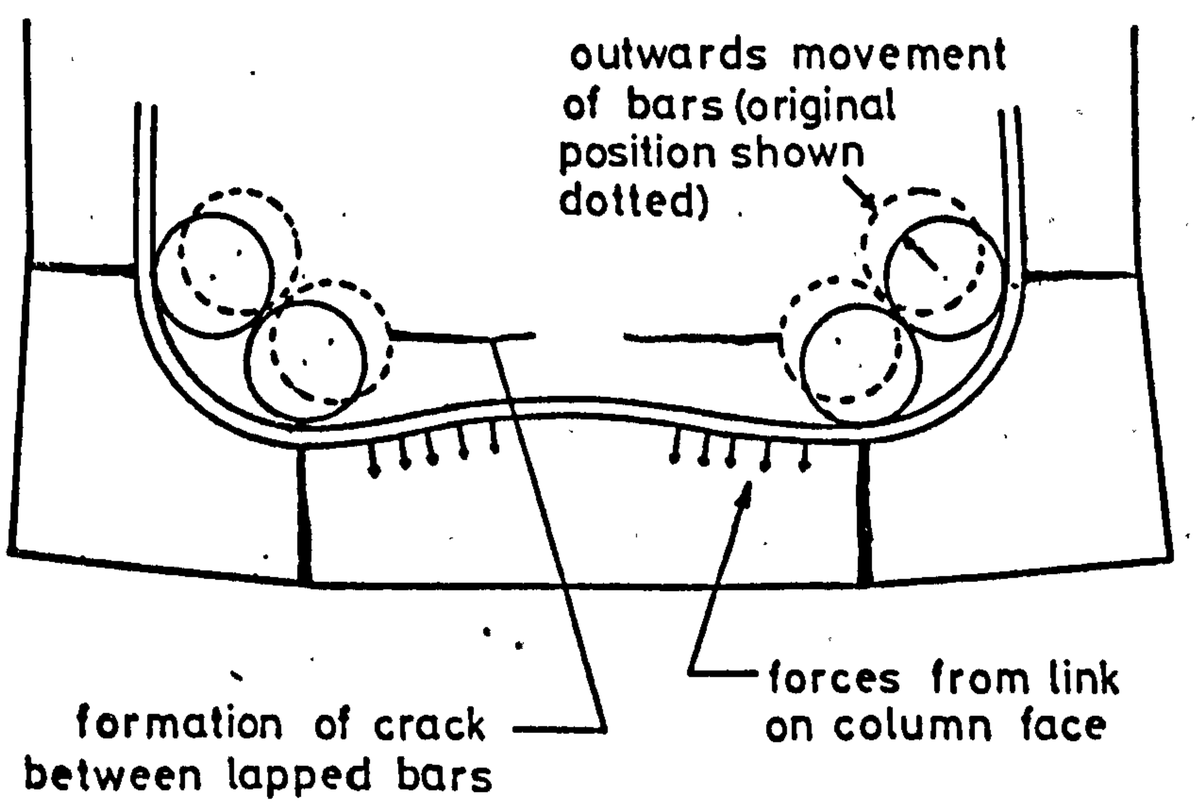

Fig. 6.2 Forces on column face.

Fig. 6.3 shows the distribution of bond stress through a 20ϕ lapped joint for a bar with bond and end bearing present. Bond stresses were calculated from strains measured on reinforcing bars by means of equation 2.1. When compared with tensile strains measured perpendicular to the bar axis on the surface of the column, shown in fig. 6.4, it may be seen that the two are related, both being high at the end of the bar, dropping to a minimum near the middle of the lapped joint, and starting to rise slowly towards the other end of the joint, but that the ratio of maximum to minimum values is considerably greater in the case of tensile strains measured on the surface of the column. However, the distribution of tensile strains over a bar on the surface of a column does reflect to a certain extent the distribution of bond stress along that bar.

The bursting forces produced by the adjacent lapped bar will also influence the transverse tensile strains in the concrete, but, according to equation 3.33, it would be expected that the bursting forces set up by bar 'A', shown in fig. 6.1, would have a greater influence on strains measured at point C than the bursting forces set up by bar 'B'

The distribution of transverse tensile strains on the surface of a column at approximately 85% of ultimate load are shown in fig. 6.5 for lapped joints where bars had end bearing only, bond only, and bond and end bearing combined. Where end bearing of the bars was not permitted, the peak tensile strain was measured within the lapped joint, unlike the other two bar conditions, where the peak tensile strain occurred outwith the lapped joint. The bar with bond and end bearing combined showed the most even distribution of tensile strains, and the bar with end bearing only produced a

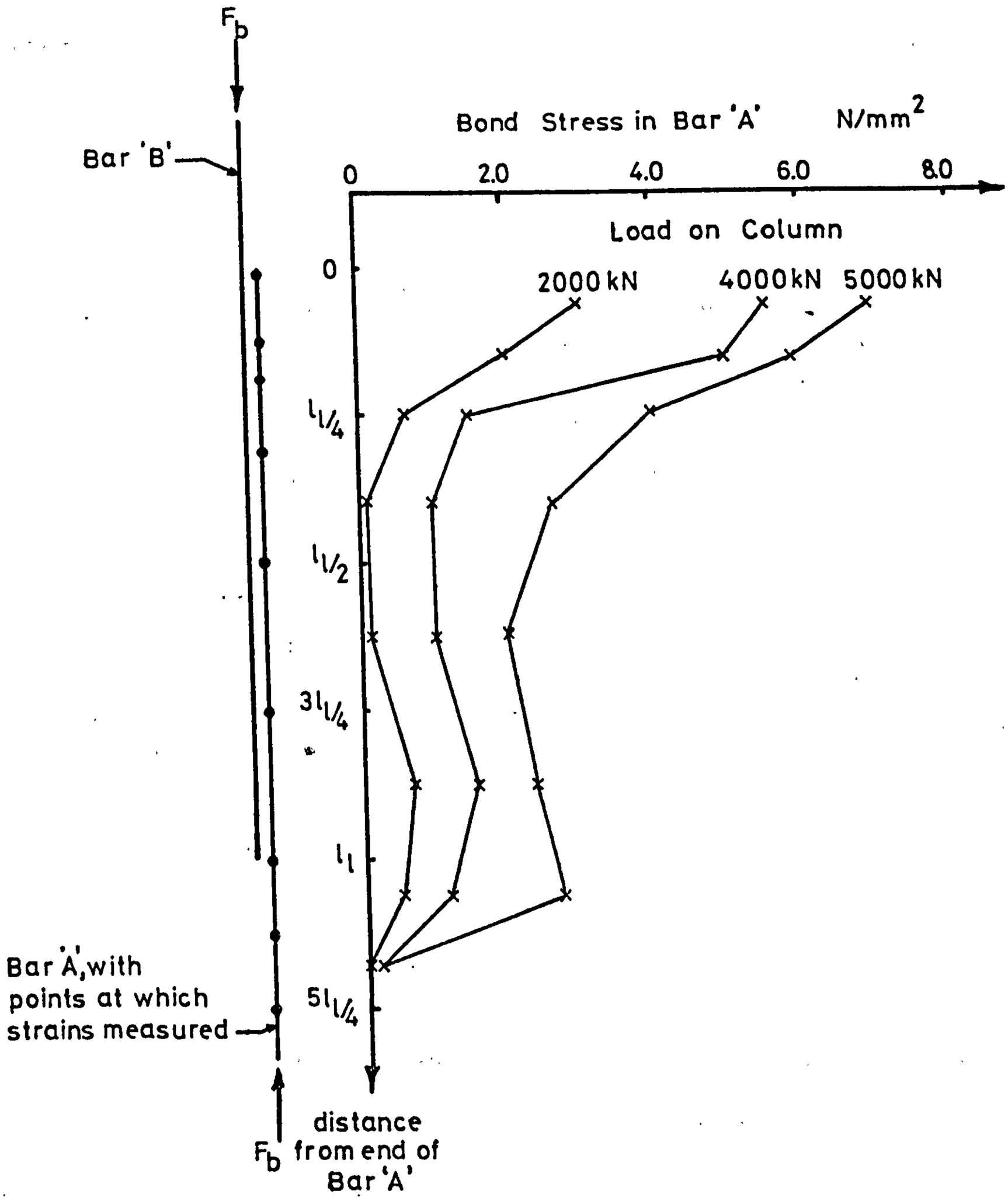

Fig. 6.3 Distribution of bond stress in 20ϕ lapped joint - bars with bond and end bearing.

very high strain over the end of the bar, but very low values were measured in the middle of the lapped joint. Fig. 6.5 therefore reflects what would have been expected for each bar condition, with the largest tensile strains occurring where transfer of force was greatest.

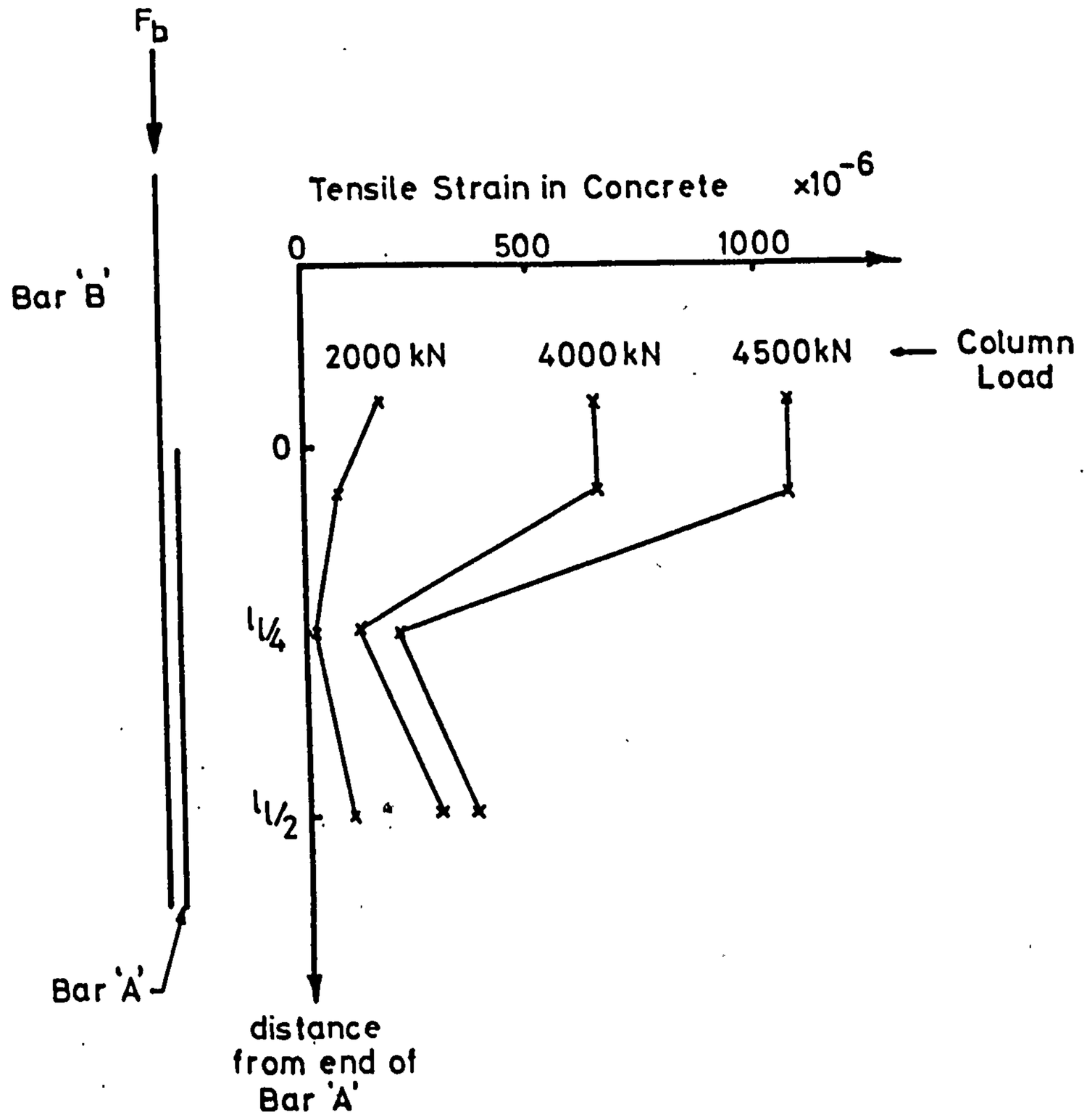

Fig. 6.4 Distribution of transverse tensile strains in concrete in 20ϕ lapped joint - bars with bond and end bearing.

Transverse tensile strains were always found to be greatest near the point where a bar was discontinued, indicating that the greatest transfer of force took place in that region. However, transverse tensile strains in the same column face were always low at the opposite end of the lapped joint, from which it may be inferred that, unlike tension lapped joints, where bond stresses are

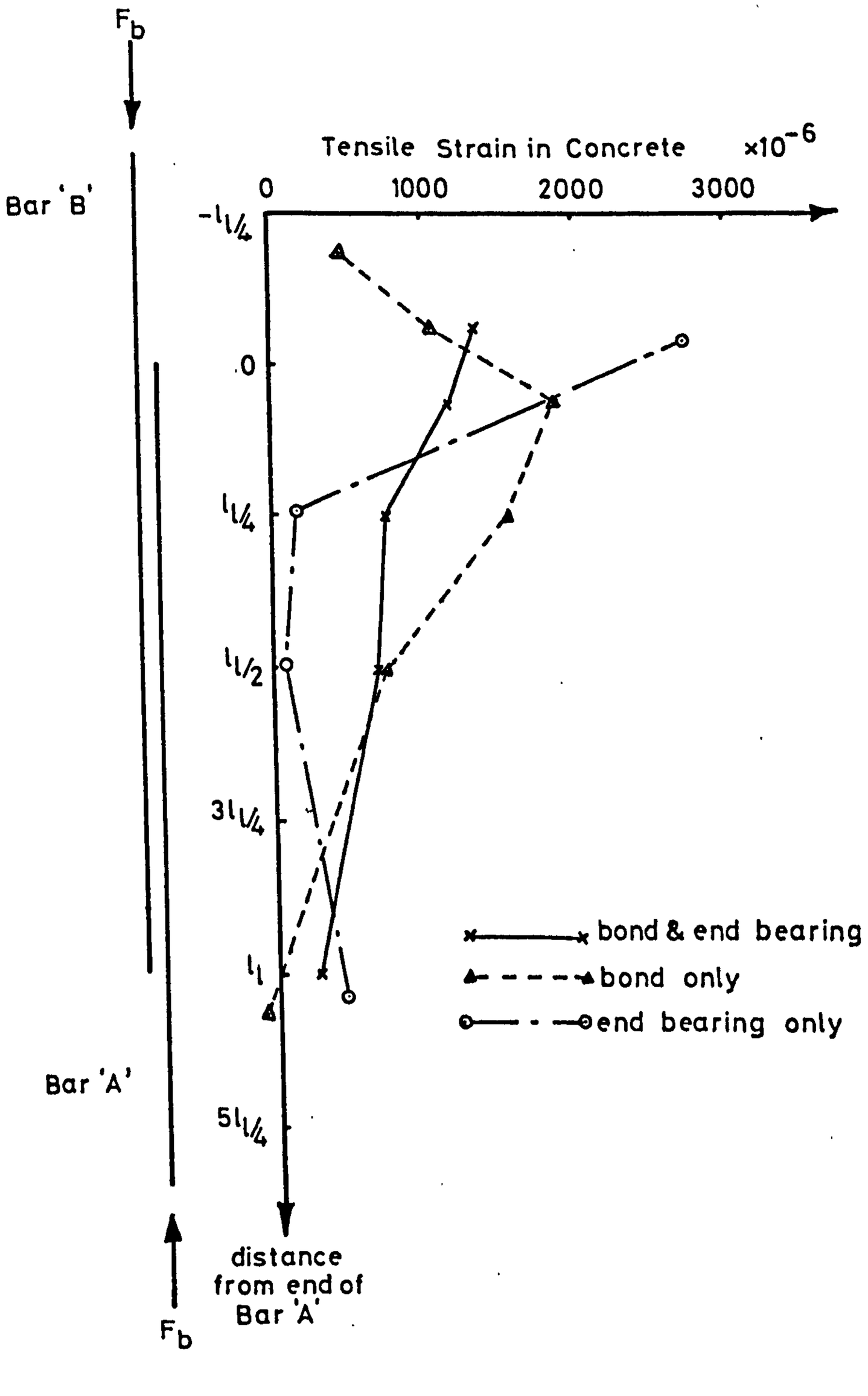

Fig. 6.5 Distribution of transverse tensile strain in concrete for various bar conditions - strains at 85% of ultimate load.

high at both ends of a lapped joint, bond stresses in a compression lapped joint are only high near the end of a bar. Higher strains were measured at point 'D' in fig. 6.1, on the leg of a link adjacent to the end of a bar, then at point 'F' on the other leg, confirming that the greatest transfer of force takes place near the end of a bar in a compression lapped joint. The bond stress distribution shown in fig. 6.3 also supports this conclusion.

The difference in the distribution of bond stress along a bar between compression and tension lapped joints is due to the interaction of concrete and reinforcement which occurs in compression lapped joints.

The resistance moment of a reinforced concrete member subjected to bending is given by the following expression

$$M = A_{st} \cdot f_{st} \cdot z \qquad 6.1$$

where M = moment to which member is subjected

A_{st} = area of tension reinforcement

f_{st} = tensile stress in reinforcement

and z = lever arm between tension steel and centroid of compression.

In most beam sections, doubling the area of reinforcement, as at a tension lapped joint, causes a relatively small change in the position of the neutral axis of the section, and hence a smaller change in the lever arm. The stress in the reinforcement in the middle of a lapped joint therefore tends to a value of half the stress in the reinforcement outwith the lapped joint.

The strength of an axially loaded short column is given by the following expression

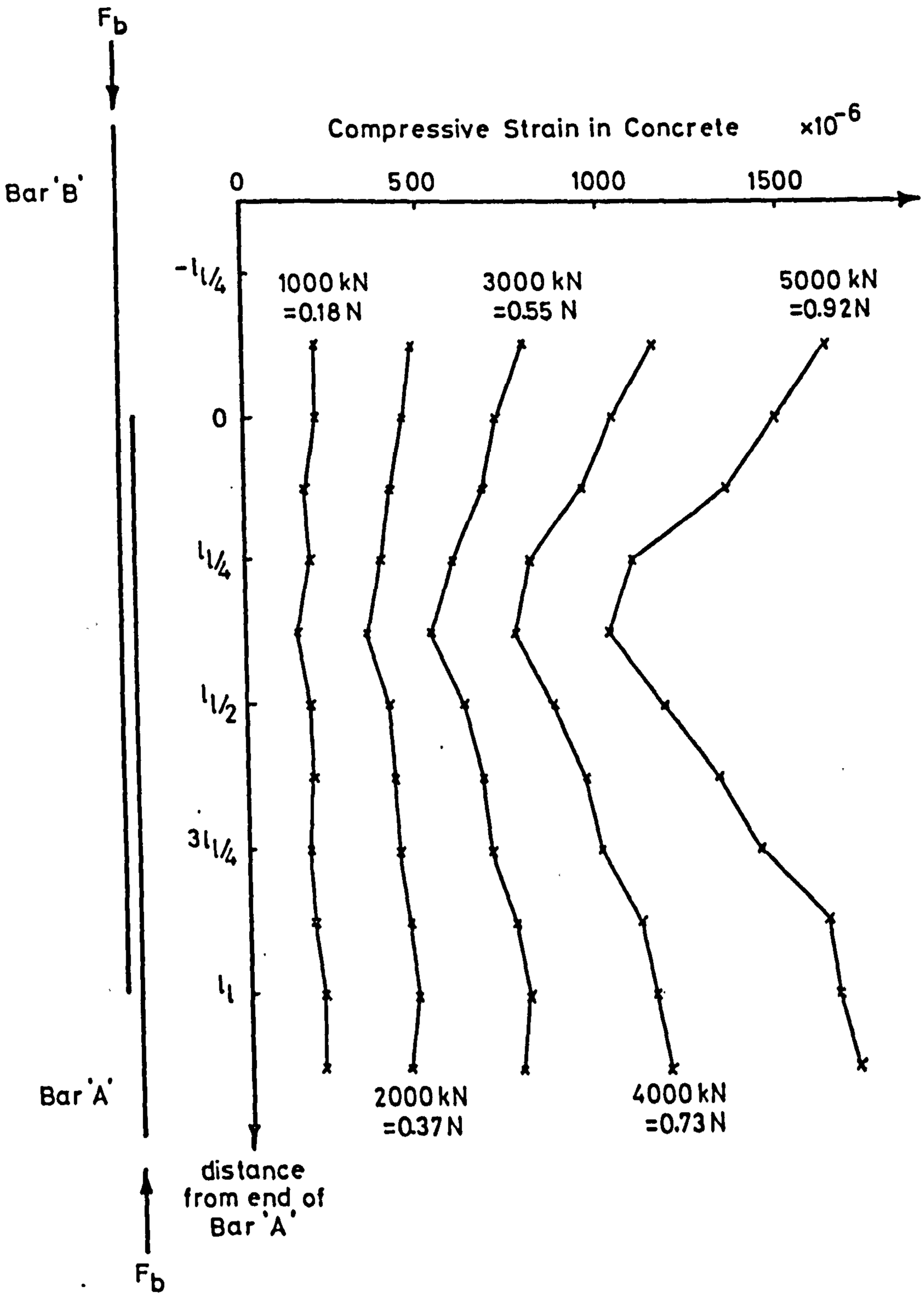

Fig. 6.6 Distribution of longitudinal compressive strain in concrete through lapped joint at various column loads.

$$N = f_c . A_c + f_{sc} . A_{sc} \qquad 6.2$$

where N = load on column

f_c = compressive stress in concrete

A_c = cross sectional area of concrete

f_{sc} = compressive stress in reinforcement

A_{sc} = cross sectional area of compression reinforcement.

Equation 6.2 may also be written

$$N = E_c . \epsilon . A_c + E_s . \epsilon . A_{sc} \qquad 6.3$$

where E_c = secant modulus of elasticity of concrete at a strain ϵ

ϵ = strain on column cross section

and E_s = modulus of elasticity of reinforcement.

In this case, doubling the area of reinforcement causes the strain on the cross section to drop to a value which will always be greater than 50% of the value outwith the lapped joint, precise values depending on the percentage of reinforcement in the column cross section and the moduli of elasticity of the steel and the concrete. This point is illustrated in fig. 3.28, where the tension case corresponds to a steel percentage of ∞ . As the stress in the reinforcement in the middle of a compression lapped joint tends to a value greater than half its value outside, the greater part of the transfer of force to a bar will take place in the half of the lap nearer to the end.

As mentioned above, the longitudinal compressive strain in the concrete in a column is lower in the middle of a lapped joint than it is outwith the lapped joint. Fig. 6.6 shows the variation of longitudinal strain on the centre line of a column face through a 20ϕ lapped joint at several column loads. The ratio of minimum to maximum strains is always greater than 0.5, and decreases with

increasing load on the column. The secant modulus of elasticity of concrete decreases with increasing strain, as may be seen from fig. 5.6, and equation 6.3 confirms that a lower modulus of elasticity should cause a greater reduction in strain at the section where the area of reinforcement is doubled.

The earliest flexural cracks to appear as a tension lapped joint is loaded form perpendicular to the bar axis at the ends of the lapped joint[24], and are due to the rapid change in strain across the discontinuity created by the stopping off of the reinforcement. All transfer of force between lapped bars must therefore take place within the lap length.

Fig. 6.3 shows that this is not the case in compression lapped joints, and that bond stresses were present in this case over a distance of up to 4ϕ beyond the end of the lapped joint for bars with bond and end bearing present. The results of strains measured on reinforcement, presented in Appendix B, show that the strain in the reinforcement increased outwith the lapped joint with all the bar conditions investigated. In calculating average bond stresses, it is assumed that bond stresses develop over a length of bar of 2.5ϕ longer than the lap length.

Despite extensive splitting of the concrete cover to the reinforcement, in no test did a corner of a column spall until the column was well beyond its ultimate load. Fig. 6.1 shows that, with the joint detail used, there was a space between the links confining the lapped bars and the lapped bars at the corners of the links. As has been shown in section 3.2, the radial component of bond stress exerts a force on the concrete cover to the reinforcement, trying to push it outwards. In the lapped joints examined in the present investigation, this sets up shear stress on planes on either side of

the links to resist the outwards movement of the corner of the column, as shown in fig. 6.7. The vertical compressive stress in the concrete will greatly enhance the shear strength of the concrete on a plane perpendicular to the direction of the compressive stress. Failure takes place on inclined surfaces above and below the links, where the principal tensile stress in the concrete exceeds the tensile strength of the concrete. The failure surface is shown diagrammatically by the dotted line in fig. 6.7, and in fig. 5.4.

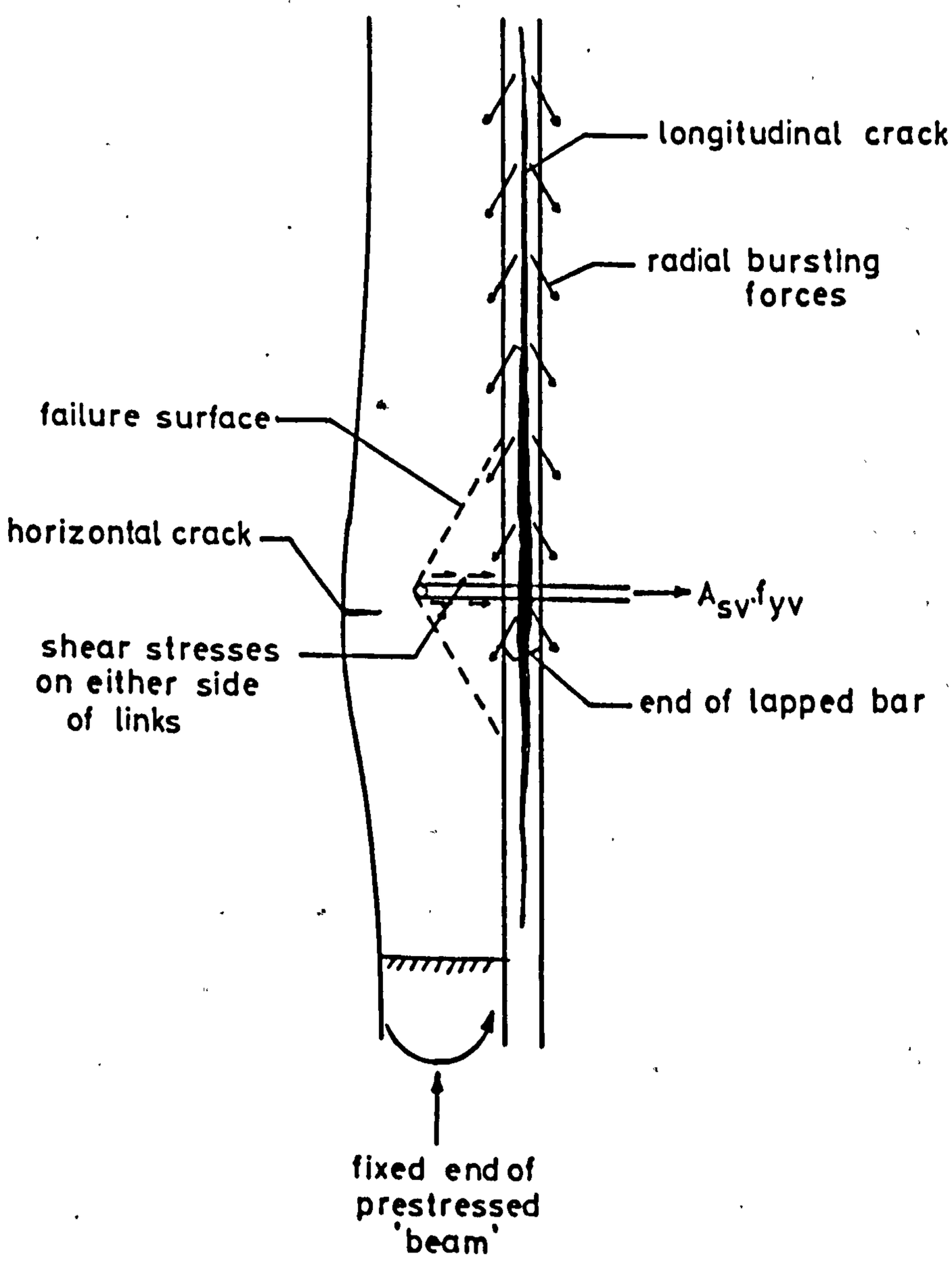

Fig. 6.7 Forces on corner of column.

Between links, the corner of a column acts as a vertical prestressed beam, loaded on one side by the radial component of bond stress. In addition, the ends of the prestressed beam will effectively be held fixed in position and direction at the point to which cracks extend outwith the lapped joint. Any outwards movement of the corner of a column therefore causes restraining moments to be set up in the prestressed beam. As has been shown above, the maximum transverse tensile strain, and hence the maximum outwards movement of the corner of the column, occurs at the end of a lapped joint, and so horizontal tensile stresses may develop in the outer edge of the corner of a column, causing the horizontal cracks observed at the ends of lapped joints in some tests.

It is extremely difficult to evaluate the forces that could be mobilised to resist spalling of the corner of a column, due to the complex state of stress in the concrete confined by links and uncertainty of crack lengths. However, it does seem likely that other joint details, where less concrete is confined between links and lapped bars, would provide lower resistance to spalling of the concrete cover. In such cases, bond strength might be reduced on one side of a bar.

After the failure of the lapped joints, which was accompanied by an outwards movement of the corners of the columns, causing shear failure of the concrete confined under the links and of the "prestressed beam" at a distance outwith the lapped joint, complete failure took place by crushing of the concrete within the lapped joint.

6.3 Effect of Bar Deformations

As stated in section 6.1, two types of ribbed deformed bars were used in tests on lapped joints. Although both had crescent shaped ribs inclined at the same angle to the bar axis, there were differences in rib spacing and in the area of each rib above the core of the bar. Details of the bar profiles are given in table 4.3.

A comparison of results of tests with each type of reinforcement showed that 'Hybar' reinforcement produced consistently higher results. However, no firm conclusion could be reached, as stronger secondary reinforcement was also used in these tests. This also has an influence on joint strength, and is discussed in section 6.7.

To investigate the effect of bar deformations on bond strength, a small number of push-in tests were conducted, as described in section 4.6. In fig. 6.8 the maximum stress developed by a reinforcing bar once the concrete cylinder had cracked is plotted against the resistance to splitting of the specimen, given in terms of the number of turns of wire in the confining spiral. The 'best fit' straight line to the results for the 'Unisteel 410' reinforcement is also shown.

Fig. 6.8 shows that the 'Hybar' reinforcement, which had the higher projected rib area per unit length of bar of the two types of reinforcement, developed stresses an average of 22 N/mm^2 higher than 'Unisteel 410' reinforcement, equivalent to a difference of 0.8 N/mm^2 in average bond stress. Investigations conducted by Clark[49] and Tepfers[4] have also shown that more heavily ribbed bars develop higher bond stresses.

6.4 Contribution of End Bearing

Results of tests on lapped joints of varying lengths are shown in table 6.1 for specimens with end bearing only, bond only, and bond and end bearing combined. Only results of tests on specimens with

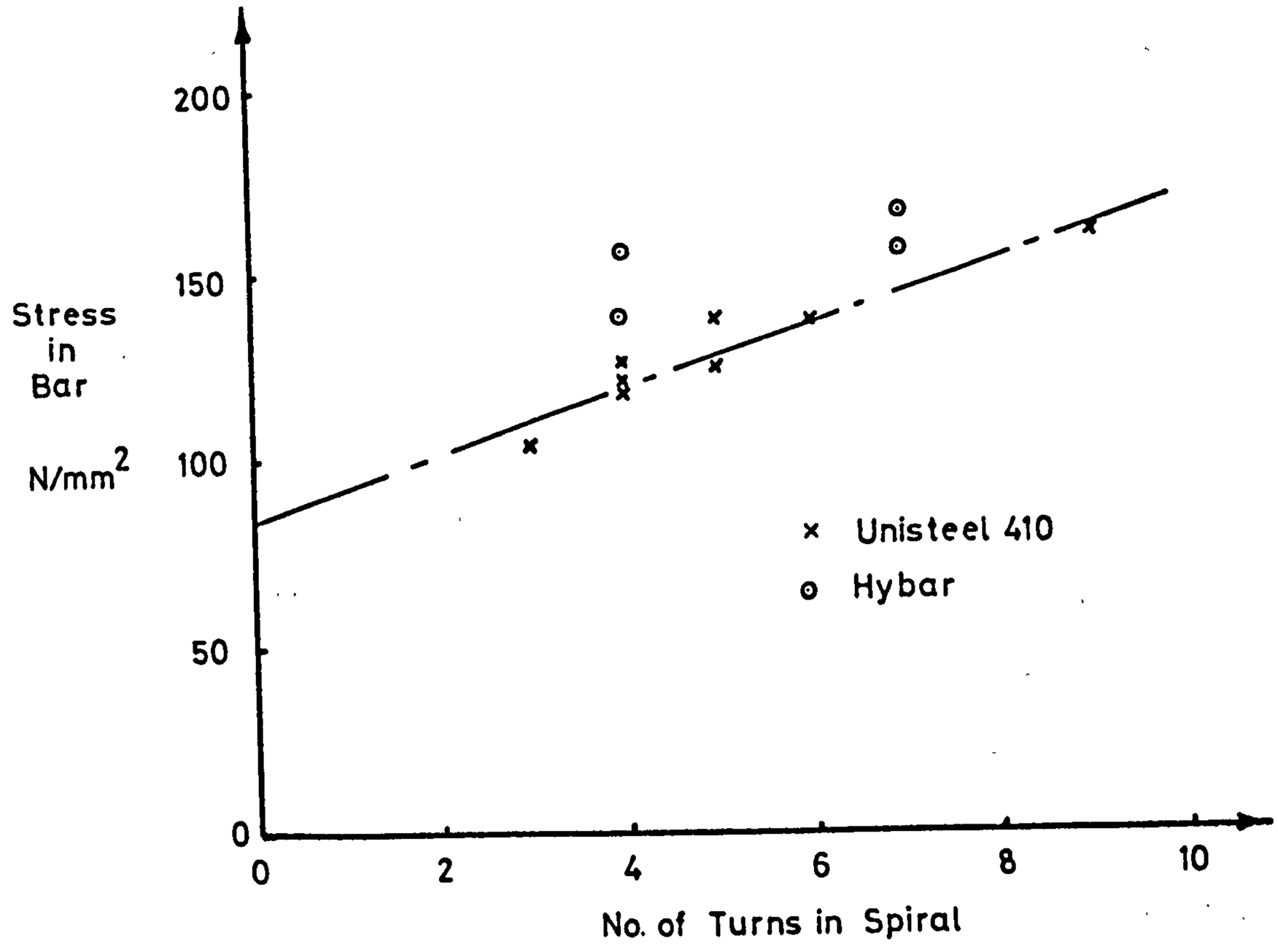

Fig. 6.8 Results of Push-in Tests

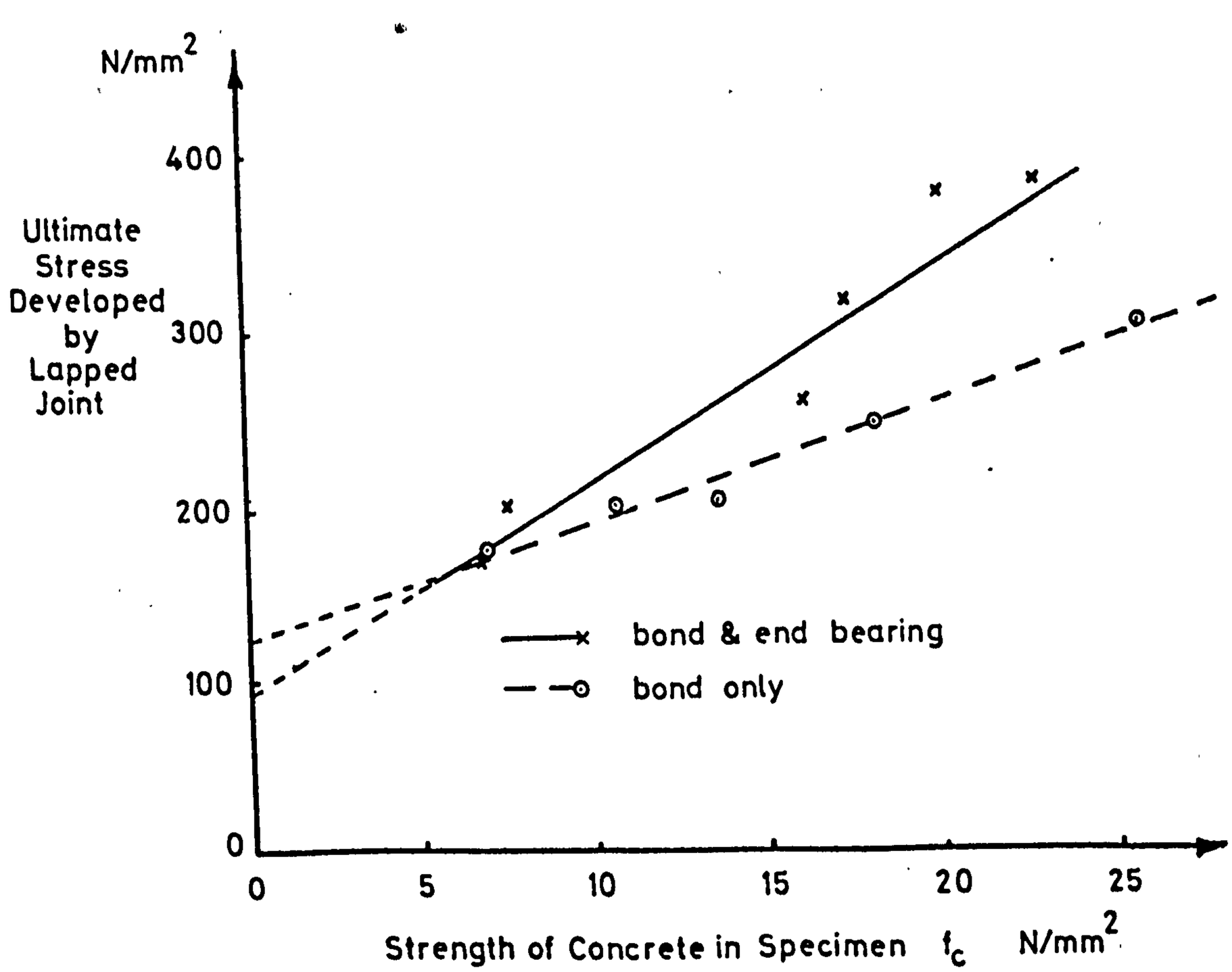

Fig. 6.9 Relationship between concrete strength and ultimate strength of lapped joint.

'Unisteel 410' reinforcement are included, and no correction has been made for differences in concrete strength. The results presented in table 6.1 show that the strength of lapped joints where bond and end bearing were present is less than the sum of the strengths of lapped joints with bond only and with end bearing only.

Fig. 6.9 shows the relationship between the stress developed by a 10ϕ lapped joint and the strength of the concrete in the specimen. The results shown are for specimens with 'Hybar' reinforcement. Two 'best fit' straight lines are also shown, one for specimens with bond and end bearing of the bars present, the other for specimens with bond only. The projection of both lines intercept the steel stress axis at approximately the same value, but the line for columns without end bearing has a flatter slope. The difference between the lines is the net contribution of end bearing to joint strength, and is approximately 80 N/mm^2 for a concrete strength of 20 N/mm^2.

TABLE 6.1 RESULTS OF INVESTIGATION ON CONTRIBUTION OF END BEARING TO JOINT STRENGTH)SPECIMENS WITH 'UNISTEEL 410' REINFORCEMENT.

		Stress Developed By Lapped Joint N/mm^2			
Bar Condition	Bar Diameter mm	Lap Length 10ϕ	15ϕ	20ϕ	
Bond and end bearing	32			443	
	40	332	>315,336	291*	430
Bond only	32			288	
	40	249	291		
End Bearing only	32			180	
	40	223	201,221	181	

* Failed outwith lapped joint.

Bond stresses and the stress in the steel close to the end of a lapped bar due to end bearing calculated from strains measured on the main reinforcing bars within the lap length are shown in table 6.2, and it may be seen that stresses due to end bearing were substantially lower where bond was also present. However, bond strength also appears to be reduced where end bearing is present, as the bond stresses developed in column A 304B where end bearing of reinforcement was eliminated were as high as those developed in columns with bond and end bearing present, despite the concrete strength being 15% lower.

TABLE 6.2 BOND STRESS AND END BEARING STRESS CALCULATED FROM STRAINS MEASURED ON REINFORCEMENT.

Column	Strains Measured at load of kN	Percentage of Ultimate Load.	Average Bond Stress N/mm^2 Distance from end of bar 2.5ϕ	5ϕ	10ϕ	20ϕ	Stress in Bar 10mm from end	Max Stress Recorded 10mm from end of Bar during Loading
A 301	5000	97	-	6.4	5.2	-	67	90
A 303B	5250	96	6.6	6.3	5.2	3.2	77	77
A 304B	4000	97	6.7	6.1	5.2	-	-	-
A 308B	3750	96	-	-	-	-	102	110

Observations of crack behaviour have shown that both bond and end bearing set up tensile stresses in the concrete cover to the reinforcement, and that, close to the ultimate load of a column, all resistance to the bursting forces is provided by the secondary reinforcement confining the lapped bars. If the same total resistance to bursting is present, in this case the same strength of secondary reinforcement, the force available to resist each is lower where

both are present, and the strength of the combination is lower than the sum of the strength of each part separately. The fact that the strength of bond or end bearing individually is lower than the strength of the combination also suggests that the strength of lapped joints is not proportional to the available resistance to bursting, as has been assumed by the reports of Tepfers[4], and the C.U.R.[3], and Ferguson and Krishnaswamy[5].

Fig. 6.10 shows the variation of longitudinal strain in the steel near the end of a reinforcing bar with column load. The strain in the bar is a measure of the bearing stress on the end of the bar. Fig.6.10 shows that, in column A 301, end bearing reached a maximum at 90% of the ultimate load of the column, but had dropped to 65% of its maximum value by the time ultimate load was reached. Leonhardt and Teichen's[2] tests produced similar results. It appears that either the maximum values of bond and end bearing occur at different values of bar-concrete slip, or that, as the ultimate strength of a lapped joint is approached, increases in bond stress take a larger proportion of the available resistance to bursting.

As mentioned in section 4.3, cones punched out by end bearing of bars were often recovered, and the angle at the apex of the cone measured, from which the angle of internal friction of the concrete could be calculated by equation 3.6. The values of the angle of internal friction calculated in this way are plotted against concrete strength in fig. 6.11.

Triaxial compression tests by the author and others [42] [43] have shown that the angle of internal friction of concrete decreases with increasing cell pressures. Fig. 6.11 shows that the angle of internal friction calculated from the dimensions of the concrete cones increased with increasing concrete strength, which shows,

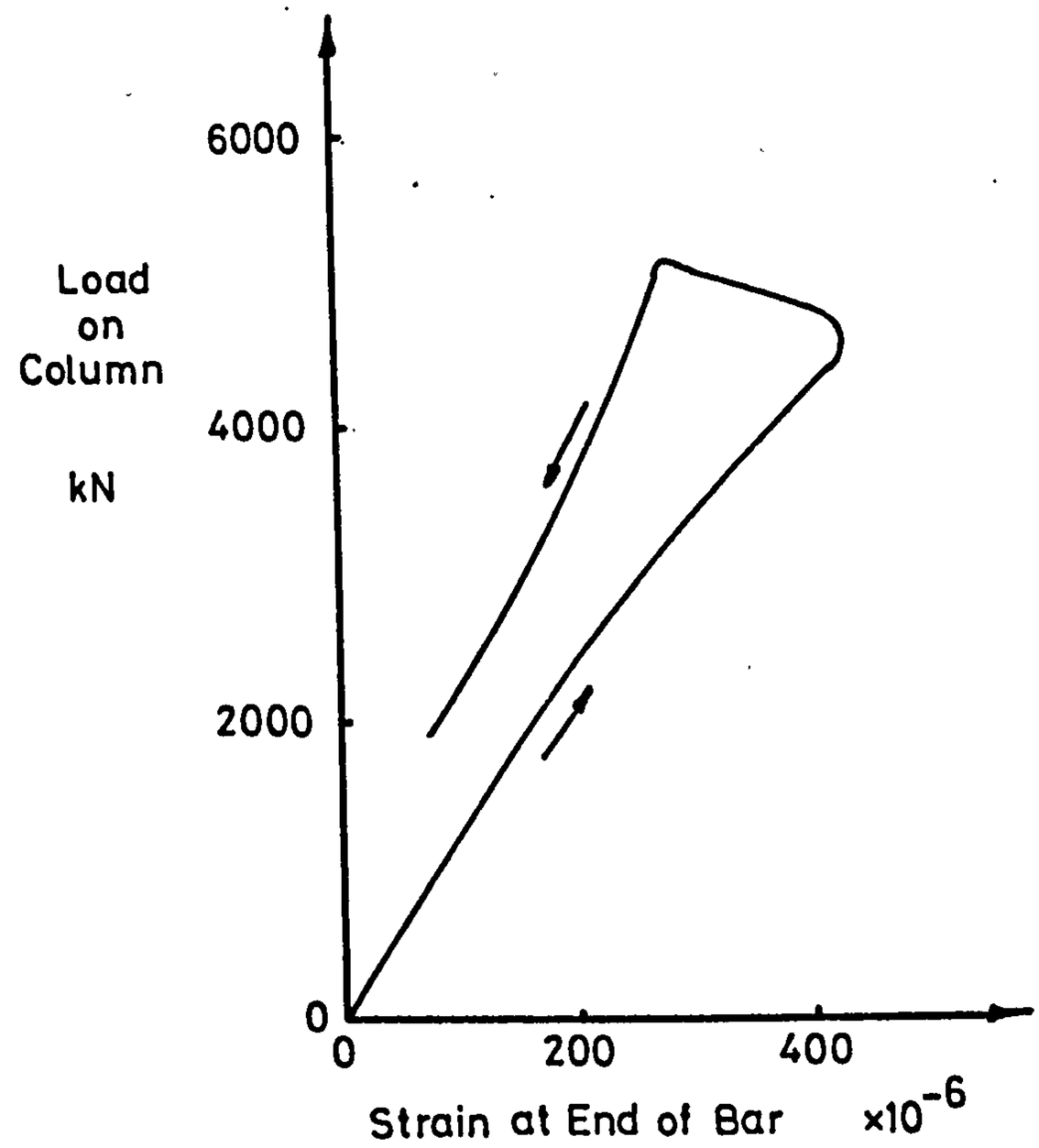

Fig. 6.10 Variation of strain at end of bar with column load - column with bond and end bearing present.

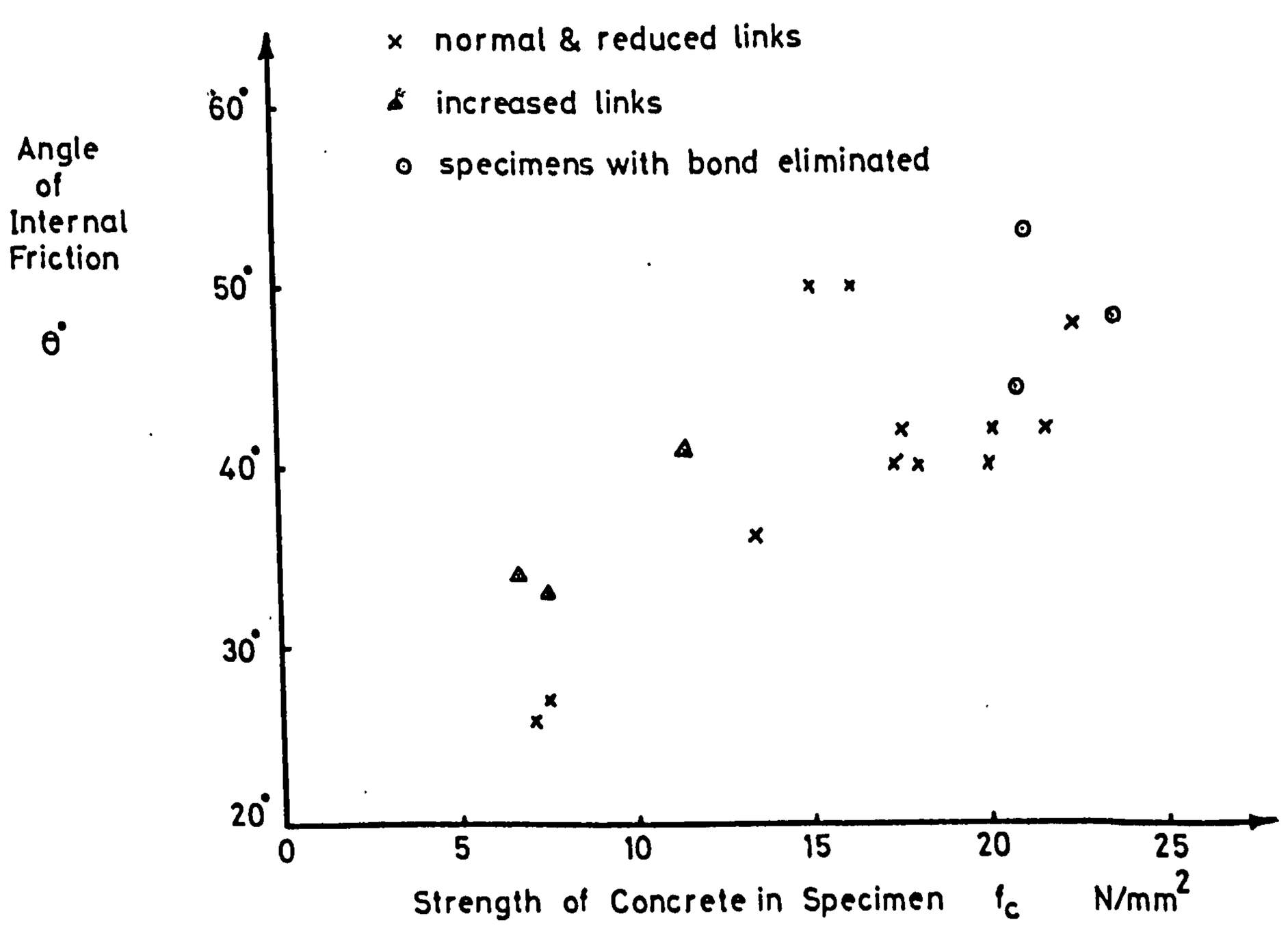

Fig. 6.11 Relationship between angle of internal friction, calculated from equation 3.6 and concrete strength.

according to Coulomb-Mohr theory, that the restraining force on cones is lower at higher concrete strengths. However, as tests with bond eliminated also produced higher values of the angle of internal friction of concrete, it is most unlikely that this is correct. The author has been unable to find any explanation for the variations in the value of θ, although it is possible that the shape of the cones was influenced by the shear stress on either side of the link at the end of the lapped joint, mentioned in section 6.2

6.5 Influence of Concrete Strength

6.5.1 Fig. 6.9 shows the influence of concrete strength on the stress developed by a 10ϕ lapped joint for bars with bond and end bearing combined and bars with bond only. The 'best fit' lines for both bar conditions show a linear variation of joint strength with concrete strength.

To allow corrections to be made for variations in concrete strength, it is assumed that the relationships between joint strength and concrete strength for 10ϕ lapped joints can be represented by the following expressions for $6\ N/mm^2 < f_c < 26\ N/mm^2$

For bars with bond only

$$f_{sc} = 110 + 7.5\, f_c \qquad 6.4$$

For bars with bond and end bearing combined

$$f_{sc} = 110 + 11.25\, f_c \qquad 6.5$$

A change in concrete strength is therefore considered to cause a change of $7.5.\Delta f_c$ in the ultimate stress developed in a bar by bond, and a change of $3.75.\Delta f_c$ in the ultimate stress developed in a bar by end bearing. The results presented later in figs. 6.14 and 6.15, and discussed in section 6.6, indicate concrete strength has little influence on the stress developed by 20ϕ lap lengths. As there is

insufficient data to determine the influence of concrete strength on the strength of 15ϕ lapped joints, corrections for concrete strength are only made to the results of test specimens with a lap length of 10ϕ. The corrections are assumed to be applicable to lapped joints with 'Hybar' reinforcement. For 'Unisteel 410' reinforcement, the factors associated with concrete strength in equations 6.4 and 6.5 are reduced to 6.7 and 10.45 respectively, in accordance with the results of the push-in tests.

The limited number of tests conducted on specimens with bond of bars eliminated do not allow any evaluation of the influence of concrete strength on joint strength to be made for that condition, but there are indications that joint strength decreases with concrete strength.

As the concrete cover to the reinforcement was extensively split along the line of the reinforcement at ultimate load in all the tests, the increase in joint strength due to an increase in the strength of the concrete in a specimen cannot be attributed to an increase in the confining force on a bar. It appears that both bond strength and end bearing strength are composed of two separate contributions, one due to the confinement of the bars by secondary reinforcement, and the other related to the compressive strength of the concrete in the specimen. The latter contribution does not exert bursting forces on the surrounding concrete. The lower joint strengths obtained when bond or end bearing were eliminated can therefore be explained by the absence of the non-bursting component of whichever bar condition was eliminated.

The results of the push-in tests, shown in fig. 6.8, indicated that bond strength varied linearly with confining force, but that

there was also a constant contribution of 85 N/mm^2, equivalent to an average bond stress of 3.1 N/mm^2, to the stress developed by 'Unisteel 410' reinforcement. The value of bond stress would be approximately 3.9 N/mm^2 for 'Hybar' reinforcement. As in tests on lapped joints, the concrete cover to the reinforcement in push-in tests was cracked at ultimate load, and this contribution to bond strength could not be attributed to the resistance to bursting of the cylinder.

The relationship between cube compressive strength and cylinder compressive strength is usually taken to be

$$f_c' = 0.78\ f_{cu} \qquad 6.7$$

where f_c' = cylinder compression strength

f_{cu} = cube compression strength.

From equation 6.7 and table 4.4, the strength of concrete in push-in specimens was approximately 0.78 x 36 = 28.1 N/mm^2. From equation 6.4, a concrete strength of 28.1 N/mm^2 would be expected to contribute 7.5 x 28.1 = 211 N/mm^2 to the stress developed by bond only in 10ϕ lapped joint. Assuming a bond length of (10 + 2.5)ϕ that is equivalent to an average bond stress of 4.2 N/mm^2, which agrees well with the results of the push-in tests on 'Hybar' reinforcement.

6.5.2 The influence of concrete strength on load at which longitudinal cracks were first detected in the concrete over the reinforcing bars was also examined. Cracks were detected as described in section 5.1.

The load at which cracks were first detected is plotted against concrete strength in fig. 6.12. The results are for 10ϕ lapped joints with bond and end bearing of bars present, and for both types of reinforcement. Fig. 6.12 shows that the load at which cracks

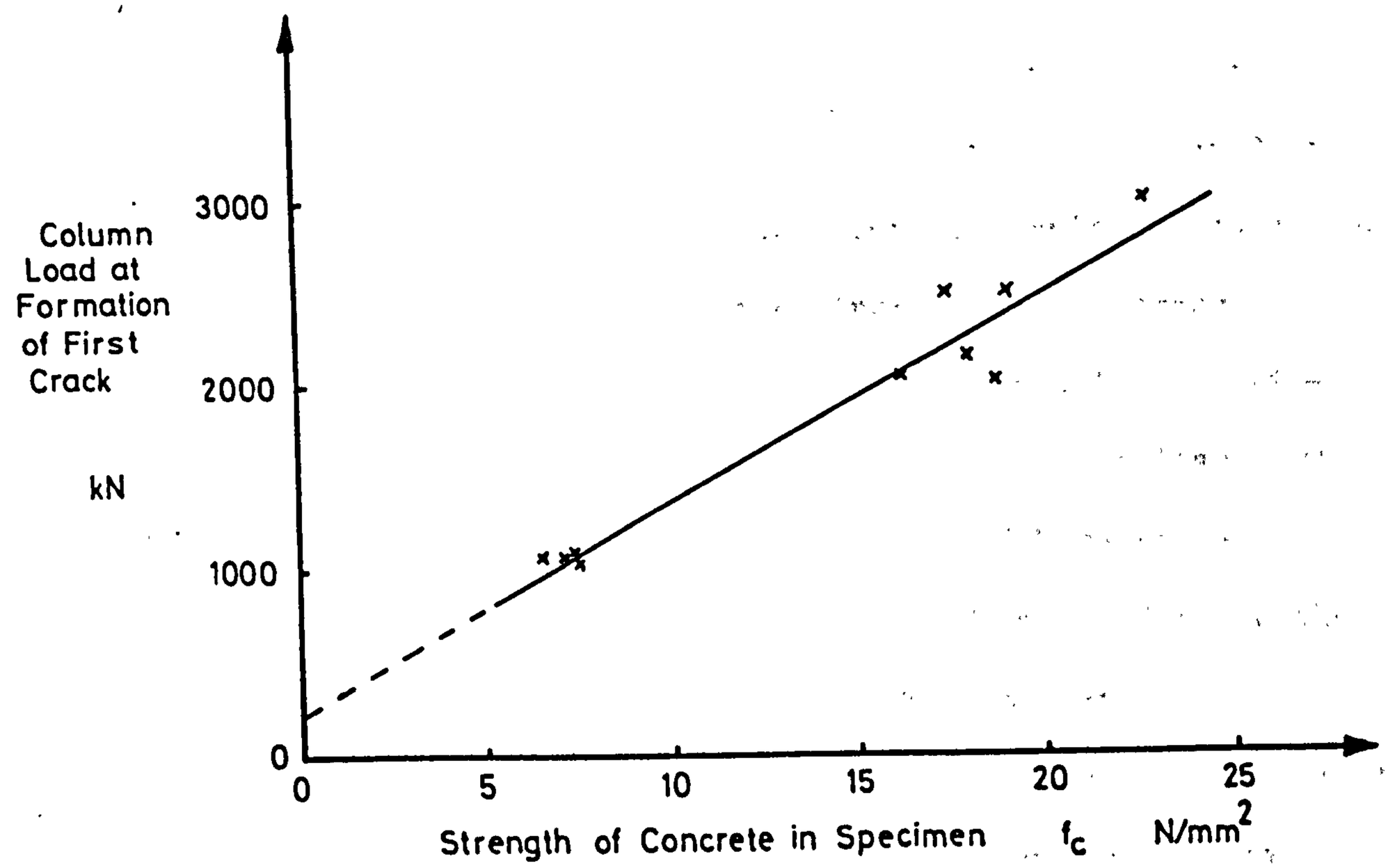

Fig. 6.12 Relationship between column load at formation of first longitudinal crack and concrete strength - specimens with bond and end bearing.

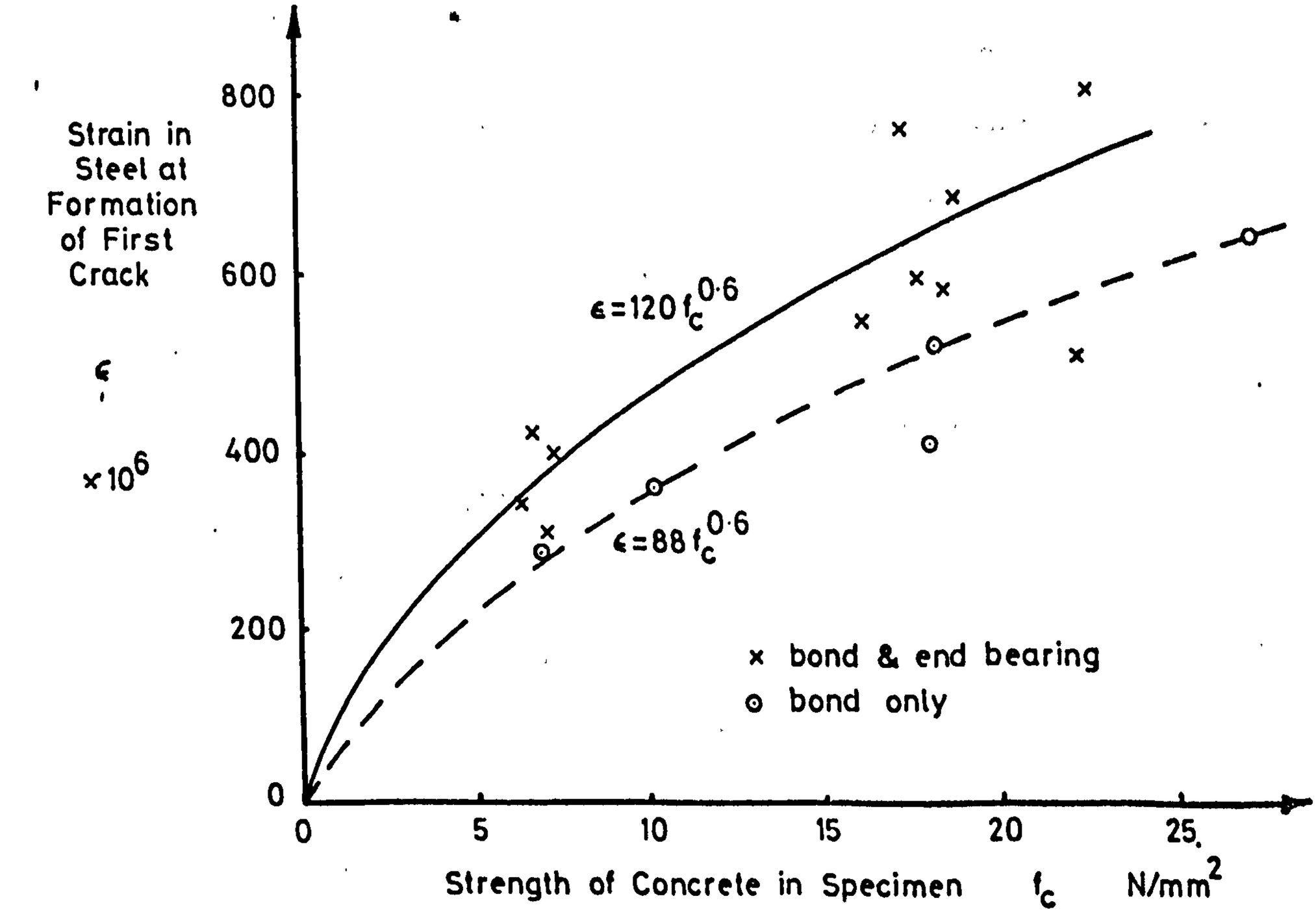

Fig. 6.13 Relationship between strain in reinforcement at formation of first crack and concrete strength.

first developed was roughly proportional to the strength of the concrete in the specimen. However, if the strain in the reinforcement at first cracking, taken to be the average strain on the column outwith the lapped joint, is plotted against concrete strength, as shown in fig. 6.13, a curve results, with the strain in the reinforcement at first cracking proportional to $f_c^{0.6}$. A similar curve results for lapped joints in which end bearing of bars was eliminated.

The curves obtained in fig. 6.13 are of a similar form to the square root expression that has been found to represent the relationship between the ultimate strength of a tension lapped joint without secondary reinforcement and the compressive strength of the concrete in the member, and indicates that the formation of the first cracks over the reinforcing bars is controlled by the tensile strength of the concrete.

As the strain in the reinforcement at a given load is affected by the modulus of elasticity of the concrete in the test specimen, which varies with the square root of concrete strength, as shown in fig. 5.8, the load at which cracks first form is approximately proportional to concrete compressive strength.

6.6 Effect of Lap Length

The range of lap lengths tested in the present investigation was small, due to the fact that 20ϕ lapped joints, the longest tested, developed stresses close to the yield strength of the reinforcement, and so stresses developed by longer lapped joints would have been limited by the yield strength of the reinforcement. Lap lengths shorter than 10ϕ were felt to be too short and too impracticable to be worthwhile investigating. The experimental programme was therefore designed to investigate a small range of lap lengths with controlled variations of other parameters. The results,

corrected to a concrete strength of 20 N/mm^2 by the method described in section 6.5.1, are plotted in fig. 6.14. The compressive strength of the concrete in the specimens lay within the range 16 N/mm^2 to 23.7 N/mm^2. Where tests were replicated, the average of the results is plotted. The results of three of Pfister and Mattock's[1] tests on tied columns are also plotted.

With the exception of the results of tests on specimens with bond of bars eliminated, all but one of the lines in fig. 6.14 have a similar slope, corresponding to an average bond stress of 2.6 N/mm^2. Projections of the lines to zero lap length intercept the steel stress axis at values between 240 N/mm^2 and 35 N/mm^2.

The line shown dotted in fig. 6.14 represents the results of tests in which end bearing of bars was eliminated. The line has a slope similar to that of bars with bond and end bearing present, and intercepts the steel stress axis at zero lap length at a value of 130 N/mm^2.

As discussed in section 6.2, a lapped joint in compression develops most of the stress in the reinforcement near the end of a lapped bar. The stress which develops on an additional length of lapped joint will therefore be relatively low, as may be seen from a comparison of strains in the reinforcement in 10ϕ and 20ϕ lapped joints, shown in figs. B.1 and B.2. Pfister and Mattock[1] assumed that the stress on the end of a bar would be half the value of the stress developed by a lapped joint with zero lap length, and that this value could be found by linear extrapolation of results of tests on specimens with lap lengths of 5ϕ to 30ϕ. The validity of this assumption must be questioned, however, in the light of results presented here.

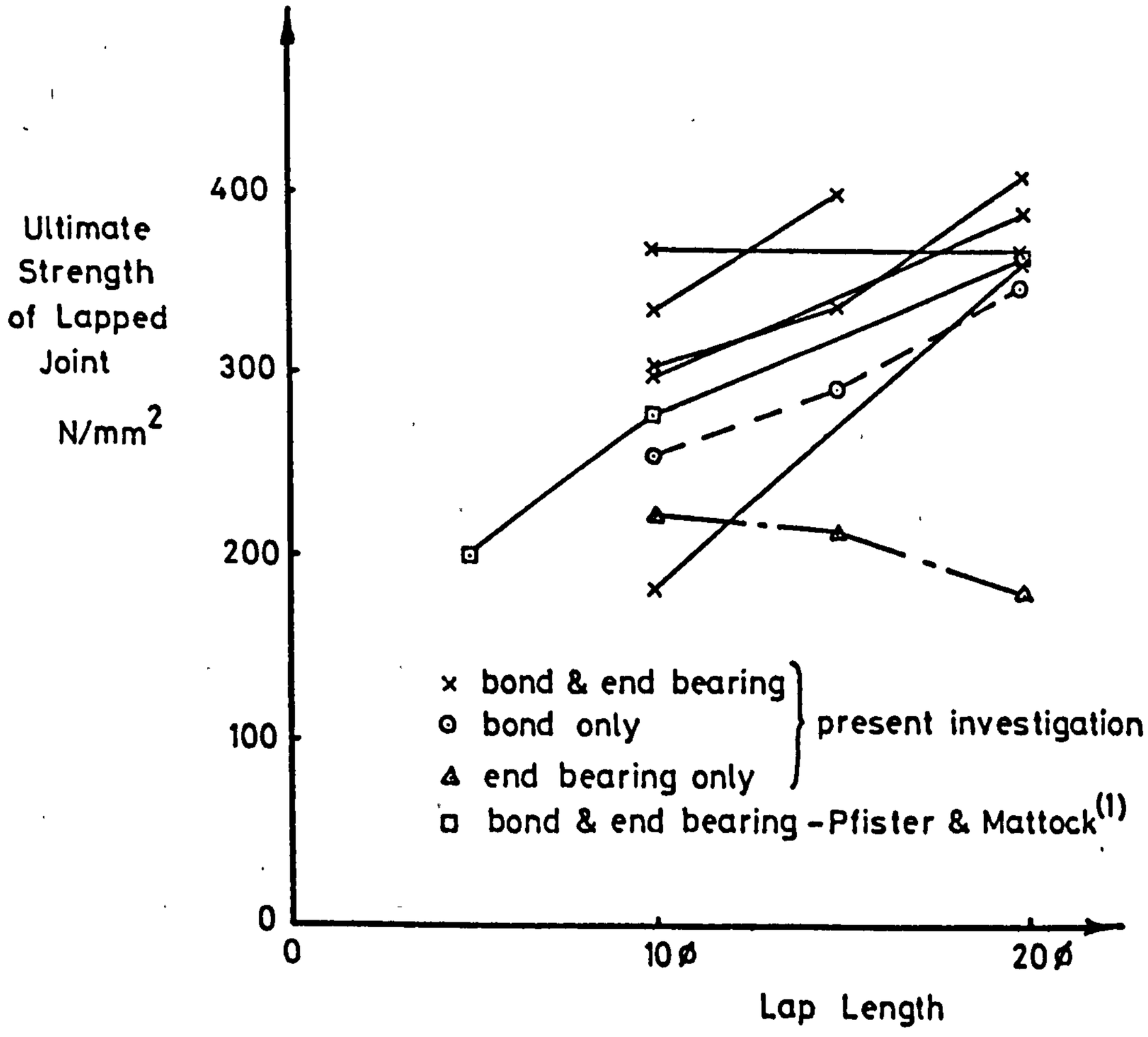

Fig. 6.14 Relationship between ultimate joint strength and lap length - results of present investigation corrected to f_c = 20 N/mm^2.

The strength of lapped joints with bond of bars eliminated decreases slightly with increasing lap length, according to fig. 6.14. The reduction in strength is small, but it may be that the corrections to the strength of lapped joints described in section 6.5.1 are not applicable to the results of tests where bond of the bars was eliminated.

Fig. 6.15 shows the variation of joint strength with lap length for columns with concrete strengths of between 7 N/mm^2 and 14 N/mm^2. The results are corrected to a concrete strength of 12 N/mm^2 by the method described in section 6.5.

The lines in fig. 6.15 slope more steeply than those shown in fig. 6.14, and the slopes correspond to an average bond stress of

approximately 3.8 N/mm^2, but the intercept with the steel stress axis at zero lap length is only 50 N/mm^2. Although 10ϕ lapped joints develop a lower stress with weaker concretes, as shown in fig. 6.9, 20ϕ lapped joints develop stresses as high as those obtained with stronger concretes.

Fig. 3.26 shows that a weaker concrete produces a more uniform distribution of bond stress, and failure of a lapped joint is therefore less likely to be due to a peak bond stress. In addition, any links in the middle of a lapped joint are likely to be better utilized. A further factor is that weaker concretes fail at higher strains, and this will also encourage a more uniform distribution of bond stress. As shown in fig. 5.1, the failure of specimens of weak concrete was much more ductile than the failure of specimens of higher strength concretes.

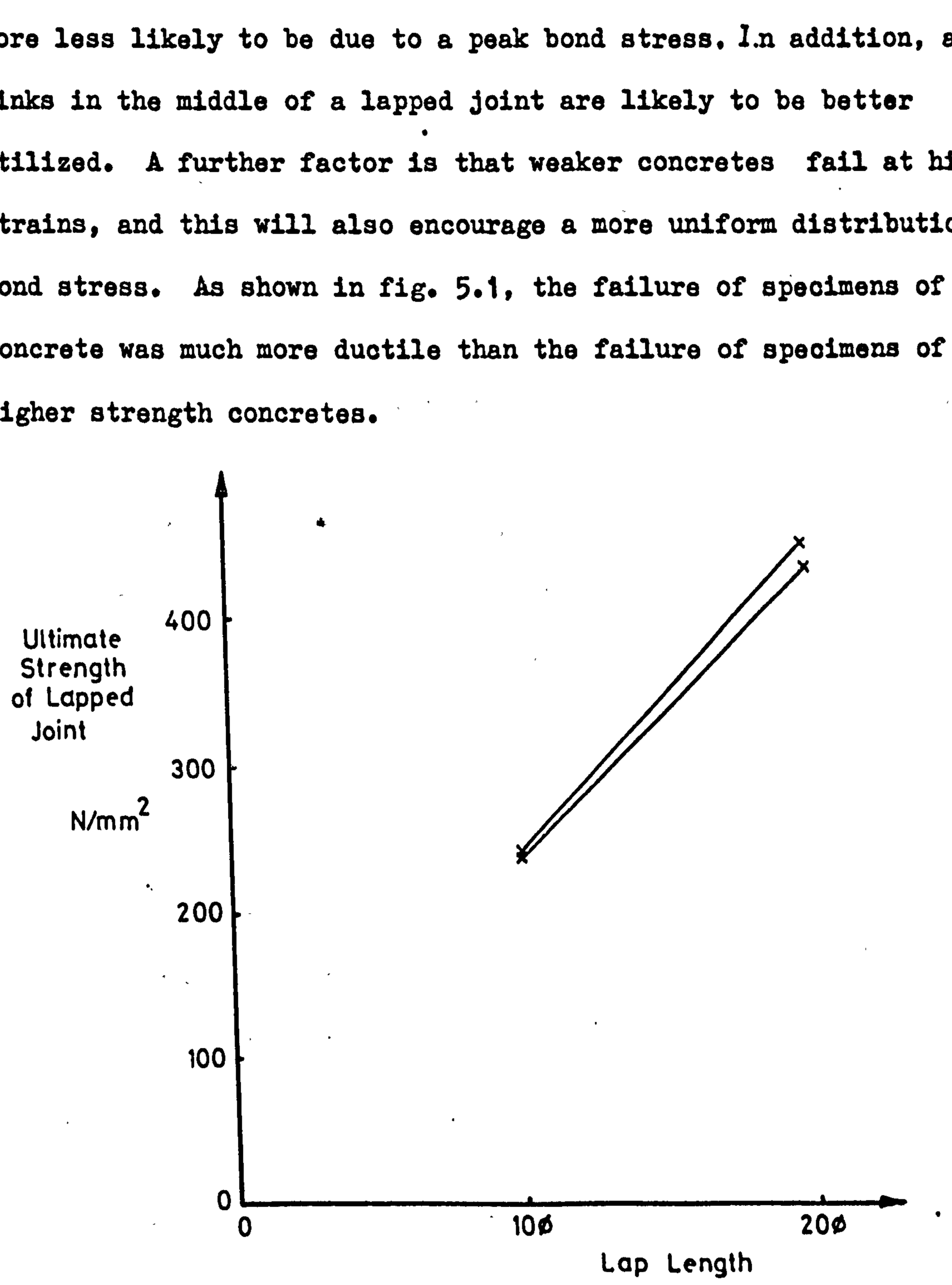

Fig. 6.15 Relationship between ultimate joint strength and lap length - results corrected to f_c = 12 N/mm^2.

6.7 Influence of Secondary Reinforcement

At the ultimate strength of a lapped joint, cracks usually extended through the length of the lapped joint in both faces adjacent to pairs of lapped bars. Resistance to the bursting forces produced by transfer of force between bars must therefore be provided almost entirely by secondary reinforcement crossing the cracks.

From observations of the growth of crack widths, it could be inferred that failure of lapped joints took place as the links confining the lapped bars exceeded their yield strength. This is confirmed in fig. 6.16, which shows strains measured on links at various positions within the specimens. The strain at which links reached their yield strength was found to be 1500×10^{-6}. As may be seen from fig. 6.16, failure of lapped joints took place as the strain in the link at the end of a lapped joint exceeded the yield strain of the steel.

Strains measured on a link in the middle of a 20ϕ lapped joint were only slightly greater than strains measured on links outwith the lapped joints. As shown in figs. 6.4 and 6.5, transverse tensile strains measured on the faces of the columns over the lapped bars were also found to be low in the middle of a 20ϕ lapped joint. From fig. 6.3 it can be seen that bond stresses were present throughout the lap length, but were lower in the middle of the lapped joint than at the end of the bar. It appears that the bond stresses in the middle of the lapped joint were insufficient to set up significant bursting forces in the concrete. As bond stresses of $\frac{1}{3}$rd of the maximum value of bond stress measured in the lapped joint developed in the middle of the lapped joint, it follows from the above that the non-bursting component of bond stress is mobilised before the bursting component, and that the bursting component of bond stress is mobilised

over a relatively small proportion of the lapped joint shown in fig.6.3. The limited mobilisation of the bursting component of bond strength causes failure to take place at the ends of the lapped joints, without the links in the middle of the lapped joints being fully utilised. The increase in joint strength with lap length is therefore largely due to an increase in the non-bursting component of joint strength, with little increase due to the bursting component of joint strength. This is reflected in the low slopes of the lines in fig. 6.14, and explains the non-zero intercept found for bars with [redacted] end bearing eliminated. The non-bursting component of bond strength for a concrete strength of 20 N/mm^2 is, from equations 6.4 and 2.1.

$$f_{bs} = \frac{7{\cdot}5\, f_c \cdot \phi}{4 \cdot l_b} = \frac{7{\cdot}5 \times 20}{4(10+2{\cdot}5)} = 3{\cdot}0\ N/mm^2 \qquad 6.8$$

The value of bond stress found from equation 6.8 is slightly greater than the average value of bond stress of 2.6 N/mm^2 found from fig. 6.14 for the difference between 10ϕ and 20ϕ lapped joints.

Plots of joint strength against lap length showed steeper slopes for weaker concretes, as shown in fig. 6.15. As discussed in the previous section, bond stresses are more uniformly distributed with weaker concretes, and links away from the ends of lapped joints will be more highly strained. In this case, the increase in joint strength with lap length is due to an increase in both the bursting and non-bursting components of joint strength.

The results of the short series of push-in tests, presented in fig. 6.8, indicated that ultimate bond strength varies linearly with confining force. A number of tests were also conducted on lapped joints to examine the influence of secondary reinforcement. The results, corrected to a concrete strength of 20 N/mm^2 by the method described in section 6.5.1, are presented in table 6.3 There is a

fairly large difference between the results of two similar tests, but their average is used in the discussion. 'Normal' links used in this investigation were quarter of the main bar diameter, and at a spacing of 10 times the main bar diameter, to comply with the requirements of B.S.C.P.110:1972, but their yield strength was considerably greater than the characteristic yield strength usually assumed for plain round mild steel reinforcing bars.

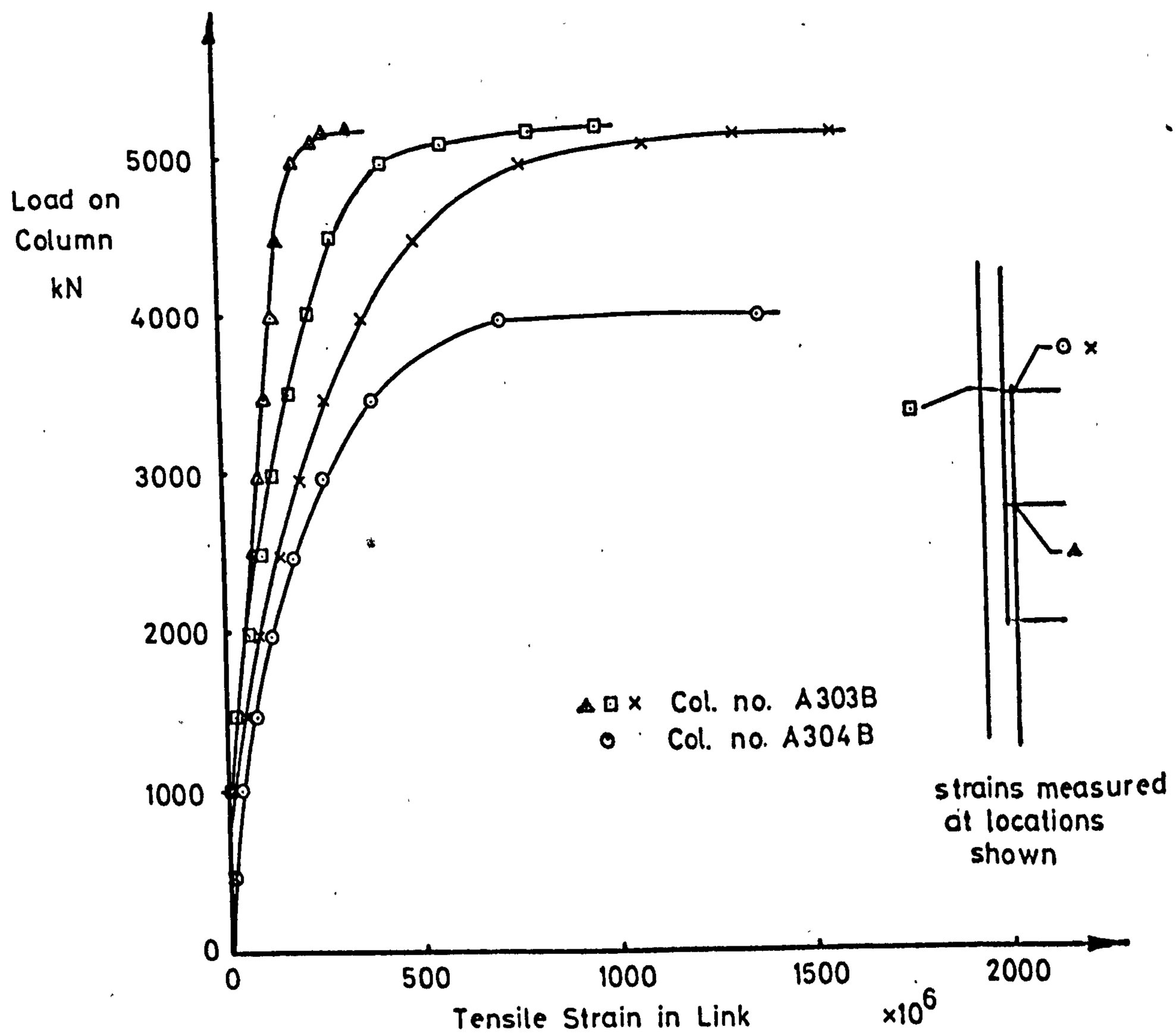

Fig. 6.16 Strains measured on links.

It may be seen from table 6.3 that, although a decrease in the amount of secondary reinforcement confining the lapped bars produced a drop in joint strength, an increase above the 'normal' amount did not produce a corresponding rise in joint strength. The specimens with increased links were the only ones in which bars sheared the

concrete along a surface across the tops of the bar ribs, producing the type 1 failure described in section 3.3. As concluded by Orangun, Jirsa and Breen[25], increasing the amount of secondary reinforcement above a certain value produces no increase in joint strength.

TABLE 6.3 INFLUENCE OF SECONDARY REINFORCEMENT ON JOINT STRENGTH - SPECIMENS WITH 'HYBAR' REINFORCEMENT.

Secondary Reinforcement		10ϕ Lap Length			20ϕ Lap Length		
Diameter (mm)	Yield strength N/mm^2	No. of links within lapped joint	$\frac{A_{sv} \cdot f_{yv}}{\phi \cdot l_l}$ N/mm^2	Steel stress at ultimate N/mm^2	No. of links within lapped joint	$\frac{A_{sv} \cdot f_{yv}}{\phi \, l_l}$ N/mm^2	Steel stress at ultimate N/mm^2
8	240	2	1.5	300	3	1.13	386
10	387	1	1.9	221,133	2	1.9	325
10	387	2*	3.8	335	3*	2.8	449
10	387	4	7.6	351	5	4.8	430

* - 'Normal' links.

Of the specimens with reduced links, two of the test specimens had weaker links positioned in the same way as 'normal' links, and three had a reduced number of links of the same strength as normal links. In the latter case, links were positioned away from the ends of the lapped joints, as shown in fig. 4.1. Although all specimens with reduced links were weaker than those with normal links, those with the reduced number of links showed the greater drop in joint strength, despite the reduction in the total strength of links being smaller. Fig. 6.17 shows that larger tensile strains were recorded on a column face over the end of a bar where there were no links at the end of a lapped joint. The greater reduction in joint strength where links were not positioned at the ends of the lapped joint is

probably due to the leverage obtained on the link by the bursting forces near the end of the bars, as indicated in fig.6.18(a) and (b). A greater outwards movement of the end of the bar will be required to develop the same force in the link for the case shown in fig.6.18(a). Obviously links are best positioned at the ends of lapped joints, where their strength may be mobilised to confine the lapped bars most quickly.

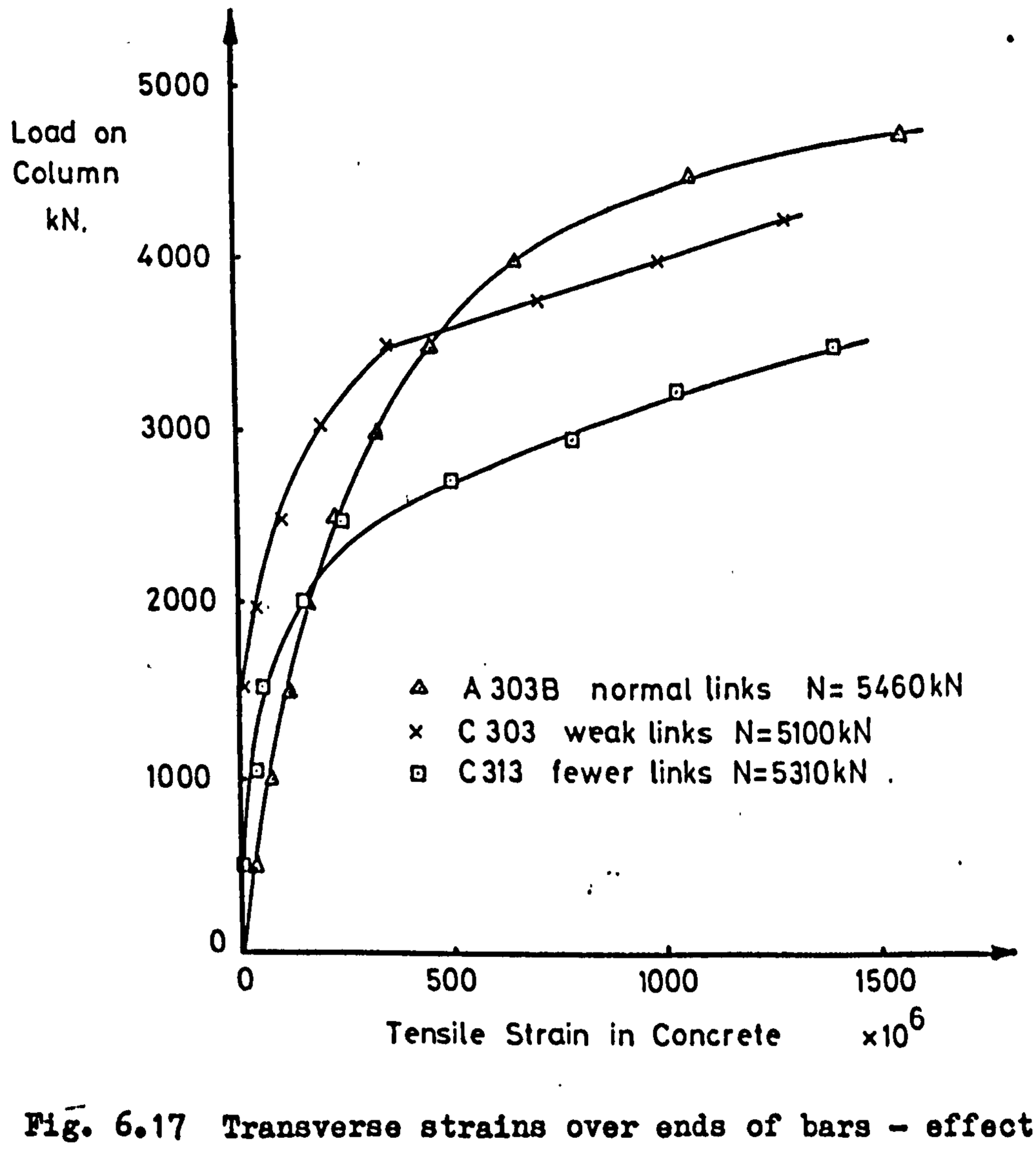

Fig. 6.17 Transverse strains over ends of bars - effect of positioning of links.

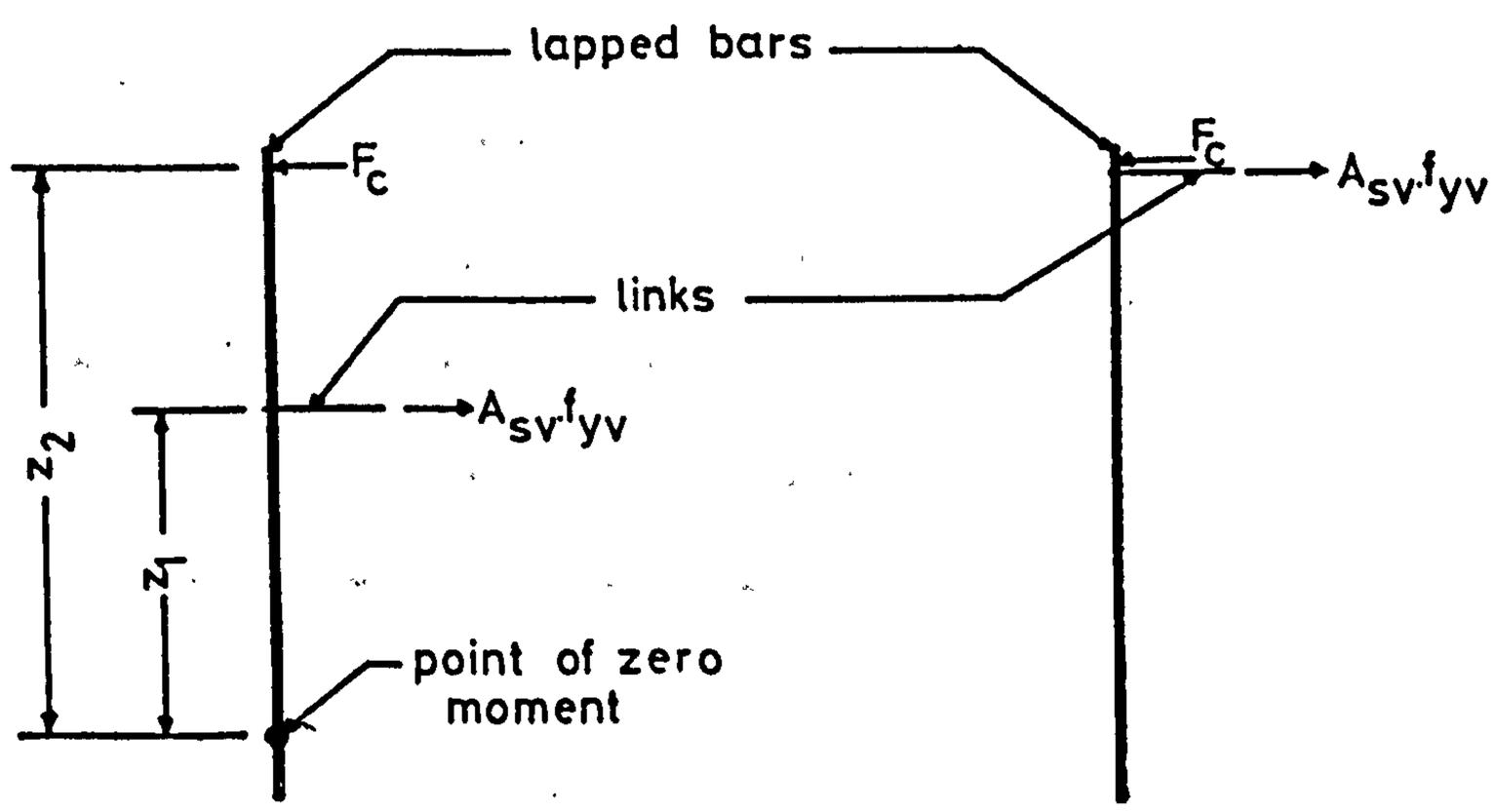

(a) link away from end of lapped bar.

(b) link at end of lapped bar.

Fig. 6.18 Effect of positioning of links on confining force on bar.

CHAPTER 7

COMPARISON WITH THEORETICAL ANALYSIS

7.1 Introduction

In sections 3.3 to 3.6, expressions were derived for the ultimate stress developed by deformed reinforcing bars in push-in specimens and in lapped joints. The analysis showed that bond strength and end bearing strength were each made up of two components, one related to the compressive strength of the concrete around a bar, and the other related to force available to resist the radial forces exerted by bond or end bearing of the reinforcement. The latter component tends to split the concrete cover along the line of reinforcement in test specimens.

The theoretical analysis is therefore in agreement in principle with the conclusions reached in chapter 6.

7.2 Push-in Tests

The stress developed by a ribbed deformed bar in a push-in test calculated from equation 3.32, is plotted against the strength of the confining spiral in fig. 7.1. Equation 3.32 is evaluated using the dimensions obtained for 40mm diameter 'Unisteel 410' reinforcement, presented in table 4.3. Results obtained from push-in tests on 40mm diameter 'Unisteel 410' reinforcement are also shown in fig. 7.1.

Fig. 7.1 shows that equation 3.32 greatly overestimates the stress developed in a bar in push-in specimens. However, theoretical and 'best fit' experimental lines do intercept the steel stress axis at zero confining force at approximately the same value. It therefore appears that the theoretical analysis estimates the non-bursting component of bond strength accurately, but overestimates the influence of the confining spiral.

The wire used for the confining spiral in the experimental

investigation was smooth and clean, and little concrete cover was provided to the spiral in the test specimens. During tests, cracks usually appeared over the wire on the surface of the concrete cylinder, indicating that there was slip between the concrete and the wire, and that the strain in the wire would be fairly even at all points in the spiral. Another reason for concluding that slip must have taken place between reinforcement and concrete is that the wire spiral rarely broke, even when wide cracks developed. The total extension of one turn of the wire spiral is therefore

$$x = \pi \cdot \phi_c \cdot \epsilon \qquad 7.1$$

where x = total extension of one turn of spiral

ϕ_c = spiral diameter $\fallingdotseq$ cylinder diameter = 150mm

and ϵ = strain in wire

Cracks in the push-in specimens usually formed at three positions as shown in fig. 7.2 and hence the width of each crack will be

$$w = \frac{x}{3} = \frac{1}{3}\pi \cdot \phi_c \cdot \epsilon \qquad 7.2$$

Hence, as shown in fig.7.3, the relative movement between bar and concrete will be

$$a = \frac{w}{2}\cot\alpha = \frac{\pi}{6}\phi_c \cdot \epsilon \cdot \cot\alpha \qquad 7.3$$

Evaluating equation 7.3 for a value of α of 29°, found from equations 3.6 and 3.15, and an average wire strain of 0.0015, a value lower than the strain at which the wire yields, gives the relative movement between bar and concrete as 0.21mm.

In tests on the bearing strength of concrete blocks, Meyerhof[50] found that a 32mm diameter punch developed on ultimate bearing stress similar to that under a rib in the push-in tests at a deflection of approximately 0.3mm. As the maximum height of the ribs of the reinforcing bars used in the push-in tests was 3mm, it must be concluded

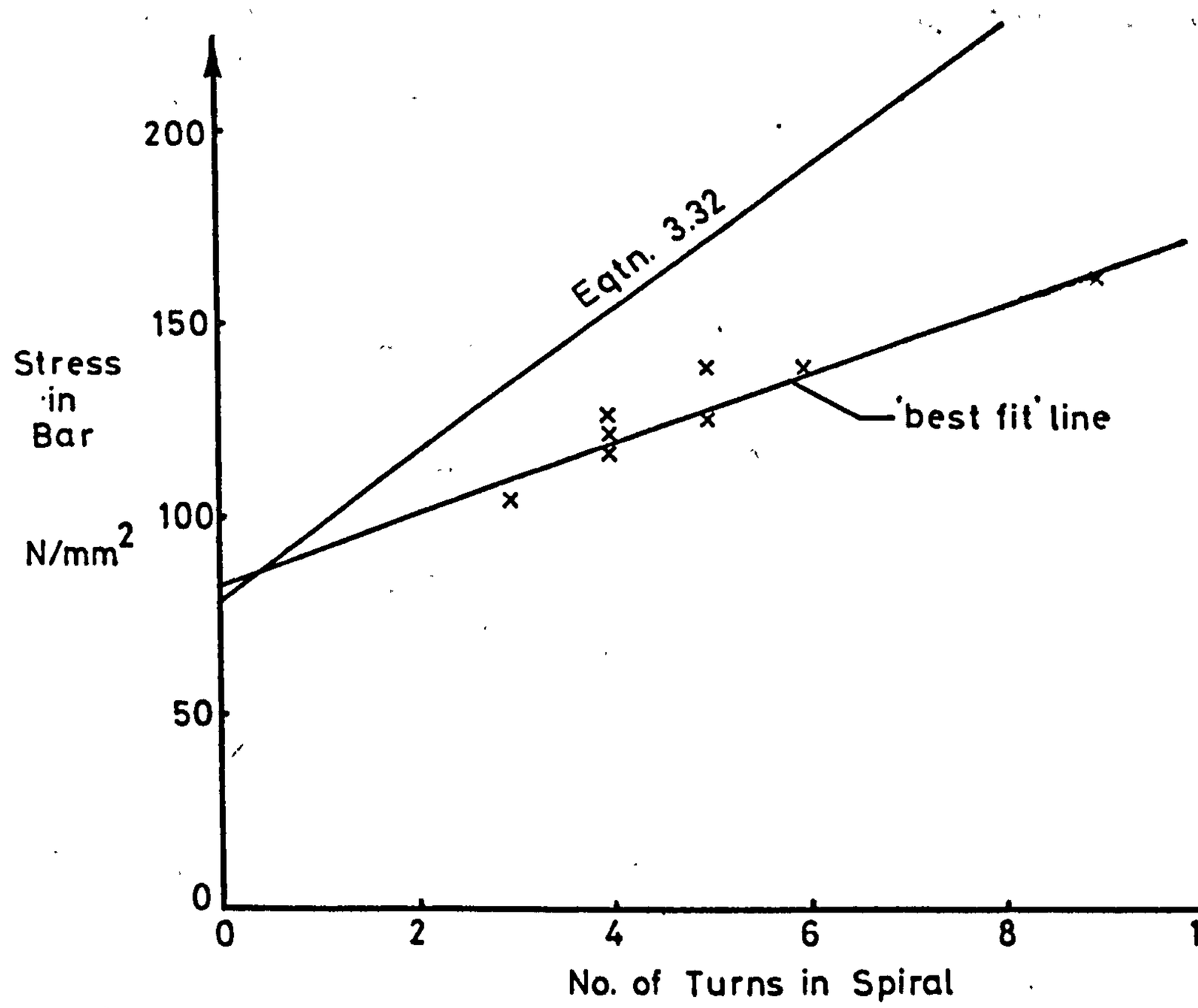

Fig. 7.1 Comparison of theoretical analysis and experimental results for push-in tests.

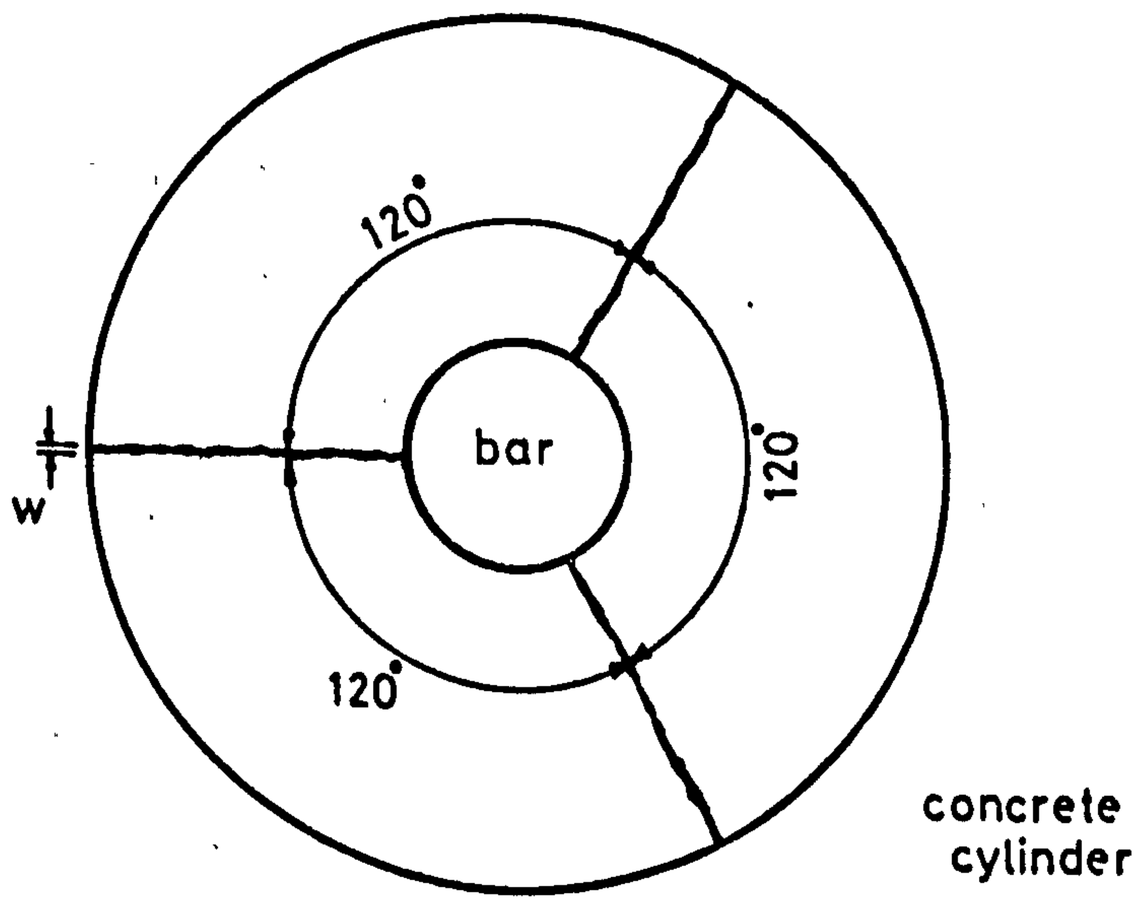

Fig. 7.2 Typical crack formation in push-in specimen.

that the wire spiral did not yield until the ultimate load of push-in specimens had been passed.

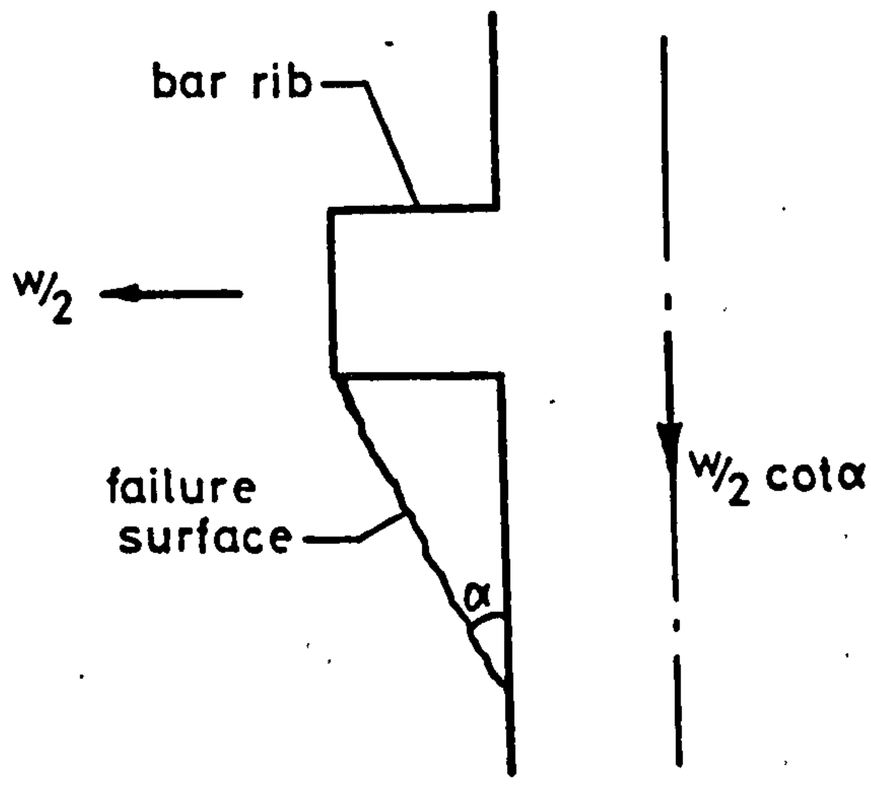

Fig. 7.3 Bar - concrete slip.

The restraint to splitting of the specimens from the platen of the testing machine may also have influenced the results of the push-in tests. However, Hyland and Chen[31] found that the ultimate bearing capacity of concrete blocks was not influenced significantly by varying degrees of platen restraint, and it is considered that platen restraint will have little influence on the ultimate strength of push-in specimens.

The results of push-in tests showed that the specimens with 'Hybar' reinforcement developed stresses an average of $22N/mm^2$ higher than the specimens with 'Unisteel 410' reinforcement. Evaluating equation 3.32 for the dimensions of 'Hybar' and 'Unisteel 410' reinforcement shows a difference of $22N/mm^2$ in the stress developed by each bar over a bond length of 275mm. Equation 3.32 therefore shows excellent agreement with experimental results in this respect. The difference in bond strength between bars is due to an increase in the non-bursting component of bond strength with the more heavily ribbed 'Hybar' reinforcement.

In tests on tension lapped joints, Tepfers[4] found that bars with annular ribs developed the same joint strength as bars with inclined crescent shaped ribs, even though the projected rib area/unit length of the bar with annular ribs was half that of the bar with crescent shaped ribs. As stated above, equation 3.32 shows that an increase in the projected rib area/unit length of bar produces an increase in the ultimate bond strength of a bar. In section 3.3, it was also shown that bars with crescent shaped ribs would be expected to develop lower stresses than bars with annular ribs, for the same confining force. As Tepfers' experimental results were mainly for tension lapped joints without secondary reinforcement, a quantitative evaluation is impossible, but it may be seen that the theoretical analysis is consistent with Tepfers' results.

7.3. Lapped Joints

7.3.1 Bars with bond only. In section 3.6, expressions were derived for the ultimate stress developed by lapped joints with bars with bond only. Upper and lower limits, given by equations 3.43 and 3.44, were derived for joint strength for the joint detail used in the experimental investigation.

The strength of 10 ϕ lapped joints, calculated from equation 3.43 and 3.44, is plotted against concrete strength in fig. 7.4. Equations 3.43 and 3.44 are evaluated for the dimensions of 'Hybar' reinforcement, and for links of one quarter of the diameter of the main reinforcement with a yield strength of 387N/mm^2. It is assumed that the non-bursting component of joint strength acts over a length of 12.5ϕ, for the reasons outlined in section 6.2. The results of tests on 10ϕ lapped joints with 'Hybar' reinforcement and end bearing of bars eliminated are also shown in fig. 7.4.

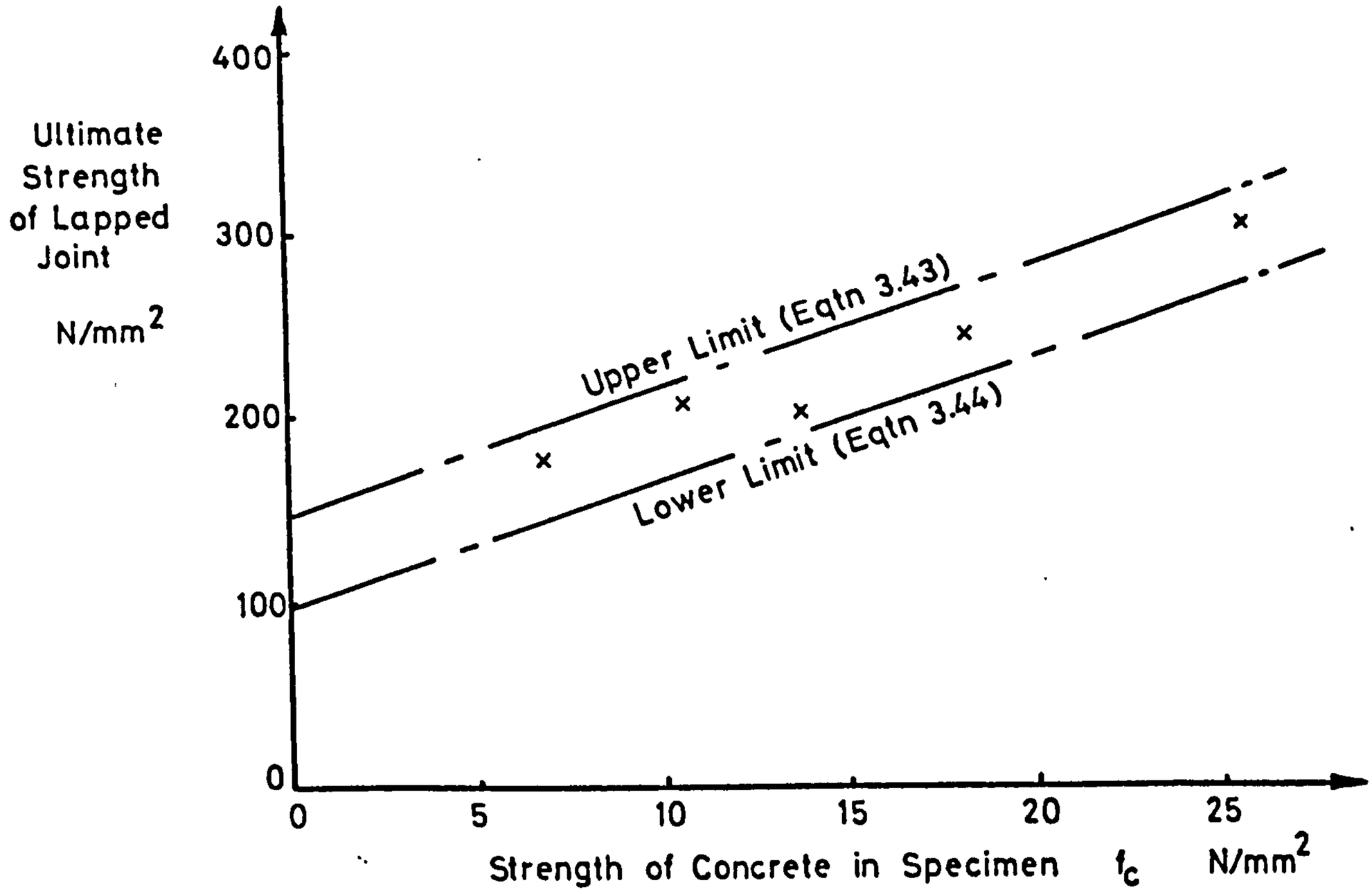

Fig. 7.4 Comparison of theoretical analysis and experimental results for ultimate strength of lapped joints with end bearing eliminated.

All the experimental points lie within the limits of joint strength calculated from equations 3.43 and 3.44. The 'best fit' line to the experimental results is approximately parallel to the upper and lower limits, and it is concluded that the theoretical analysis gives a good representation of the behaviour of short lapped joints with varying concrete strength.

In table 7.1, the strength of lapped joints calculated from equations 3.43 and 3.44 are compared with the experimental results for columns in which end bearing of reinforcement was eliminated. In two cases of 20 ϕ lapped joints, both equation 3.43 and equation 3.44 overestimate the strength of the lapped joint. This may

TABLE 7.1 LAPPED JOINTS - BARS WITHOUT END BEARING.

Column No.	Lap Length Factor l_l/ϕ	Upper Limit of Joint Strength Calculated From Eqtn. 3.43 - f_{sc_u} N/mm²	Lower Limit of Joint Strength Calculated From Eqtn. 3.44 - f_{sc_l} N/mm²	Experimentally Determined Joint Strength f_{sc} N/mm²	f_{sc}/f_{sc_u}	f_{sc}/f_{sc_l}
B 304 B	10	189	161	175	0.93	1.09
314	10	215	186	204	0.95	1.10
334	10	313	283	299	0.96	1.06
334 B	10	275	234	240	0.87	1.03
A 304 B	10	207	184	249	1.20	1.35
305	15	354	275	291	0.82	1.06
306 B	20	415+	322	348	0.84	1.08
202 B	20	435+	361	288	0.66	0.80
114	10	237	207	199	0.84	0.96
116	20	472+*	376	260	0.55	0.69
				averages	0.86	1.02

indicate that the assumption of the non-bursting component of bond stress being fully developed throughout the bond length is in error. However, there are insufficient results to justify any conclusion.

7.3.2. Bars with end bearing only. In section 3.6, expressions were derived for the ultimate bearing strength of the end of a reinforcing bar for the joint detail used in the experimental part of the investigation. As in the case of specimens with end bearing eliminated, expressions were derived for upper and lower limits of end bearing stress.

From equations 3.45 and 3.46, the upper and lower limits for the ultimate end bearing strength of bars in column A 308B are 134N/mm^2 and 110N/mm^2 respectively. Strains measured on reinforcement in column A 308B showed that the ultimate end bearing strength of bars varies from 98N/mm^2 to 112N/mm^2, with an average strength of 107N/mm^2. These values show good agreement with the lower limit of bearing strength calculated from equation 3.46.

The ratio of the bearing stress of the end of a lapped bar to the stress in the reinforcement outwith the lapped joint decreases with increasing column load, but cannot be less than 0.5 when the end bearing stress is a maximum, as if the ratio falls to a lower value, the total load carried by the steel within the lapped joint will be less than the load carried by the steel outwith the lapped joint, which must represent failure of the lap. Strains measured on reinforcement in column A 308B showed that, at the maximum value of end bearing stress, the ratio varied from 0.52 to 0.55. The latter value is therefore used in calculating the lower limit of joint strength, and a value of 0.5 is used in calculating the upper limit of joint strength. From equations 3.45 and 3.46, this leads

to the following expressions for upper and lower limits to

Upper limit:

$$f_{sc_u} = 2.\sigma_q = 3{\cdot}6\left[\frac{4.F_c}{\phi^2} + f_c\right] \leq f_y \qquad 7.4$$

Lower limit:

$$f_{sc_l} = 1{\cdot}8\,\sigma_q = 3{\cdot}24\left[\frac{4.F_c}{\phi^2} + f_c\right] \leq f_y \qquad 7.5$$

The upper limit and lower limit of joint strength calculated from equations 7.4 and 7.5 for each test specimen in which bond of reinforcement was prevented are compared with the experimental results in table 7.2. The lower limit given by equation 7.5, is in good agreement with test results.

7.3.3 Bars with bond and end bearing. As stated in the introduction to this chapter, the theoretical analysis of the bond strength and the bearing strength of deformed reinforcing bars derived in chapter 3 showed that the strength of each depended on the force available from secondary reinforcement to balance the bursting forces that each produced. Consequently, if the same amount of secondary reinforcement is present, the strength of the combination of bond and end bearing will be less than the sum of the strengths of bond and end bearing individually. The theoretical analysis also showed that bond and end bearing have a component which does not produce bursting forces, and so the strength of the combination of bond and end bearing will be greater than the strength of either bond or end bearing individually. The theoretical analysis is therefore in agreement with the conclusions reached in chapter 6.

The greatest difficulty in a theoretical analysis of the strength of lapped joints of bars with bond and end bearing present lies in apportioning the available resistance to bursting to each. As shown in section 3.4.2, the force transferred to a bar by the bursting

TABLE 7.2 STRENGTH OF LAPPED JOINTS - BARS WITHOUT BOND

Column No.	Lap Length Factor l_l/ϕ	Upper Limit of Joint Strength Calculated From Eqtn. 3.45 f_{sc_u} N/mm²	Lower Limit of Joint Strength Calculated From Eqtn. 3.46 f_{sc_l} N/mm²	Experimentally Determined Joint Strength f_{sc} N/mm²	f_{sc}/f_{sc_u}	f_{sc}/f_{sc_l}
A 307	10	299	210	223	0.75	1.06
308	15	299	209	201	0.67	0.96
308 B	15	288	200	221	0.77	1.11
308 C	15	365	249	159*	0.44*	0.64*
308 D	15	355	247	271	0.76	1.12
309	20	282	192	181	0.64	0.94
203	20	312	219	181	0.58	0.83
				Average	0.70	1.00

* Results determined from cube strength - omitted from average of results.

component is greater for end bearing than for bond of bars with crescent shaped ribs for the same bursting force. The relative proportions of the total bursting force produced by bond and by end bearing will therefore affect the stress developed by a bar.

Analysis of the strength of a lapped joint with bars having bond and end bearing may be considered as the sum of three parts-

1) the strength of an equivalent lapped joint with bars with end bearing eliminated.
2) the component of end bearing due to the unit cohesion of the concrete, i.e. the non-bursting component.
3) an additional component due to the greater efficiency of end bearing in transferring force.

The contribution of (3) will depend on many factors, such as concrete strength, steel percentage, lap length, strength and positioning of links, etc. The many variables preclude an accurate assessment of the contribution to joint strength. However, the contribution is not likely to be large. The difference between the end bearing stress at ultimate load calculated from strains measured on reinforcement in columns A 301 and A 303B and the non-bursting component of end bearing calculated from equation 3.46 has an average of only $23N/mm^2$. Evaluating equation 3.26 and equation 3.28 for the dimensions of 'Hybar' and 'Unisteel' reinforcement shows that the additional component of joint strength due to the bearing of the end of a bar will be approximately 25% of the bursting component of end bearing. The contribution of (3) will therefore be small, and is neglected in the succeeding analysis.

From equation 3.23, the non-bursting component of end bearing stress is

$$\sigma_q = 2\delta . \cot\alpha = 1.8 f_c \qquad 7.6$$

In section 7.3.2, it was shown that, in the case of bars with bond of reinforcement within the lapped joint eliminated, between 80% and 100% of the total force transmitted by end bearing of a bar at ultimate load was transferred to the adjacent bar. Assuming that the average of the above two values may be used in the case of lapped joints where bond and end bearing are present, leads to the following expression for the stress developed in a lapped joint by the non-bursting component of end bearing strength.

$$f_{sc} = 3{\cdot}42\ f_c \qquad 7.7$$

This is in good agreement with the net contribution of end bearing to the stress developed by a 10ϕ lapped joint, found from the difference between equations 6.4 and 6.5 to be

$$f_{sc} = 3{\cdot}75\ f_c \qquad 7.8$$

The value of f_{sc} from equation 7.7 may therefore be added to the right hand side of equations 3.43 and 3.44 to obtain expressions for the stress developed by lapped joints with bond and end bearing of bars.

At the upper limit

$$f_{sc_u} = \left[\frac{0{\cdot}71\, n.A_{sv}.f_{yv}}{\phi.h_r} + \frac{f_c.l_b}{s_r}\right]\frac{A_r.7{\cdot}2}{\pi.\phi^2} + 3{\cdot}42 f_c \leq f_y \qquad 7.9$$

At the lower limit

$$f_{sc_l} = \left[\frac{0{\cdot}93\ A_{sv}\ f_{yv}}{\phi.h_r} + \frac{f_c.l_b}{s_r}\right]\frac{A_r.7{\cdot}2}{\pi.\phi^2} + 3{\cdot}42 f_c \leq f_y \qquad 7.10$$

The upper and lower limits of joint strength, calculated from equations 7.9 and 7.10 for each specimen with bond and end bearing of bars present, are compared with the experimental results in table 7.3.

The results presented in table 7.3 show that the upper limit of joint strength, calculated from equation 7.9, gives a reasonable

representation of the strength of lapped joints with 'normal' links and with links of reduced strength. Both equations 7.9 and 7.10 overestimate the stress developed by a lapped joint when links are not positioned close to the ends of the joint, as in the cases of columns C 311, C 311B and C 313. The equations also overestimate the strength of columns C 321, C 324 and C 324B, where type 1 failures occurred due to the additional links provided in these specimens.

Excluding the results of the above six columns and column C 326, which also had additional links, the average value of the ratio f_{sc}/f_{sc_u} in column 4 of table 7.3 is 0.98, and the average value of the ratio f_{sc}/f_{sc_l} in column 5 is 1.13. The standard deviation of the results is 0.126 and 0.173 respectively.

The good agreement shown between the upper limit of joint strength, calculated from equation 7.9, and the experimental results indicates that a value of ψ close to unity is reasonable. The additional contribution to joint strength of the bursting component of end bearing was also neglected in the analysis, which would cause equations 7.9 and 7.10 to tend to underestimate the stresses developed, and hence to overestimate the ratios of the experimental to the theoretical results.

TABLE 7.3 STRENGTH OF LAPPED JOINTS - BARS WITH BOND AND END BEARING

Column No.	Lap Length Factor l_1/ϕ	Upper Limit of Joint Strength Calculated From Eqtn. 7.9 - f_{sc_u} N/mm^2	Lower Limit of Joint Strength Calculated From Eqtn. 7.10 - f_{sc_l} N/mm^2	Experimentally Determined Joint Strength f_{sc} N/mm^2	f_{sc}/f_{sc_u}	f_{sc}/f_{sc_l}	Notes
A111	10	348	319	371	1.07	1.16	
113	20	472$^+$	425	362	0.77	0.85	
201	20	361	282	443	1.23	1.57	
201B	20	442$^+$	431	454	1.03	1.05	
301	10	304	281	332	1.09	1.18	
302	15	347	268	>315	0.91	1.17	
302B	15	348	268	336	0.97	1.25	
302C	15	415$^+$	388	397	0.96	1.02	
303	20	436	357	291*	-	-	
303B	20	445$^+$	369	412	0.93	1.12	
B301	10	212	182	167	0.79	0.92	
301B	10	220	190	198	0.90	1.04	
311	10	305	276	256	0.84	0.93	
321	10	319	289	311	0.97	1.08	
331	10	372	342	378	1.02	1.10	
313	20	415$^+$	322	449	1.08	1.39	
C301	10	234	223	275	1.18	1.23	3
303	20	393	352	387	0.98	1.10	3
311	10	259	259	210	0.81	0.81	1
311B	10	309	309	175	0.57	0.57	1
313	20	415$^+$	415$^+$	363	0.87	0.87	1
321	10	415$^+$	415$^+$	341	0.82	0.82	2

TABLE 7.3 Contd.

Column No.	Lap Length Factor l_l/ϕ	Upper Limit of Joint Strength Calculated From Eqtn. 7.9 - f_{sc_u} N/mm^2	Lower Limit of Joint Strength Calculated From Eqtn. 7.10 - f_{sc_l} N/mm^2	Experimentally Determined Joint Strength f_{sc} N/mm^2	f_{sc}/f_{sc_u}	f_{sc}/f_{sc_l}	Notes
324	10	355	296	173	0.49	0.58	2
324B	10	363	305	191	0.53	0.63	2
326	20	415$^+$	406	430	1.04	1.06	2

+ - yield strength of reinforcement

* - column failed outwith lapped joint

Notes 1 - no links at ends of lapped joint

2 - double links at ends of lapped joint - type 1 failure

3 - weaker links

CHAPTER 8

COMPARISON WITH EXISTING DESIGN RULES.

8.1 Introduction

The design of compression lapped joints may often be critical to the strength of a structure. Failure of a column in a multi-storey structure is potentially much more serious than failure of a flexural member. Compression lapped joints usually have to be designed to develop the full design strength of the reinforcement, as, unlike tension lapped joints, they cannot be positioned where stress in the reinforcement is low.

Although cracking was observed in all test specimens prior to ultimate load, the associated deformations would not be great enough to cause signs of distress in decorative cladding, and it is not considered that signs of impending failure would be noticed. In most tests in this investigation, but particularly those with higher strength concretes, the load capacity of a column dropped rapidly after ultimate load. Despite the fact that failure of the lapped joints takes place by yielding of the links confining the lapped bars, failure of compression lapped joints in reinforced concrete columns must be regarded as a compression failure, and an adequate factor of safety must be used in their design. The cost of additional lap length is low compared with the potential cost of failure.

In the following section, the ultimate limit state philosophy of B.S.C.P.110:1972[9] is used to formulate design rules for compression lapped joints from results obtained in the experimental investigation and from the theoretical analysis of joint strength.

8.2 The influence of the positioning of links on joint strength was discussed in section 6.7. The results of the experimental investigation showed that there was a considerable reduction in joint

strength when links were not positioned close to the ends of a lapped joint. It is therefore recommended that links be provided at both ends of lapped joints.

In section 7.3.3 it was shown that equation 7.6 gave a good representation of the strength of compression lapped joints in which links were provided at both ends of the lapped joint. The mean of the ratio of joint strength determined experimentally to joint strength calculated from equation 7.6 was 0.98, and the standard deviation of the results was 0.126. The characteristic joint strength below which not more than 5% of results fall is therefore

$$f_{sc_{char}} = f_{sc_{mean}} - 1{\cdot}64\,\sigma_d = 0{\cdot}77\,f_{sc_{eqtn.\,7{\cdot}6}} \qquad 8.1$$

where $f_{sc_{char}}$ = value below which not more than 5% of results fall

$f_{sc_{mean}}$ = mean of results

σ_d = standard deviation of results

and $f_{sc_{eqtn\,7.6}}$ = joint strength calculated from equation 7.6.

B.S.C.P.110:1972 requires that partial safety factors of 1.5 and 1.15 be applied to the ultimate strength of concrete and reinforcement yielding in tension respectively. Inserting the partial safety factors in equation 7.6, and allowing for the difference between characteristic and mean values, leads to the following expression.

$$f_{sc} = 0{\cdot}77\left\{\left[\frac{0{\cdot}71.n.A_{sv}.f_{yv}}{1{\cdot}15.\phi.h_r} + \frac{f_c.l_b}{1{\cdot}5.s_r}\right]\frac{A_r.7{\cdot}2}{\pi.\phi^2} + \frac{3{\cdot}42\,f_c}{1{\cdot}5}\right\} \qquad 8.2$$

Simplifying equation 8.2 leads to

$$f_{sc} = \left[\frac{0{\cdot}47\,n.A_{sv}.f_{yv}}{\phi.h_r} + 0{\cdot}51\,\frac{f_c.l_b}{s_r}\right]\frac{A_r.7{\cdot}2}{\pi.\phi^2} + 1{\cdot}74\,f_c \qquad 8.3$$

Equation 8.3 is presented in terms of the compressive strength of the concrete in the test specimen. To convert equation 8.3 to concrete cube strength, it is assumed that the relationship between concrete cube strength and 'in-situ' concrete strength is given by

$$f_c = 0{\cdot}67\, f_{cu} \qquad 5.3$$

where f_c = 'in-situ' concrete strength

and f_{cu} = characteristic concrete cube compressive strength.

The partial safety factor of 1.5 on concrete strength incorporated in equation 8.3 allows for the reduction in strength of concrete subjected to long term loading, which accounts for the difference in the factors associated with concrete cube strength in equations 5.3 and 5.15.

Equation 8.3 applies only to the joint detail used in the current investigation, and shown in figs. 4.1 and 3.19. As was shown in 3.6.4, the confining force on the lapped bars may be reduced to 45% of the value used in equation 8.3 where the joint detail shown in fig. 3.23 is used.

Allowing for the difference in joint details, and putting equation 8.3 in terms of concrete cube strength, leads to

$$f_{sc} = \left[\frac{0{\cdot}45 \times 0{\cdot}47 n.A_{sv} f_{yv}}{\phi.h_r} + \frac{0{\cdot}67 \times 0{\cdot}51\, f_{cu}.l_b}{s_r}\right]\frac{A_r.7{\cdot}2}{\pi.\phi^2} + 0{\cdot}67 \times 1{\cdot}74\, f_{cu} \qquad 8.4$$

simplifying equation 8.4 leads to

$$f_{sc} = \left[\frac{0{\cdot}21\, n.A_{sv}.f_{yv}}{\phi.h_r} + 0{\cdot}34\,\frac{f_{cu}.l_b}{s_r}\right] A_r.\frac{7{\cdot}2}{\pi.\phi^2} + 1{\cdot}17\, f_{cu} \qquad 8.5$$

B.S.C.P.110:1972 requires ribbed deformed bars to have a mean area of ribs above the core of a bar projected on a plane normal to the axis of the bar of not less than $0.15\,\phi.s_r$ mm^2, where ϕ is the nominal diameter of the bar and s_r is the spacing of the rib along the bar axis. Assuming that the proportions of rib area to $\int_{-\frac{\pi}{2}}^{+\frac{\pi}{2}} \frac{\phi}{2}.h_r \cos\mu.d\mu$ found for 'Hybar' reinforcement are generally applicable to bars with crescent shaped ribs, then

$$\int_{-\frac{\pi}{2}}^{+\frac{\pi}{2}} \frac{\phi}{2}.h_r \cos\mu.d\mu. = \phi.h_r = \frac{94}{220}.0{\cdot}15\phi.s_r = 0{\cdot}064.\phi.s_r \qquad 8.6$$

Substituting for the above in equation 8.5 leads to the

following expression for the design stress developed by a ribbed reinforcing bar.

$$f_{sc} = 0.34\left[\frac{3.28\, n.\, A_{sv}.\, f_{yv}}{\phi^2} + \frac{0.34\, f_{cu}\, l_b}{\phi}\right] + 1.17\, f_{cu} \qquad 8.7$$

For the design of lapped joints, it is necessary to find the lap length required to develop a certain stress in the reinforcement. Solving equation 8.5 for lap length leads to the following expression.

$$\frac{l_l}{\phi} = \frac{l_b}{\phi} - 2.5 = \left[(f_{sc} - 1.17\, f_{cu})2.94 - \frac{3.28\, n.\, A_{sv}.\, f_{yv}}{\phi^2}\right]\frac{2.94}{f_{cu}} - 2.5$$

$$= \left[(f_{sc} - 1.17\, f_{cu}) - \frac{1.1\, n.\, A_{sv}.\, f_{yv}}{\phi^2}\right]\frac{8.64}{f_{cu}} - 2.5 \qquad 8.8$$

From B.S.C.P.110:1972, the design strength of compression reinforcement at the ultimate limit state is

$$f_{sc} = \frac{f_y}{1.15 + \frac{f_y}{2000}} \qquad 8.9$$

For a steel with a characteristic yield strength of 410 N/mm^2, the design stress of the reinforcement is 303 N/mm^2.

The characteristic yield strength of plain round mild steel reinforcement, the type generally used for links, is usually taken to be 250 N/mm^2. B.S.C.P.110:1972 [9] specifies that the diameter of links must be at least one quarter of the diameter of the main reinforcing bars, and links must be spaced at not more than 12 times the diameter of the main bar.

Substituting for f_{sc} and $A_{sv}.f_{yv}$ in equation 8.8 leads to

$$\frac{l_l}{\phi} = \left[303 - 1.17\, f_{cu} - 13.5\, n\right]\frac{8.64}{f_{cu}} - 2.5 \qquad 8.10$$

The value of n, the number of links in the lap length, is

$$n = \frac{l_l}{12.\phi} \qquad 8.11$$

the value obtained from equation 8.11 being rounded up to the next whole number. The design lap length for ribbed deformed bars may then be calculated by substituting for n in equation 8.10.

Values of l_l/ϕ obtained from equation 8.10 for various concrete strengths are presented in table 8.1. The values obtained are considerably greater than the lap lengths specified by B.S.C.P.110:1972, shown in table 2.1, suggesting that the Code rules are unsafe for this case.

The German code of practice, D I N 1045[35], specifies that 3 links of at least 0.4 times the diameter of the lapped bars must be provided at both ends of lapped joints. Substituting in equation 8.8 for $f_{sc} = 303$ N/mm^2, $f_{yv} = 250$ N/mm^2 and $A_{sv} = 0.04\pi.\phi^2$, and putting $n = 6$, leads to the following expression for the design lap length of bars with crescent shaped ribs and a projected rib area of $0.15\,\phi.s_r$ mm^2.

$$l_l/\phi = \left[303 - 1.17\,f_{cu} - 207\right]\frac{8.64}{f_{cu}} - 2.5$$

$$= \left[96 - 1.17\,f_{cu}\right]\frac{8.64}{f_{cu}} - 2.5 \qquad 8.12$$

Values of l_l/ϕ obtained from equation 8.12 for various concrete strengths are also presented in table 8.1. The values obtained are lower than the lap lengths specified by D I N 1054, particularly at higher concrete strengths. The comparison indicates that the requirements of D I N 1045 for compression lapped joints are quite adequate.

The Recommendations of the C.E.B.[37] is vague about the amount of confining reinforcement to be provided at lapped joints, and so a comparison with the proposed design rules is not possible.

The links used in specimens in the current investigation were always of plain round mild steel reinforcement. However, in the United States, links are generally of hot rolled ribbed bars, and it is therefore considered that a comparison of the proposed design rules with the requirements of the current American code of practice[36] could not be justified without further research.

TABLE 8.1 DESIGN LAP LENGTHS BASED ON REQUIREMENTS FOR SECONDARY REINFORCEMENT OF CURRENT CODES OF PRACTICE.

Secondary Reinforcement to Comply with -	Lap Length l_l/ϕ Characteristic Cube Strength N/mm^2		
	20	30	40
B.S.C.P.110:1972[4] (Equation 8.10)	78	55	42
D I N 1045[35] (Equation 8.12)	29	15	9

In the majority of current codes of practice, the design strength of compression reinforcement at the ultimate limit state is taken to be the yield strength of the reinforcement, and is not as given in equation 8.9. However, differences in partial safety factors for loads and for materials generally result in the design load of a column being approximately the same.

Removing partial safety factors for materials from equation 8.10 leads to the following expression.

$$l_l/\phi = \left[f_{sc} - 1{\cdot}5 \times 1{\cdot}17\, f_{cu} - 1{\cdot}15 \times 13{\cdot}5 n\right] \frac{8{\cdot}64}{1{\cdot}5\, f_{cu}} - 2{\cdot}5$$

$$= \left[f_{sc} - 1{\cdot}75\, f_{cu} - 15{\cdot}5 n\right] \frac{5{\cdot}76}{f_{cu}} - 2{\cdot}5 \qquad 8.13$$

Evaluating equation 8.13 for $f_{sc} = 410$ N/mm^2 and $f_{cu} = 30$ N/mm^2, and substituting for n from equation 8.11, gives a value of lap length of 52ϕ, a value close to that obtained from equation 8.10.

Removing partial safety factors for materials from equation 8.12 leads to the following expression.

$$l_l/\phi = \left[f_{sc} - 1{\cdot}75\, f_{cu} - 238\right] \frac{5{\cdot}76}{f_{cu}} - 2{\cdot}5 \qquad 8.14$$

Evaluating equation 8.14 for f_{sc} = 410 N/mm^2 and f_{cu} = 30 N/mm^2 gives a value of l_d/ϕ of 21, a value 40% greater than that obtained from equation 8.12, but still less than the requirements of D.I.N.1045.

Although the choice of design method does influence the lap length required by the design rules derived in this chapter, in both cases the requirements of the German code[35] of practice appear to be adequate, but the requirements of B.S.C.P.110:1972[9] appear to be unsafe.

Although the requirements of B.S.C.P.110:1972[9] appear to be inadequate, no failures of compression lapped joints have been recorded in structures designed to this code. However, as B.S.C.P.110:1972 was published only 3½ years ago, few structures that were designed to its specifications will be in full use. The previous British code of practice B.S.C.P.114:1969[51], was not based on ultimate limit state philosophy, and so direct comparisons are difficult, but, partly because B.S.C.P.114:1969 did not allow higher bond stresses for ribbed deformed bars than for square twisted bars, and partly because it did not allow high strength bars to be utilised as efficiently as B.S.C.P.110:1972, approximately 30% greater lap lengths were required by the earlier code. The requirements for secondary reinforcement were also more severe in the earlier code, with every compression bar near a column face having to be adequately confined by links.

Another factor that will reduce the probability of failure is that ribbed reinforcing bars generally have a greater projected rib area than the minimum of $0.15\phi.s_r$ specified for Type 2 (ribbed) deformed bars in B.S.C.P.110:1972. The only ribbed reinforcement with a projected rib area as low as this that the author is aware of is the Swedish Ks 40 reinforcement, which has annular ribs. As discussed in sections 3.3 and 7.2, it would be expected that bars

with annular ribs would develop higher stresses than bars with crescent shaped ribs, if all other factors were held constant.

However, as mentioned in section 6.2, joint strength might decrease if the concrete cover to the reinforcement was less securely held by links than was the case in the present investigation, and the theoretical analysis discussed in section 3.7 indicated that lower percentages of reinforcement might have an adverse effect on joint strength.

Despite the fact that no failures of compression lapped joints designed to comply with B.S.C.P.110:1972 have been recorded, it is considered advisible that increased links should be provided at compression lapped joints, as is required by D I N 1045. It is considered that the best design solution is that which will use the same links as are required outwith the lapped joint. Plain round mild steel bars are preferred for accuracy of positioning of reinforcement, as the inside radius of the links will equal the diameter of the main reinforcement.

Solving equation 8.10 for n, the number of links in the lap length, gives the following expression.

$$n = 0{\cdot}074\left[303 - 1{\cdot}17 f_{cu} - \frac{f_{cu}}{8{\cdot}64}\left(\frac{l_l}{\phi} + 2{\cdot}5\right)\right] \qquad 8.15$$

Table 8.2 shows the number of links required to develop the ultimate design strength of compression reinforcement with a yield strength of 410 N/mm^2 in the lap lengths specified by B.S.C.P.110:1972, calculated from equation 8.15 for the joint detail shown in fig. 8.1. The number of links required is large, and the spacing of links would have to be small to accommodate the required number. However, it is possible to increase link spacing by placing links in pairs, as shown in fig. 8.1, but the density of secondary reinforcement in

the column core must not be such that it would impede the flow of concrete during casting, and prevent proper compaction. Sufficient space must also be left to allow the insertion of an internal vibrator. An alternative method of increasing link spacing would be to bundle links.

For lapped joints other than that considered here, with three pairs of lapped bars, a different number of links will be required. The bottom line of table 8.2 gives the number of links required in the lap length for each pair of lapped bars in one face of a column. (The value given in the bottom line of table 8.2 may be less than one third of the value in the second from bottom line, as values in that line were rounded up to the nearest whole number). Any detail which complies with the requirements of B.S.C.P.110:1972[9] may be used, but the number of links confining the corner bars must be at least the value given in the bottom line of table 8.2. It is also necessary to distribute the links within the lapped joint in such a way that they are concentrated close to the ends of the lapped joint, say by positioning at least one third of the required number of links within a distance of 15% of the lap length from both ends of the lapped joint as shown in fig. 8.2.

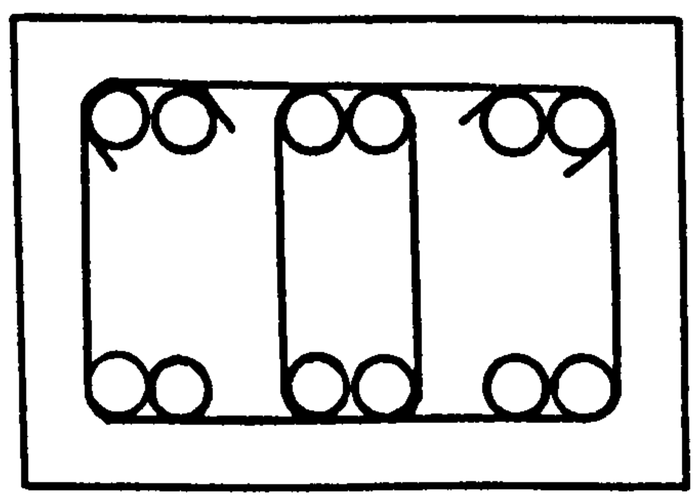

Fig. 8.1 Suggested joint detail.

TABLE 8.2 NO. OF LINKS REQUIRED TO DEVELOP ULTIMATE DESIGN STRENGTH OF COMPRESSION REINFORCEMENT WITH LAP LENGTHS SPECIFIED IN B.S.C.P.110:1972 - f_y = 410 N/mm^2.

	Concrete Grade			
	20	25	30	40
Lap Lengths Specified in B.S.C.P.110:1972[9]	28	25	22	19
No. of Links Required for Joint Detail Shown in Fig. 3.23	16	15	14	12
Min. No. of Links Required per Pair of Lapped Bars in One Column Face	5.2	4.9	4.6	4.0

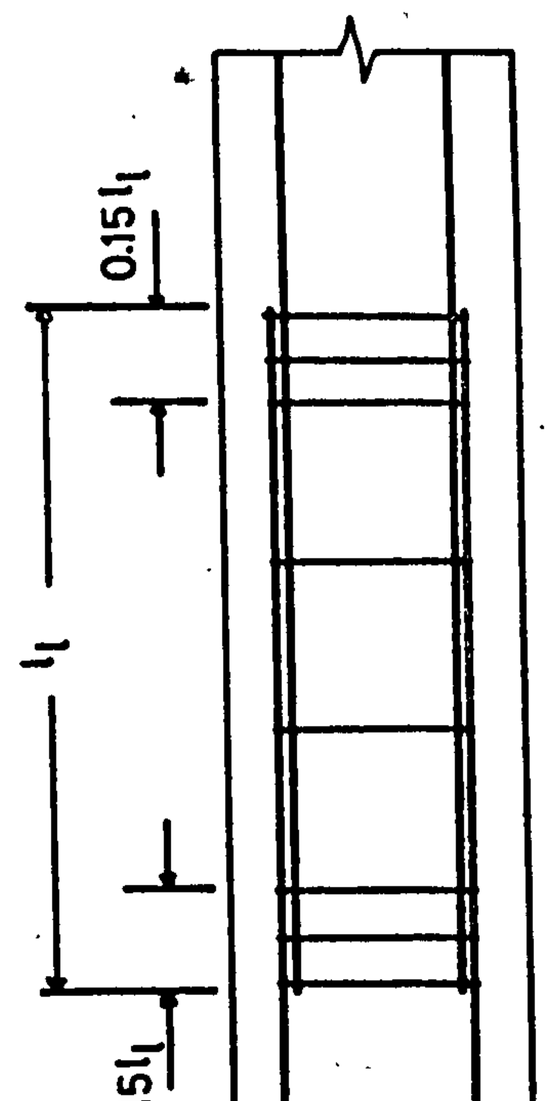

Fig. 8.2 Recommended distribution of links in lapped joint.

CHAPTER 9

CONCLUSIONS AND RECOMMENDATIONS

9.1 The following conclusions can be drawn from the investigation reported in this thesis.

1) Force is transferred between deformed bars in compression lapped joints by bond stresses on the circumference of the reinforcing bars and also by bearing of the ends of the bars. The ultimate strength of bond and of end bearing is dependent on the resistance available to counteract the bursting forces exerted by both effects on the surrounding concrete, and also on the compressive strength of the concrete. Bond strength also depends on the dimensions of the ribs of the reinforcing bars.

2) The positioning of secondary reinforcement within a compression lapped joint influences the strength of the joint. Failure to provide links close to the ends of lapped joints was found to weaken the joint.

3) For the joint detail used in the current investigation and the range of parameters investigated, the ultimate strength of compression lapped joints in which bond and end bearing of bars were present could be predicted to within $\pm$ 21% with 95% confidence by the following expression

$$f_{sc} = \left[\frac{0{\cdot}71\, n.A_{sv}.f_{yv}}{\phi.h_r} + (l_l + 2{\cdot}5\phi)\frac{f_c}{s_r}\right]\frac{A_r.7{\cdot}2}{\pi.\phi^2} + 3{\cdot}42\, f_c \leq f_y \qquad 7.9$$

for links of plain round mild steel reinforcement.

This expression applies only when failure takes place by yielding of the secondary reinforcement confining the lapped bars due to the outwards movement of the lapped bars along the inclined failure surface below the ribs of the bars. Equation 7.9 overestimates the strength of specimens in which links are not provided close to the ends of the lapped joint. Equation 7.9 and the ultimate limit state philosophy of B.S.C.P.110:1972 were used to develop the following

expression for the design lap length of compression lapped joints.

$$\frac{l_l}{\phi} = \left[f_{sc} - 1{\cdot}17 f_{cu} - \frac{1{\cdot}1 n. A_{sv}. f_{yv}}{\phi^2} \right] \frac{8{\cdot}64}{f_{cu}} - 2{\cdot}5 \qquad 8.8$$

4) The requirements of B.S.C.P.110:1972 do not appear to provide an adequate factor of safety against failure of compression lapped joints. To ensure the safety of the lap lengths specified by the Code, it is recommended that increased links be provided at compression lapped joints as specified below, and that the links should be distributed so that at least one third of the links required are positioned within a distance of 15% of the lap length from both ends of the lapped joint. The detailing of the lapped joint should also comply with the current requirements of B.S.C.P.110:1972.

Concrete Grade	20	25	30	40
Min. No. of Links Required /Pair of Lapped Bars in Any Column Face	5.2	4.9	4.6	4.0

9.2 It is recommended that research be undertaken in the following areas.

1) The strength of different joint details. It is anticipated that an experimental investigation would be fairly short, as it is believed that some of the parameters which have a strong influence on the strength of tension lapped joints, such as spacing of lapped bars and cover to reinforcement, would have little influence on the strength of compression lapped joints.

2) The influence of rib dimensions of deformed reinforcing bars on joint strength. Most of the data available at present relates to specimens in which heavy confining reinforcement was provided to prevent failure by splitting of the specimens. It is suggested that

the push-in specimens described in this thesis might be suitable for an examination of the influence of rib dimensions where specimens may fail by splitting.

3) The strength of lapped joints confined by links of ribbed deformed reinforcing bars.

4) The strength of compression lapped joints in flexural members.

5) The strength of compression lapped joints under fluctuating loads.

REFERENCES

1. PFISTER, J.S. and MATTOCK, A.H. High strength bars as concrete reinforcement, Part 5, lapped splices in concentrically loaded columns. Journal of the Portland Cement Association. Vol. 5, No. 2. May 1963. pp 27-40.

2. LEONHARDT, F. and TEICHEN, K.T. Drucke-Stöße von Bewehrungsstäben (Compression joints of reinforcing bars). H E F T 222, Deutscher Ausschuss fur Stahlbeton. 1972, pp 59.

3. C.U.R. report no. 23. An investigation of the bond of deformed steel bars in concrete. C.and C.A. Translation No. 112. London. Cement and Concrete Association. 1964. pp 28.

4. TEPFERS, R. A theory of bond applied to overlapped tensile reinforcement splices for deformed bars. Chalmers University of Technology, Publication No.73:2. Gothenburg. 1973. pp 328.

5. FERGUSON, P.M. and KRISHNASWAMY, C.N. Tensile lap splices, Part 2, Design recommendations for retaining wall splices and large bar splices. Center for Highway Research, University of Texas at Austin. Research report 113-3. April 1971. pp 60.

6. HAJNAL KONYI, K. Bond between concrete and steel. Structural Concrete, Vol. 1, No. 9, May/June 1963. pp 373-390.

7. AMERICAN CONCRETE INSTITUTE COMMITTEE 408. Opportunities in bond research. Proceedings of the American Concrete Institute. Vol. 67, No. 11. Nov. 1970. pp 857-867.

8. AMERICAN CONCRETE INSTITUTE COMMITTEE 408. Bond stress - the state of the art. Proceedings of the American Concrete Institute, Vol. 63, No. 11. Nov. 1966. pp 1161-1188.

9. BRITISH STANDARDS CODE OF PRACTICE C.P.110: PART1: 1972. The structural use of concrete. London. British Standards Institution. 1972.

10. ROBERTS, N.P. and CHUNG-TAI HO, R. Behaviour and design of tensile lapped joints in reinforced concrete beams. Civil Engineering and Public Works Review. Vol. 68, No. 798. Jan. 1973. pp 33-45.

11. ROBERTS, N.P. Development length bond stress and limit state design. Concrete. Vol. 2, No. 9. Sept. 1968. pp 364-372

12. ABRAMS, D.A. Tests of bond between concrete and steel. University of Illinois Bulletin. Bulletin No. 71. 1913. pp 238.

13. SNOWDEN, L.C. Classifying reinforcing bars for bond strength. B.R.S. Current Paper 36/70. London. Building Research Station. Nov. 1970. pp 40.

14. FERGUSON, P.M. and THOMPSON, J.N. Development length for large high strength reinforcing bars. Proceedings of the American Concrete Institute. Vol. 62, No. 1. Jan. 1965. pp 71-91.

15. LEONHARDT, F. On the need to consider the influence of lateral stresses on bond. Symposium on bond and crack formation in reinforced concrete. Vol. 1. R I L E M. Stockholm. 1957. pp 29-34.

16. MAINS, R.M. Measurement of the distribution of tensile and bond stresses along reinforcing bars. Proceedings of the American Concrete Institute. Vol. 48. Nov. 1951. pp 225-252.

17. BERNANDER, K.G. An investigation of bond by means of strain measurements in high tensile bars embedded in long cylindrical pull-out specimens. Symposium on bond and crack formation in reinforced concrete. Vol. 1. R I L E M. Stockholm. 1957. pp 203-210.

18. MATHEY, R.G. and WATSTEIN, D. Investigation of bond in beam and pullout specimens with high yield strength deformed bars. Proceedings of the American Concrete Institute. Vol. 57, No. 9. Mar. 1961. pp 1071-1090.

19. FERGUSON, P.M., BREEN, J.E. and THOMPSON, J.N. Pullout tests on high strength reinforcing bars. Proceedings of the American Concrete Institute. Vol. 62, No. 8. Aug. 1965. pp 933-949.

20. UNTRAVER, R.E. and HENRY, R.L. Influence of normal pressure on bond strength. Proceedings of the American Concrete Institute. Vol. 62, No. 5. May 1965. pp 577-586.

21. KUPFER, H., HILSDORF, H.K. and RUSCH, H. Behaviour of concrete under biaxial stresses. Proceedings of the American Concrete Institute. Vol. 66, No.8. Aug. 1969. pp 656-666.

22. REHM,G. The basic principle of the bond between steel and concrete. C.and C.A. Translation No.134. London. Cement and Concrete Associaiton. 1968. pp 45.

23. LUTZ, L.A. Information on the bond of deformed bars from special pullout tests. Proceedings of the American Concrete Institute. Vol. 67, No. 11. Nov. 1970. pp 885-887.

24. FERGUSON, P.M. and BREEN, J.E. Lapped splices for high strength reinforcing bars. Proceedings of the American Concrete Institute. Vol. 62, No. 9. Sept. 1965. pp 1063-1077.

25. ORANGUN, C.O., JIRSA, J.O. and BREEN, J.E. The strength of anchor bars : A re-evaluation of test data on development length and splices. Center for Highway-Research, University of Texas at Austin. Research Report 154-3F. Jan. 1975.

26. RICHART, F.E. and BROWN, R.L. An investigation of reinforced concrete columns. University of Illinois Bulletin. Bulletin No, 267. June 1934. pp 91.

27. PLOWMAN, J.M. Stresses in column reinforcement. Structural Engineer. Vol. 41, No. 3. Mar. 1963. pp 109-116.

28. SOMERVILLE, G. and TAYLOR, H.P.J. The influence of reinforcement detailing on the strength of concrete structures. Structural Engineer. Vol. 50, No. 1. Jan. 1972. pp 7-19.

29. SOMERVILLE, G., MORRIS, G.G. and CLEMENTS, S.W. Tests on the P.B. column-column joint, having high percentage of reinforcement. C. and C.A. Departmental Note DN/ 3007. London. Cement and Concrete Association. Mar. 1968.

30. HAWKINS, N.M. The bearing strength of concrete loaded through rigid plates. Magazine of Concrete Research. Vol. 20, No. 62. Mar. 1968. pp 31-40.

31. HYLAND, M.W. and CHEN, W.F. Bearing capacity of concrete blocks. Proceedings of the American Concrete Institute. Vol. 67, No. 3. Mar. 1970. pp 228-236.

32. ZIELINSKI, J. and ROWE, R.E. An investigation of the stress distribution in the anchorage zones of post tensioned concrete members. London. Cement and Concrete Association. Sept. 1960. Research Report 9. pp 32.

33. COWAN, H.J. The strength of plain, reinforced, and prestressed concrete under the action of combined stresses, with particular reference to the combined bending and torsion of rectangular sections. Magazine of Concrete Research. No. 14. Dec. 1953. pp 75-86.

34. CHEN, W.F. and DRUCKER, D.C. The bearing capacity of concrete blocks or rock. Proceedings of the American Society of Civil Engineers, Engineering Mechanics Division. Vol. 95, EM4. Aug. 1969. pp 955-978.

35. GERMAN STANDARD D I N 1045. Concrete and reinforced concrete structures : Design and construction. (English translation) London. British Standards Institution. 1972.

36. A.C.I. STANDARD 318-71. Building Code requirements for reinforced concrete. Detroit. American Concrete Institute. 1971.

37. C.E.B. and F.I.P. International recommendations for the design and construction of concrete structures : Principles and Recommendations. 6th Congress of the Federation Internationale de la Precontrainte. Prague. June 1970.

38. GOTO, Y. Cracks formed in concrete around deformed tension bars. Proceedings of the American Concrete Institute. Vol. 70, No. 4. April 1970. pp 244-251.

39. GOODE, C.D. and HELMY, M.A. The strength of concrete under combined shear and direct stress. Magazine of Concrete Research. Vol. 19, No. 59. June 1967. pp 105-112.

40. OJHA, S.K. The shear strength of rectangular reinforced and prestressed concrete beams. Magazine of Concrete Research. Vol. 19, No. 60. Sept. 1967. pp 173-184.

41. JENSEN, B.C. Lines of discontinuity for displacements in the theory of plasticity of plain and reinforced concrete. Magazine of Concrete Research. Vol. 27, No. 92. Sept. 1975. pp 143-150.

42. SMEE, D.J. The effect of aggregate size and concrete strength on the failure of concrete under triaxial compression. Civil Engineering Transactions of the Institution of Engineers, Australia. Vol. C E 9, No. 2. Oct. 1967. pp 339-344.

43. RICHART, F.E., BRAENDTZAEG, A. and BROWN, R.L. A study of the failure of concrete under combined compressive stresses. University of Illinois Bulletin. Bulletin No. 185. April 1929. pp 72.

44. BRITISH STANDARDS INSTITUTION. B.S.4408 Part 5. Recommendations for non-destructive methods of test for concrete. Part 5. Measurement of the velocity of ultrasonic pulses in concrete. London. British Standards Institution. Feb. 1974.

45. McHENRY, D. and SHIDELER, D.D. Review of data on effect of speed in mechanical testing of concrete. Symposium on speed of testing of non-metallic materials. Philadelphia American Society for Testing Materials. S T P 185. 1956. pp 72-82.

46. ANSON, M. and NEWMAN, K. The effect of mix proportions and methods of testing on Poisson's ratio for mortars and concretes. Magazine of Concrete Research. Vol. 18, No. 56. Sept. 1966. pp 115-130.

47. TAKABAYASHI, T. Comparison of dynamic Young's modulus and static Young's modulus for concrete. Proceedings, International Symposium on Non-Destructive Testing of Materials and Structures. Vol. 1. RILEM, Paris. 1954. pp 34-44.

48. PHILLEO, R.E. Comparison of three methods for determining Young's Modulus of Elasticity of concrete. Proceedings of the American Concrete Institute. Vol. 51, No. 5. Jan. 1955. pp 461-469.

49. CLARK, A.P. Comparative bond efficiency of deformed concrete reinforcing bars. Proceedings of the American Concrete Institute. Vol. 43. Dec. 1946. pp 381-400.

50. MEYERHOF, G.G. The bearing capacity of concrete and rock. Magazine of Concrete Research. No. 12. April 1953. pp 107-116.

51. THE COUNCIL FOR CODES OF PRACTICE C.P. 114 Part 2:1969. The structural use of reinforced concrete in buildings. Part 2: Metric units. London. British Standards Institution.

APPENDIX A

RESULTS OF TRIAXIAL COMPRESSION TESTS

A short series of triaxial tests on mortar specimens was conducted to determine the angle of internal friction to be used in theoretical calculations of bond strength. A total of 18 tests were conducted on specimens of two different strengths.

Cylindrical specimens 76.2mm high by 38.1mm diameter were chosen to fit a standard triaxial cell. The maximum grain size to be used in the mortar was determined from an analysis of the sand in the wedges of concrete which adhered to the bearing of ribs after joint failure. It was found that a maximum grain size of 1.18mm was reasonable, and only sand passing this sieve size was used in the manufacture of specimens. A water/cement ratio of 0.6 and a sand/cement ratio of 2.5 were selected to give a mix of suitable workability and strength. The specimens were compacted by vibration, and cured in air in the laboratory. Tests were conducted at ages of between 10 and 23 days.

Prior to testing the ends of the specimens were smoothed by grinding, and the circumference covered with a layer of 'Plasticine' to prevent puncturing of the impervious membrane.

Tests were carried out in a brass triaxial cell with a 38.1mm diameter piston, with specimens in a dry condition. The cell pressure was supplied from a small reservoir of oil held under constant pressure, which was maintained by intermittent pumping. Deviator stress was applied by a 50 tonne screw type testing machine, and loading to failure took between two and five minutes. During tests, one end of the specimen was open to the atmosphere, to ensure that pore pressures did not affect results.

The results of these tests are presented in table A.1, and Mohr circles and envelopes for both mortar strengths are shown in fig. A.1. The envelopes are curved, with a unit cohesion of approximately 0.25 times the unconfined cylinder strength, and an initial value of the angle of internal friction of 43°.

From known values of link strength, rib height, etc., equations 3.5 and 3.13 can be used to show that normal stresses at failure will be in the range of 20 N/mm^2 to 50 N/mm^2.

If the equation of the chord to the Mohr envelope between normal stresses of 20 N/mm^2 and 40 N/mm^2 is used to estimate the shear strength of the mortar, then

$$\tau = 0.55\ f_c' + \sigma_n \tan 32^{\circ} \qquad \text{A.1}$$

for tests 1 to 3, and

$$\tau = 0.47\ f_c' + \sigma_n \tan 32^{\circ} \qquad \text{A.2}$$

for tests 4 to 6, where

τ = shear strength of mortar

f_c' = unconfined cylinder strength

and σ_n = normal stress on the failure plane.

The average of these expressions is therefore used in theoretical calculations of bond strength, equation 3.15

$$\tau = 0.5\ f_c' + \sigma_n \tan 32^{\circ} \qquad \text{3.15}$$

TABLE A.1 RESULTS OF TRIAXIAL COMPRESSION TESTS ON MORTAR.

Test No.	Cell Pressure N/mm^2	Deviator Stress N/mm^2	Test No.	Cell Pressure N/mm^2	Deviator Stress N/mm^2
1	0	12.7	4	0	20.8
	6.9	46.2		2.8	38.6
	13.8	66.0		6.9	55.7
2	0	13.2	5	0	21.9
	6.9	46.5		5.5	44.6
	13.8	71.5		9.7	61.0
3	0	12.2	6	0	23.0
	2.8	24.5		6.9	57.9
	6.9	44.4		12.4	77.0

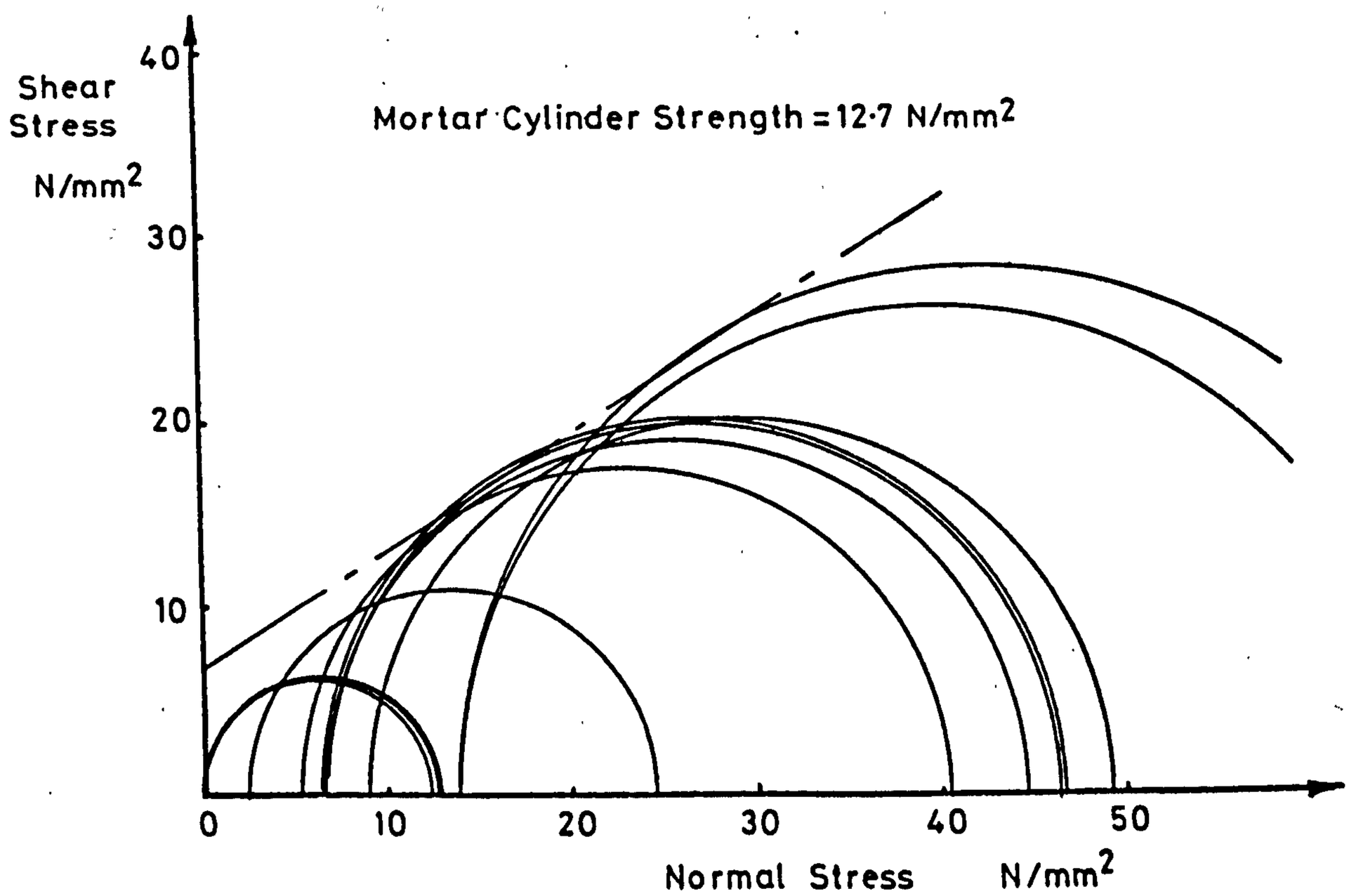

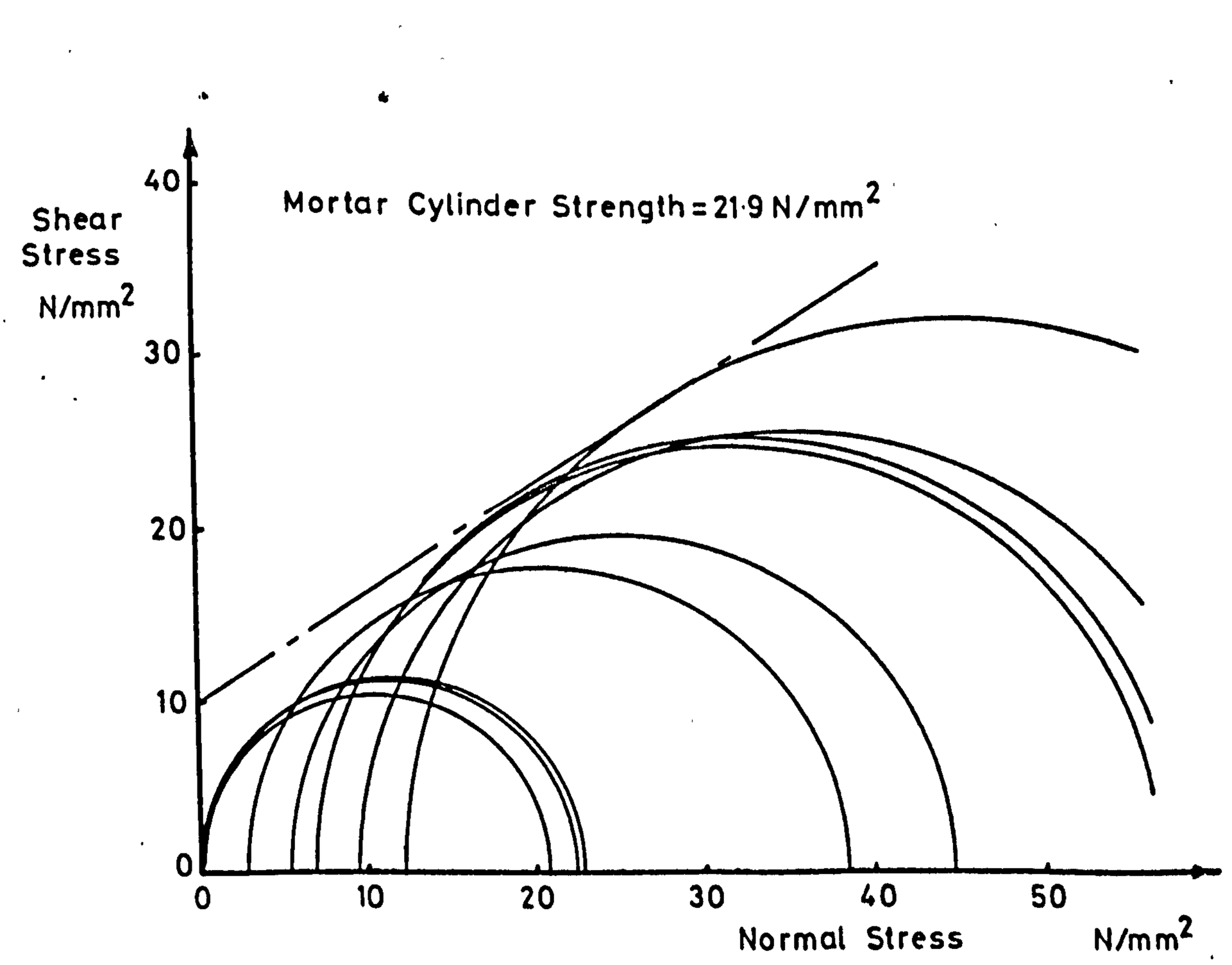

Fig. A.1 Mohr envelopes for shear strengths of mortar.

APPENDIX B

STRAINS MEASURED ON REINFORCING BARS

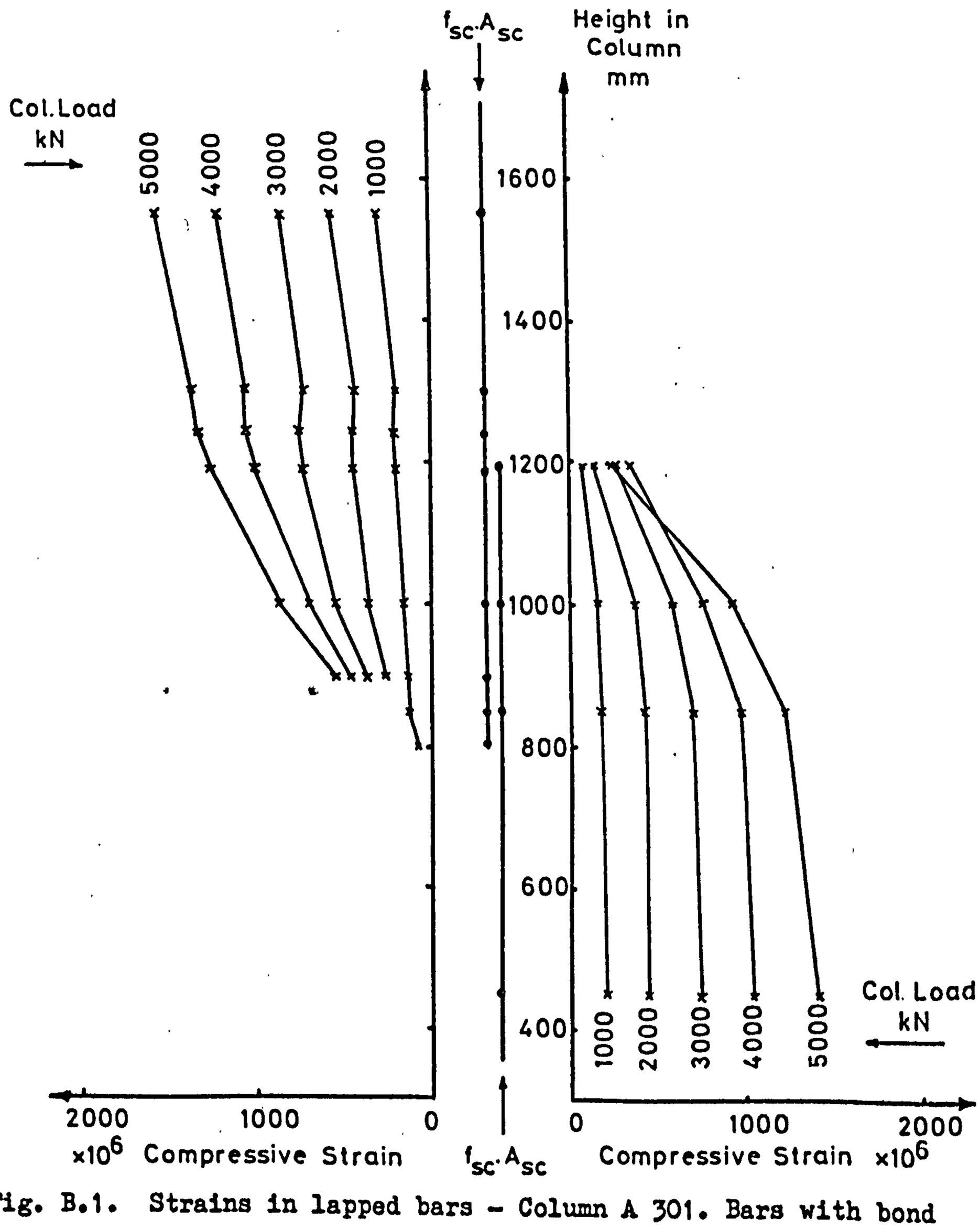

Fig. B.1. Strains in lapped bars - Column A 301. Bars with bond and end bearing.

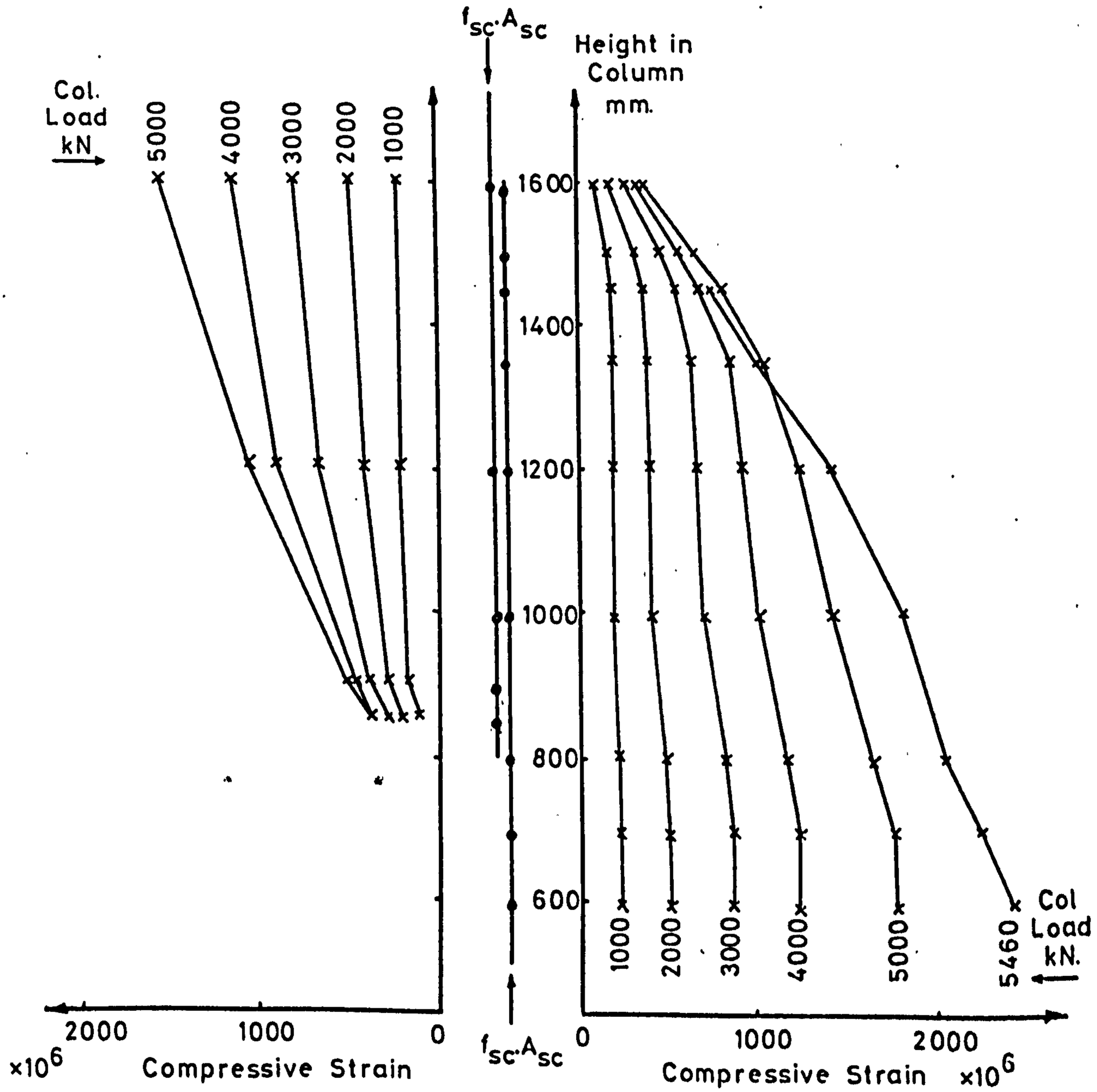

Fig. B.2. Strains in lapped bars - Column A 303B.

Bars with bond and end bearing.

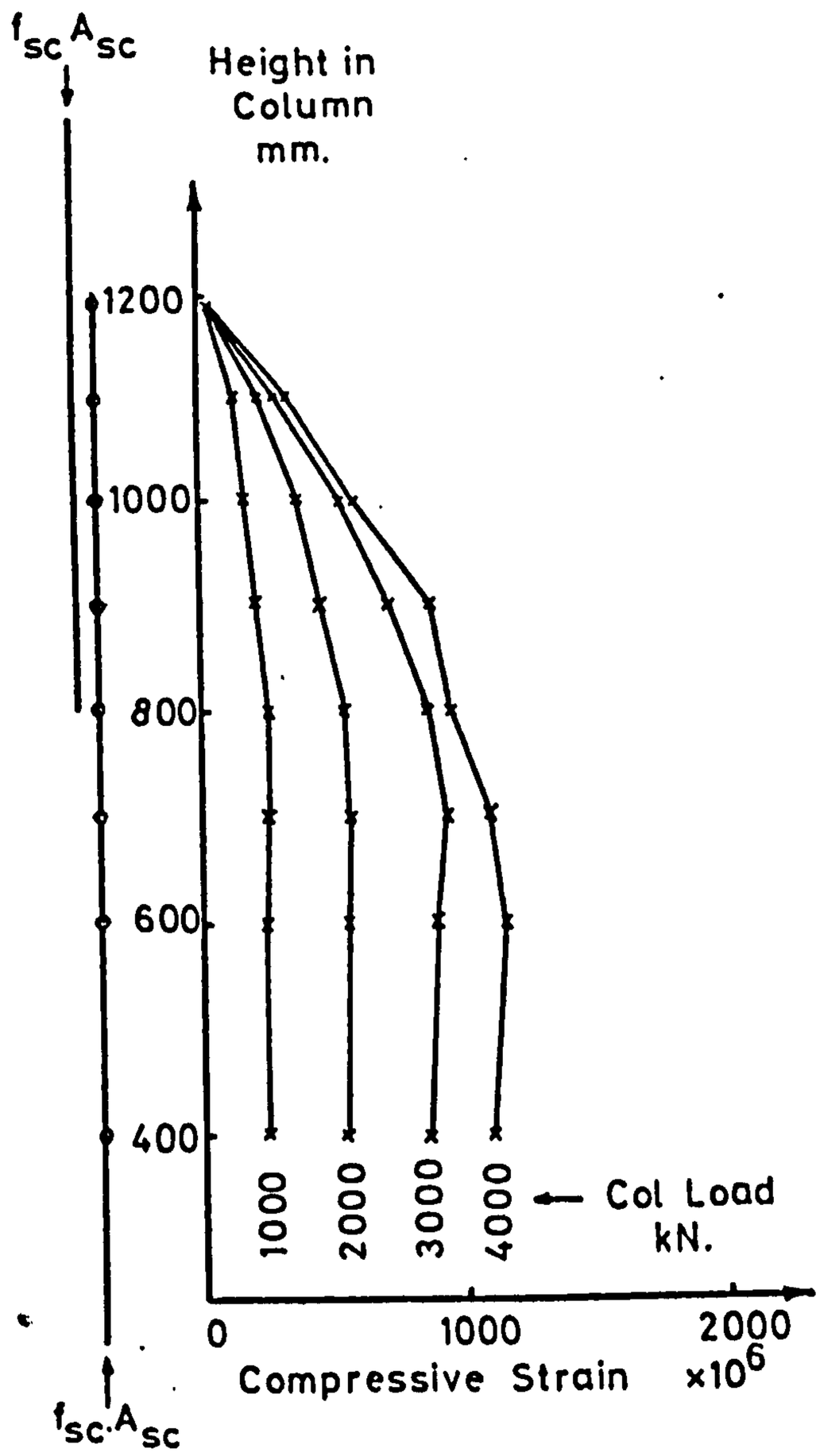

Fig. B.3 Strains in lapped bars - Column A 304B. Bars with Bond only.

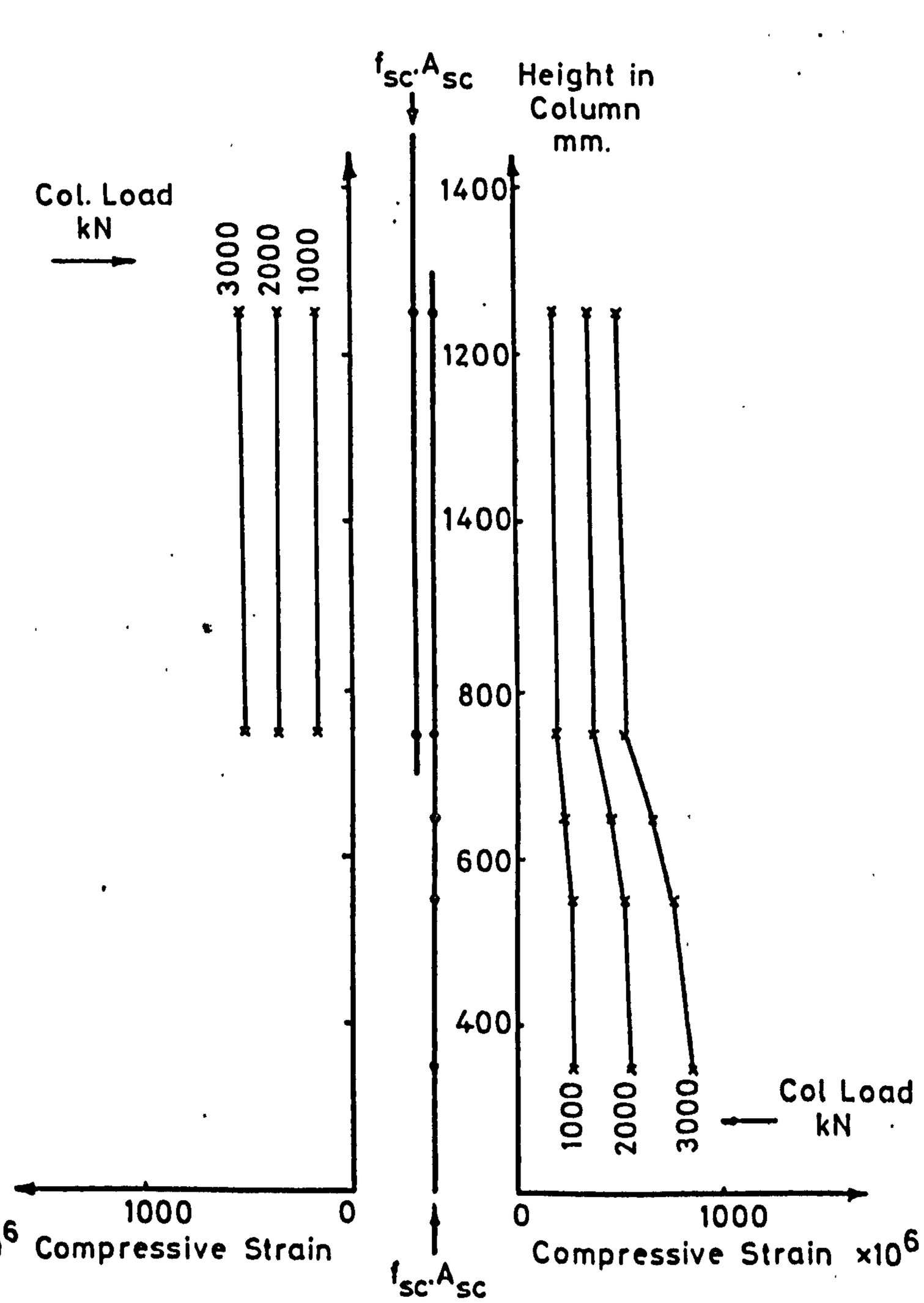

Fig. B.4 Strains in lapped bars - Column A 308B. Bars with end bearing only.

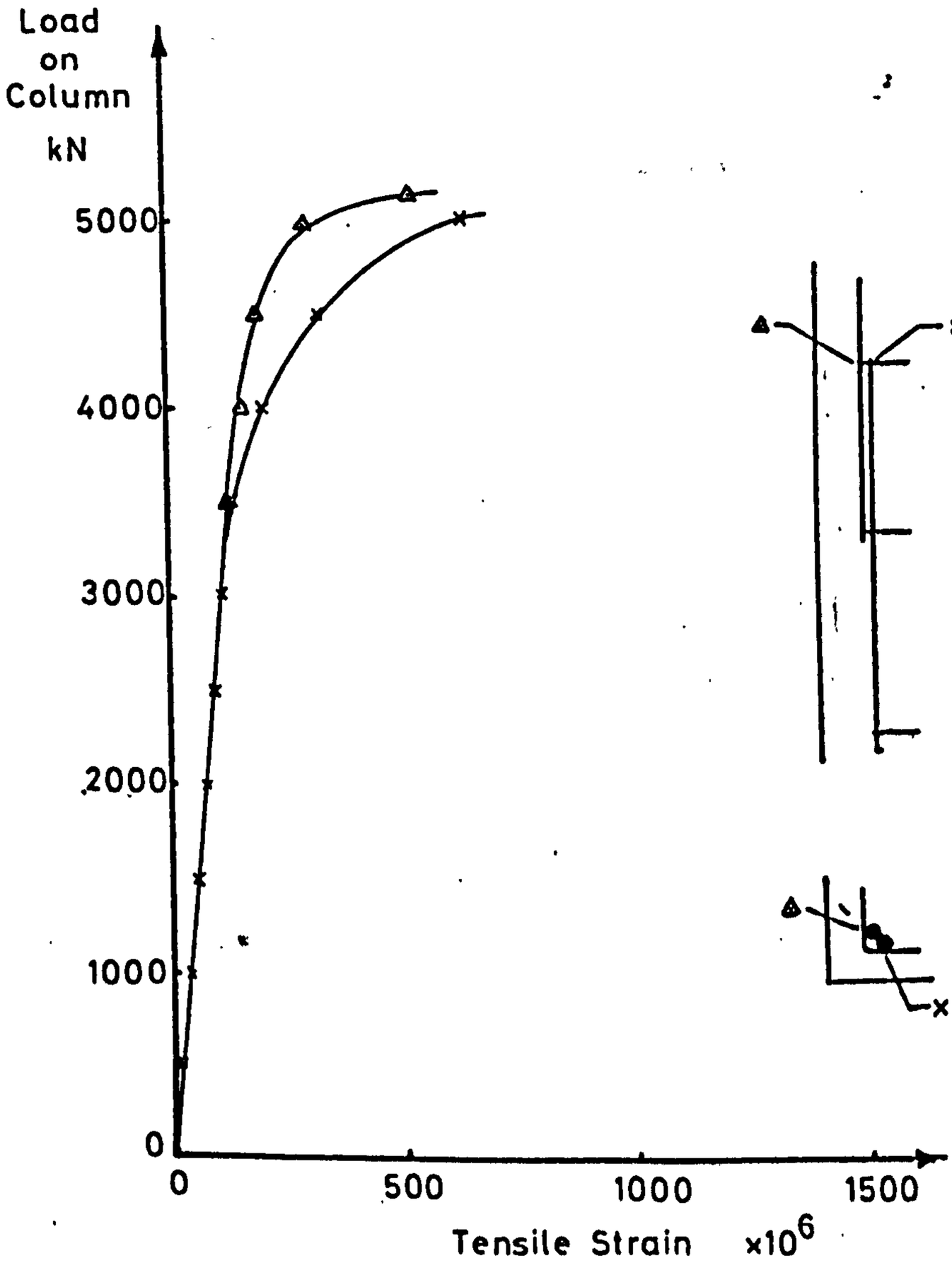

Fig. B.5 Strains measured on links – Column A 301.

Bars with bond and end bearing.

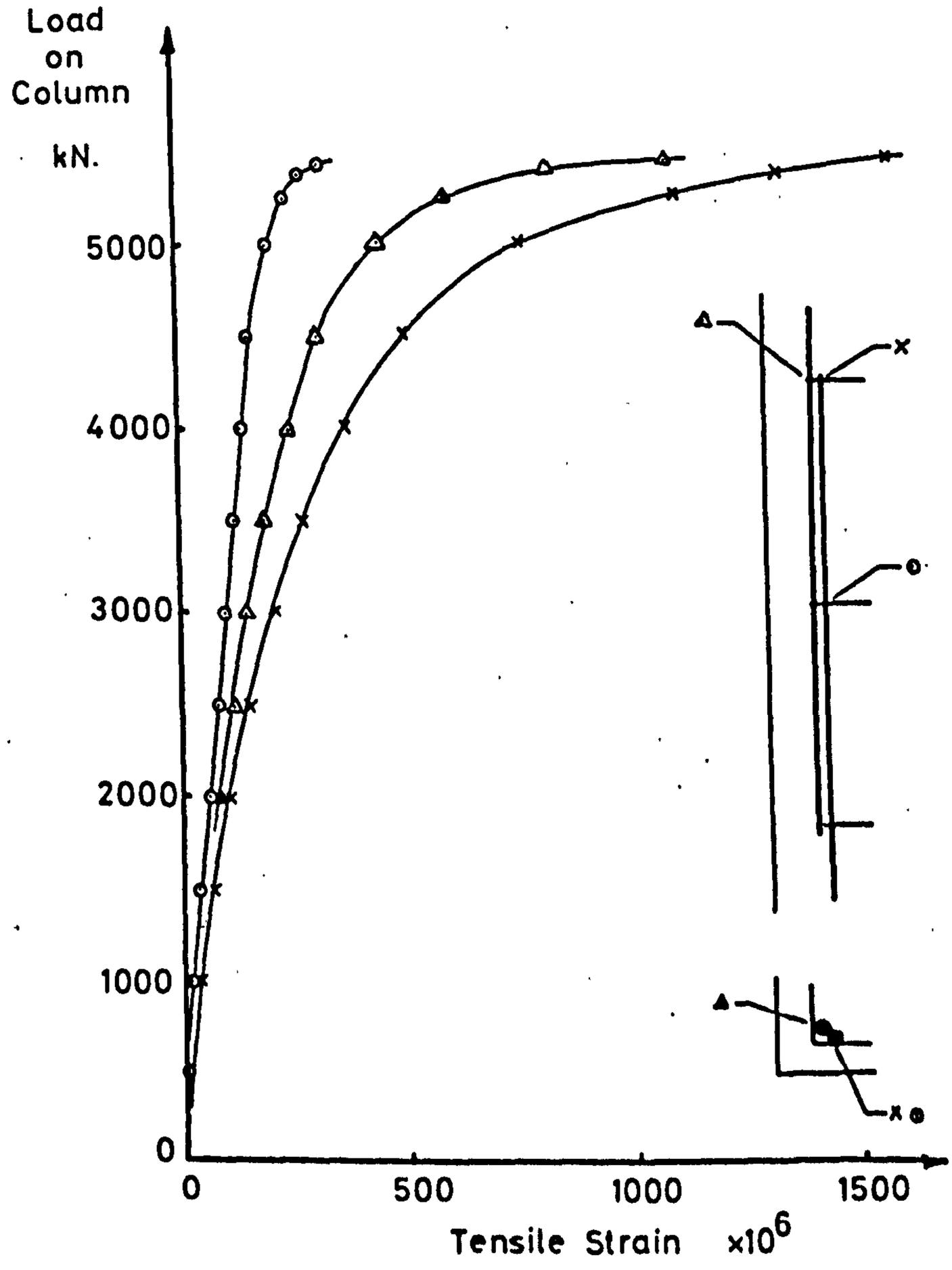

Fig. B.6 Strains measured on links - Column A 303B.

Bars with bond and end bearing.

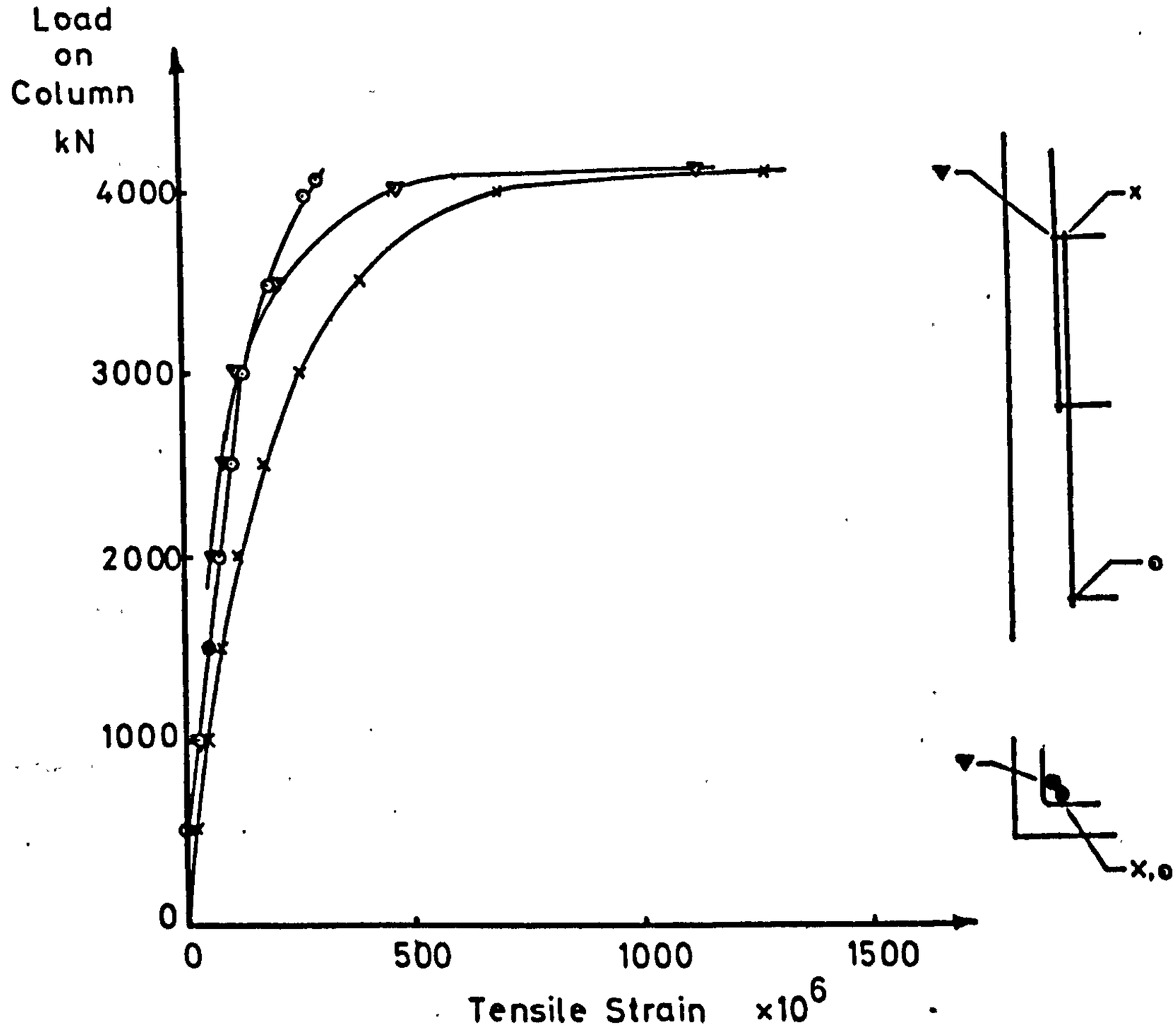

Fig. B.7 Strains Measured on links - Column A 304B.

Bars with bond only.

APPENDIX C

SPECIMEN CALCULATIONS FOR A TYPICAL COLUMN (COL. A 302C)

The actual cross sectional areas of reinforcement and concrete were used in calculations of joint strength. For column A 302C, these were

nett cross sectional area of concrete - at gauge height - 159,000mm^2

- at ends of lapped joint -

157,000mm^2

cross sectional area of reinforcement - 5,020mm^2

The Young's modulus of the reinforcing steel was 207 kN/mm^2.

Strains measured outwith the lapped joint on each column face are shown for various load increments up to 80% of ultimate load in table C.1, columns 2-5, and their average is shown in column 6. The load carried by the reinforcing bars is calculated from the properties of the reinforcement and the average strain in the column, column 7, and is subtracted from the total load on the column to give the load carried by the concrete, column 8. Dividing the load carried by the concrete by the cross sectional area of concrete at the gauge height and the average strain in the column gives the secant modulus of elasticity of the concrete, shown in column 9 of table C.1.

Values of secant modulus are then plotted against strain, as shown in fig. C.1, and a straight line fitted to the points to evaluate the coefficients in the stress-strain relationship. The equation of the 'best fit' straight line in fig. C.1 is

$$E_c = -6{\cdot}1.\epsilon \times 10^{+6} + 23{\cdot}6 \times 10^{3} \quad N/mm^2 \qquad C.1$$

Multiplying both sides of equation C.1 by ϵ leads to the following expression for the stress-strain relationship of the concrete in the test specimen

$$E_c . \epsilon = \sigma = -6{\cdot}1\,\epsilon^2 \times 10^{+6} + 23{\cdot}6\,\epsilon \times 10^{+3} \quad N/mm^2 \qquad C.2$$

TABLE C.1 CALCULATION OF SECANT MODULUS OF ELASTICITY OF CONCRETE FROM STRAINS MEASURED ON COLUMN A 302C

Column Load	Measured Strains $\times 10^6$					Steel Load	Concrete Load	Secant Modulus
kN	1	2	3	4	Average	kN	kN	kN/mm^2
500	100	120	100	100	105	110	390	23.4
1000	220	250	220	220	227	240	760	21.1
1500	320	370	350	320	340	350	1150	21.3
2000	450	500	470	450	467	490	1510	20.3
2500	570	620	620	550	590	610	1890	20.1
3000	750	750	770	650	730	760	2240	19.3
3500	900	950	950	850	887	920	2580	18.3
4000	1070	1070	1100	1000	1060	1100	2900	17.2
4500	1270	1250	1270	1170	1240	1290	3210	16.3

From equation 5.10, the ultimate strength of the concrete is then

$$f_{cg} = \frac{(23.6)^2}{4 \times 6.1} = 22.8 \ N/mm^2 \qquad C.3$$

The values of ultrasonic pulse velocity measured at the gauge height and through the lapped joint were 4.10 km/sec. and 4.05 km/sec. respectively. From equation 5.14, the strength of the concrete through the lapped joint is

$$f_{cj} = 22.8 \left(\frac{4.05}{4.10}\right)^4 = 21.7 \ N/mm^2 \qquad C.4$$

The ultimate load of the column was 5400 kN, and the stress developed in the reinforcement is given by equation 5.2

$$f_{sc} = \frac{5400 \times 10^3 - 21.7 \times 157,000}{5020} = 397 \ N/mm^2 \qquad C.5$$

Expressions for the upper and lower limits of joint strength derived from the theoretical analysis are given by equations 3.43 and 3.44.

In column A 302C, there were a total of 3 links of 10mm diameter with a yield strength of 387 N/mm^2, arranged as shown in fig. 4.1. 40mm diameter 'Hybar' reinforcement was used in this column, and the rib dimensions are as given in table 4.3. The length of the lapped joint was 600mm, or 15 times the diameter of the main reinforcement, and it is assumed that bond stresses develop over a distance of 2.5ϕ more than the lap length. The strength of the concrete in the specimen was as given above.

The upper limit to joint strength is, from equation 3.43

$$f_{scu} = \left[\frac{0.71 \times 3 \times 78.5 \times 387}{94} + \frac{21.7 \times 700}{24}\right] \frac{220 \times 7.2}{\pi . 1600} + 3.42 \times 21.7$$

$$= 491 \ N/mm^2$$

This is greater than the yield strength of the reinforcement,

which was 415 N/mm^2 and the yield strength is therefore taken to be the upper limit of joint strength in this case. The ratio of the experimental result to the joint strength calculated from equation 3.43 is

$$f_{sc}/f_{sc_u} = \frac{397}{415} = 0.96 \qquad C.7$$

The lower limit to joint strength is, from equation 3.44

$$f_{sc_l} = \left[\frac{0.93 \times 78.5 \times 387}{94} + \frac{21.7 \times 700}{24}\right] \frac{220 \times 7.2}{\pi . 1600} + 3.42 \times 21.7$$

$$= 368\ N/mm^2 \qquad C.8$$

The ratio of the experimental result to the joint strength calculated from equation 3.44 is

$$f_{sc}/f_{sc_l} = \frac{397}{368} = 1.08 \qquad C.9$$

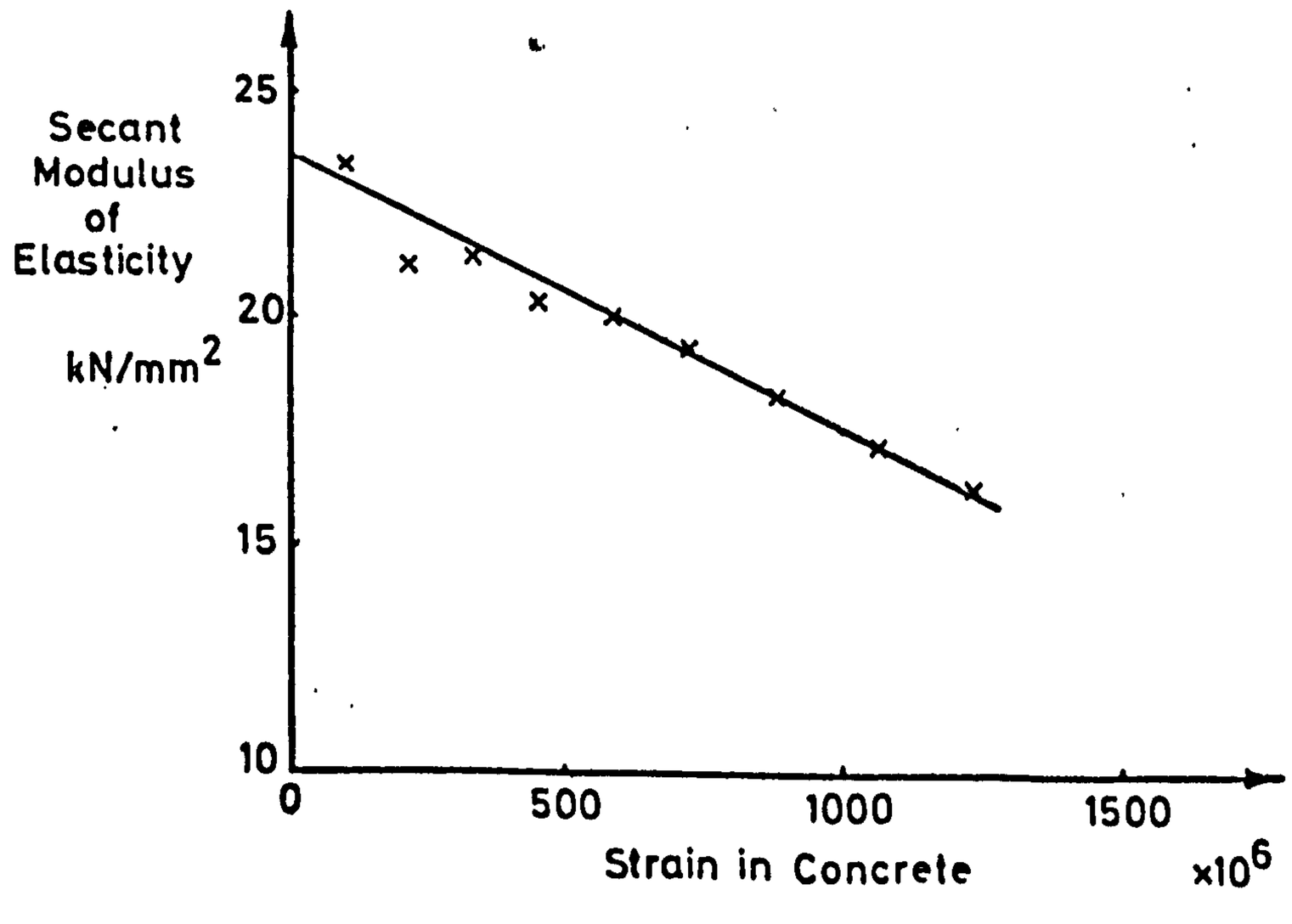

Fig. C.1 Secant modulus of elasticity vs. strain in concrete - Column A 302 C.

UNIVERSITY LIBRARY